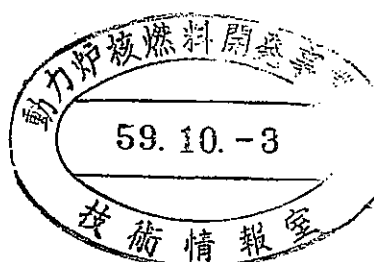


本資料は2001年7月31日付けて
登録区分変更する。[技術展開部技術協力課]

SHIELDING ANALYSES
OF
JOYO MK-II (I)-C



JUNE, 1984

POWER REACTOR AND NUCLEAR FUEL DEVELOPMENT CORPORATION
HITACHI Ltd.

TABLE OF CONTENTS

ABSTRACT

CHAPTER 1	INTRODUCTION	1-1
CHAPTER 2	CROSS-SECTION GENERATION AND UPPER AXIAL 2-D ANALYSIS	
2.1	INTRODUCTION	2-1
2.2	CALCULATIONAL MODEL	2-1
2.3	GENERATION AND CONDENSATION OF CROSS-SECTIONS	2-8
2.4	UPPER AXIAL 2-D CALCULATION	2-52
CHAPTER 3	COMPARISON OF THE CALCULATION RESULTS WITH MEASUREMENTS	
3.1	MEASUREMENT	3-1
3.2	COMPARISON	3-5
CHAPTER 4	CONCLUSIONS	4-1
REFERENCES		
ACKNOWLEDGEMENTS		



NOT FOR PUBLICATION
PNC/J/J 202 84-06 (Tr)
June, 1984

Shielding Analysis of JOYO MK-II (I) - C*

Noboru Nakao**
Tatsuo Amada**
Junnosuke Horie***
Jun Takeuchi***
Hiroyuki Handa***
Masao Sebata***

* This work was performed under the contracts between Power Reactor and Nuclear Fuel Development Corporation and Hitachi Ltd.

** Hitachi Works, Hitachi Ltd.

*** Hitachi Engineering Company

ABSTRACT

Shielding analyses of the JOYO MK-II have been performed in order to confirm the shielding design method for the prototype fast breeder reactor, MONJU, and to obtain the data for estimation of the shielding design margin. The method used here is almost the same as the design method of MONJU. The only difference is the cross-sections that are generated from the JENDL-2. The calculational flux distributions have been first obtained by a series of the ANISN and DOT calculations, then compared with measurements.

The primary results obtained in this analysis are as follows:

- (1) The calculational results agreed with the measurement within a factor of 5 in a wide range of the reactor, taking into consideration the effect of fuels in an in-vessel fuel storage rack, the flux-to-reaction rate conversion factors and the effect of the detector guide tube on the measurement.
- (2) The fuels in the in-vessel fuel rack have a strong effect on fast neutron flux levels in the fuel rack, but have a little effect on neutron flux levels outside the rack.
- (3) The comparison of the one dimensional calculation results obtained by the JENDL-2 base cross-section data and the ENDF/B-IV base cross-section data have revealed that the calculation with the JENDL-2 base data gives smaller flux levels than that with the ENDF/B-IV base data.

CHAPTER 1

INTRODUCTION

In order to confirm the shielding design method and to evaluate the design margin, acquisition of the evaluation data and experience is required. It is one of the most effective way to obtain shielding design information through the analysis and measurements of the operational reactor. The shielding analyses of JOYO was first performed by the "Committee on the Fast Reactor Core Design (Shield Design)" from 1977 to 1979⁽¹⁾ and followed by the "Supplemental Analyses Work."⁽¹¹⁾ Many fruitful results were obtained in these analyses and the analysis method developed in these studies have been being applied to the shielding design of MONJU.

The shielding analysis of JOYO MK-II have been performed in this study under the different condition from MK-I analyses. The primary differences are as follows:

- (1) The JENDL-2 base multigroup cross-section data were used in place of the ENDF/B-IV base cross-section data used in the MK-I analysis. (3), (4), (5), (6), (7)
- (2) There is no blanket assembly around the fuel assembly in the MK-II structure, while the fuel assemblies in the MK-I structure were surrounded by the blanket assemblies.
- (3) The composition of the control rod is changed.

The actual MK-II core have been being operated with some special fuels in the fuel storage rack just outside the inner neutron shield. Although the evaluation of the effect of the fuels in the fuel storage rack on the flux distribution in the reactor system is very important, the detailed analysis was out of scope in this study.

The primary objectives in this study are the analysis of the neutron and gamma-ray flux distribution in the reactor vessel and the streaming analysis in the reactor cavity. The ways of evaluation are the comparison of the calculational results between MK-I and MK-II analysis and the comparison of the calculation with the measurement.

Main part of the calculation will be described in chapter 2, where the analysis procedure, calculational results and the comparison with the MK-I results will be performed. In chapter 3, the comparison of the calculational results with the measurement will be described.

CHAPTER 2
CROSS-SECTION GENERATION
AND
UPPER AXIAL 2-D ANALYSIS

2.1 Introduction

It was described that the JENDL-2 (Japanese Evaluated Nuclear Data Library) cross-section data is used in this study of the JOYO shielding analysis, and that one of primary objectives of this study is to give the neutron and gamma-ray boundary fluxes to perform further analysis for the upper reactor radiation distribution including the streaming analysis around the support ledge. In this chapter we will describe the geometrical model for the DOT calculation,⁽²⁾ the generation and condensation of the cross-sections using the RADHEAT code and the ANISN code⁽⁸⁾. Then the results obtained by using the JENDL-2 based cross-section data are compared with the results by the ENDF/B-IV based cross-section data. The JENDL-2 based cross-section data is used for the upper axial two dimensional analysis and the results are compared with the measurements.

2.2 Calculational Model

The shielding configuration used for the upper axial two dimensional calculation is shown in Fig. 2.2.1. To perform the calculation by use made of the bootstrap method the full region was devided into two regions. One is the region inside the reactor vessel where usual angular quadrature set is enough to obtain the neutron and gamma-ray flux distribution, and the other outside the reactor vessel where special many angular quadrature set is necessary to calculate the streaming neutrons and gamma-rays at the reactor cavity. Therefore, the calculation was devided into two serial steps, one for inside the reactor vessel and the other for outside the reactor vessel. Each calculational step has a common overlapping region to obtain the well defined boundary fluxes. The geometric models used for the two steps of this DOT series for the upper axial region are shown in Figs. 2.2.2 and 2.2.3. The calculational regions for the two steps are also shown in Fig. 2.2.1.

The upper axial full region was devided into 35,997 mesh intervals (169 mesh intervals radially and 213 intervals axially). The fuel region extends from a core mid-plane level to a level 775 cm above the core mid plane and from a core center axis to a radius of 500 cm. The first step includes 1 to 120 mesh interval (0 to 285 cm) in the radial direction and 1 to 213 mesh interval (0 to 775cm) in the axial direction. The total mesh intervals is 25,560. The second step extends radially from 74 to 169 mesh interval (150 to 500 cm) and axially from 1 to 142 mesh interval (0 to 540.5 cm). Space mesh structures in radial and axial directions are shown in Tables 2.2.1 and 2.2.2 for convenience.

The cross-sections needed for the DOT calculations are generated based on the JENDL-2 data as is described in the next section.

Table 2-2-1 Space Mesh Structure in Radial Direction

(Unit : cm)

I	R(I)	I	R(I)	I	R(I)	I	R(I)
1	2.47	51	94.50	101	218.50	151	413.33
2	4.95	52	97.00	102	221.50	152	417.78
3	6.49	53	99.50	103	224.25	153	422.22
4	8.18	54	102.00	104	227.00	154	426.67
5	9.87	55	104.50	105	228.50	155	431.11
6	12.84	56	107.00	106	231.75	156	435.56
7	15.80	57	109.50	107	235.50	157	440.00
8	16.93	58	112.00	108	238.00	158	445.00
9	17.66	59	114.50	109	241.50	159	450.00
10	20.37	60	115.78	110	245.00	160	455.00
11	21.65	61	117.06	111	247.50	161	460.00
12	22.93	62	118.33	112	250.00	162	465.00
13	25.49	63	119.61	113	256.00	163	470.00
14	27.73	64	120.89	114	260.50	164	475.00
15	29.98	65	122.17	115	265.00	165	480.00
16	32.22	66	123.44	116	268.00	166	485.00
17	34.46	67	124.72	117	272.75	167	490.00
18	36.70	68	126.00	118	277.50	168	495.00
19	38.81	69	130.80	119	281.25	169	500.00
20	40.92	70	135.60	120	285.00		
21	43.03	71	140.40	121	290.00		
22	45.14	72	145.20	122	294.00		
23	47.25	73	150.00	123	298.00		
24	49.00	74	156.17	124	302.00		
25	50.50	75	162.33	125	306.00		
26	52.25	76	168.50	126	310.00		
27	54.00	77	171.75	127	314.00		
28	55.00	78	175.00	128	318.00		
29	56.50	79	176.25	129	320.00		
30	58.00	80	177.50	130	320.95		
31	59.50	81	178.75	131	321.90		
32	61.00	82	180.00	132	329.08		
33	63.00	83	181.25	133	336.26		
34	65.00	84	182.50	134	343.43		
35	67.00	85	185.00	135	350.61		
36	68.25	86	186.20	136	357.79		
37	69.93	87	187.40	137	364.97		
38	71.50	88	190.20	138	372.14		
39	73.50	89	193.00	139	379.32		
40	75.00	90	196.00	140	386.50		
41	76.50	91	199.00	141	388.17		
42	77.50	92	201.50	142	389.83		
43	79.50	93	203.50	143	391.50		
44	82.00	94	204.50	144	393.17		
45	83.00	95	206.50	145	394.83		
46	84.50	96	209.50	146	396.50		
47	86.00	97	211.50	147	398.25		
48	87.00	98	213.50	148	400.00		
49	89.50	99	215.00	149	404.44		
59	92.00	100	216.50	150	408.89		

Table 2-1-2 Space Mesh Structure in Axial Direction

(Unit : cm)

J	Z (J)	J	Z (J)	J	Z (J)	J	Z (J)	J	Z (J)
1	3.94	51	130.00	101	360.10	151	569.75	201	732.75
2	7.89	52	133.00	102	365.00	152	573.20	202	735.00
3	11.83	53	135.27	103	370.10	153	575.20	203	740.50
4	15.78	54	137.53	104	375.20	154	577.20	204	744.00
5	19.72	55	140.00	105	380.30	155	580.60	205	747.50
6	23.66	56	145.33	106	385.40	156	584.00	206	751.00
7	27.61	57	150.67	107	390.50	157	586.00	207	754.50
8	28.81	58	156.00	108	395.60	158	588.80	208	757.50
9	30.48	59	159.87	109	400.70	159	591.60	209	758.50
10	32.16	60	163.75	110	405.80	160	594.40	210	762.50
11	33.83	61	167.62	111	410.90	161	597.20	211	767.00
12	35.43	62	171.50	112	416.00	162	599.55	212	771.00
13	37.02	63	175.50	113	420.87	163	601.90	213	775.00
14	38.61	64	179.50	114	425.75	164	605.45		
15	40.21	65	182.00	115	430.62	165	609.00		
16	41.80	66	184.50	116	435.50	166	615.45		
17	43.40	67	189.55	117	440.37	167	621.90		
18	44.99	68	194.60	118	445.25	168	623.95		
19	46.59	69	199.65	119	450.12	169	626.00		
20	48.18	70	204.70	120	455.00	170	629.50		
21	49.19	71	209.75	121	457.14	171	633.00		
22	50.58	72	214.80	122	459.29	172	637.33		
23	51.97	73	219.85	123	461.43	173	641.67		
24	53.36	74	224.90	124	463.57	174	646.00		
25	54.75	75	229.95	125	465.71	175	648.05		
26	56.15	76	235.00	126	467.86	176	650.10		
27	57.54	77	240.00	127	470.00	177	653.70		
28	58.93	78	245.00	128	473.00	178	658.85		
29	62.27	79	250.00	129	476.00	179	664.00		
30	65.62	80	255.00	130	480.50	180	667.05		
31	68.97	81	260.00	131	485.75	181	670.10		
32	72.31	82	265.00	132	491.00	182	672.15		
33	75.66	83	270.00	133	496.50	183	674.20		
34	79.01	84	275.00	134	499.50	184	678.00		
35	82.35	85	280.12	135	504.40	185	683.50		
36	85.70	86	285.25	136	509.30	186	689.00		
37	89.04	87	290.37	137	514.20	187	694.20		
38	92.39	88	295.50	138	519.10	188	696.25		
39	95.74	89	300.62	139	524.00	189	698.30		
40	99.08	90	305.75	140	529.50	190	700.00		
41	102.98	91	310.87	141	535.00	191	702.00		
42	106.89	92	316.00	142	540.50	192	704.00		
43	110.79	93	320.90	143	546.00	193	707.33		
44	114.69	94	325.80	144	547.50	194	710.67		
45	116.19	95	330.70	145	549.00	195	714.00		
46	117.69	96	335.60	146	552.50	196	718.30		
47	120.30	97	340.50	147	555.95	197	720.30		
48	123.00	98	345.40	148	559.40	198	722.10		
49	126.09	99	350.30	149	562.85	199	726.30		
50	128.04	100	355.20	150	566.30	200	730.50		

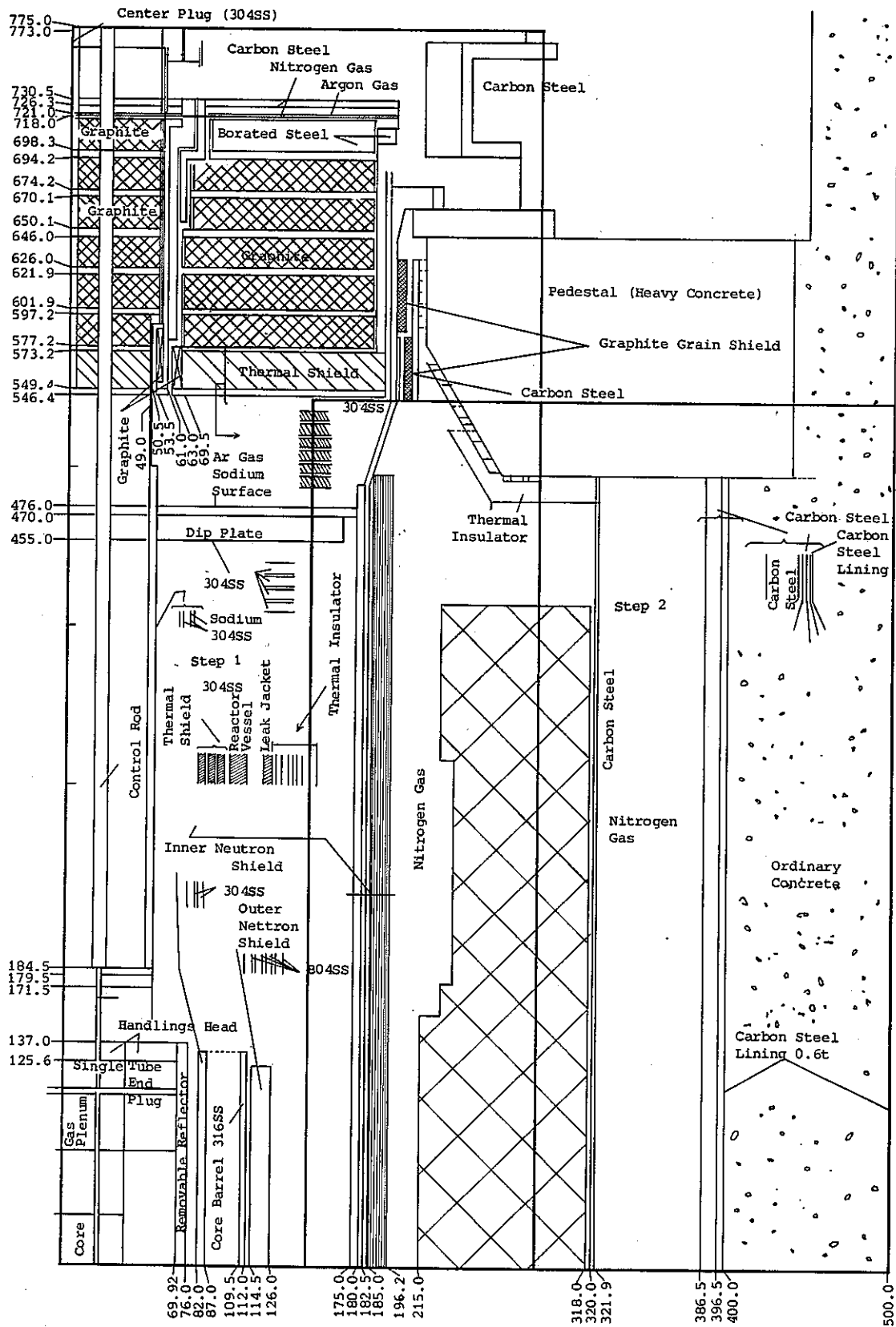


Fig. 2-2-1 Main Shield Configuration for Analysis Base.

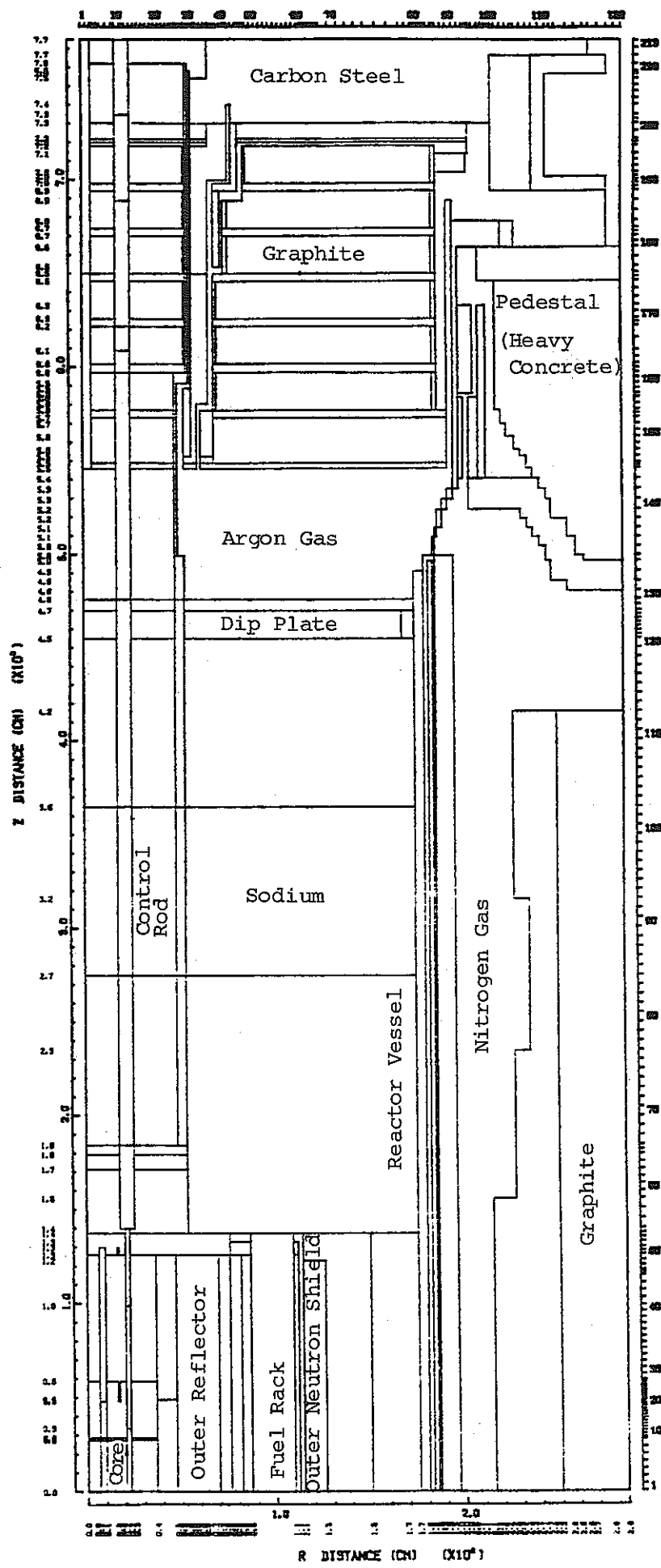


Fig. 2.2.2 Calculational Geometry for Step 1

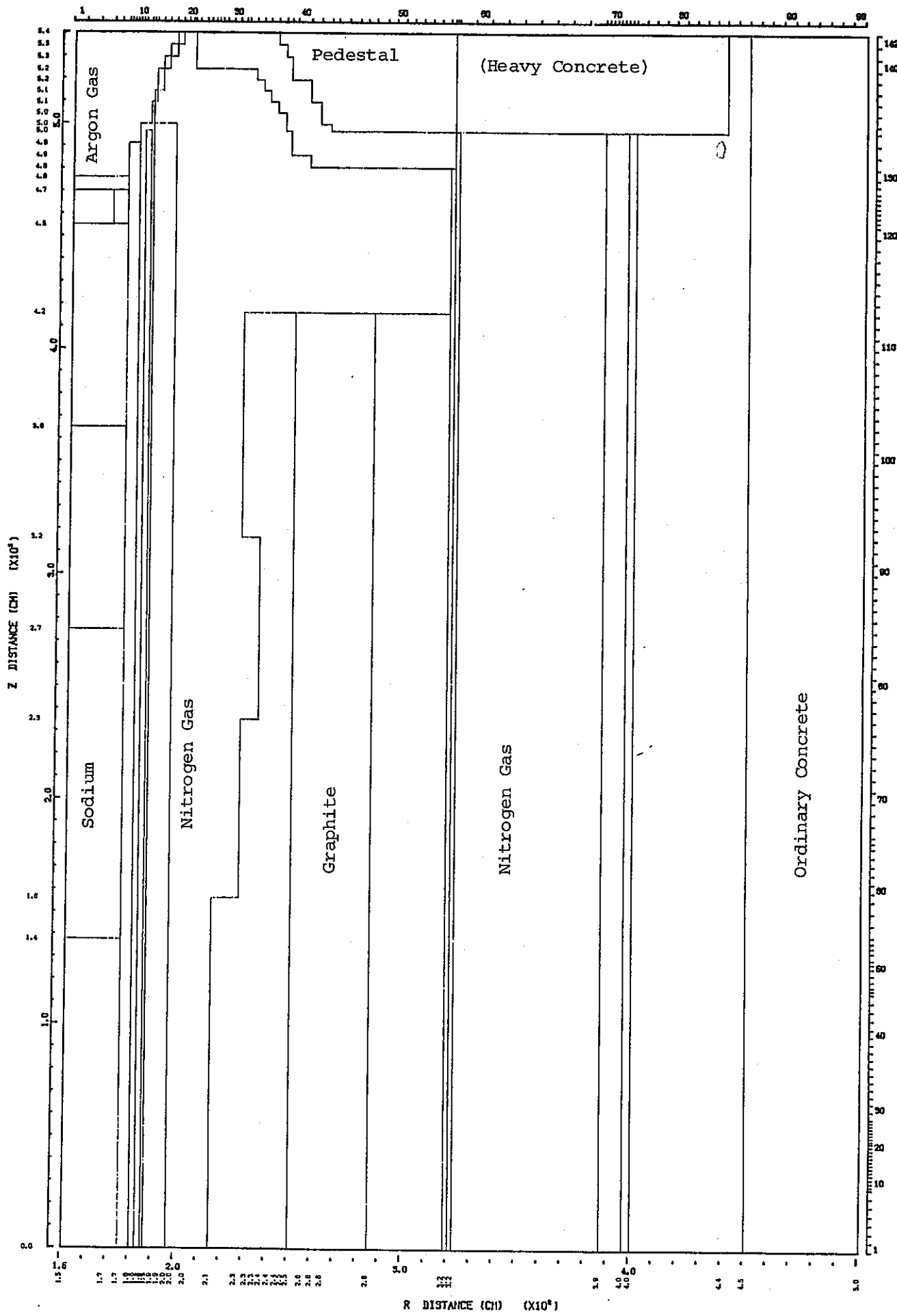


Fig. 2.2.3 Calculational Geometry for Step 2

2.3 Generation and condensation of cross-sections

2.3.1 Generation of a 120 group cross-section data

The RADHEAT code was used to generate 100 group neutron and 20 group gamma-ray cross-section data for 38 materials. The infinitely diluted cross-section file generated from the JENDL-2 data and the self-shielding factor file, JFT-200, were used to generate the 100 group effective neutron cross-sections. The structure of the infinitely diluted cross-section file is the same as the JSD-100 file which was based on the ENDF/B-IV. The secondary gamma-ray production data were from the POPOP4 library. In table 2.3.1 the coupled 120 group structure is shown. The material compositions are shown in Table 2.3.2.

Table 2.3.1 Energy group structure. (120 Group)

Neutron Energy Group (100 Groups)								Gamma-Ray Energy Group (20 Groups)	
1	1.4918+7	31	7.4274+5	61	7.1017+3	91	39.279+0	1	1.4+7
2	1.3499+7	32	6.7206+5	62	5.5308+3	92	3.0590+0	2	1.2+7
3	1.2214+7	33	6.0810+5	63	4.3074+3	93	2.3824+0	3	1.0+7
4	1.1052+7	34	5.5023+5	64	3.3546+3	94	1.8554+0	4	8.0+6
5	1.0000+7	35	4.9787+5	65	2.6126+3	95	1.4450+0	5	6.5+6
6	9.0484+6	36	4.5049+5	66	2.0347+3	96	1.1254+0	6	5.0+6
7	8.1873+6	37	4.0762+5	67	1.5846+3	97	8.7642-1	7	4.0+6
8	7.4082+6	38	3.6883+5	68	1.2341+3	98	6.8256-1	8	3.0+6
9	6.7032+6	39	3.3373+5	69	9.6112+2	99	5.3158-1	9	2.5+6
10	6.0653+6	40	3.0197+5	70	7.4852+2	100	4.1399-1	10	2.0+6
11	5.4881+6	41	2.7324+5	71	5.8295+2			11	1.66+6
12	4.9659+6	42	2.4724+5	72	4.5400+2			12	1.33+6
13	4.4933+6	43	2.2371+5	73	3.5357+2			13	1.0+6
14	4.0657+6	44	2.0242+5	74	2.7536+2			14	8.0+5
15	3.6788+6	45	1.8316+5	75	2.1445+2			15	6.0+5
16	3.3287+6	46	1.6573+5	76	1.6702+2			16	4.0+5
17	3.0119+6	47	1.4996+5	77	1.3007+2			17	3.0+5
18	2.7253+6	48	1.3569+5	78	1.0130+2			18	2.0+5
19	2.4660+6	49	1.2277+5	79	7.8893+1			19	1.0+5
20	2.2313+6	50	1.1109+5	80	6.1442+1			20	5.0+4
21	2.0190+6	51	8.6517+4	81	4.7851+1				2.0+4
22	1.8268+6	52	6.7379+4	82	3.7267+1				
23	1.6530+6	53	5.2475+4	83	2.9023+1				
24	1.4957+6	54	4.0868+4	84	2.2603+1				
25	1.3534+6	55	3.1828+4	85	1.7603+1				
26	1.2246+6	56	2.4788+4	86	1.3710+1				
27	1.1080+6	57	1.9305+4	87	1.0677+1				
28	1.0026+6	58	1.5034+4	88	8.3153+0				
29	9.0718+5	59	1.1709+4	89	6.4760+0				
30	8.2085+5	60	9.1188+3	90	5.0435+0				

* Unit : eV

** Upper Energy

Table 2.3.2 Atomic Number Densities (ATOM/BARN. CM) (1/8)

NO.	JY0001	JY0002	JY0003	JY0004	JY0005
NAME	DRIV5	CROD 3	REFI3	REFA	REFB
NUCLIDE					
H	0.0	0.0	0.0	0.0	0.0
C	0.0	0.0	0.0	0.0	0.0
N	0.0	0.0	0.0	0.0	0.0
O	1.67183-2	0.0	0.0	0.0	0.0
NA	8.73043-3	1.57995-2	6.22030-3	6.41819-3	4.55693-3
MG	0.0	0.0	0.0	0.0	0.0
SI	0.0	0.0	0.0	0.0	0.0
K	0.0	0.0	0.0	0.0	0.0
CA	0.0	0.0	0.0	0.0	0.0
CR	3.54388-3	5.05839-3	1.14204-2	1.16230-2	1.40591-2
MN	3.45275-4	4.92831-4	9.40500-4	8.58037-4	1.22558-3
FE	1.26643-2	1.80765-2	4.43127-2	4.25462-2	4.82251-2
NI	2.49242-3	3.55758-3	5.62835-3	5.97534-3	6.06183-3
MO	2.82449-4	4.03156-4	9.60800-5	1.22881-4	0.0
B10	0.0	0.0	0.0	0.0	0.0
B11	0.0	0.0	0.0	0.0	0.0
U235	7.44374-4	0.0	0.0	0.0	0.0
U238	5.33415-3	0.0	0.0	0.0	0.0
PU39	1.79231-3	0.0	0.0	0.0	0.0
PU40	5.09499-4	0.0	0.0	0.0	0.0
PU41	8.53612-5	0.0	0.0	0.0	0.0
PU42	2.07508-5	0.0	0.0	0.0	0.0
CO59	0.0	0.0	0.0	0.0	0.0

Table 2.3.2 (Continued) (2/8)

NO.	JY0006	JY0007	JY0008	JY0009	JY0010
NAME	SPFB5-J	SPFC5-J	CROD2	REFI2	SPFB2-J
NUCLIDE					
H	0.0	0.0	0.0	0.0	0.0
C	0.0	0.0	6.21170-3	0.0	0.0
N	0.0	0.0	0.0	0.0	0.0
O	3.91671-3	1.20817-2	0.0	0.0	0.0
NA	1.26795-2	1.07380-2	1.30130-2	1.23827-2	1.32462-2
MG	0.0	0.0	0.0	0.0	0.0
SI	0.0	0.0	0.0	0.0	0.0
K	0.0	0.0	0.0	0.0	0.0
CA	0.0	0.0	0.0	0.0	0.0
CR	4.63369-3	3.97069-3	2.85614-3	8.04695-3	4.34583-3
MN	4.51454-4	3.86859-4	2.78269-4	7.15524-4	4.23408-4
FE	1.65588-2	1.41895-2	1.02066-2	2.77988-2	1.55301-2
NI	3.25889-3	2.79260-3	2.00873-3	3.82233-3	3.05644-3
MO	2.69308-4	3.16466-4	2.27636-4	1.09164-4	3.46365-4
B10	0.0	0.0	2.24508-2	0.0	0.0
B11	0.0	0.0	2.26885-3	0.0	0.0
U235	1.74629-4	5.01093-4	0.0	0.0	0.0
U238	1.25139-3	3.67402-3	0.0	0.0	0.0
PU39	4.22962-4	1.39633-3	0.0	0.0	0.0
PU40	1.15701-4	3.82255-4	0.0	0.0	0.0
PU41	1.90395-5	6.40725-5	0.0	0.0	0.0
PU42	4.45808-6	1.27749-5	0.0	0.0	0.0
CO59	0.0	0.0	0.0	0.0	0.0

Table 2.3.2 (Continued) (3/8)

NO.	JY0011	JY0012	JY0013	JY0014	JY0015
NAME	SPFB3 J	SPFB4-J	SPFC2-J	SPFC3 J	FREF5
NUCLIDE					
H	0.0	0.0	0.0	0.0	0.0
C	0.0	0.0	0.0	0.0	0.0
N	0.0	0.0	0.0	0.0	0.0
O	0.0	4.28168-3	0.0	0.0	0.0
NA	1.26795-2	1.26795-2	1.07838-2	1.22973-2	1.45305-2
MG	0.0	0.0	0.0	0.0	0.0
SI	0.0	0.0	0.0	0.0	0.0
CA	0.0	0.0	0.0	0.0	0.0
CR	5.92993-3	4.63369-3	3.94006-3	7.03616-3	4.01421-3
MN	5.77744-4	4.51454-4	3.83874-4	6.85524-4	3.12664-3
FE	2.11910-2	1.65588-2	1.40800-2	2.51442-2	1.46851-2
NI	4.17054-3	3.25889-3	2.77106-3	4.94856-3	2.98980-3
MO	4.72618-4	3.69308-4	3.14024-4	5.60786-4	3.31825-4
B10	0.0	0.0	0.0	0.0	0.0
B11	0.0	0.0	0.0	0.0	0.0
U235	0.0	4.40238-6	0.0	0.0	0.0
U238	0.0	2.16904-3	0.0	0.0	0.0
PU39	0.0	0.0	0.0	0.0	0.0
PU40	0.0	0.0	0.0	0.0	0.0
PU41	0.0	0.0	0.0	0.0	0.0
PU42	0.0	0.0	0.0	0.0	0.0
CO59	0.0	0.0	0.0	0.0	0.0

Table 2.3.2 (Continued) (4/8)

NO.	JY0016	JY0017	JY0018	JY0019	JY0020
NAME	SPFAS-M	DRIV1	DRIV2	DRIV3	DRIV4
NUCLIDE					
H	0.0	0.0	0.0	0.0	0.0
C	0.0	0.0	0.0	0.0	0.0
N	0.0	0.0	0.0	0.0	0.0
O	1.54785-2	0.0	0.0	0.0	0.0
NA	8.98626-3	1.59522-2	8.83207-3	8.73042-3	1.81256-2
MG	0.0	0.0	0.0	0.0	0.0
SI	0.0	0.0	0.0	0.0	0.0
K	0.0	0.0	0.0	0.0	0.0
CA	0.0	0.0	0.0	0.0	0.0
CR	3.84507-3	3.61913-3	3.47589-3	9.03127-3	3.54388-3
MN	3.74619-4	3.52607-4	3.38650-4	8.79904-4	3.45275-4
FE	1.37406-2	1.29532-2	1.24213-2	3.22739-2	1.26643-2
NI	2.70425-3	2.54535-3	2.44460-3	6.35172-3	2.49242-3
MO	3.06454-4	2.88447-4	2.77029-4	7.19797-4	2.82449-4
B10	0.0	0.0	0.0	0.0	0.0
B11	0.0	0.0	0.0	0.0	0.0
U235	6.72115-4	0.0	0.0	0.0	1.86367-5
U238	4.69013-3	0.0	0.0	0.0	9.18220-3
PU39	1.78785-3	0.0	0.0	0.0	0.0
PU40	4.86987-4	0.0	0.0	0.0	0.0
PU41	8.14451-5	0.0	0.0	0.0	0.0
PU42	1.62499-5	0.0	0.0	0.0	0.0
CO59	0.0	0.0	0.0	0.0	0.0

Table 2.3.2 (Continued) (5/8)

NO.	JY0021	JY0022	JY0023	JY0024	JY0025
NAME	CROD 1	SPFC4-J	FREF2	RFLCTR	CR OUT
NUCLIDE					
H	0.0	0.0	0.0	0.0	0.0
C	0.0	0.0	0.0	0.0	0.0
N	0.0	0.0	0.0	0.0	0.0
O	0.0	1.19632-2	0.0	0.0	0.0
NA	2.06168-2	1.07380-2	1.33194-2	4.56060-3	2.13720-2
MG	0.0	0.0	0.0	0.0	0.0
SI	0.0	0.0	0.0	0.0	0.0
K	0.0	0.0	0.0	0.0	0.0
CA	0.0	0.0	0.0	0.0	0.0
CR	1.83577-3	3.97069-3	5.40064-3	1.34280-2	1.32770-3
MN	1.78857-4	3.86859-4	3.26679-3	0.0	0.0
FE	6.56025-3	1.41895-2	1.97786-2	4.79030-2	4.83430-3
NI	1.29111-3	2.79260-3	4.02459-3	6.18920-3	8.50770-4
MO	1.46312-4	3.16466-4	4.46356-4	0.0	9.56590-5
B10	0.0	0.0	0.0	0.0	0.0
B11	0.0	0.0	0.0	0.0	0.0
U235	0.0	1.37681-5	0.0	0.0	0.0
U238	0.0	5.96784-3	0.0	0.0	0.0
PU39	0.0	0.0	0.0	0.0	0.0
PU40	0.0	0.0	0.0	0.0	0.0
PU41	0.0	0.0	0.0	0.0	0.0
PU42	0.0	0.0	0.0	0.0	0.0
CO59	0.0	0.0	0.0	0.0	0.0

Table 2.3.2 (Continued) (6/8)

NO.	JY0026	JY0027	JY0028	JY0029	JY0030 *
NAME	CR IN	ORD CON	HVY COC	GRAFITE	C. STEEL
NUCLIDE					
H	0.0	6.51300-3	4.98800-3	0.0	0.0
C	5.57600-3	3.03900-4	2.35200-4	8.00700-2	9.45900-4
N	0.0	0.0	0.0	0.0	0.0
O	0.0	4.21600-2	3.26300-2	0.0	0.0
NA	1.30400-2	6.54900-4	5.06900-4	0.0	0.0
MG	0.0	0.0	0.0	0.0	0.0
SI	0.0	1.72100-2	1.33200-2	0.0	4.49700-4
K	0.0	2.78700-4	2.15700-4	0.0	0.0
CA	0.0	2.81000-3	2.17500-3	0.0	0.0
CR	3.43600-3	0.0	0.0	0.0	0.0
MN	0.0	0.0	0.0	0.0	6.89400-4
FE	1.25110-2	6.23300-4	1.96300-2	3.45100-6	8.36500-2
NI	2.20180-3	0.0	0.0	0.0	0.0
MO	2.47570-4	0.0	0.0	0.0	0.0
B10	2.06170-2	0.0	0.0	8.42300-8	0.0
B11	1.68760-3	0.0	0.0	3.61400-7	0.0
U235	0.0	0.0	0.0	0.0	0.0
U238	0.0	0.0	0.0	0.0	0.0
PU39	0.0	0.0	0.0	0.0	0.0
PU40	0.0	0.0	0.0	0.0	0.0
PU41	0.0	0.0	0.0	0.0	0.0
PU42	0.0	0.0	0.0	0.0	0.0
CO59	0.0	0.0	0.0	0.0	0.0

Table 2.3.2 (Continued) (7/8)

NO.	JY0031 *	JY0032	JY0033	JY0034 *	JY0035
NAME	SS-304	SODIUM	NITRGN	SS-316	B-STEEL
NUCLIDE					
H	0.0	0.0	0.0	0.0	0.0
C	3.12400-4	0.0	0.0	2.40900-4	1.13800-4
N	0.0	0.0	2.69000-5	0.0	0.0
O	0.0	0.0	0.0	0.0	0.0
NA	0.0	2.36500-2	0.0	0.0	0.0
MG	0.0	0.0	0.0	0.0	0.0
SI	1.77500-3	0.0	0.0	8.74800-4	4.99300-4
K	0.0	0.0	0.0	0.0	0.0
CA	0.0	0.0	0.0	0.0	0.0
CR	1.71400-2	0.0	0.0	1.53200-2	0.0
MN	1.70800-3	0.0	0.0	1.42900-3	8.09800-4
FE	5.67900-2	0.0	0.0	5.67200-2	8.22900-2
NI	7.99099-3	0.0	0.0	1.07500-2	0.0
MO	0.0	0.0	0.0	1.19500-3	0.0
B10	0.0	0.0	0.0	0.0	1.19500-4
B11	0.0	0.0	0.0	0.0	5.28200-4
U235	0.0	0.0	0.0	0.0	0.0
U238	0.0	0.0	0.0	0.0	0.0
PU39	0.0	0.0	0.0	0.0	0.0
PU40	0.0	0.0	0.0	0.0	0.0
PU41	0.0	0.0	0.0	0.0	0.0
PU42	0.0	0.0	0.0	0.0	0.0
CO59	1.99000-4	0.0	0.0	2.04400-5	0.0

Table 2.3.2 (Continued) (8/8)

NO.	JY0036	JY0037	JY0038		
NAME	INSLTOR	SS WOOL	C-POWDR		
NUCLIDE					
H	1.04300-2	0.0	0.0		
C	0.0	4.06100-5	4.00400-2		
N	0.0	0.0	0.0		
O	2.34500-2	0.0	0.0		
NA	0.0	0.0	0.0		
MG	7.89199-3	0.0	0.0		
SI	5.21300-3	2.30800-4	0.0		
K	0.0	0.0	0.0		
CA	0.0	0.0	0.0		
CR	0.0	2.22800-3	0.0		
MN	0.0	2.22000-4	0.0		
FE	0.0	7.38299-3	1.72600-6		
NI	0.0	1.03900-3	0.0		
MO	0.0	0.0	0.0		
B10	0.0	0.0	8.42300-8		
B11	0.0	0.0	1.80700-7		
U235	0.0	0.0	0.0		
U238	0.0	0.0	0.0		
PU39	0.0	0.0	0.0		
PU40	0.0	0.0	0.0		
PU41	0.0	0.0	0.0		
PU42	0.0	0.0	0.0		
CO59	0.0	2.58700-5	0.0		

Table 2.3.3 Energy Group Structure

	No.	No.	Energy (ev)		Lethagy Width	Remark
Neutron	1	1 - 10	1.4918+7	5.4881+6	1.0	
	2	11 - 15	5.4881+6		0.5	
	3	16 - 20	3.3287+6		0.5	
	4	21 - 25	2.0190+6		0.5	
	5	26 - 30	1.2246+6		0.5	
	6	31 - 35	7.4274+5		0.5	
	7	36 - 40	4.5049+5		0.5	
	8	41 - 45	2.7324+5		0.5	
	9	46 - 51	1.6573+5		0.9	
	10	52 - 55	6.7379+4		1.0	
	11	56 - 59	2.4788+4		1.0	
	12	60 - 63	9.1188+3		1.0	
	13	64 - 67	3.3546+3		1.0	
	14	68 - 71	1.2341+3		1.0	
	15	72 - 75	4.5400+2		1.0	
	16	76 - 80	1.6702+2		1.25	
	17	87 - 85	4.7851+1		1.25	
	18	86 - 90	1.3710+1		1.25	
	19	91 - 95	3.9279+0		1.25	
	20	96 - 99	1.1254+0		1.0	
	21	100	4.1399-1	1.0-3		
	No.	No.	Energy (ev)		Energy Width	Remark
Gamma	1	1 - 3	14.0	8.0	6.0	
	2	4 - 5	8.0		3.0	
	3	6 - 7	5.0		2.0	
	4	8 - 9	3.0		1.0	
	5	10 - 12	2.0		1.0	
	6	13 - 15	1.0		0.6	
	7	16 - 20	0.4	0.02	0.38	

Table 2.3.4 Region Geometry and Material Composition
in Axial 1-D Calculation

1	2	3	4	5	6	7	8	9	10	11	12	13	14	15	16	17	18	19	20	21	22	23	24	25	26	27	28	29	30	31	32	33

<u>Region</u>		<u>Distance from Core Center, cm (Region Thickness, cm)</u>	<u>No. of Meshes</u>	<u>Region Material</u>
1	Driver Fuel	27.61 (27.61)	13	Driver Fuel 1.0
2	Insulator	28.81 (1.20)	14	Insulator 1.0
3	Upper Reflector	58.93 (30.12)	44	Upper Reflector 1.0
4	Gas Plenum	126.09 (67.16)	79	Gas Plenum 1.0
5	Handling Head	137.53 (11.44)	84	Handling Head 1.0
6	Upper Core Structure 1	171.50 (33.97)	99	Sodium 0.74, SS-316 0.26
7	Upper Core Structure 2	179.50 (8.00)	104	Sodium 0.38, SS-316 0.62
8	Upper Core Structure 3	184.50 (5.00)	110	SS-316 1.0
9	Sodium	275.00 (90.50)	131	Sodium 1.0
10	Sodium	365.00 (90.00)	152	Sodium 1.0
11	Sodium	455.00 (90.00)	173	Sodium 1.0
12	Dip Plate	470.00 (15.00)	203	Sodium 0.2, SS-304 0.8
13	Sodium	476.00 (6.00)	205	Sodium 1.0
14	Argon Gas	546.00 (70.00)	225	Nitrogen Gas 1.0
15	Stainless Steel	549.00 (3.00)	229	SS-304 1.0
16	Thermal Shield	573.20 (24.20)	254	SS-304 0.13, C-Steel 0.12, SS Wool 0.75
17	Carbon Steel	577.20 (4.00)	259	Corbon Steel 1.0
18	Graphite	597.20 (20.00)	267	Graphite 1.0
19	Carbon Steel	601.90 (4.70)	272	Carbon Steel 1.0
20	Graphite	621.90 (20.00)	280	Graphite 1.0
21	Carbon Steel	626.00 (4.10)	284	Carbon Steel 1.0
22	Graphite	646.00 (20.00)	292	Graphite 1.0
23	Carbon Steel	650.10 (4.10)	296	Carbon Steel 1.0
24	Graphite	670.10 (20.00)	304	Graphite 1.0
25	Carbon Steel	674.20 (4.10)	308	Carbon Steel 1.0
26	Graphite	694.20 (20.00)	316	Graphite 1.0
27	Carbon Steel	698.30 (4.10)	320	Carbon Steel 1.0
28	Graphite	718.30 (20.00)	328	Graphite 1.0
29	Argon Gas	720.30 (2.00)	329	Nitrogen Gas 1.0
30	Stainless Steel	722.10 (1.80)	333	SS-304 1.0
31	Cavity	730.50 (8.40)	337	Nitrogen Gas 1.0
32	Boron Steel	762.50 (32.00)	397	Boron Steel 1.0
33	Stainless Steel	773.00 (10.50)	408	SS-304 1.0

Table 2.3.5 Region Geometry and Material Composition
in Radial 1-D Calculation

2	4	5	6	7	8	9	10	11	12	13	14	15	16	17	18	19	20	21	22	23	24	25	26	27	28	29	30	31	32	33	
1	3																														

<u>Region</u>		<u>Distance from Core Center, cm (Region Thickness, cm)</u>		<u>No. of Meshes</u>	<u>Region Material</u>
1	Core 1	6.49	(6.49)	7	Driver Fuel 1.0
2	Core 2	9.87	(3.38)	10	Speical Fuel 0.666, Refector 0.333
3	Core 3	20.37	(10.49)	20	Driver Fuel 1.0
4	Control Rod (Out)	22.93	(2.55)	23	Control Rod Adaptor 1.0
5	Core 4	36.70	(13.77)	36	Driver Fuel 1.0
6	Inner Reflector	47.25	(10.55)	56	Inner Reflector 1.0
7	Outer Reflector 1	69.93	(22.67)	100	Outer Reflector (A) 1.0
8	Outer Reflector 2	76.00	(6.06)	112	Outer Reflector (B) 100
9	Sodium	82.00	(6.00)	115	Sodium 1.0
10	Inner Radial Shield	87.00	(5.00)	125	Sodium 0.2, SS-304 0.8
11	Fuel Storage Rack	109.50	(22.50)	140	Sodium 1.0
12	Core Barrel	112.00	(2.50)	146	SS-316 1.0
13	Sodium	114.50	(2.50)	148	Sodium 1.0
14	Outer Radial Shield	126.00	(11.50)	181	Sodium 0.26, SS-304 0.74
15	Sodium	150.00	(24.00)	191	Sodium 1.0
16	Sodium	175.00	(25.00)	201	Sodium 1.0
17	Thermal Shield	180.00	(5.00)	209	Sodium 0.4, SS-304 0.6
18	Reactor Vessel	182.50	(2.50)	215	SS-304 1.0
19	Cavity	185.00	(2.50)	217	Nitrogen Gas 1.0
20	Leak Jacket	186.20	(1.20)	220	SS-304 1.0
21	Thermal Insulator	196.20	(10.00)	225	SS-304 0.04
22	Cavity	215.00	(18.80)	231	Nitrogen Gas 1.0
23	Graphite	250.00	(35.00)	246	Graphite 1.0
24	Graphite	285.00	(35.00)	261	Graphite 1.0
25	Graphite	318.00	(33.00)	276	Graphite 1.0
26	Cavity	320.00	(2.00)	278	Nitrogen Gas 1.0
27	Carbon Steel	321.90	(1.90)	283	Carbon Steel 1.0
28	Cavity	386.50	(64.60)	305	Nitrogen Gas 1.0
29	Carbon Steel	396.50	(10.00)	340	Carbon Steel 1.0
30	Liner	400.00	(3.50)	350	Carbon Steel 0.43
31	Concrete	450.00	(50.00)	400	Ordinary Cancrete 1.0
32	Concrete	500.00	(50.00)	450	Ordinary Cancrete 1.0
33	Carbon Steel	500.60	(0.60)	452	Carbon Steel 1.0

2.3.2 Condensation of cross-sections

The 120 group cross-section data were condensed into 21 group neutron and 7 group gamma-ray cross-section data which would be used for the DOT calculation. The weighting spectrum was obtained from the one dimensional neutron and gamma-ray calculation using the ANISN code with the coupled 120 group cross-section data. The energy group structure of the coupled 28 group is shown in Table 2.3.3.

The ANISN calculations were performed both in the radial and in the axial directions. The radial calculation was performed along the core mid plane within the range from the core center to the outer edge of the concrete biological shield. The region geometry is shown in Table 2.3.4. The axial calculation was performed along the core center axis within the range from the core mid plane to the top surface of the shield plug. In the axial calculation the control rod region at the center of the core was neglected to obtain the adequate neutron and gamma-ray energy spectrum information. The region geometry is shown in Table 2.3.5.

In these calculations the scattering cross-sections up to P_5 expansion components were used, and the S_8 angular quadrature set was used. The neutrons generated by the fissions in the core were taken as the source term, the neutrons generated from the special fuel assembly located at the fuel storage rack outside the inner radial shield were not taken into account in these calculation.

The calculational results are shown in Fig. 2.3.1 for the radial neutron flux distribution and in Figs. 2.3.2 (1) to 2.3.2 (7) for the neutron energy spectra at various positions in the region. The axial neutron flux distribution is shown in Fig. 2.3.3 and the energy spectra at various positions are shown in Fig. 2.3.4 (1) to 2.3.4 (6).

*** JOYO MK-II *** SHIELD CALC 1-D RADIAL (JENDL-2) NO 6

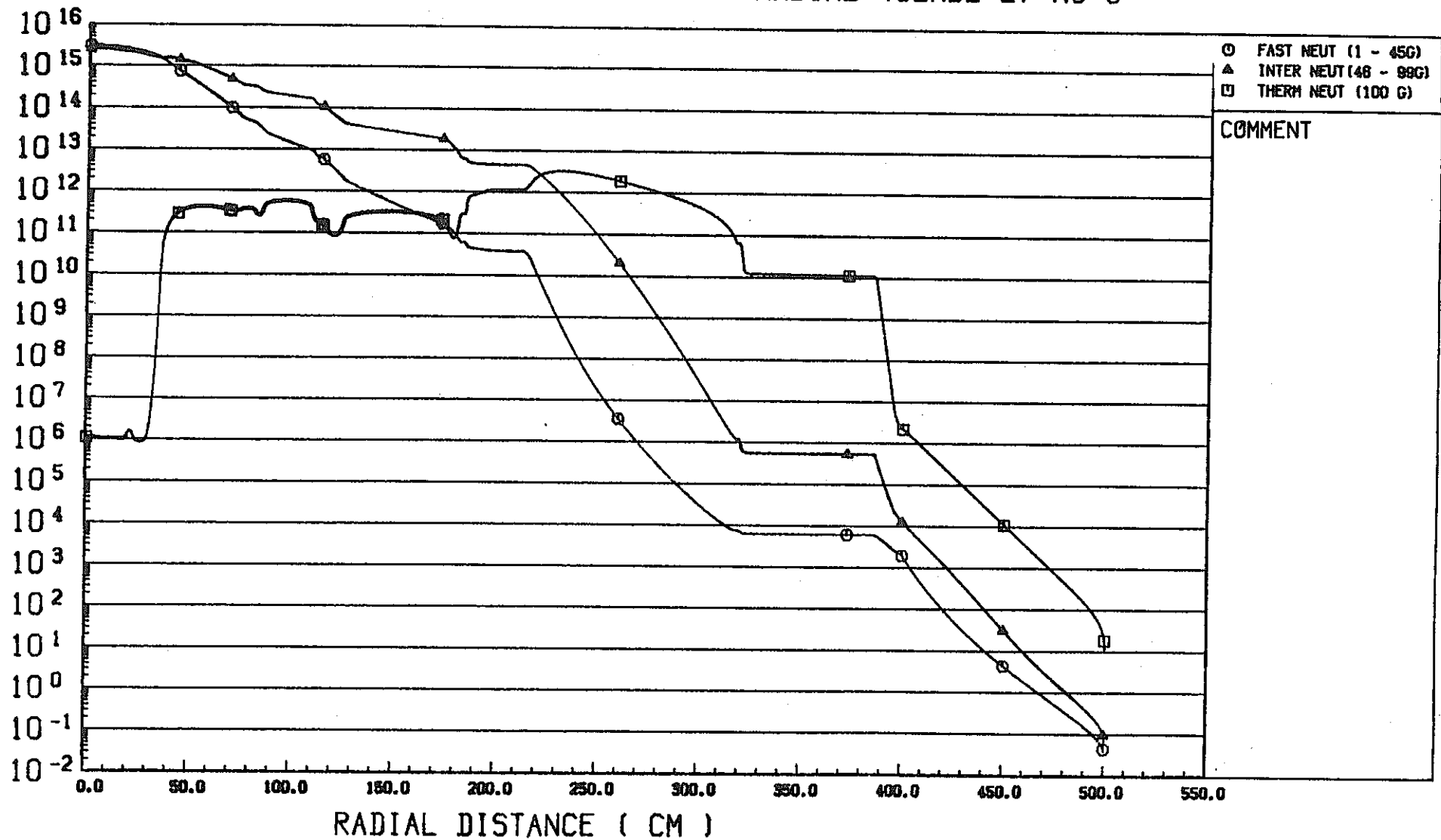


Fig. 2.3.1 Radial Neutron Flux Distribution from 1-D Calculation (JENDL-2)

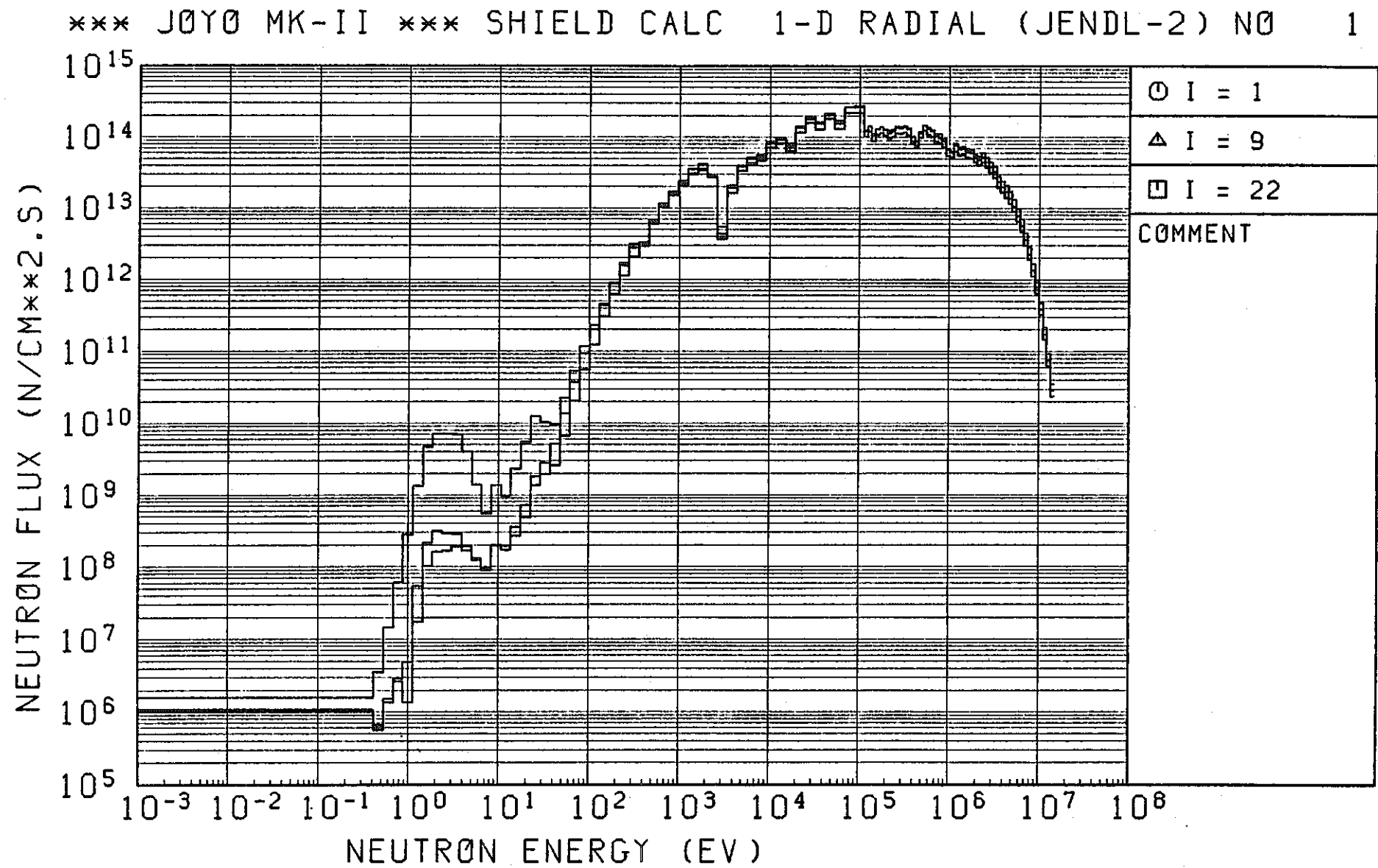


Fig. 2.3.2 (1) Neutron Spectrum from 1-D Radial Calculation (JENDL-2) (1/7)

*** JOYO MK-II *** SHIELD CALC 1-D RADIAL (JENDL-2) NO 2

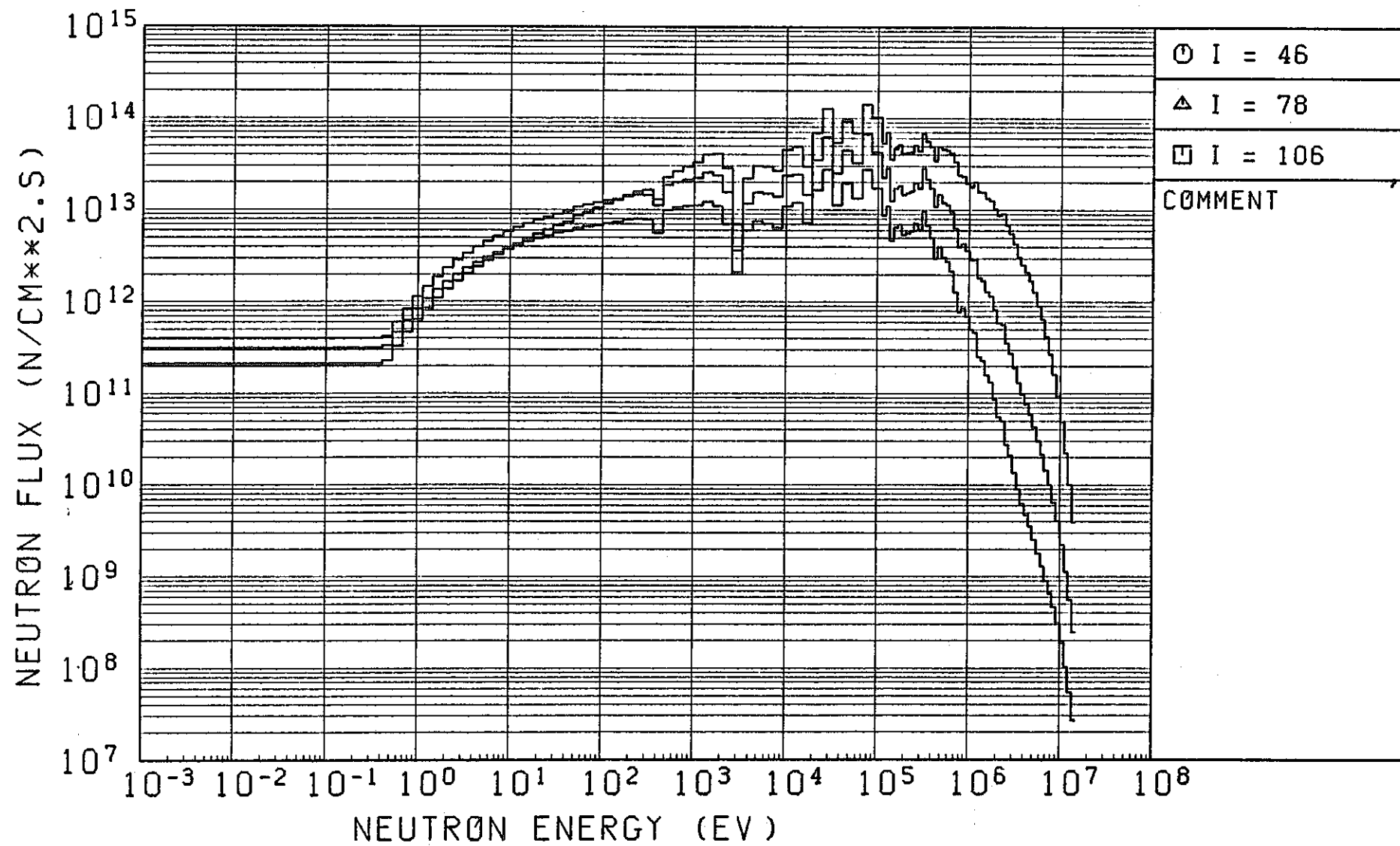


Fig. 2.3.2 (2) (Continued) (2/7)

*** JOYO MK-II *** SHIELD CALC 1-D RADIAL (JENDL-2) NO 3

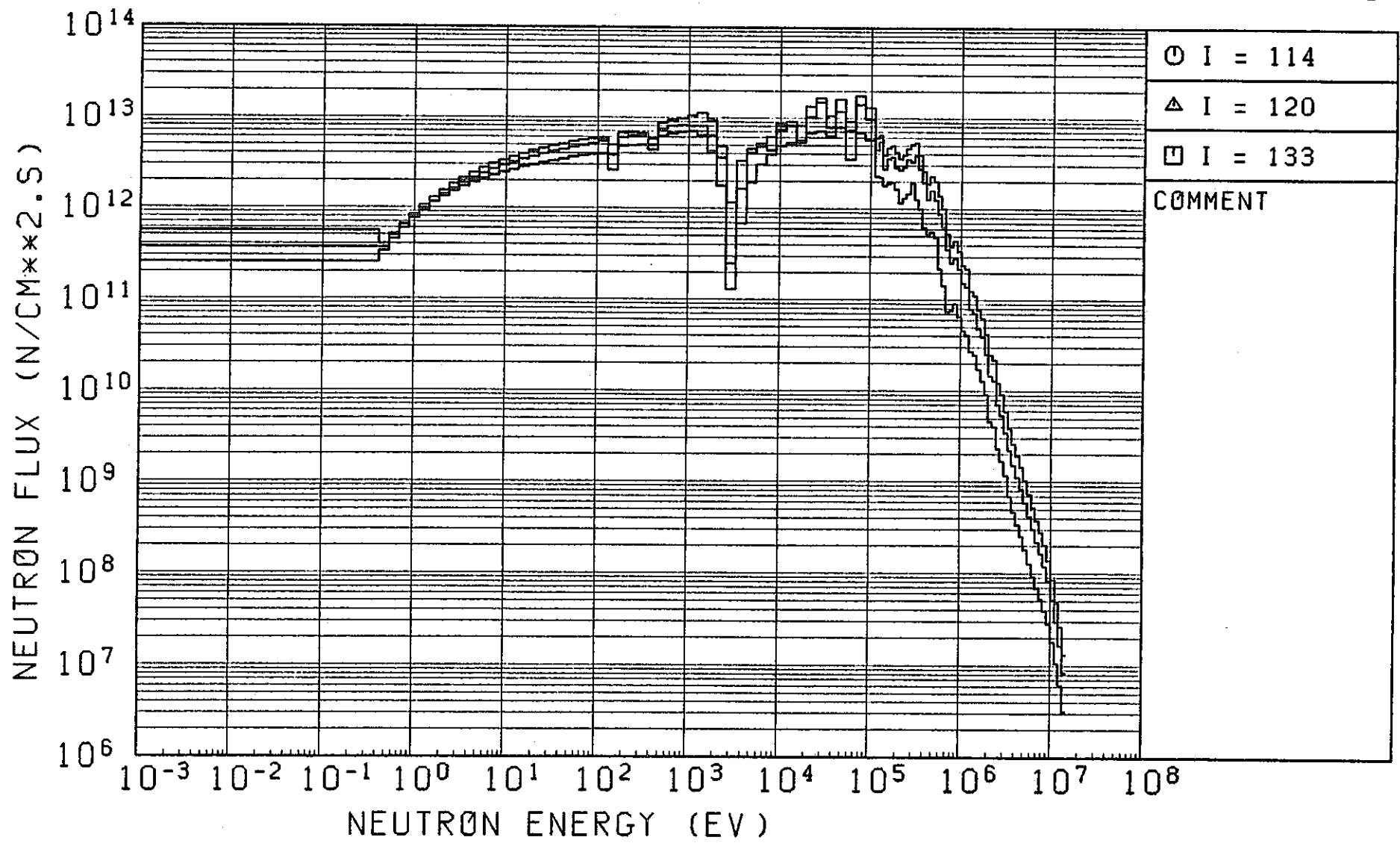


Fig. 2.3.2 (3) (Continued) (3/7)

*** JOYO MK-II *** SHIELD CALC 1-D RADIAL (JENDL-2) NO 4

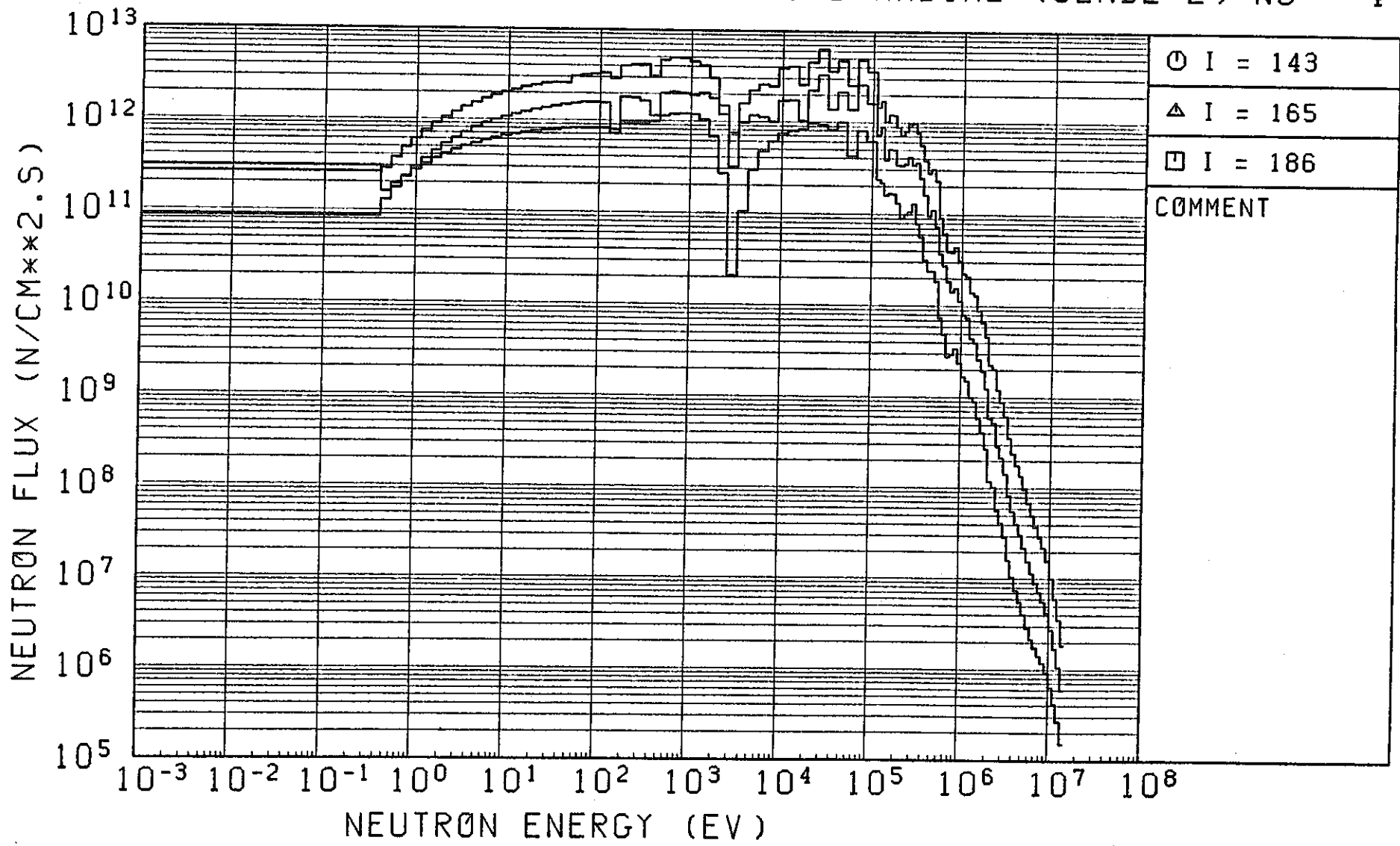


Fig. 2.3.2 (4) (Continued) (4/7)

*** JOYO MK-II *** SHIELD CALC 1-D RADIAL (JENDL-2) NO 6

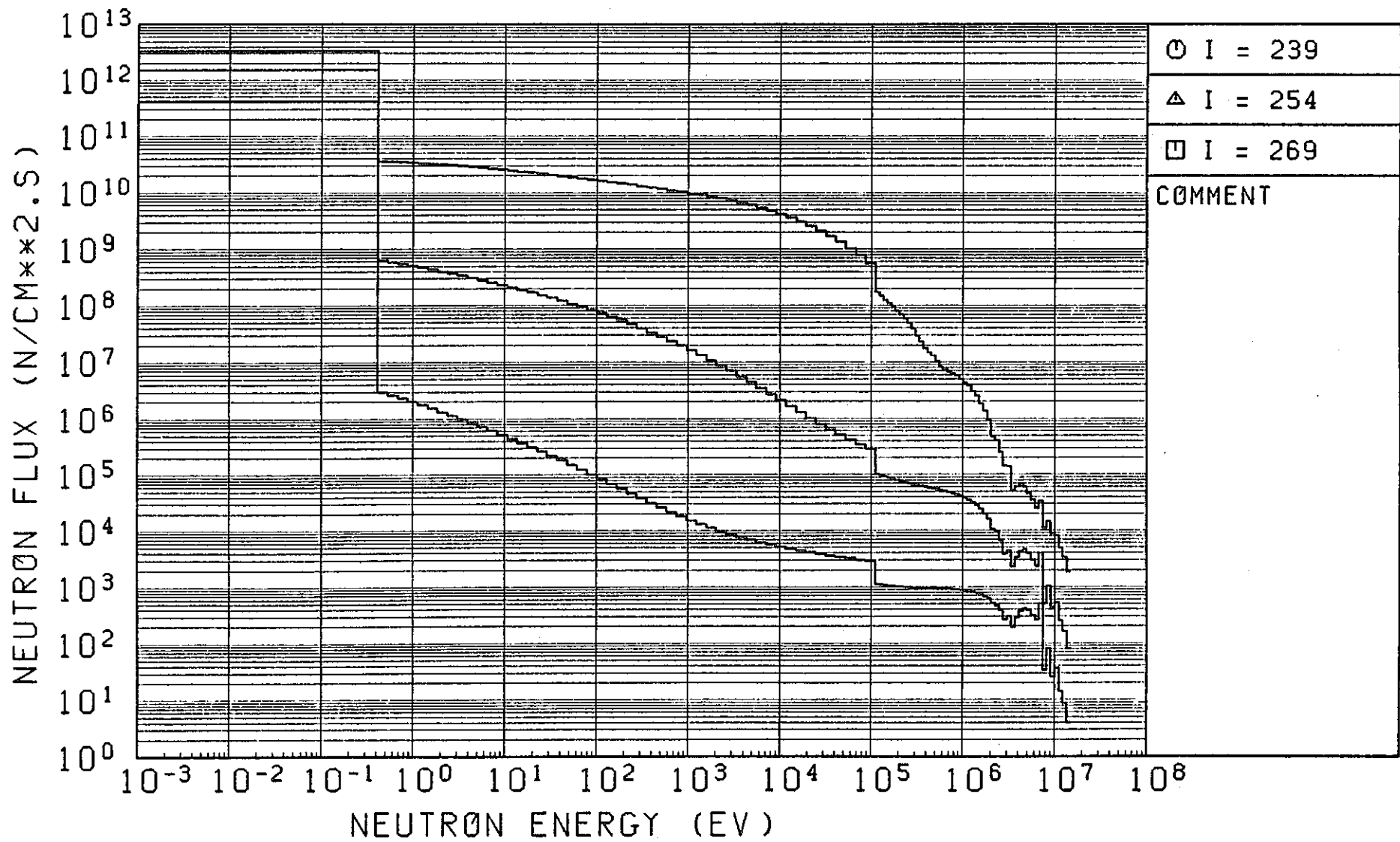


Fig. 2.3.2 (5) (Continued) (5/7)

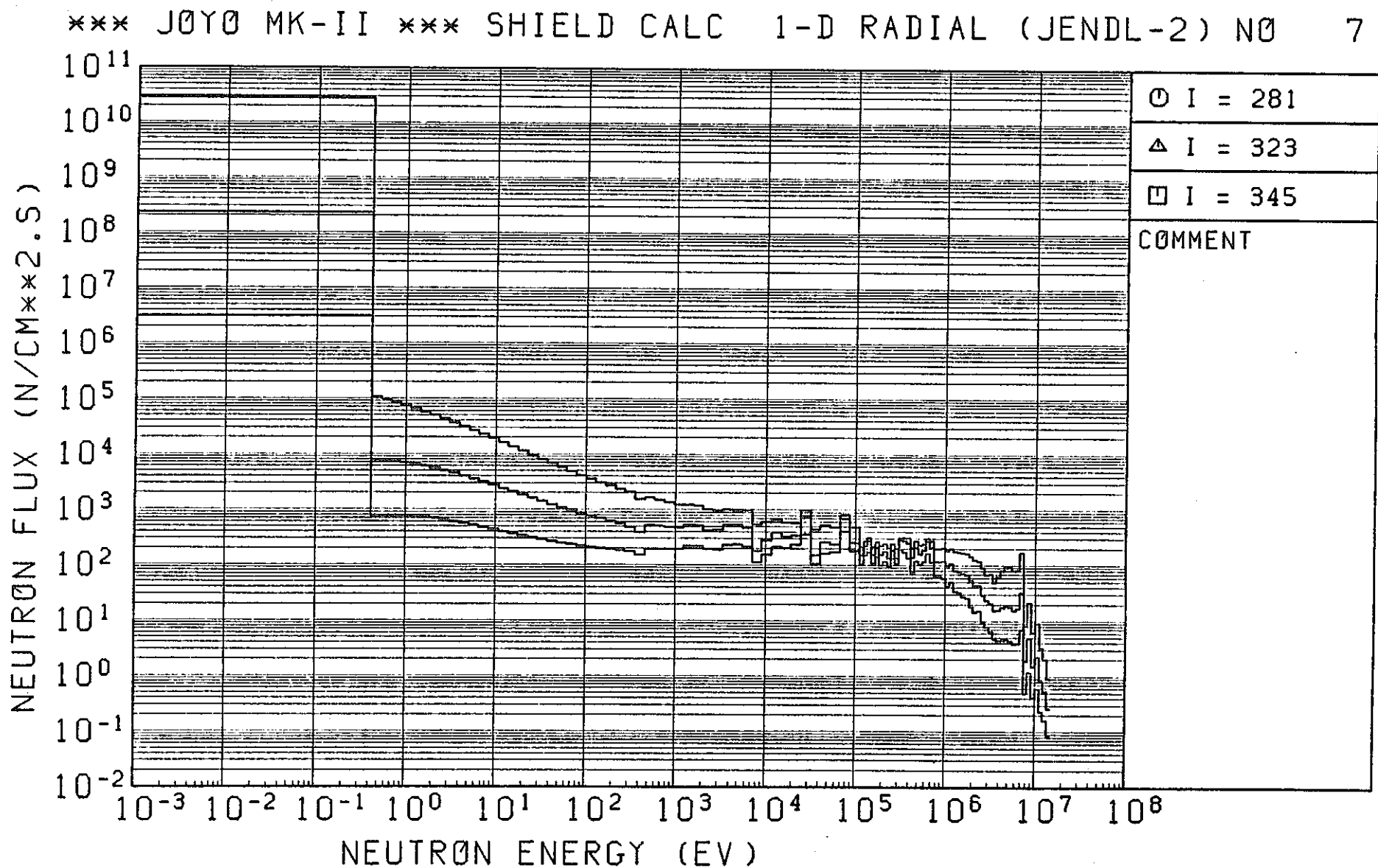


Fig. 2.3.2 (6) (Continued) (6/7)

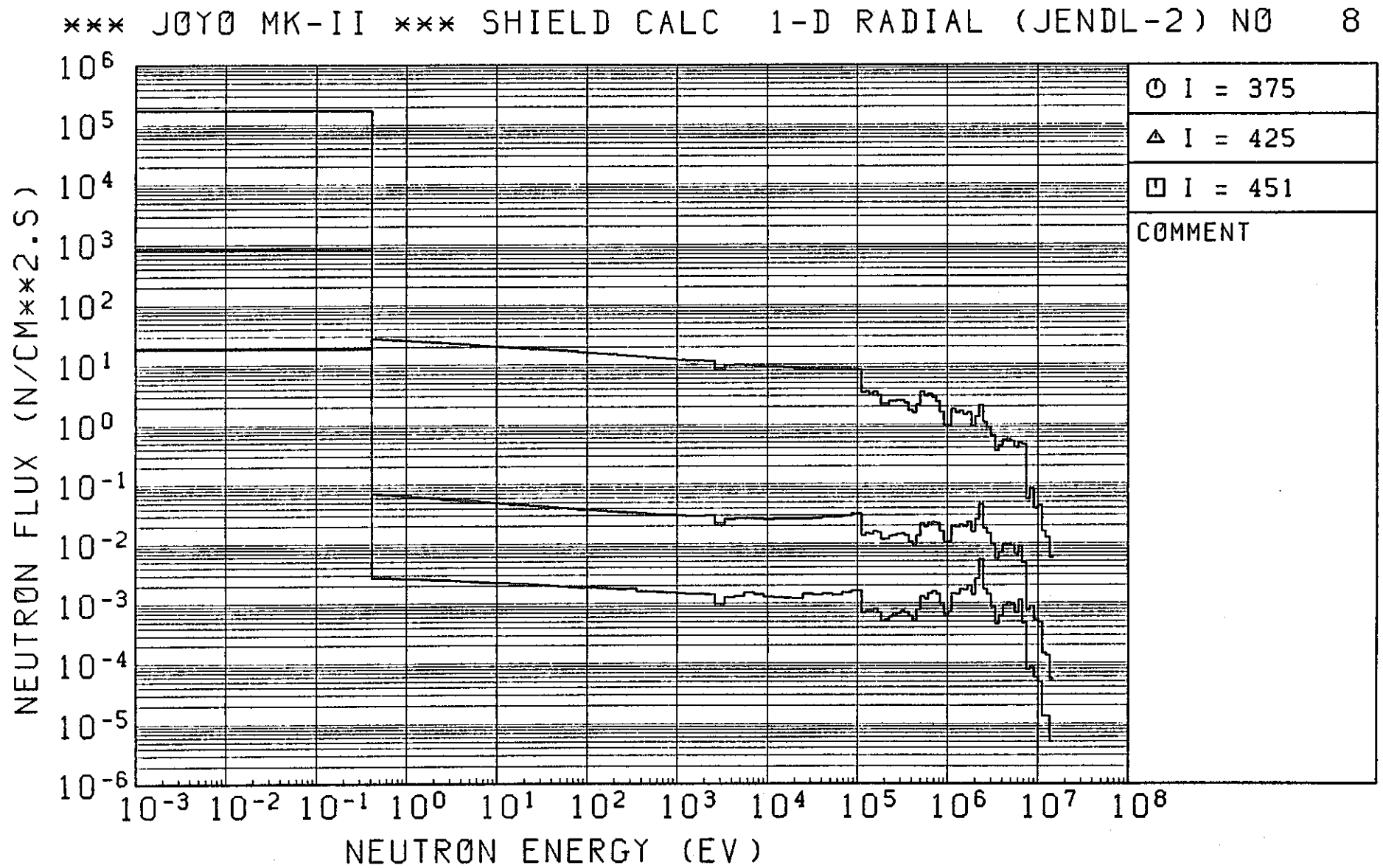


Fig. 2.3.2 (7) (Continued) (7/7)

*** JOYO MK-II *** SHIELD CALC 1-D AXIAL (JENDL-2) NO 6

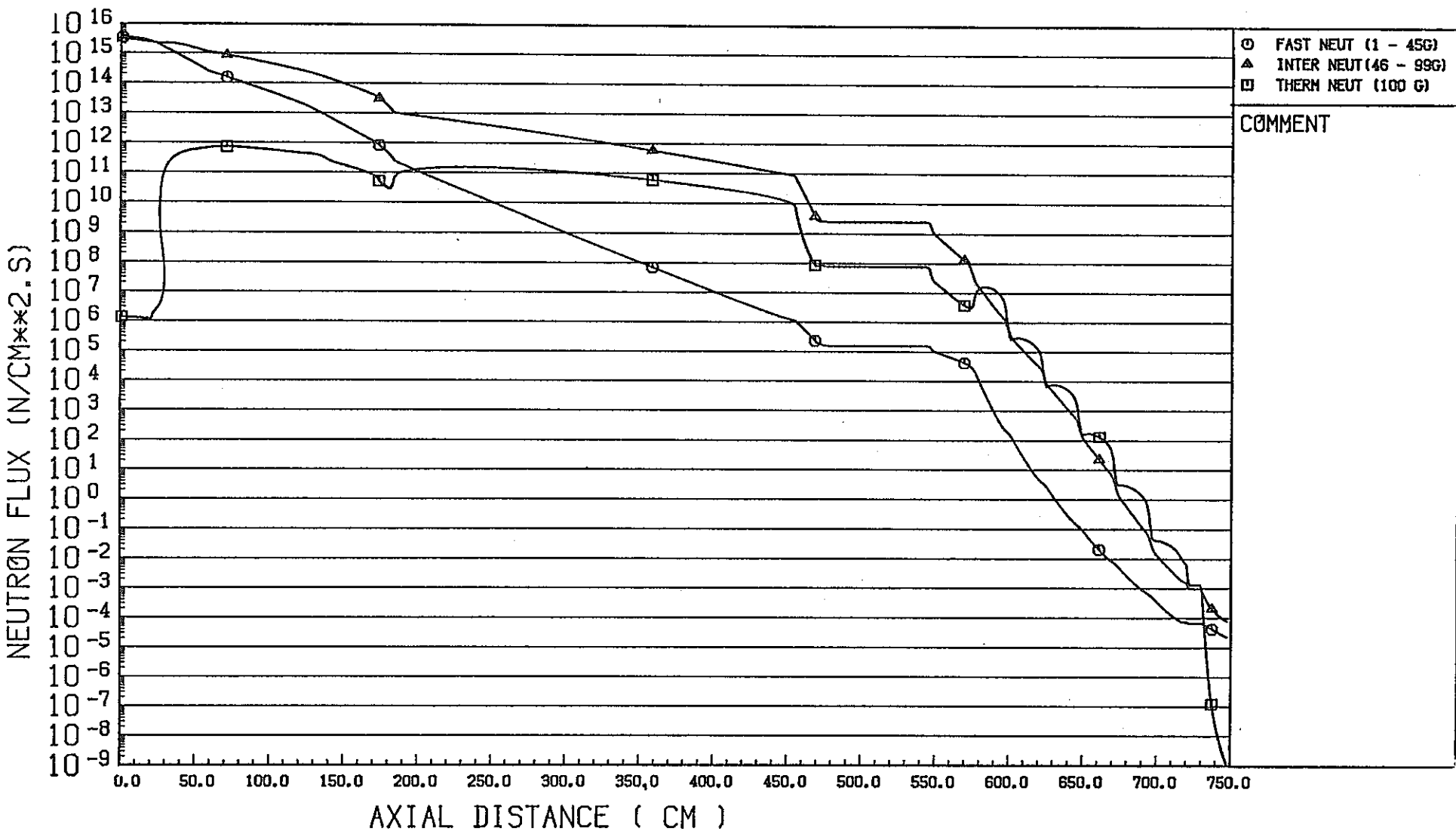


Fig. 2.3.3 Axial Neutron Flux Distribution from 1-D Calculation (JENDL-2)

*** JOYO MK-II *** SHIELD CALC 1-D AXIAL (JENDL-2) NO 1

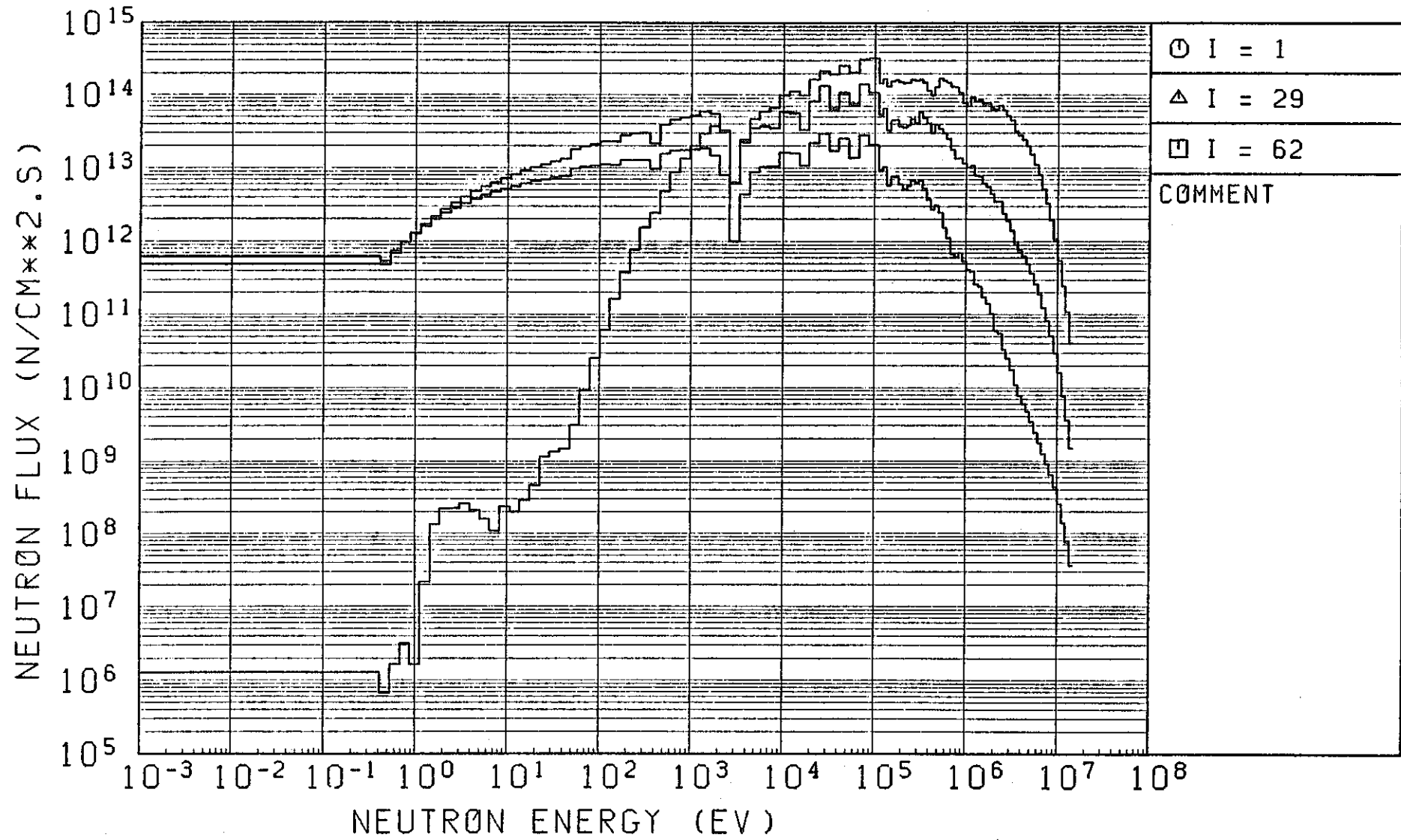


Fig. 2.3.4 (1) Neutron Spectrum from 1-D Axial Calculation (JENDL-2) (1/6)

*** JOYO MK-II *** SHIELD CALC 1-D AXIAL (JENDL-2) NO 2

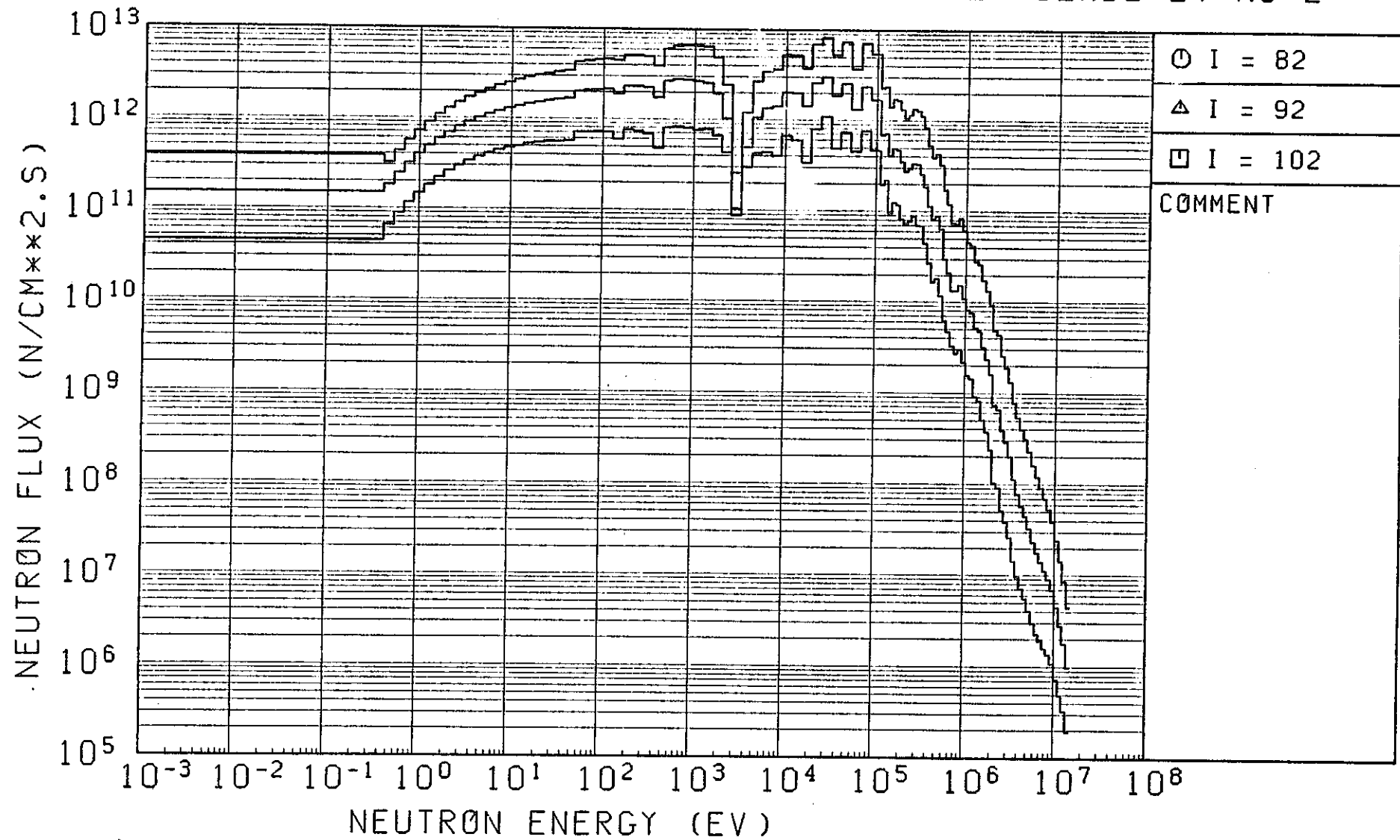


Fig. 2.3.4 (2) (Continued) (2/6)

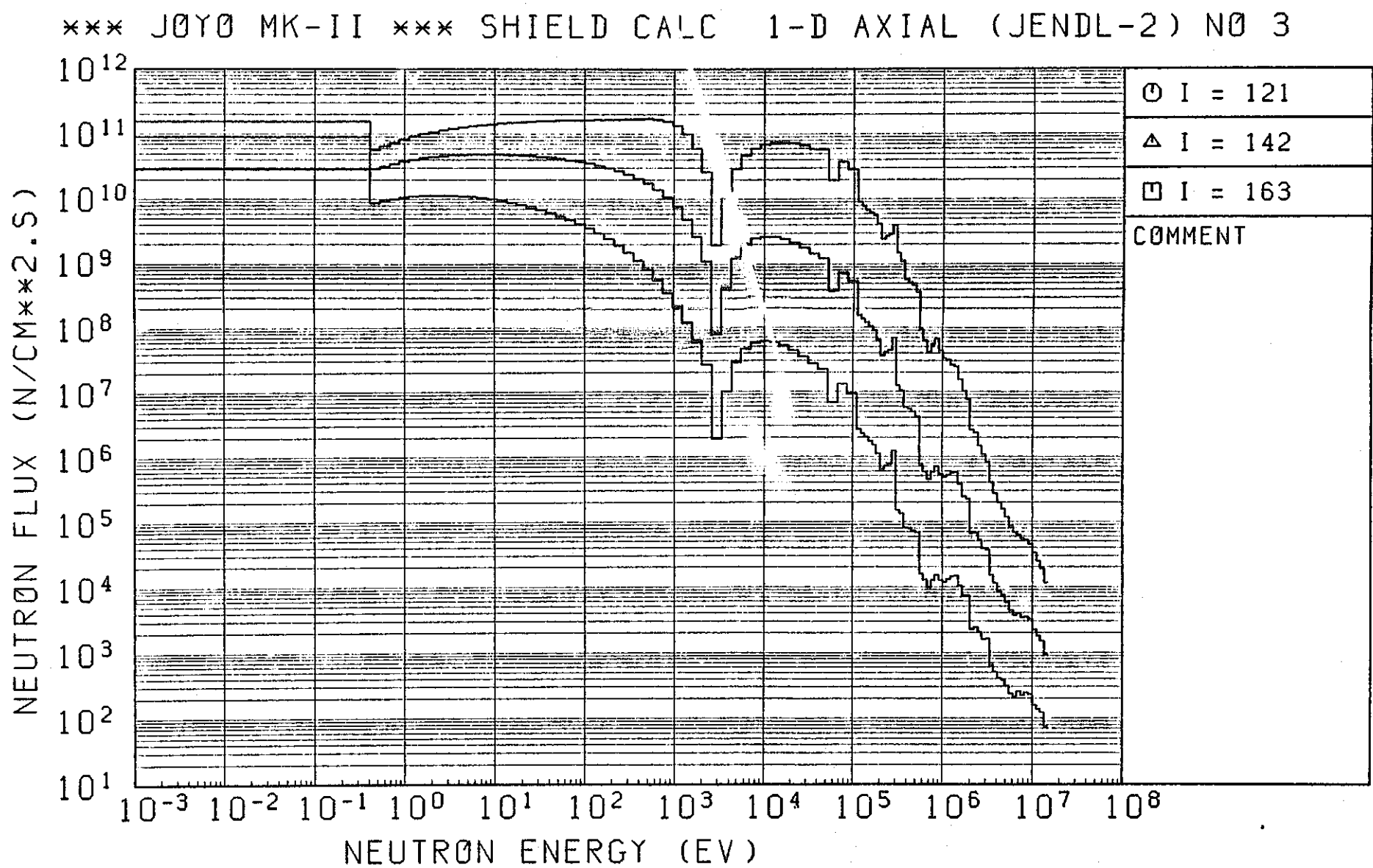


Fig. 2.3.4 (3) (Continued) (3/6)

*** JOY MK-II *** SHIELD CALC 1-D AXIAL (JENDL-2) NO 7

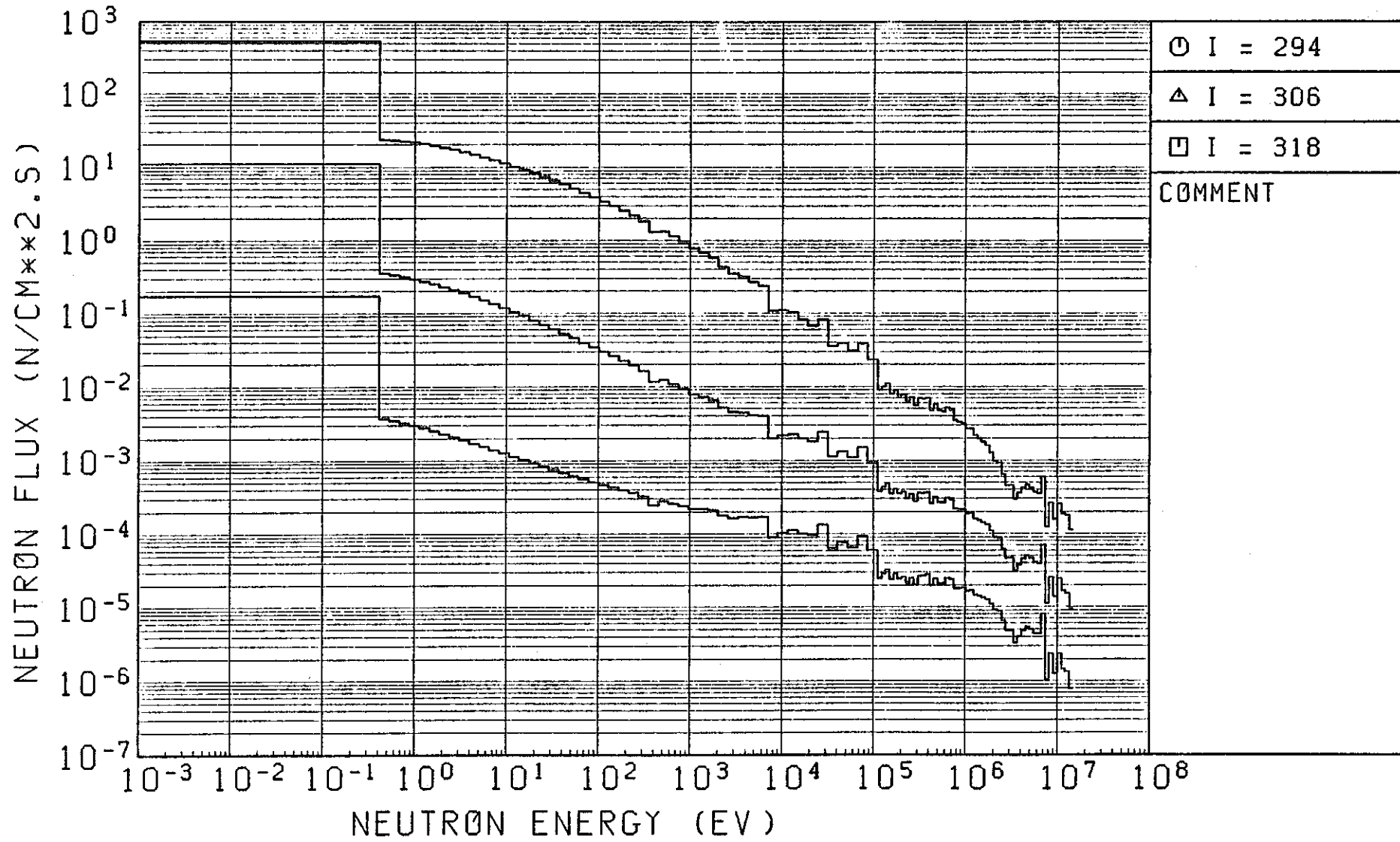


Fig. 2.3.4 (4) (Continued) (4/6)

*** JOYO MK-II *** SHIELD CALC 1-D AXIAL (JENDL-2) NO 8

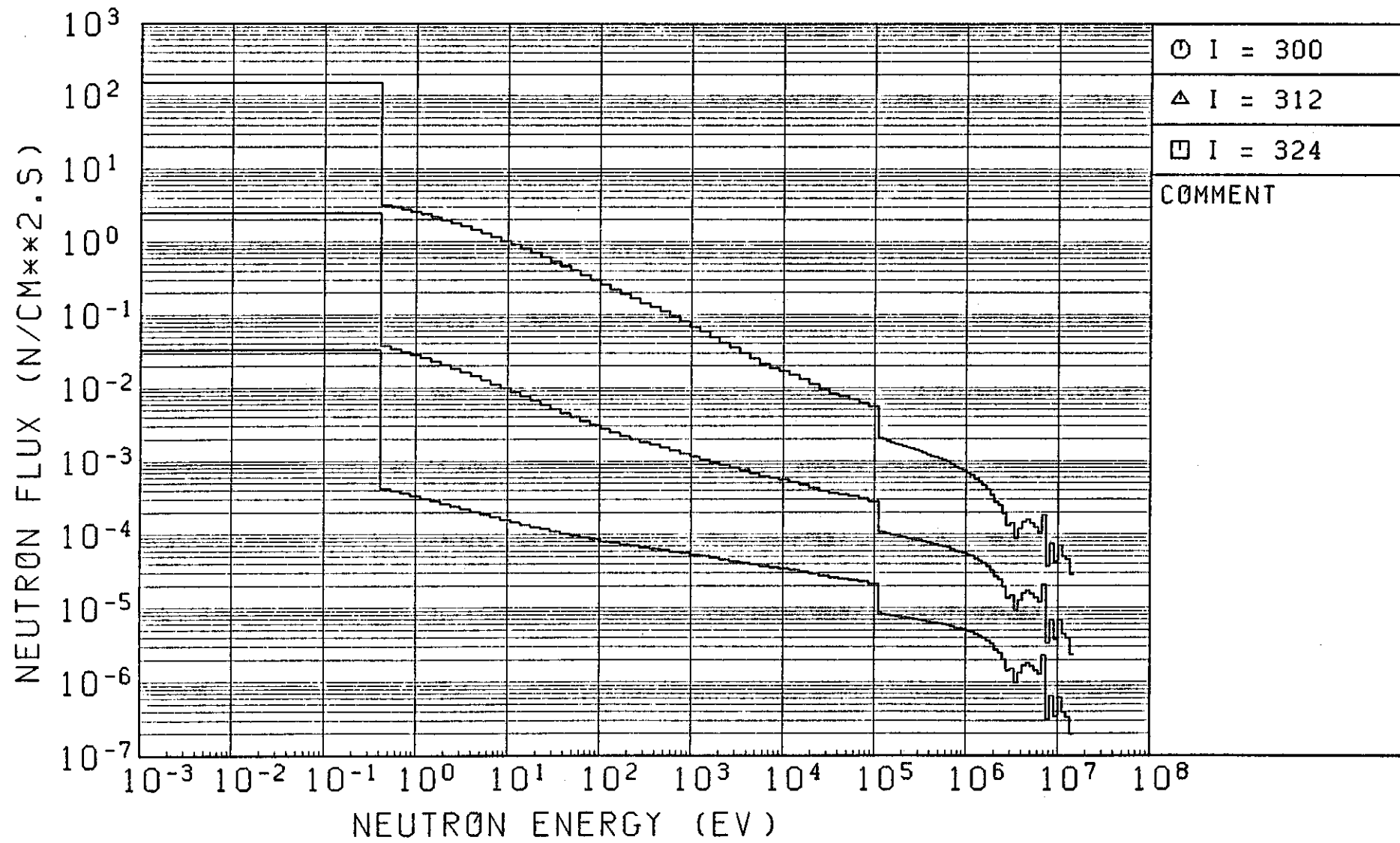


Fig. 2.3.4 (5) (Continued) (5/6)

*** JOYO MK-II *** SHIELD CALC 1-D AXIAL (JENDL-2) NO 9

2 - 34

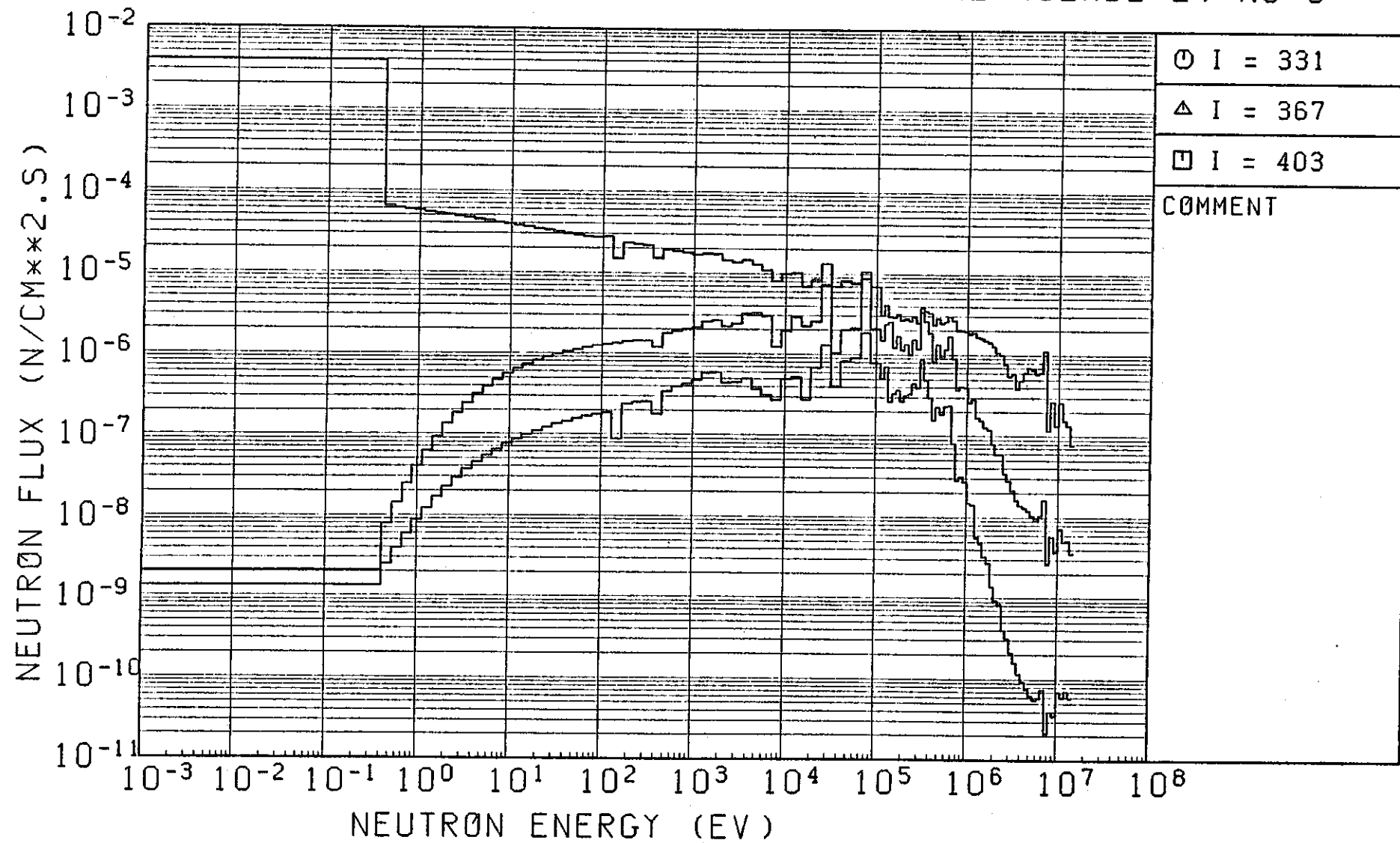


Fig. 2.3.4 (6) (Continued) (6/6)

2.3.3 Comparison of the 120 group cross-section data

The 120 group cross-section data generated from the JSD-100 file which is based on the ENDF/B-IV have been used for the previous JOYO shielding analysis. This is the first time for the JOYO shielding analysis to use the cross-sections based on the JENDL-2. In order to investigate how much the fluxes obtained by the new cross-section data agrees or disagrees with the fluxes by the previous cross-section data, the one-dimensional ANISN calculation using the cross-sections from JSD-100 was performed and the results were compared with the results of the preceeding section.

The region geometry and parameters are the same as those in the preceeding section. The radial neutron flux distribution is shown in Fig. 2.3.5 and the neutron energy spectra are shown in Figs. 2.3.6 (1) to 2.3.6 (4). The axial neutron flux distribution is shown in Fig. 2.3.7 and the neutron energy spectra are shown in Figs. 2.3.8 (1) to 2.3.8 (4).

In Table 2.3.6, the fast, intermediate, thermal and total neutron fluxes in each region of the radial calculation geometry are shown for the JENDL-2 base and JSD-100 base calculations. The ratio of the JENDL-2 base flux to the JSD-100 base flux for the fast energy region decreases with the distance. The magnitude of the decrease is large in the graphite regions. The ratios of the JENDL-2 base to the JSD-100 base fluxes for the intermediate and thermal neutron energy regions have the same tendency as for the fast flux.

In Table 2.3.7, the fast, intermediate, thermal and total neutron fluxes in each region of the axial calculation geometry are shown for the JENDL-2 base and JSD-100 base calculations. The ratio of the JENDL-2 base to the JSD-100 base fluxes have the same decrease as for the radial calculation. The magnitudes of the decrease are large in the graphite and the concrete regions.

It may be concluded that the JENDL-2 base cross-section data generally gives a little stronger attenuation than the JSD-100 base cross-section data, and that the JENDL-2 base cross-section data for the graphite and the concrete are different in the scattering matrixes from the JSD-100 base data.

Table 2.3.6 Comparison of the Calculated Value by JSD-100 with
the one by JENDL-2 (R-Direction) (1/4)

Mesh No.	Zone	Fast Neutron Flux	Intermediate Neutron Flux	Thermal Neutron Flux	Total Neutron Flux	Total Gamma-Ray Flux
1	Core 1	* ¹ 3.90+15	1.74+15	3.51+5	5.64+15	8.68+14
		* ² 3.82+15	1.71+15	1.09+6	5.53+15	8.78+14
		* ³ 0.98	0.98	3.09	0.98	1.10
9	Core 2	3.70+15	1.74+15	3.20+05	5.44+15	8.03+14
		3.63+15	1.71+15	9.95+05	5.34+15	8.10+14
		0.98	0.98	3.11	0.98	1.01
15	Core 3	3.57+15	1.60+15	3.26+05	5.17+15	7.99+14
		3.51+15	1.56+15	1.00+06	5.07+15	8.08+14
		0.98	0.98	3.07	0.98	1.01
22	Control Rod (out)	3.09+15	1.49+15	9.45+05	4.58+15	7.44+14
		3.03+15	1.45+15	1.58+06	4.49+15	7.49+14
		0.98	0.97	1.67	0.98	1.01
30	Core 4	2.53+15	1.24+15	6.08+05	3.77+15	6.01+14
		2.49+15	1.19+15	1.17+06	3.68+15	6.05+14
		0.98	0.96	1.92	0.98	1.01
46	Inner Reflector	1.25+15	1.25+15	1.85+11	2.50+15	1.83+14
		1.22+15	1.18+15	2.12+11	2.41+15	1.83+14
		0.98	0.95	1.15	0.96	1.00
78	Outer Reflector (A)	4.10+14	7.82+14	3.55+11	1.19+15	6.16+13
		3.84+14	7.33+14	3.98+11	1.12+15	6.02+13
		0.94	0.94	1.12	0.94	0.98
106	Outer Reflector (B)	1.40+14	3.95+14	2.98+11	5.35+14	3.21+13
		1.27+14	3.65+14	3.16+11	4.92+14	3.07+13
		0.91	0.92	1.06	0.92	0.96
114	Sodium	9.41+13	3.17+14	3.58+11	4.11+14	3.02+13
		8.36+13	2.92+14	3.63+11	3.76+14	2.84+13
		0.89	0.92	1.01	0.91	0.94
120	Inner Radial Shield	6.93+13	2.65+14	2.53+11	3.35+14	2.41+13
		6.08+13	2.43+14	2.54+11	3.04+14	2.27+13
		0.88	0.92	1.00	0.91	0.94

*¹ Calculated value by JSD-100

*² Calculated Value by JENDL-2

*³ (Value by JENDL-2) / (Value by JSD-100)

Table 2.3.6 (Continued) (2/4)

Mesh No.	Zone	Fast Neutron Flux	Intermediate Neutron Flux	Thermal Neutron Flux	Total Neutron Flux	Total Gamma-Ray Flux
133	Fuel Storage Rack	* ¹ 3.42+13	1.96+14	5.86+11	2.31+14	2.53+13
		* ² 2.88+13	1.78+14	5.59+11	2.08+14	2.34+13
		* ³ 0.84	0.91	0.95	0.90	0.92
143	Core Barrel	2.11+13	1.49+14	2.65+11	1.70+14	1.80+13
		1.74+13	1.34+14	2.58+11	1.52+14	1.67+13
		0.83	0.90	0.97	0.89	0.93
148	Sodium	1.66+13	1.21+14	1.89+11	1.38+14	1.53+13
		1.36+13	1.09+14	1.84+11	1.23+14	1.41+13
		0.82	0.90	0.98	0.89	0.92
165	Outer Radial Shield	9.36+12	7.22+13	8.81+10	8.16+13	8.66+12
		7.60+12	6.40+13	8.54+10	7.17+13	7.92+12
		0.81	0.89	0.97	0.88	0.91
186	Sodium	3.11+12	3.84+13	3.41+11	4.18+13	6.86+12
		2.38+12	3.33+13	3.01+11	3.60+13	6.10+12
		0.77	0.87	0.88	0.86	0.89
196	Sodium	1.10+12	2.63+13	3.27+11	2.77+13	5.49+12
		7.90+11	2.25+13	2.87+11	2.36+13	4.86+12
		0.72	0.86	0.88	0.85	0.88
205	Thermal Shield	5.28+11	1.64+13	1.08+11	1.71+13	2.88+12
		3.71+11	1.40+13	9.57+10	1.44+13	2.53+12
		0.70	0.85	0.89	0.84	0.88
212	Reactor Vessel	3.27+11	9.91+12	1.35+11	1.04+13	2.12+12
		2.30+11	8.26+12	1.13+11	8.61+12	1.84+12
		0.70	0.83	0.83	0.83	0.87
216	Cavity	2.47+11	7.53+12	3.41+11	8.12+12	1.92+12
		1.74+11	6.21+12	2.82+11	6.66+12	1.65+12
		0.70	0.82	0.83	0.82	0.86
219	Leak Jacket	2.16+11	6.73+12	5.39+11	7.49+12	1.84+12
		1.52+11	5.51+12	4.47+11	6.11+12	1.57+12
		0.70	0.82	0.83	0.82	0.85

*¹ Calculated Value by JSD-100*² Calculated Value by JENDL-2*³ (Value by JENDL-2) / (Value by JSD-100)

Table 2.3.6 (Continued) (3/4)

Mesh No.	Zone	Fast Neutron Flux	Intermediate Neutron Flux	Thermal Neutron Flux	Total Neutron Flux	Total Gamma-Ray Flux
(223)	Thermal Insulator	* ¹ 1.73+11	5.75+12	1.07+12	6.99+12	1.62+12
		* ² 1.22+11	4.67+12	8.90+11	5.68+12	1.38+12
		* ³ 0.70	0.81	0.83	0.81	0.85
(228)	Cavity	1.57+11	5.50+12	1.34+12	7.00+12	1.60+12
		1.11+11	4.45+12	1.12+12	5.68+12	1.36+12
		0.70	0.81	0.83	0.81	0.85
(239)	Graphite	2.95+09	1.02+12	4.04+12	5.06+12	9.92+11
		1.67+09	7.98+11	3.30+12	4.10+12	8.45+11
		0.57	0.78	0.82	0.81	0.85
(254)	Graphite	6.06+06	9.57+09	1.89+12	1.90+12	2.68+11
		2.00+06	7.13+09	1.53+12	1.53+12	2.26+11
		0.33	0.74	0.81	0.81	0.84
(269)	Graphite	1.82+05	3.09+07	5.10+11	5.10+11	8.81+10
		3.47+04	2.22+07	4.11+11	4.11+11	7.34+10
		0.19	0.72	0.81	0.81	0.83
(278)	Cavity	5.63+04	1.85+06	7.75+10	7.75+10	5.62+10
		8.98+03	1.20+06	6.35+10	6.35+10	4.62+10
		0.16	0.65	0.82	0.82	0.82
(281)	Carbon Steel	5.29+04	1.34+06	3.47+10	3.47+10	4.57+10
		8.38+03	8.32+05	2.80+10	2.80+10	3.74+10
		0.16	0.62	0.81	0.81	0.82
(294)	Cavity	4.80+04	9.13+05	1.45+10	1.45+10	3.21+10
		7.55+03	5.33+05	1.14+10	1.14+10	2.61+10
		0.16	0.58	0.79	0.79	0.81
(323)	Carbon Steel	3.50+04	2.25+05	3.21+08	3.21+08	7.65+09
		5.28+03	9.63+04	2.31+08	2.31+08	6.18+09
		0.15	0.43	0.72	0.72	0.81
(345)	Liner	2.17+04	6.29+04	4.84+06	4.92+06	1.74+09
		3.11+03	1.67+04	3.08+06	3.10+06	1.41+09
		0.14	0.27	0.64	0.63	0.81

*¹ Calculated Value by JSD-100*² Calculated Value by JENDL-2*³ (Value by JENDL-2) / (Value by JSD-100)

Table 2.3.6 (Continued) (4/4)

*1 Calculated Value by JSD-100

*2 Calculated Value by JENDL-2

*3 (Value by JENDL-2) / (Value by JSD-100)

Table 2.3.7 Comparison of the Calculated Value by JSD-100
with the one by JENDL-2 (Z-Direction) (1/4)

Mesh No.	Zone	Fast Neutron Flux	Intermediate Neutron Flux	Thermal Neutron Flux	Total Neutron Flux	Total Gamma-Ray Flux
1	Driver Fuel	* ¹ 4.53+15	2.06+15	4.23+05	6.58+15	1.03+15
		* ² 4.12 +15	2.00+15	1.30+06	6.42+15	1.03+15
		* ³ 0.98	0.97	3.06	0.98	1.01
14	Insulator	3.57+15	1.78+15	3.82+05	5.35+15	8.48+14
		2.25+15	1.68+15	5.97+10	3.93+15	8.84+14
		0.97	0.96	1.08	0.96	1.04
29	Upper Reflector	1.04+15	1.62+15	4.53+11	2.66+15	1.82+14
		9.79+14	1.54+15	4.91+11	2.52+15	1.78+14
		0.94	0.95	1.08	0.94	0.98
62	Gas Plenum	1.44+14	5.47+14	6.13+11	6.91+14	6.93+13
		1.23+14	5.01+14	6.22+11	6.24+14	6.53+13
		0.85	0.92	1.02	0.90	0.94
82	Handling Head	3.21+13	2.06+14	3.99+11	2.38+14	3.03+13
		2.54+13	1.82+14	3.86+11	2.08+14	2.77+13
		0.79	0.88	0.97	0.87	0.91
92	Upper Core Structure 1	9.40+12	9.03+13	1.59+11	9.99+13	1.44+13
		6.97+12	7.73+13	1.50+11	8.44+13	1.28+13
		0.74	0.86	0.94	0.84	0.89
102	Upper Core Structure 2	2.59+12	3.12+13	4.76+10	3.38+13	5.52+12
		1.82+12	2.55+13	4.41+10	2.74+13	4.77+12
		0.70	0.82	0.93	0.81	0.87
107	Upper Core Structure 3	1.38+12	1.71+13	3.41+10	1.86+13	3.11+12
		9.56+11	1.36+13	2.97+10	1.46+13	2.62+12
		0.69	0.80	0.87	0.79	0.84
121	Sodium	1.46+11	6.86+12	1.97+11	7.21+12	2.19+12
		8.45+10	5.24+12	1.54+11	5.47+12	1.76+12
		0.58	0.76	0.78	0.76	0.80
142	Sodium	2.98+09	1.59+12	1.18+11	1.71+12	7.16+11
		1.46+09	1.19+12	9.06+10	1.29+12	7.16+11
		0.49	0.75	0.77	0.75	0.78

*1 Calculated Value by JSD-100

*2 Calculated Value by JENDL-2

*3 (Value by JENDL-2) / (Value by JSD-100)

Table 2.3.7 (Continued) (2/4)

Mesh No.	Zone	Fast Neutron Flux	Intermediate Neutron Flux	Thermal Neutron Flux	Total Neutron Flux	Total Gamma-Ray Flux
163	Sodium	* ¹ 5.31+07	2.86+11	3.74+10	3.32+11	2.71+11
		* ² 2.50+07	2.15+11	2.86+10	2.43+11	2.10+11
		* ³ 0.47	0.75	0.77	0.75	0.77
188	Dip Plate	3.52+06	2.33+10	5.14+08	2.38+10	1.84+10
		1.73+06	1.65+10	4.01+08	1.69+10	1.40+10
		0.49	0.71	0.78	0.71	0.76
205	Sodium	1.21+06	3.91+09	1.11+08	4.02+09	4.31+09
		5.80+05	2.56+09	7.96+07	2.64+09	3.19+09
		0.48	0.66	0.72	0.66	0.74
215	Argon Gas	1.15+06	3.77+09	1.05+08	3.88+09	4.10+09
		5.49+05	2.48+09	7.56+07	2.55+09	3.04+09
		0.48	0.66	0.72	0.66	0.74
227	Stainless Steel	9.95+05	2.78+09	6.09+07	2.84+09	2.93+09
		4.74+05	1.80+09	4.41+07	1.84+09	2.16+09
		0.48	0.65	0.72	0.65	0.74
242	Thermal Shield	4.72+05	5.31+08	1.16+07	5.43+08	7.18+08
		2.16+05	3.11+08	8.03+06	3.19+08	5.16+08
		0.46	0.59	0.69	0.59	0.72
257	Carbon Steel	2.15+05	9.40+07	6.10+06	1.00+08	1.73+08
		9.06+04	4.77+07	3.40+06	5.12+07	1.20+08
		0.42	0.51	0.56	0.51	0.70
263	Graphite	2.68+04	1.42+07	3.18+07	4.60+07	1.21+08
		7.87+03	6.14+06	1.58+07	2.20+07	8.42+07
		0.29	0.43	0.50	0.48	0.70
270	Carbon Steel	2.56+03	1.67+06	1.49+06	3.16+06	2.65+07
		4.97+02	6.12+05	7.05+05	1.32+06	1.79+07
		0.19	0.37	0.47	0.42	0.68
276	Graphite	3.94+02	2.94+05	6.94+05	9.88+05	1.69+07
		5.42+01	9.94+04	2.70+05	3.69+05	1.16+07
		0.14	0.34	0.39	0.37	0.68

*1 Calculated Value by JSD-100

*2 Calculated Value by JENDL-2

*3 (Value by JENDL-2) / (Value by JSD-100)

Table 2.3.7. (Continued) (3/4)

Mesh No.	Zone	Fast Neutron Flux	Intermediate Neutron Flux	Thermal Neutron Flux	Total Neutron Flux	Total Gamma-Ray Flux
282	Carbon Steel	*1 6.18+01	5.02+04	5.58+04	1.06+05	4.34+06
		*2 6.21+00	1.70+04	2.08+04	3.78+04	2.96+06
		*3 0.10	0.34	0.37	0.36	0.68
288	Graphite	1.32+01	6.98+03	2.10+04	2.80+04	2.80+06
		1.04+00	2.32+03	6.99+03	9.31+03	1.93+06
		0.08	0.33	0.33	0.33	0.69
284	Carbon Steel	3.12+00	9.61+02	1.65+03	2.62+03	7.42+05
		1.87-01	3.18+02	5.41+02	8.59+02	5.10+05
		0.06	0.33	0.33	0.33	0.69
300	Carbon Steel	8.70-01	1.11+02	4.94+02	6.06+02	4.94+05
		4.13-02	3.33+01	1.54+02	1.87+02	3.41+05
		0.05	0.30	0.31	0.31	0.69
306	Carbon Steel	2.70-01	1.47+01	3.66+01	5.16+01	1.34+05
		9.99-03	3.82+00	1.12+01	1.51+01	9.22+04
		0.04	0.26	0.31	0.29	0.69
312	Graphite	8.65-02	2.07+00	9.10+00	1.13+01	9.05+04
		2.63-03	3.60-01	2.48+00	2.84+00	6.25+04
		0.03	0.17	0.27	0.25	0.69
318	Carbon Steel	3.05-02	3.99-01	6.63-01	1.09+00	2.48+04
		7.71-04	4.37-02	1.73-01	2.17-01	1.72+04
		0.03	0.11	0.26	0.20	0.69
324	Graphite	1.05-02	1.02-01	1.91-01	3.03-01	1.70+04
		2.25-04	5.83-03	3.34-02	3.95-02	1.18+04
		0.02	0.06	0.17	0.13	0.69
329	Argon Gas	4.94-03	3.89-02	4.66-02	9.04-02	8.70+03
		9.38-05	1.61-03	7.48-03	9.18-03	6.02+03
		0.02	0.04	0.16	0.10	0.69
331	Stainless Steel	4.79-03	3.35-02	2.48-02	6.31-02	5.89+03
		9.06-05	1.34-03	3.95-03	5.37-03	4.07+03
		0.02	0.04	0.16	0.09	0.69

*1 Calculated Value by JSD-100

*2 Calculated Value by JENDL-2

*3 (Value by JENDL-2) / (Value by JSD-100)

Table 2.3.7 (Continued) (4/4)

*1 Calculated Value by JSD-100

*2 Calculated Value by JENDL-2

*3 (Value by JENDL-2) / (Value by JSD-100)

*** JOYO MK-II *** SHIELD CALC 1-D RADIAL (JSD-100) NO 6

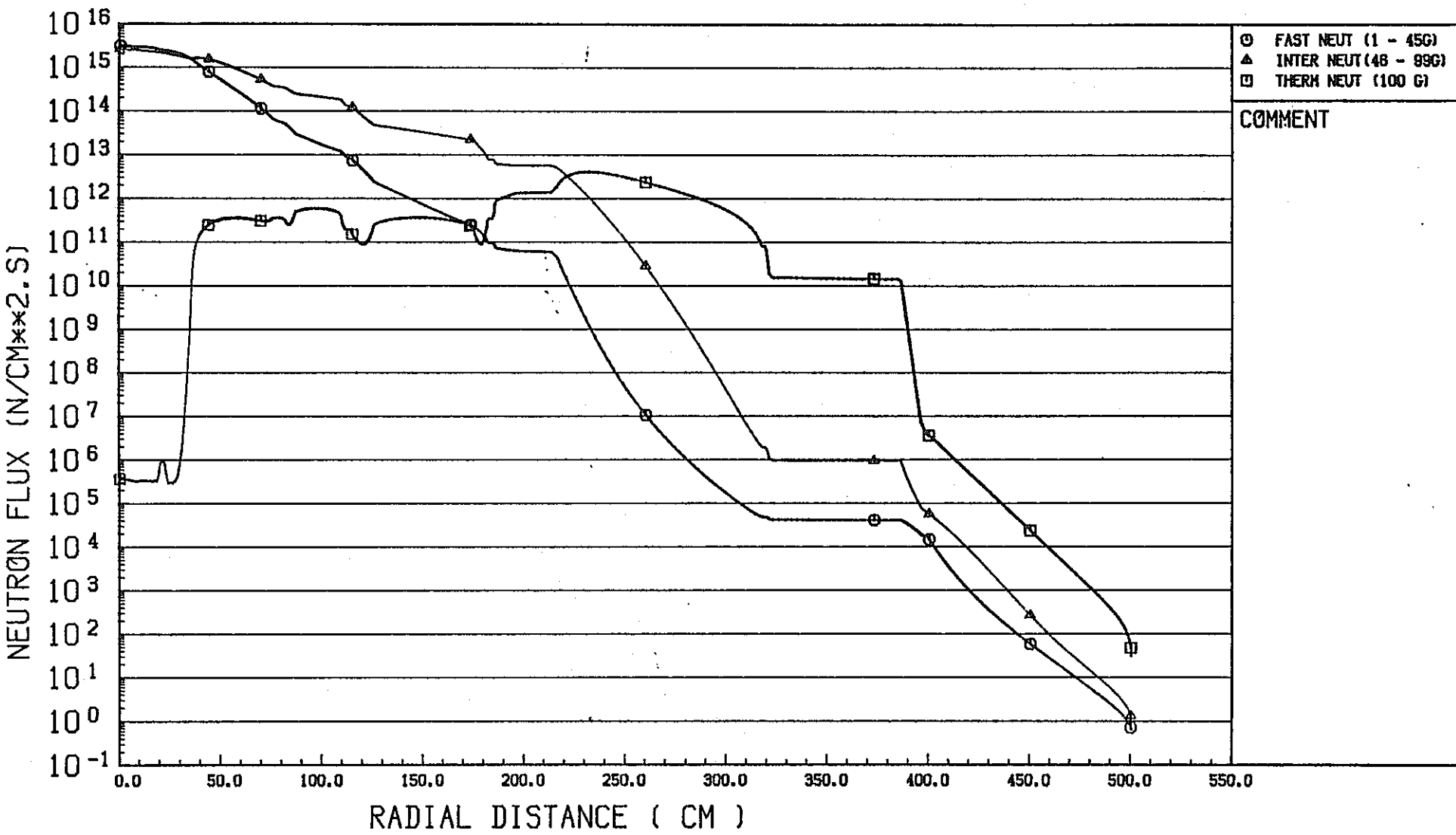


Fig. 2.3.5 Radial Neutron Flux Distribution from 1-D Calculation (JSD-100)

*** JOY MK-II *** SHIELD CALC 1-D RADIAL (JSD-100) NO 1

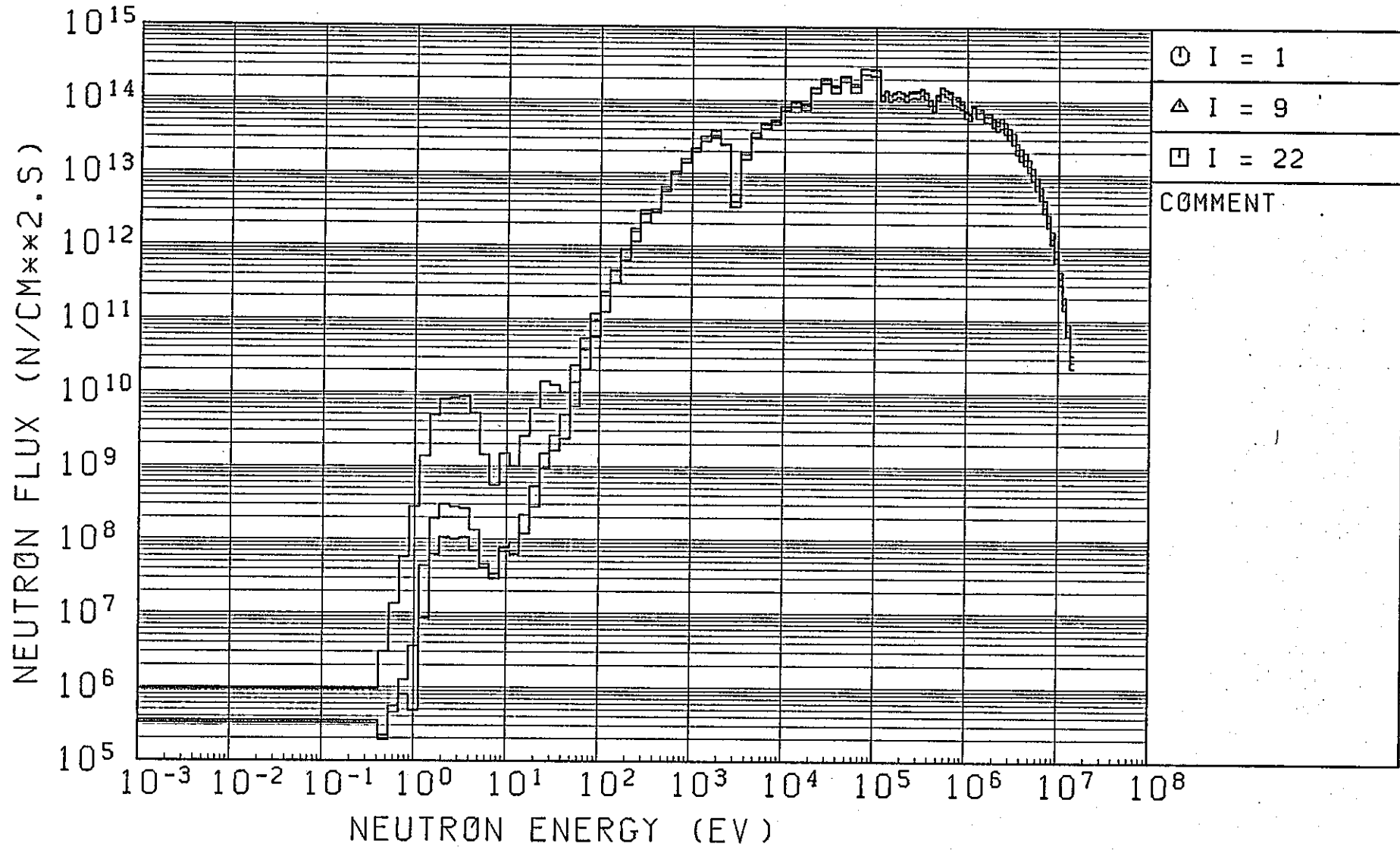


Fig. 2.3.6(1) Neutron Spectrum from 1-D Radial Calculation (JSD-100) (1/4)

*** JOYO MK-II *** SHIELD CALC 1-D RADIAL (JSD-100) NO 4

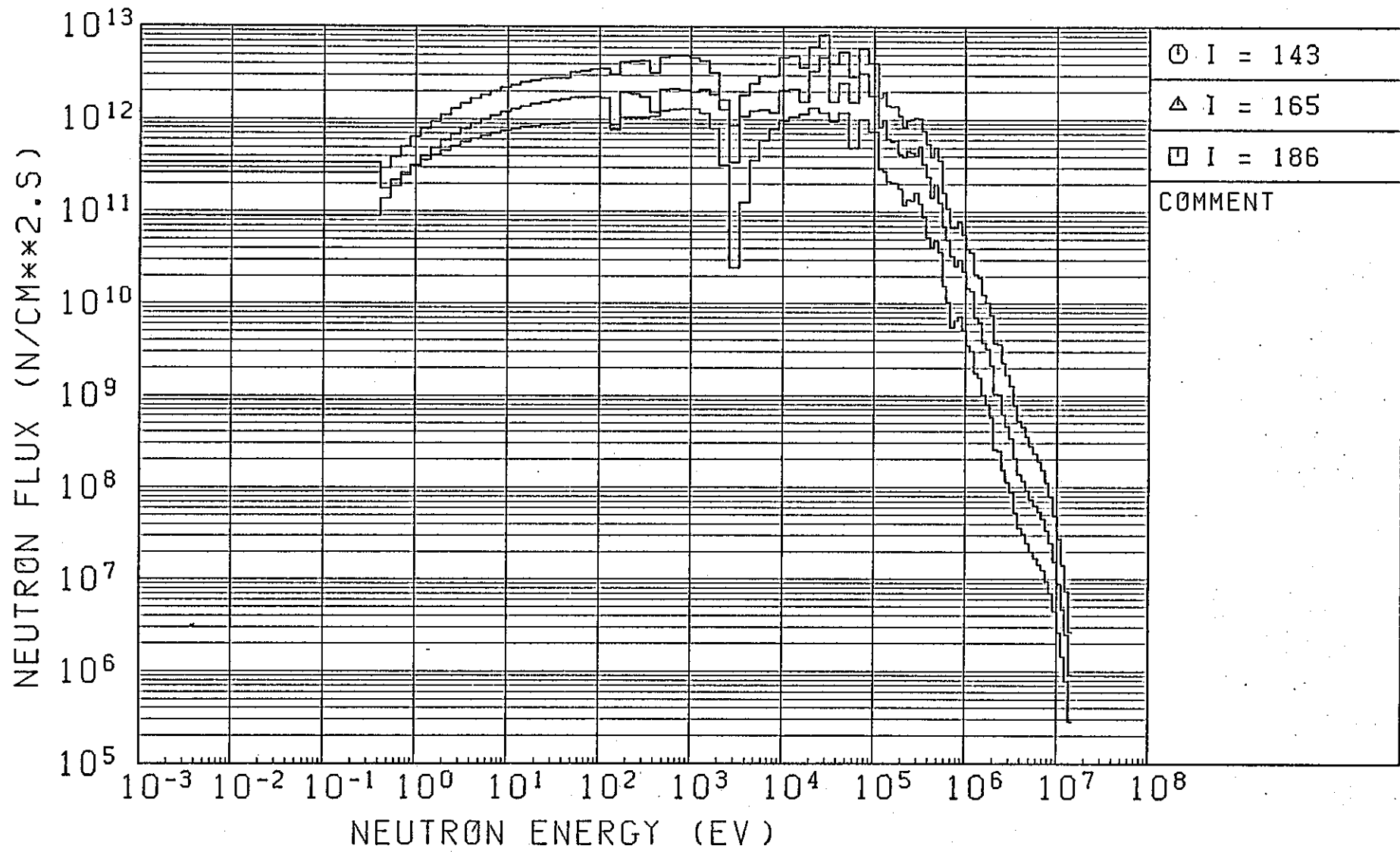


Fig. 2.3.6 (2) (Continued) (2/4)

*** JOYO MK-II *** SHIELD CALC 1-D RADIAL (JSD-100) NO 6

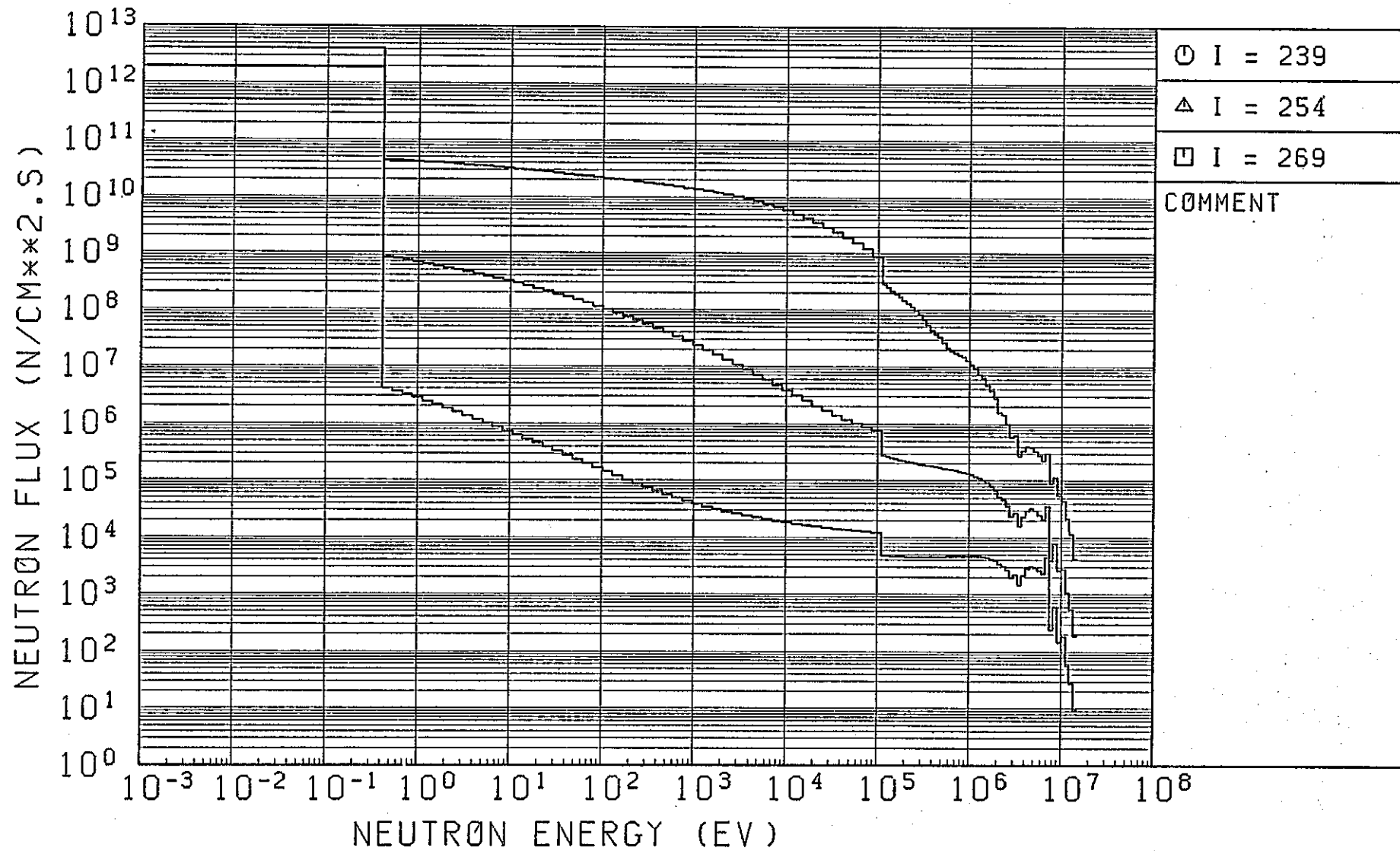


Fig. 2.3.6 (3) (Continued) (3/4)

*** JOYO MK-II *** SHIELD CALC 1-D RADIAL (JSD-100) NO 8

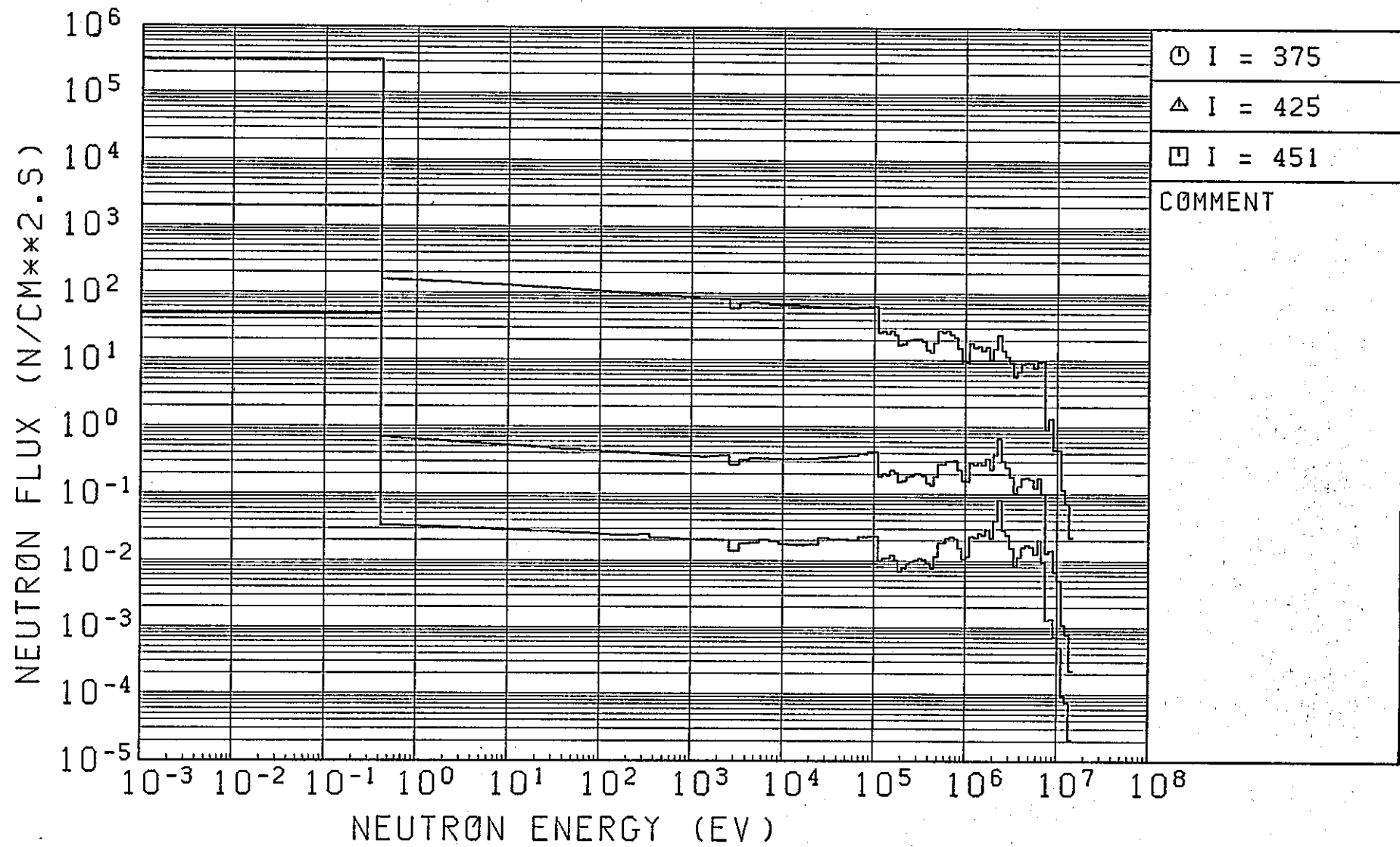


Fig. 2.3.6 (4) (Continued) (4/4)

*** JOY0 MK-II *** SHIELD CALC 1-D AXIAL (JSD-100) RST 7

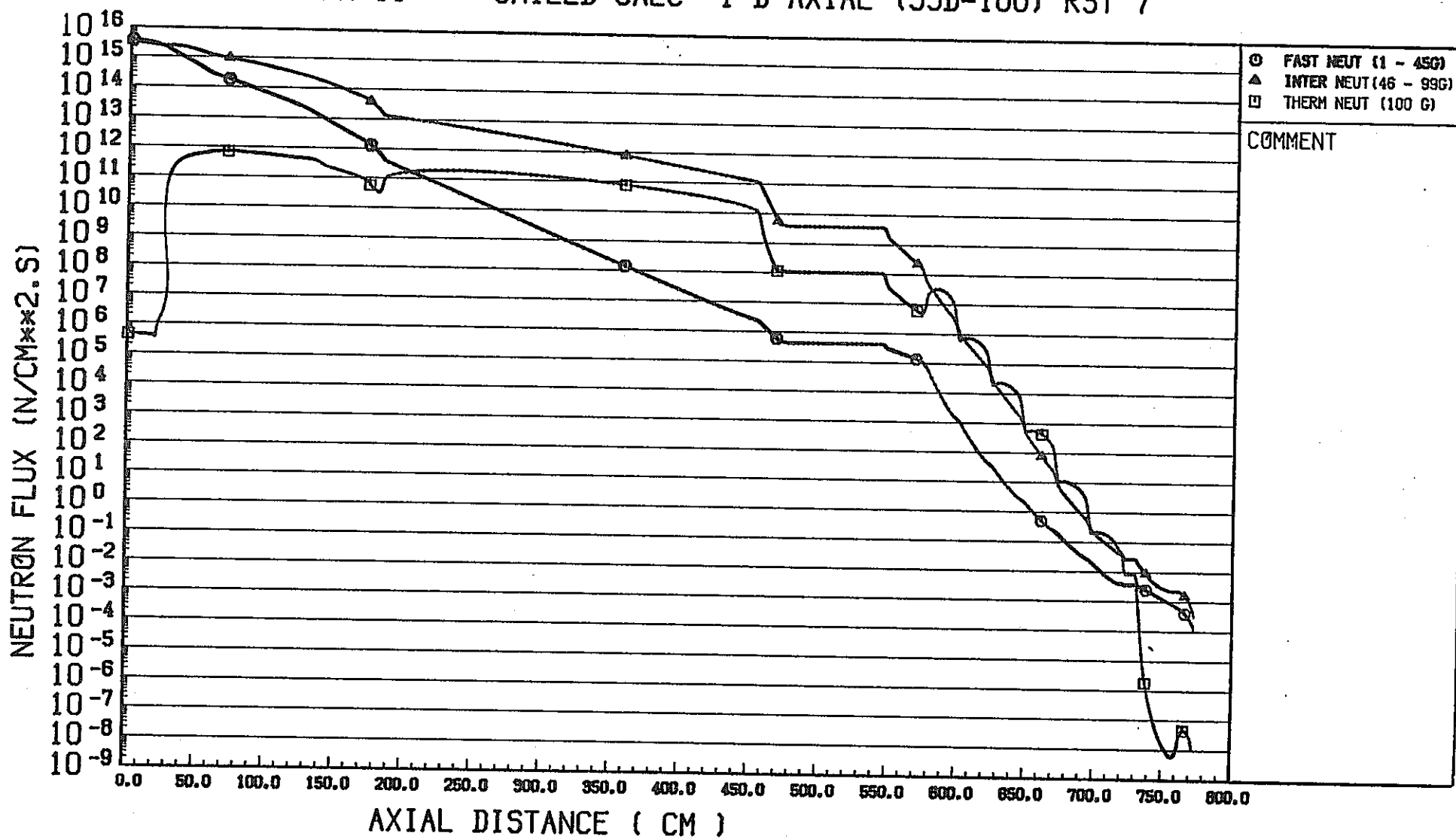


Fig. 2.3.7 Axial Neutron Flux Distribution from 1-D Calculation (JSD-100)

*** JOYO MK-II *** SHIELD CALC 1-D AXIAL (JSD-100) RST 7

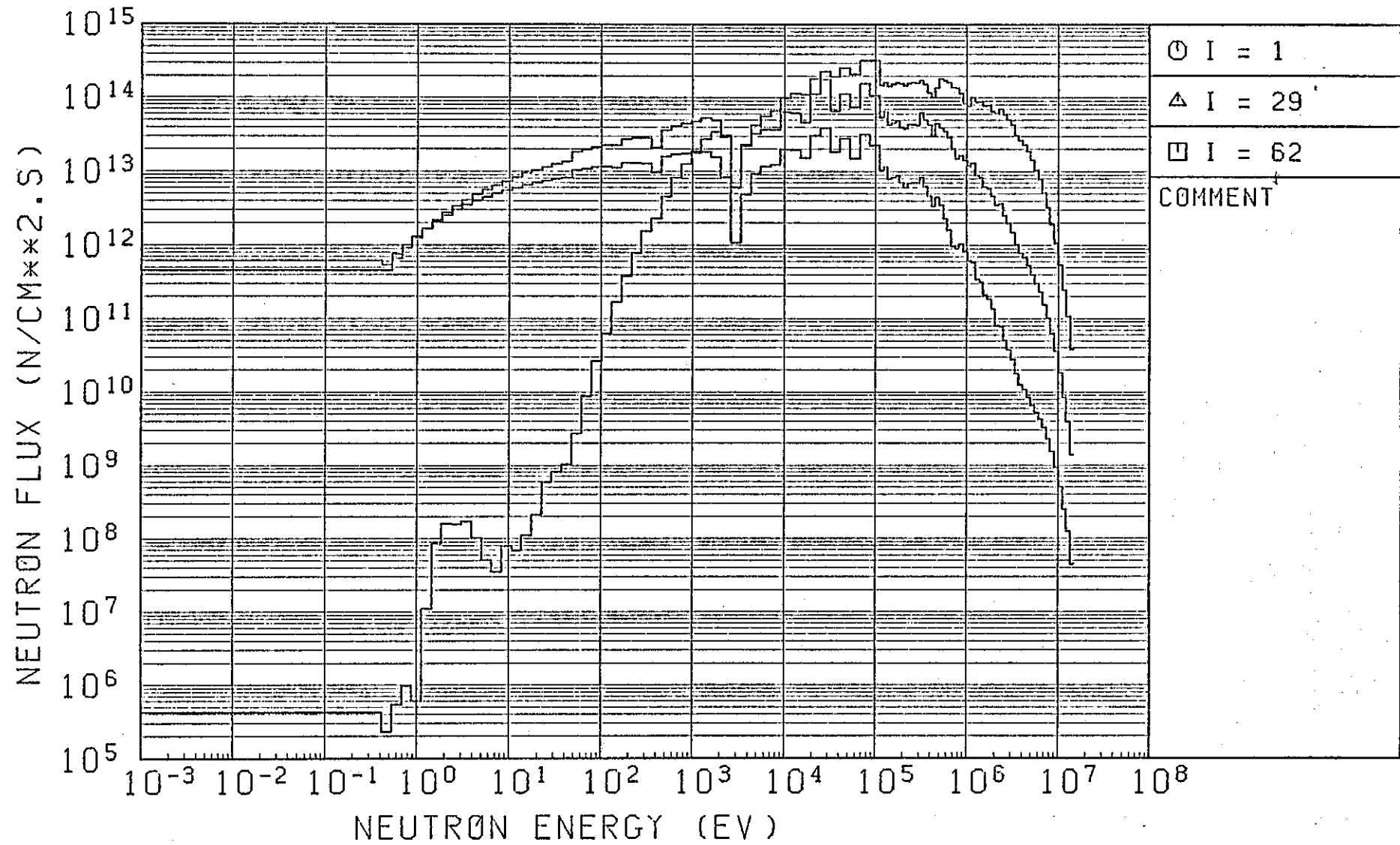


Fig. 2.3.8 (1) Neutron Spectrum from 1-D Axial Calculation (JSD-100) (1/4)

*** JOYO MK-II *** SHIELD CALC 1-D AXIAL (JSD-100) RST 7

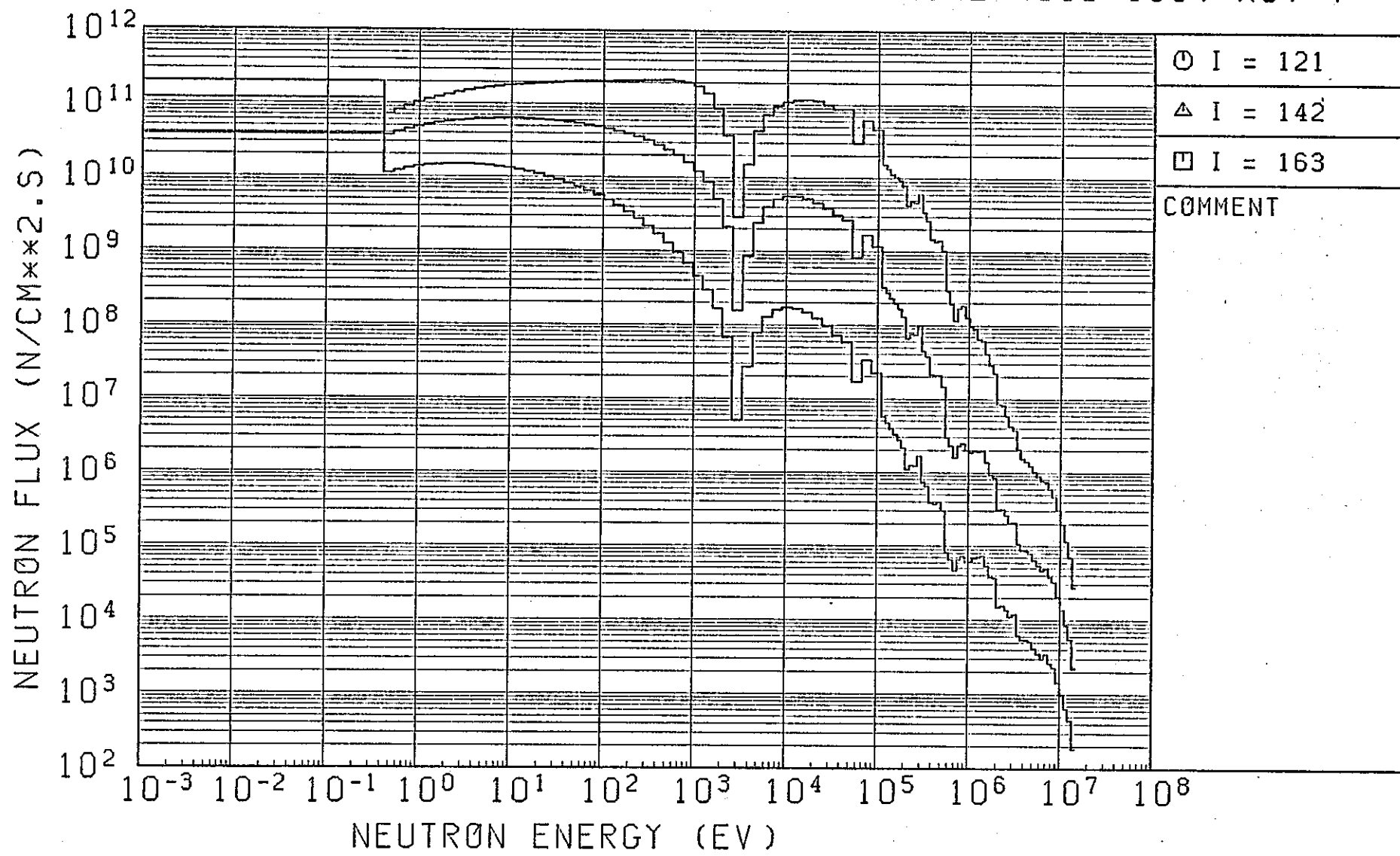


Fig. 2.3.8 (2) (Continued) (2/4)

*** JOYO MK-II *** SHIELD CALC 1-D AXIAL (JSD-100) RST 7

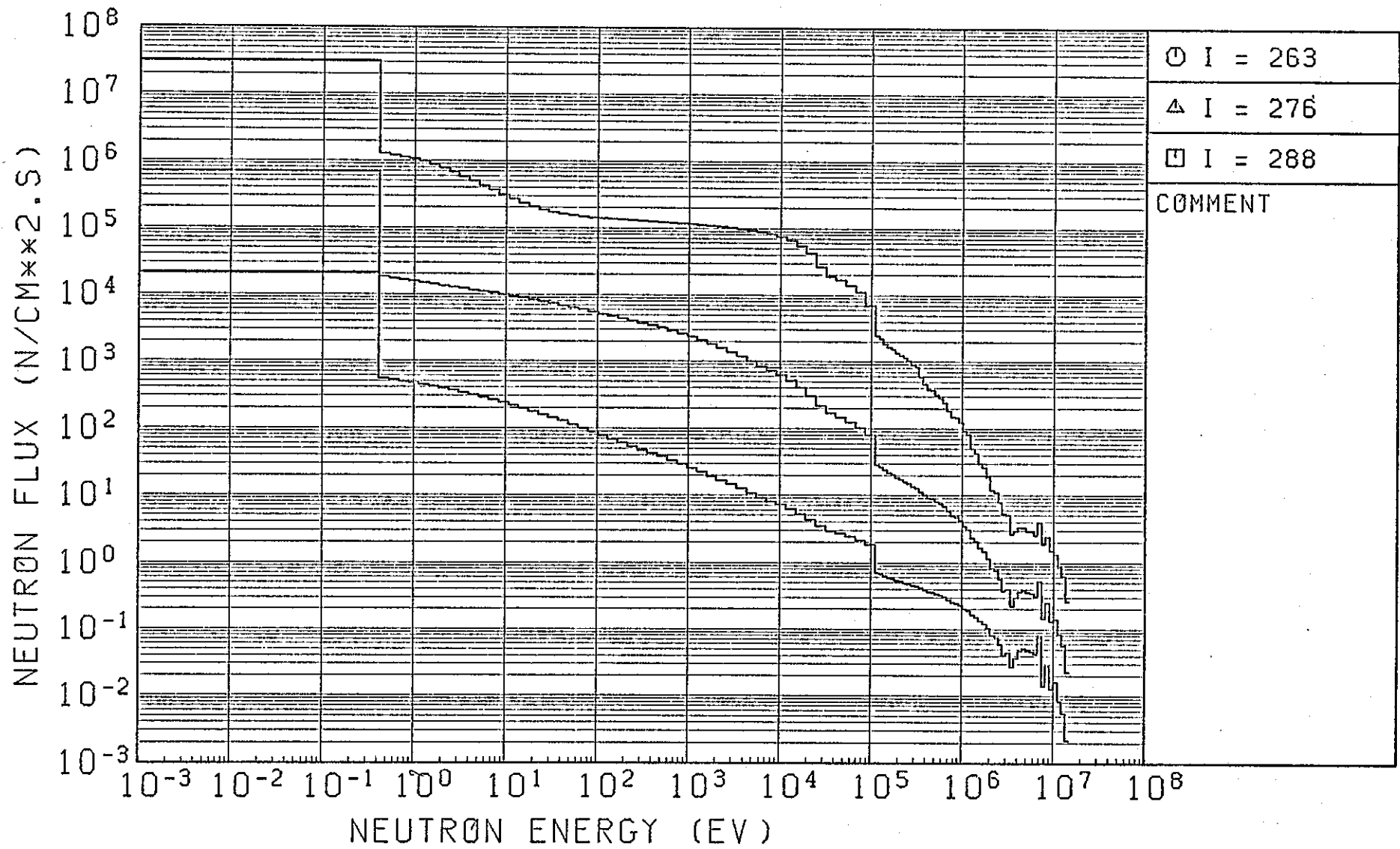
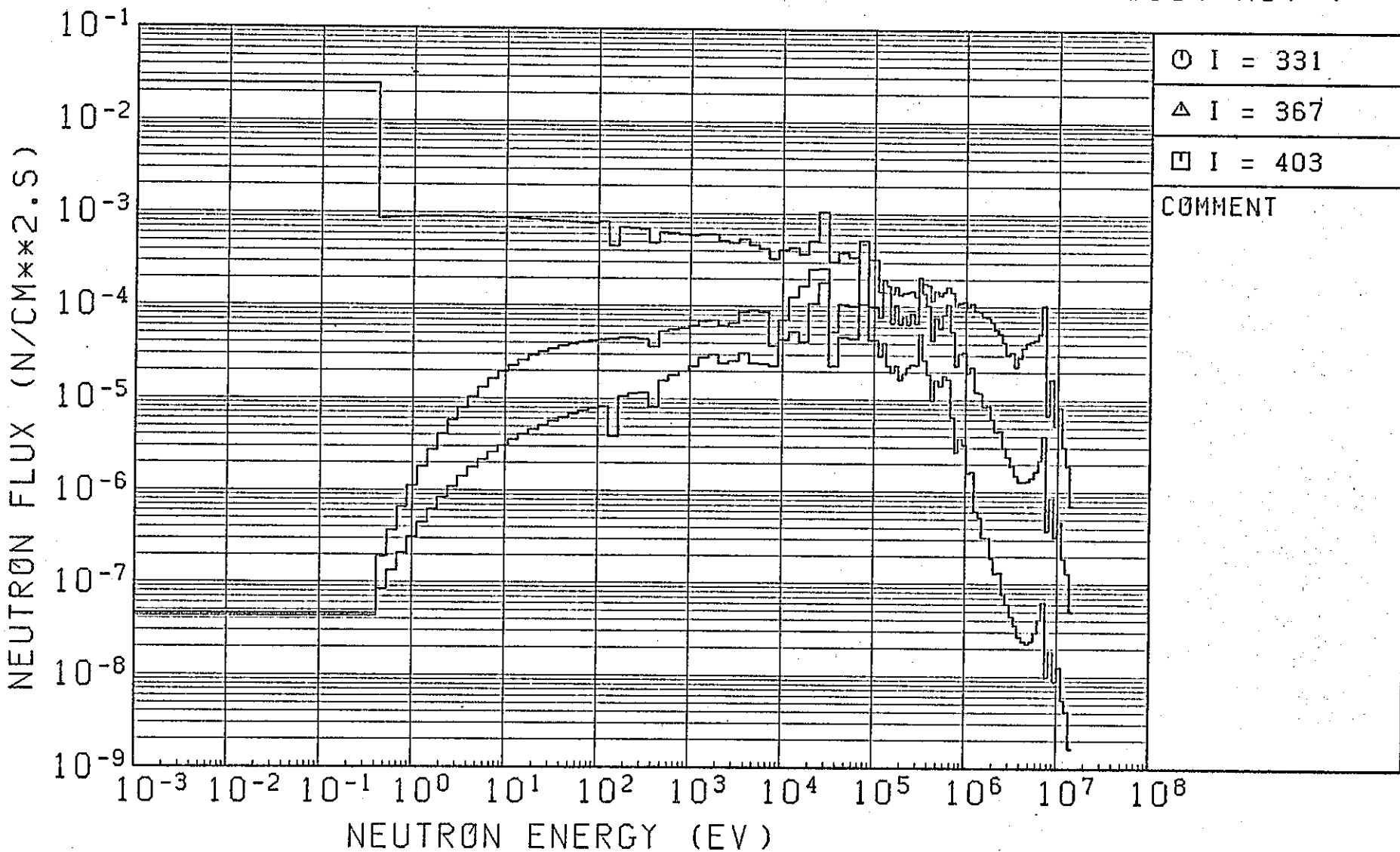


Fig. 2.3.8 (3) (Continued) (3/4)

*** JOY MK-II *** SHIELD CALC 1-D AXIAL (JSD-100) RST 7

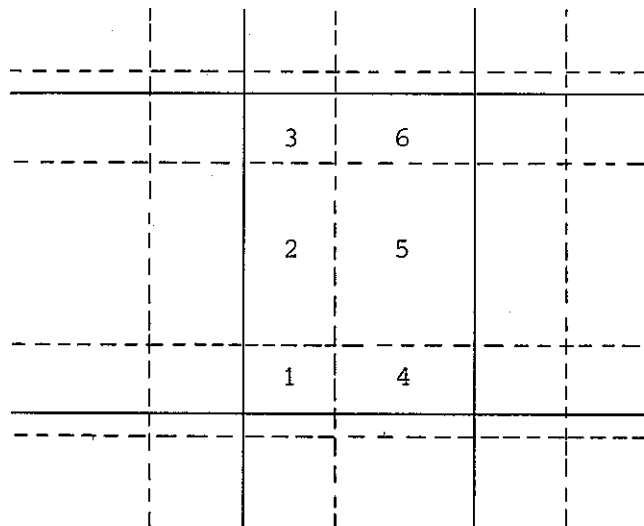


2.4 Upper axial 2-D calculation

2.4.1 Step 1 Calculation

The DOT calculation have been done for the calculational geometry described in section 2.2 with the cross-sections generated in section 2.3. The JOYO partial R-Z material compositions used in zones shown in Fig. 2.4.1 are shown in Table 2.4.1.

The neutron source distribution was calculated based on the results of the core calculation.⁽¹⁰⁾ Since the mesh structures in shielding and core calculations are different, the reutron source distribution was interpolated as follows. When the mesh structures for the shielding and core calculation are overlapped each other, the mesh boundary lines are not always correspond to each others. Overlapping is shown, for example, as a figure bellow.



Broken lines show mesh boundary in core cal.
Solidlines show mesh boundary in shield cal.

In this case, the one mesh for the DOT calculation is devided to 6 regions by the core calculation mesh spacing. The neutron sources in regions are known. The source desity in one region was multiplied by its volume and summed over 6 regions then devided by the mesh volume of the shield calculation. This value was given as the source density used in the shield calculation.

In the actual calculation, the source strength in the upper half core region was 4.05×10^{18} n/sec/100MW, while the source strength obtained by the core calculation had been given as 4.01×10^{18} n/sec. This small discrepancy was neglected because of its small difference. The comparison of the mesh spacings between core and shield calculations is shown in Table 2.4.2. The source distributions are shown in Tables 2.4.3 and 2.4.4 for the core and shield calculations, respectively.

The summary of the parameters used in the DOT calculation is shown in Table 2.4.5.

The calculation results were edited in the forms of

- (1) fast neutron flux (14.92Mev to 166 kev)
- (2) intermediate neutron flux (166 kev to 0.414 ev)
- (3) thermal neutron flux (0.414 ev to 0.001 ev)
- (4) total neutron flux
- (5) total gamma-ray flux (14 Mev to 40 kev)
- (6) neutron dose rate
- (7) gamma-ray dose rate, and
- (8) neutron plus gamma-ray dose rate.

The conversion factors for the flux to dose rate are shown in Table 2.4.6.

The iso-flux and iso-dose rate contours are shown in Figs. 2.4.2 to 2.4.9. In Figs. 2.4.10 to 2.4.18 are the radial directional and axial directional attenuations of the neutron fluxes. The energy spectra of the neutron and gamma-ray at various positions are shown in Figs. 2.4.19 and 2.4.20.

Table 2.4.1 JOYO MK-II Partial R-Z Materials in Step 1 Calculation (1/3)

<u>Zone</u>	<u>Material</u>	<u>Vol.Fraction</u>	<u>Zone</u>	<u>Material</u>	<u>Vol.Fraction</u>
1	Driver Fuel	1.0	24	Graphite	1.0
2	Special fuel Reflector	0.666 0.333	25	Driver Fuel Insulator	1.0
3	Driver Fuel	1.0	26	B-Type Fuel Insulator CMIR Reflector	0.666 0.333
4	Control Rod Adaptor	1.0	27	Driver Fuel Insulator	1.0
5	Driver Fuel	1.0	28	Driver Fuel Insulator	1.0
6	Inner Reflector	1.0	29	Upper Reflector	1.0
7	Outer Reflector (A)	1.0	30	B-Type Upper Reflector CMIR Upper Reflector	0.666 0.333
8	Outer Reflector (B)	1.0	31	Upper Reflector	1.0
9	Sodium	1.0	32	Control Rod (In)	1.0
10	Sodium SS-304	0.2 0.8	33	Upper Reflector	1.0
11	Sodium	1.0	34	B-Type Gas Plenum CMIR Upper Reflector	0.666 0.333
12	SS-316	1.0	35	Gas Plenum	1.0
13	Sodium	1.0	36	Upper Part of Inner Reflector	1.0
14	Sodium SS-304	0.26 0.74	37	Gas Plenum	1.0
15	Sodium	1.0	38	Gas Plenum	1.0
16	Sodium	1.0	39	Upper Part of Control Rod	1.0
17	Sodium SS-304	0.4 0.6	40	Handling Head	1.0
18	SS-304	1.0	41	Handling Head	1.0
19	Nitrogen Gas	1.0	42	SS-316	1.0
20	SS-304	1.0	43	SS-316	1.0
21	SS-304	0.04	44	Sodium	1.0
22	Nitrogen Gas	1.0	45	Sodium SS-316	0.74 0.26
23	Graphite	1.0			

Table 2.4.1 (Continued) (2/3)

<u>Zone</u>	<u>Material</u>	<u>Vol.Fraction</u>	<u>Zone</u>	<u>Material</u>	<u>Vol.Fraction</u>
46	Sodium SS-316	0.74 0.26	66-68	Sodium SS-304	0.2 0.8
47	Sodium	1.0	69-72	Sodium	1.0
48	Sodium SS-316	0.38 0.62	73	Nitrogen Gas	1.0
49	Sodium SS-316	0.38 0.62	74	SS-316	0.23
50	SS-316	1.0	75	Nitrogen Gas	1.0
51	SS-316	1.0	76	SS-304	0.5533
52	Sodium	1.0	77	Nitrogen Gas	1.0
53	Sodium SS-316	0.77 0.23	78	Insulator	0.0833
54	Sodium	1.0	79	SS-304	1.0
55	Sodium SS-304	0.4466 0.5533	80	Heavy Concrete	1.0
56	Sodium	1.0	81	SS-304	1.0
57	Sodium SS-316	0.77 0.23	82	Carbon Steel	1.0
58	Sodium	1.0	83	Graphite Powder	1.0
59	Sodium SS-304	0.4466 0.5533	84	Carbon Steel	1.0
60	Sodium	1.0	85	SS-304	1.0
61	Sodium	1.0	86	SS-304	1.0
62	Sodium SS-316	0.77 0.23	87	SS-316	0.94
63	Sodium	1.0	88-90	SS-304	1.0
64	Sodium SS-304	0.4466 0.5533	91-92	SS-304 Carbon Steel SS-Wool	0.13 0.12 0.75
65	Sodium	1.0	93-94	SS-304	1.0
			95	SS-304 Carbon Steel SS-Wool	0.13 0.12 0.75
			96-97	Graphite	1.0

Table 2.4.1 (Continued) (3/3)

<u>Zone</u>	<u>Material</u>	<u>Vol.Fraction</u>	<u>Zone</u>	<u>Material</u>	<u>Vol.Fraction</u>
98-100	Carbon Steel	1.0	143-145	Carbon Steel	1.0
101-102	Graphite	1.0	146-147	Graphite	1.0
103	Carbon Steel	1.0	148-149	Carbon Steel	1.0
104	Graphite	1.0	150	Graphite	1.0
105-106	Carbon Steel	1.0	151-154	Carbon Steel	1.0
107	Graphite Powder	1.0	155	SS-304	1.0
108-109	Carbon Steel	1.0	156	Carbon Steel	1.0
110	SS-304	1.0	157	Nitrogen Gas	1.0
111	Carbon Steel	1.0	158	Graphite	1.0
112-113	Graphite	1.0	159	SS-316	0.89
114-115	Carbon Steel	1.0	160	Graphite	1.0
116	Graphite	1.0	161-162	Carbon Steel	1.0
117-120	Carbon Steel	1.0	163	Boron Steel	1.0
121-122	Graphite	1.0	164	Carbon Steel	1.0
123-124	Carbon Steel	1.0	165-167	Nitrogen Gas	1.0
125	Graphite	1.0	168-171	SS-304	1.0
126-130	Carbon Steel	1.0	172-175	Nitrogen Gas	1.0
131	SS-304	1.0	176	Boron Steel	1.0
132-133	Graphite	1.0	177	SS-316	0.37
134	Carbon Steel	1.0	178	Boron Steel	1.0
135-136	SS-304	1.0	179	Carbon Steel	1.0
137	Carbon Steel	1.0	180-181	SS-304	1.0
138	Graphite	1.0	182	Sodium SS-316	0.77 0.23
139	Carbon Steel	1.0	183	SS-316	0.20
140	SS-304	1.0	184	SS-316	0.66
141-142	Nitrogen Gas	1.0	185	Boron Steel	1.0

Table 2.4.2 Mesh Structure for Core and Shield Calculations

(Unit : cm)

I=	RD(I)	RC(I)	ZD(I)	ZC(I)
1	0.0	0.0	0.0	0.0
2	2.47500	2.14783	3.94381	3.45084
3	4.95000	4.29566	7.88763	6.90168
4	6.49010	5.39287	11.83144	10.35251
5	8.18165	6.49008	15.77526	13.80335
6	9.87320	8.18162	19.71907	17.25418
7	12.83630	9.87316	23.66287	20.70502
8	15.79940	10.61920	27.60670	24.15585
9	16.92709	11.36525	28.81140	27.60670
10	17.66060	13.20502	0.0	28.20905
11	20.36790	15.04480	0.0	28.81140
12	21.64655	16.88457	0.0	0.0
13	22.92520	18.72435	0.0	0.0
14	25.49319	19.54610	0.0	0.0
15	27.73497	20.36784	0.0	0.0
16	29.97675	21.64653	0.0	0.0
17	32.21852	22.92522	0.0	0.0
18	34.46030	24.52734	0.0	0.0
19	36.70210	26.12949	0.0	0.0
20	0.0	27.98465	0.0	0.0
21	0.0	29.83981	0.0	0.0
22	0.0	31.69498	0.0	0.0
23	0.0	33.55019	0.0	0.0
24	0.0	34.33817	0.0	0.0
25	0.0	35.12614	0.0	0.0
26	0.0	35.91412	0.0	0.0
27	0.0	36.70210	0.0	0.0

RD : Radial mesh boundary for shield calculation

RC : Radial mesh boundary for core calculation

ZD : Axial mesh boundary for shield calculation

ZC : Axial mesh boundary for core calculation

Table 2.4.3 Neutron Source Distribution by Core Calculation

Radial Mesh Numbers

	1	2	3	4	5	6	7	8	9	10	
	11	12	13	14	15	16	17	18	19	20	
Axial Mesh Numbers 2 - 58	1	6.2414E+13	6.2076E+13	6.1609E+13	6.1191E+13	9.5143E+12	9.4454E+12	5.9938E+13	5.9649E+13	5.9021E+13	5.7856E+13
	2	6.1357E+13	6.1024E+13	6.0565E+13	6.0155E+13	9.3534E+12	9.2854E+12	5.8921E+13	5.8636E+13	5.8016E+13	5.6869E+13
	3	5.9327E+13	5.9007E+13	5.8565E+13	5.8169E+13	9.0454E+12	8.9793E+12	5.6972E+13	5.6694E+13	5.6091E+13	5.4980E+13
	4	5.6374E+13	5.6072E+13	5.5656E+13	5.5284E+13	8.5982E+12	8.5348E+12	5.4138E+13	5.3869E+13	5.3287E+13	5.2228E+13
	5	5.2683E+13	5.2407E+13	5.2030E+13	5.1692E+13	8.0456E+12	7.9845E+12	5.0601E+13	5.0334E+13	4.9762E+13	4.8760E+13
	6	4.8168E+13	4.7924E+13	4.7596E+13	4.7302E+13	7.3687E+12	7.3098E+12	4.6267E+13	4.6000E+13	4.5442E+13	4.4503E+13
	7	4.3160E+13	4.2959E+13	4.2701E+13	4.2467E+13	6.6302E+12	6.5714E+12	4.1467E+13	4.1179E+13	4.0605E+13	3.9714E+13
	8	3.8136E+13	3.7983E+13	3.7815E+13	3.7665E+13	5.9131E+12	5.8493E+12	3.6637E+13	3.6288E+13	3.5636E+13	3.4745E+13
	9	3.3423E+12	3.3162E+12	3.2793E+12	3.2526E+12	5.0747E+11	5.0403E+11	3.1887E+12	3.1766E+12	3.1529E+12	3.0942E+12
	10	3.1267E+12	3.1052E+12	3.0764E+12	3.0570E+12	4.7810E+11	4.7449E+11	2.9937E+12	2.9772E+12	2.9484E+12	2.8899E+12

Table 2.4.4 Neutron Source Distribution for Shield Calculation

2 - 59

Radial Mesh Numbers

	1	2	3	4	5	6	7	8	9	10
Axial Mesh Numbers	6.2199E+13	6.1791E+13	6.1169E+13	9.4942E+12	9.4267E+12	5.9256E+13	5.7463E+13	5.6203E+13	5.4539E+13	5.3394E+13
1	6.0768E+13	6.0370E+13	5.9763E+13	9.2764E+12	9.2102E+12	5.7889E+13	5.6134E+13	5.4902E+13	5.3278E+13	5.2161E+13
2	5.8142E+13	5.7764E+13	5.7187E+13	8.8777E+12	8.8138E+12	5.5382E+13	5.3697E+13	5.2519E+13	5.0969E+13	4.9905E+13
3	5.4457E+13	5.4109E+13	5.3580E+13	8.3219E+12	8.2608E+12	5.1857E+13	5.0260E+13	4.9156E+13	4.7714E+13	4.6730E+13
4	4.9798E+13	4.9491E+13	4.9029E+13	7.6225E+12	7.5639E+12	4.7388E+13	4.5887E+13	4.4875E+13	4.3569E+13	4.2691E+13
5	4.4360E+13	4.4110E+13	4.3740E+13	6.8148E+12	6.7569E+12	4.2147E+13	4.0723E+13	3.9807E+13	3.8661E+13	3.7917E+13
6	3.8725E+13	3.8546E+13	3.8306E+13	6.0027E+12	5.9404E+12	3.6637E+13	3.5201E+13	3.4356E+13	3.3365E+13	3.2780E+13
7	3.2286E+12	3.1999E+12	3.1607E+12	4.9278E+11	4.8933E+11	3.0663E+12	2.9764E+12	2.9067E+12	2.8091E+12	2.7391E+12
	11	12	13	14	15	16	17	18		
Axial Mesh Numbers	0.0	0.0	4.8385E+13	4.5821E+13	4.2973E+13	3.9812E+13	3.7469E+13	3.5754E+13		
1	0.0	0.0	4.7272E+13	4.4771E+13	4.1994E+13	3.8915E+13	3.6638E+13	3.4985E+13		
2	0.0	0.0	4.5244E+13	4.2860E+13	4.0218E+13	3.7293E+13	3.5142E+13	3.3616E+13		
3	0.0	0.0	4.2393E+13	4.0173E+13	3.7725E+13	3.5028E+13	3.3062E+13	3.1721E+13		
4	0.0	0.0	3.8770E+13	3.6758E+13	3.4562E+13	3.2166E+13	3.0449E+13	2.9372E+13		
5	0.0	0.0	3.4498E+13	3.2744E+13	3.0866E+13	2.8845E+13	2.7457E+13	2.6750E+13		
6	0.0	0.0	2.9956E+13	2.8547E+13	2.7106E+13	2.5594E+13	2.4674E+13	2.4464E+13		
7	0.0	0.0	2.4645E+12	2.3349E+12	2.1758E+12	1.9730E+12	1.7748E+12	1.5084E+12		
8	0.0	0.0								

OVERALL SOURCE STRENGTH = 4.052E+18 n/sec

Table 2.4.5 Description of Input Variables (Step 1)

Program DOT 3.5

Geometry type Two-dimensional cylinder

Problem type Fixed volume distributed source

Number of energy groups IGM = 21 + 7

Number of radial intervals IM = 120

Number of axial intervals..... JM = 213

Number of angles A04 = 30

Order of scattering A03 = 1

Flux calculational model Weighted difference mode

Convergence Pointwise scaling, G06 = 0.01

Boundary conditions

Left Reflection

Right Vacuum

Bottom Reflection

Top Vacuum

Table 2.4.6 Flux-to-Dose Rate Conversion Factor

Neutron

Group	$(\text{mrem}/\text{hr}) / (\text{n/cm}^2 \cdot \text{sec})$	Group	$(\text{mrem}/\text{hr}) / (\text{n/cm}^2 \cdot \text{sec})$
1	0.1480	11	0.004603
2	0.1460	12	0.003619
3	0.1430	13	0.003670
4	0.1355	14	0.003784
5	0.1150	15	0.003982
6	0.08266	16	0.004178
7	0.05692	17	0.004283
8	0.03882	18	0.004385
9	0.02365	19	0.004492
10	0.01089	20	0.004494
		21	0.003846

Gamma-Ray

Group	$(\text{mrem}/\text{hr}) / (\text{r/cm}^2 \cdot \text{sec})$
1	1.008-2
2	6.890-3
3	4.965-3
4	3.689-3
5	2.543-3
6	1.440-3
7	4.692-4

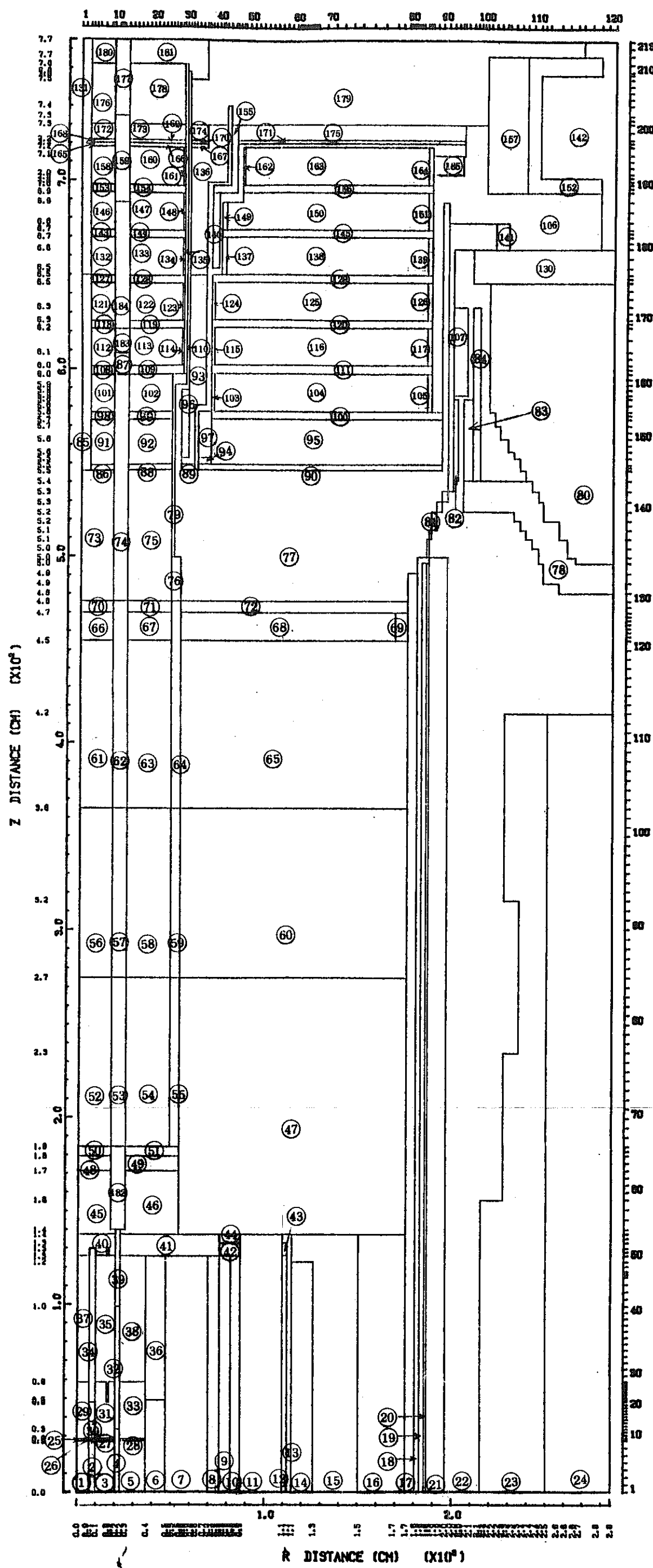


Fig. 2.4.1 Calculational Configuration for Step 1 Calculation (Zone No.)

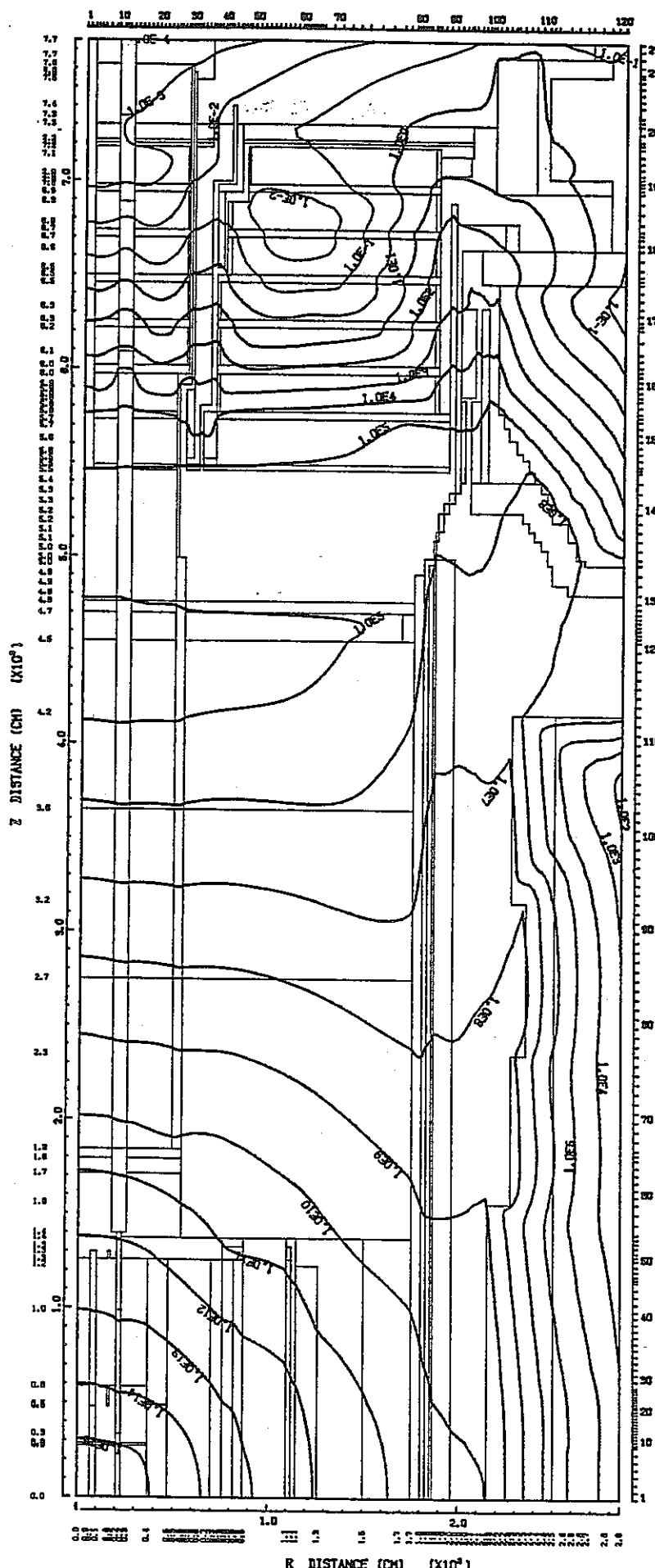


Fig. 2.4.2 Fast Neutron Isoflux Contours for Step 1 Calculation

FAST NEUTRON FLUX (N/CM**2.S) 1.4918E+07 - 1.6573E+05 (EV) (GROUP 1 - 8)

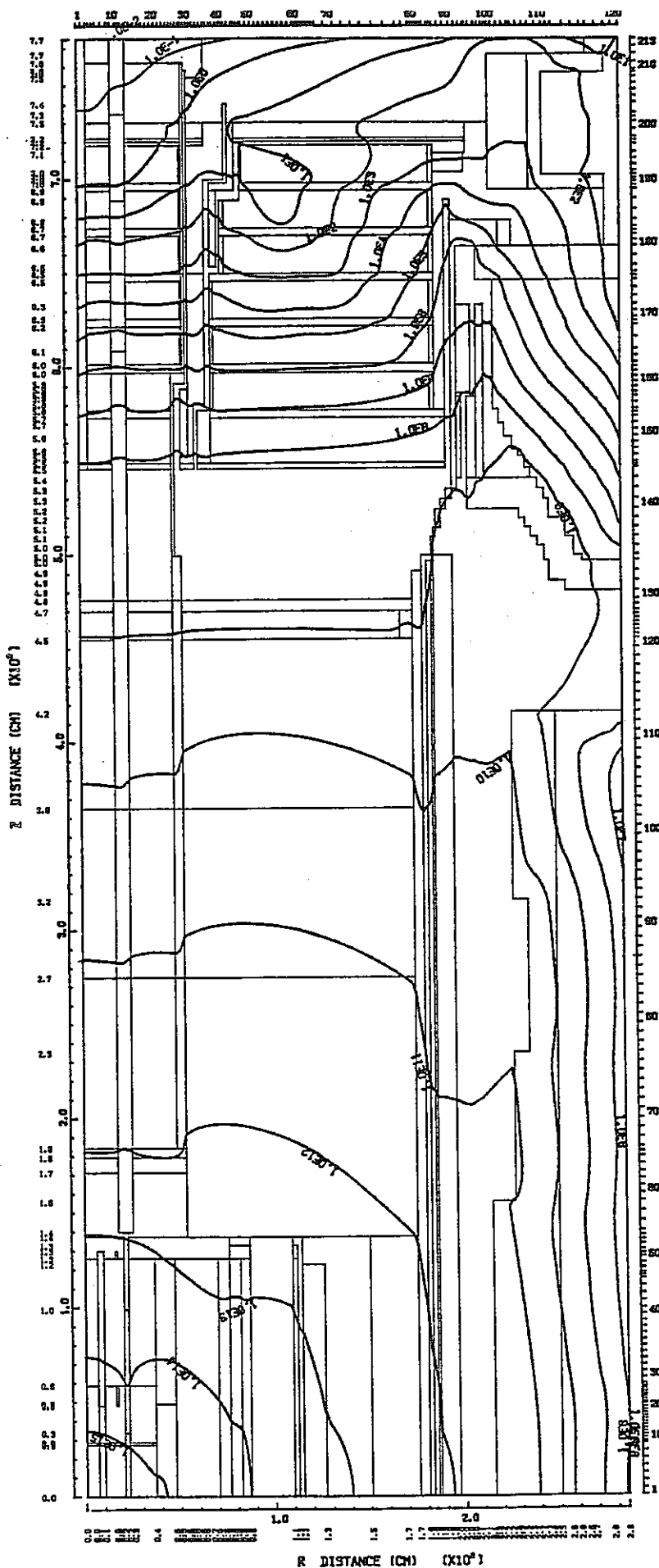


Fig. 2.4.3 Intermediate Neutron Isoflux Contours for Step 1 Calculation
 INTER NEUTRON FLUX (N/CM**2.S) 1.6573E+05 - 4.1399E-01 (EV) (GROUP 9 - 20)

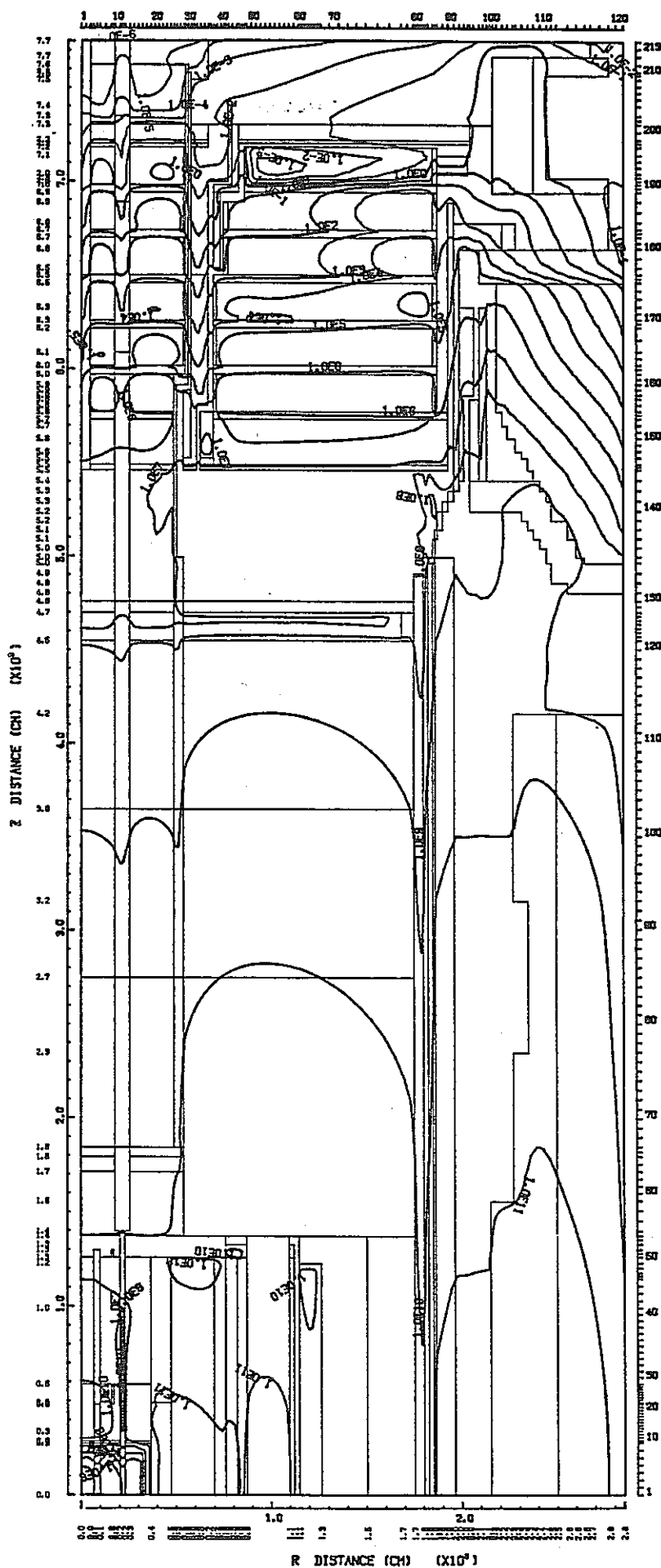


Fig. 2.4.4 Thermal Neutron Isoflux Contours for Step 1 Calculation
 NEUTRON FLUX (N/CM**2.S) 4.1399E-01 - 1.0000E-03 (EV) (GROUP 21)
 2 - 65

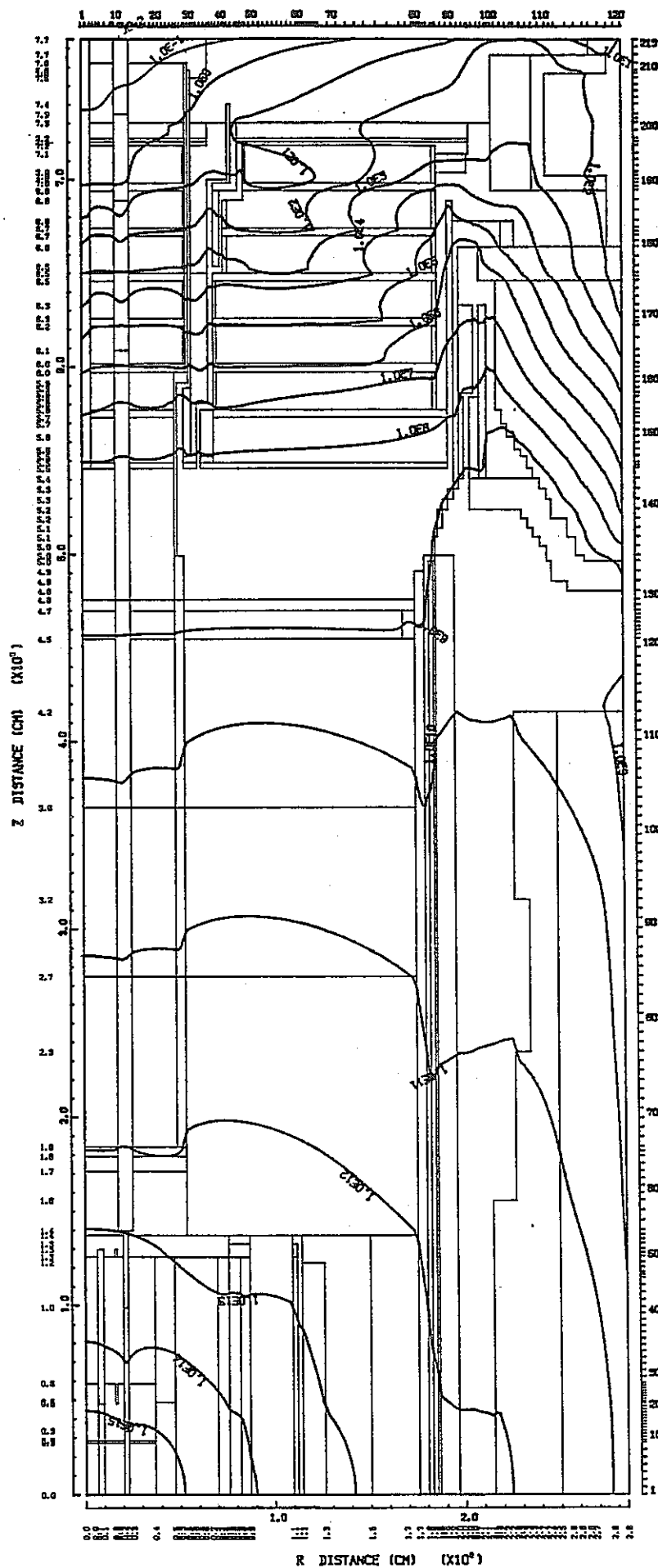


Fig. 2.4.5 Total Neutron Isoflux Contours for Step 1 Calculation
 TOTAL NEUTRON FLUX (N/CM**2.S) 1.4918E+07 - 1.0000E-03 (EV) (GROUP 1 - 21)

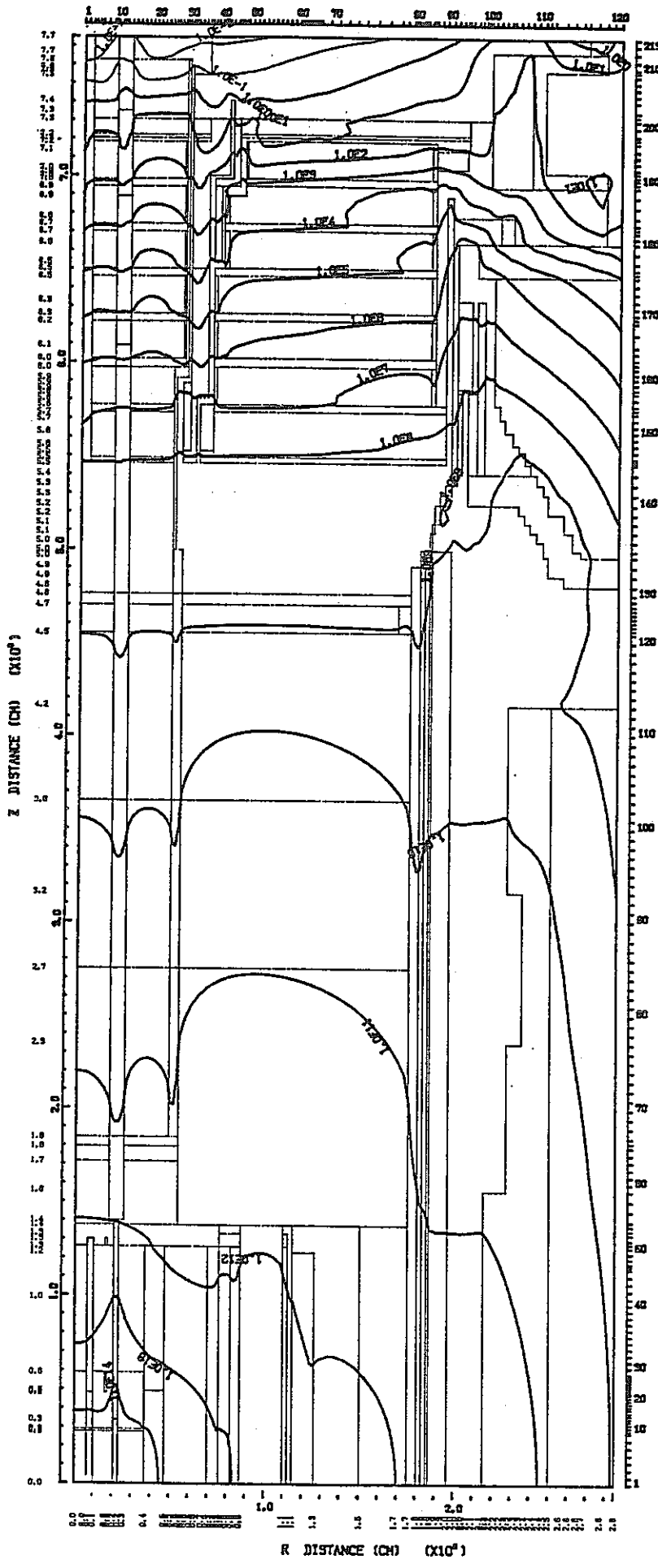


Fig. 2.4.6 Total Gamma-Ray Isoflux Contours for Step 1 Calculation
 TOTAL GAMMA FLUX (P/CM**2.S) 14.0 - 0.02 (MEV) (GROUP 22-28)

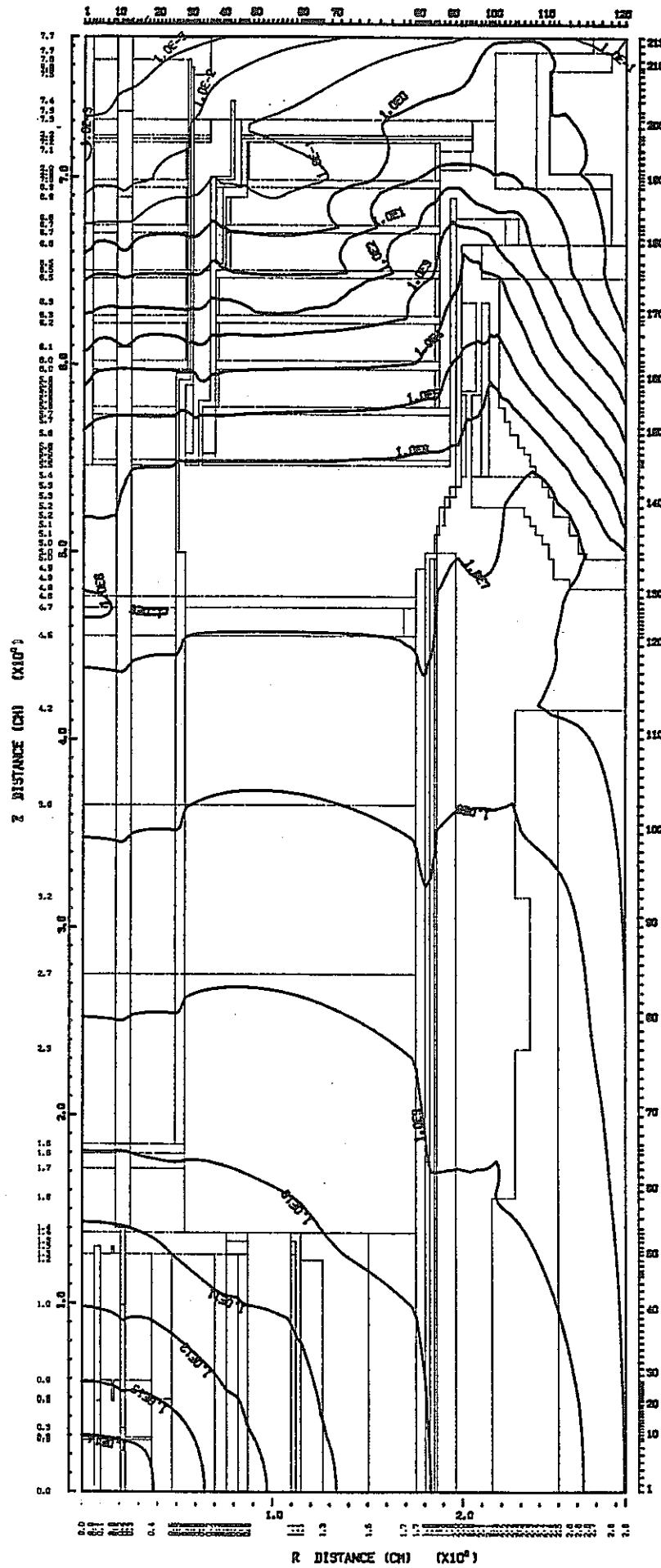


Fig. 2.4.7 Neutron Isodose Contours for Step 1 Calculation
 NEUTRON DOSE RATE (MREM/HOUR) 1.4918E+07 - 1.0000E-03 (EV) (GROUP 1-21)

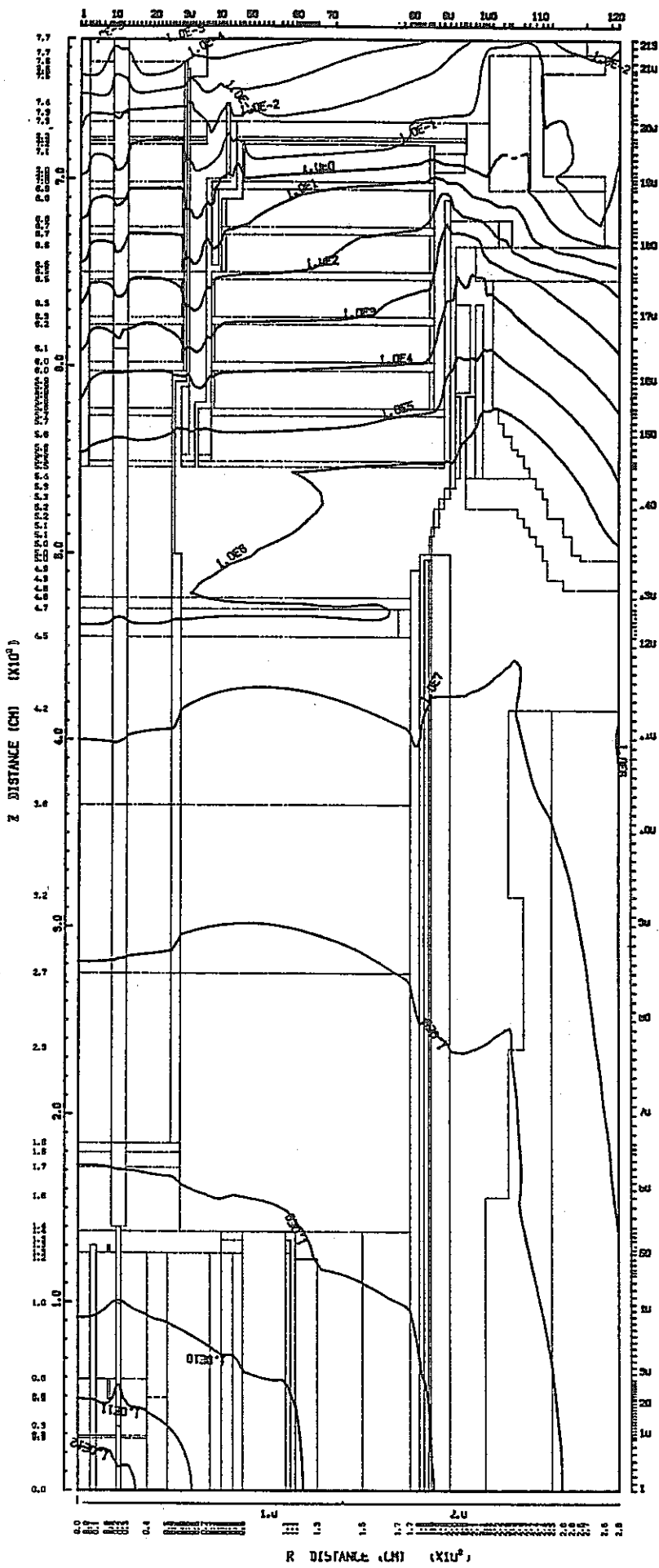


Fig. 2.4.8 Gamma-Ray Isodose Contours for Step 1 Calculation
 GAMMA DOSE RATE (MREM/HOUR) 14.0 - 0.02 (ME') (GROUP 22-28)

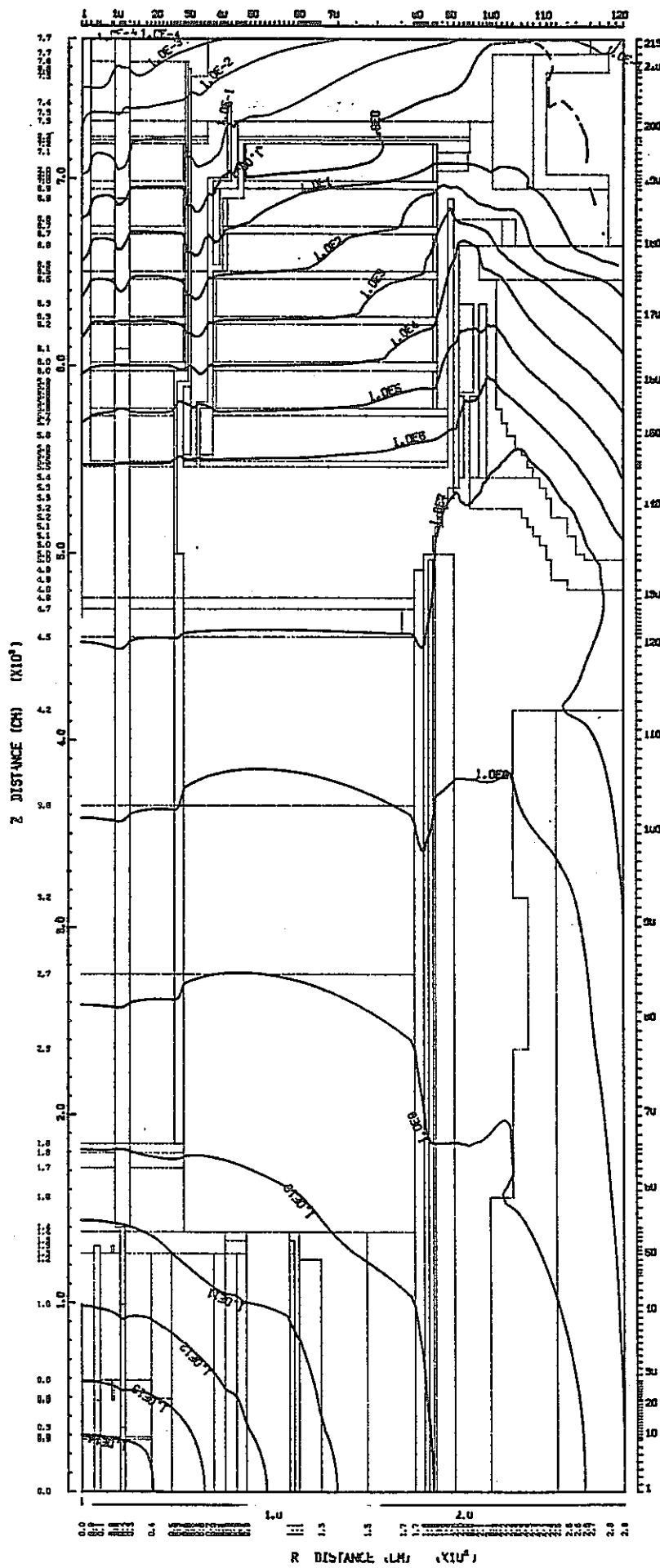
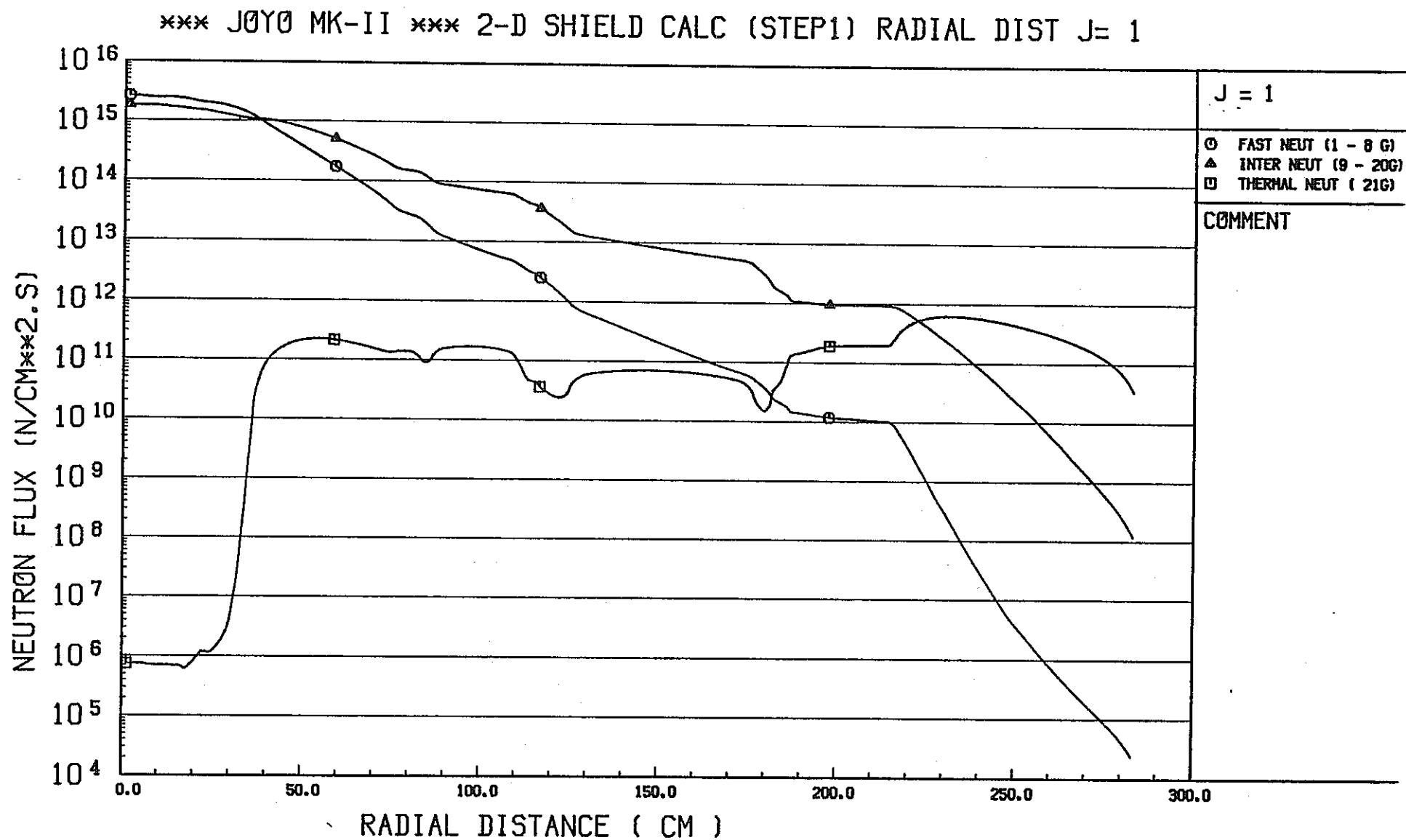


Fig. 2.4.9 Isodose Contours for Step 1 Calculation
TOTAL DOSE RATE (MREM/HOUR) NEUTRON DOSE + GAMMA DOSE (GROUP 1-28)

Fig. 2.4.10 Radial Flux Distribution for Step 1 Calculation at $Z=1.97\text{cm}$ (1/2)

*** JOY0 MK-II *** 2-D SHIELD CALC (STEP1) RADIAL DIST J= 1

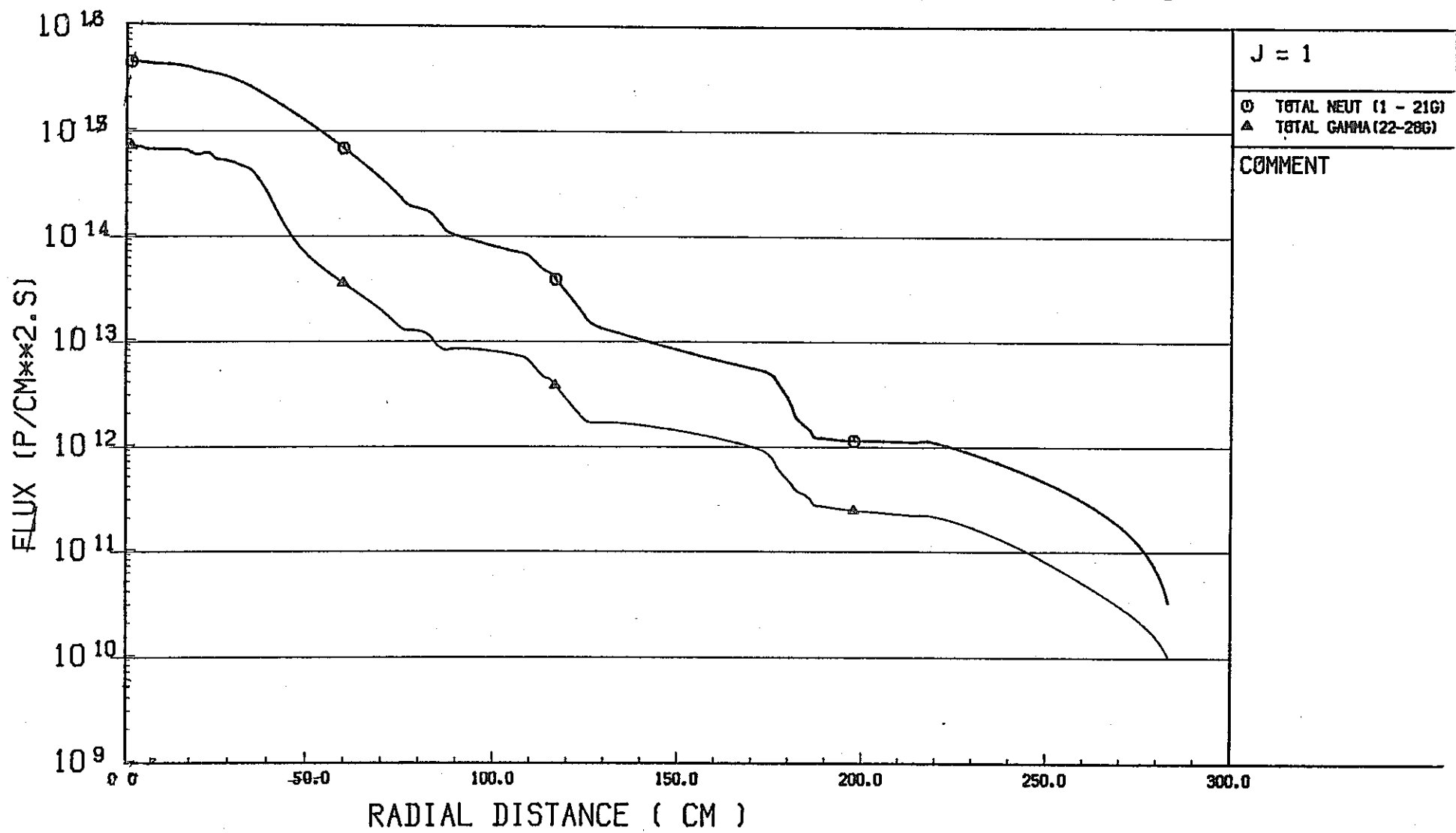


Fig. 2.4.10 (Continued) (2/2)

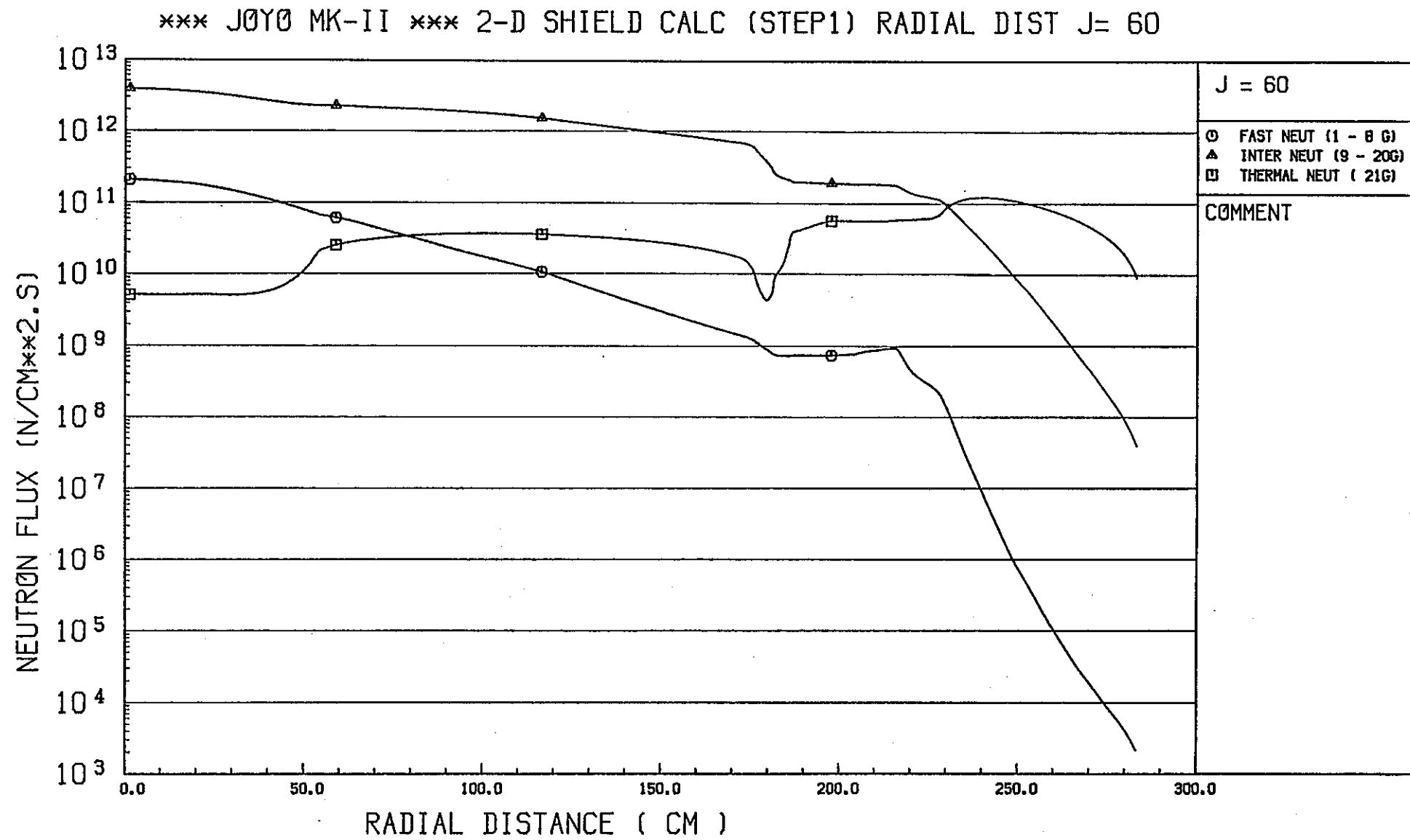


Fig. 2.4.11 Radial Flux Distribution for Step 1 Calculation at Z=161.8cm (1/2)

*** JOY0 MK-II *** 2-D SHIELD CALC (STEP1) RADIAL DIST J= 60

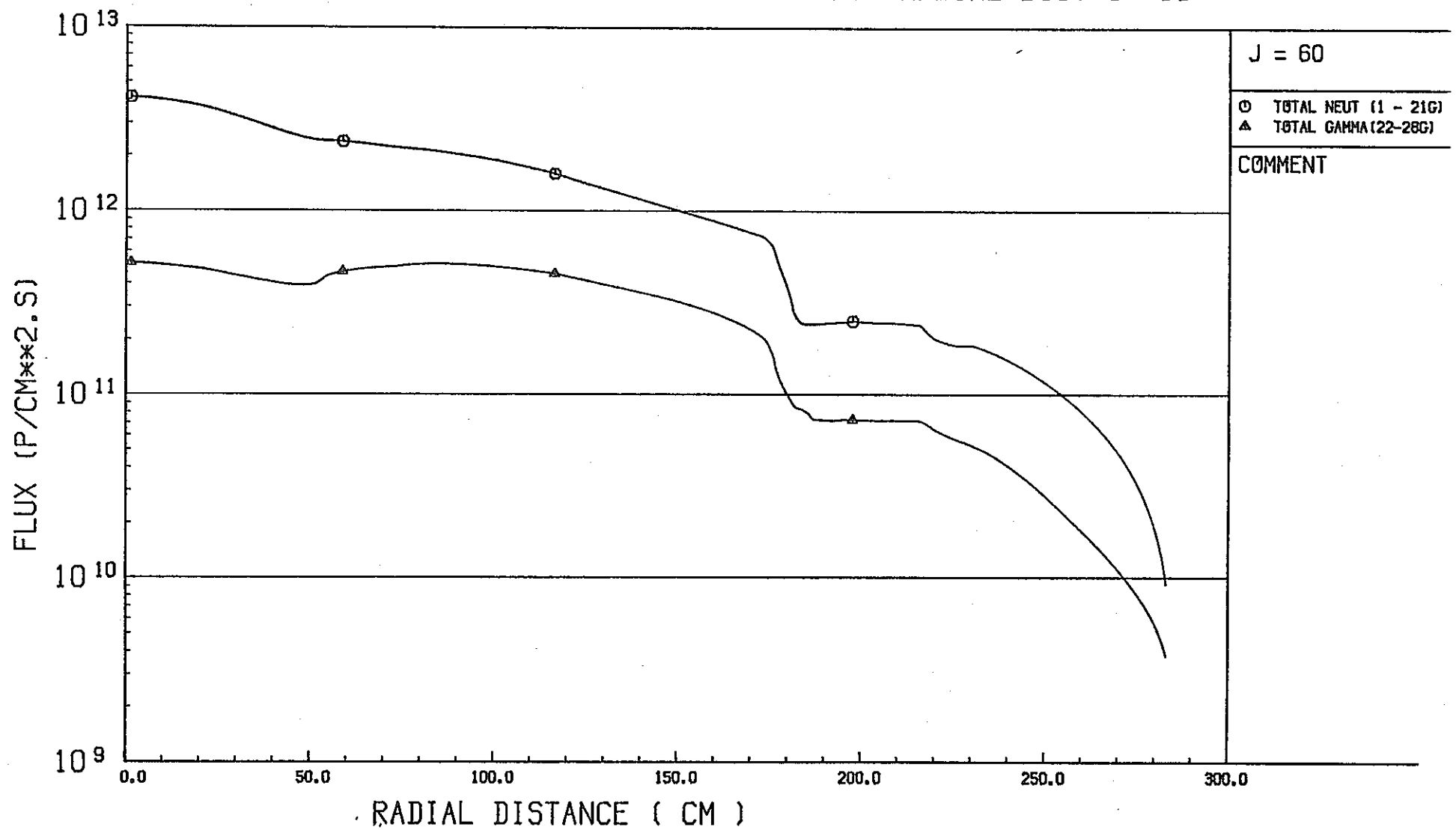


Fig. 2.4.11 (Continued) (2/2)

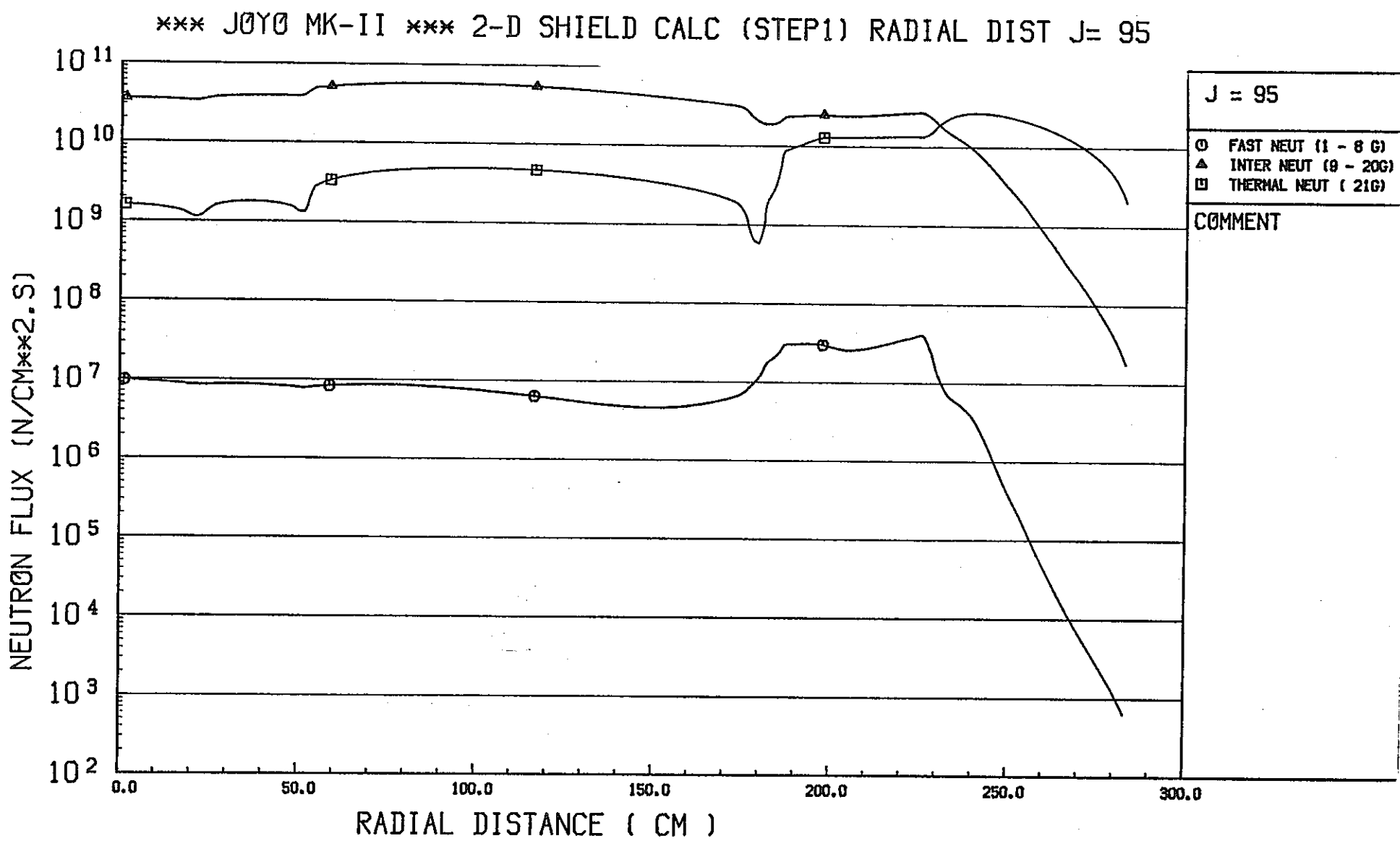


Fig. 2.4.12 Radial Flux Distribution for Step 1 Calculation at Z=328.3 cm (1/2)

*** J0Y0 MK-II *** 2-D SHIELD CALC (STEP1) RADIAL DIST J= 95

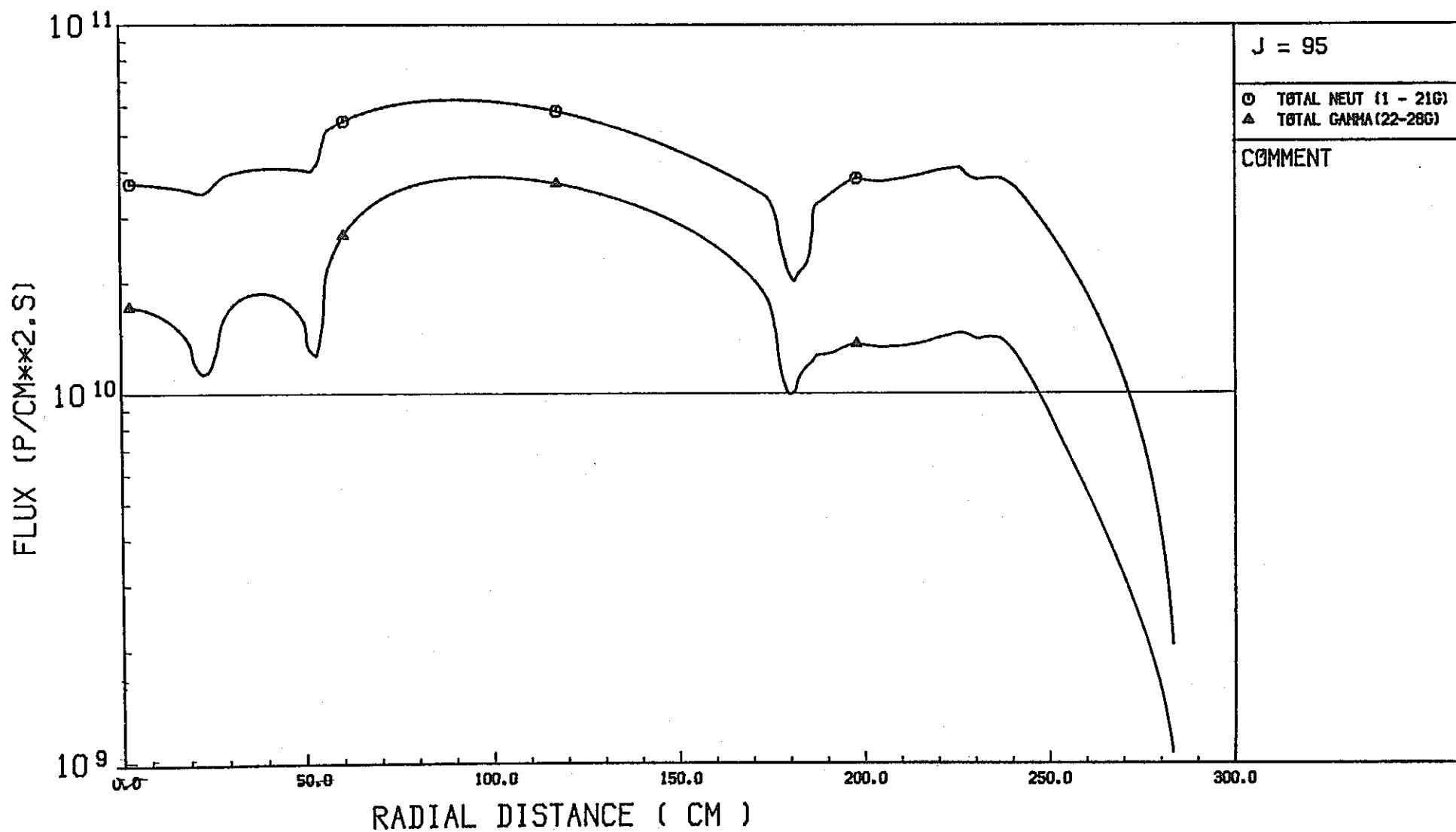


Fig. 2.4.12 (Continued) (2/2)

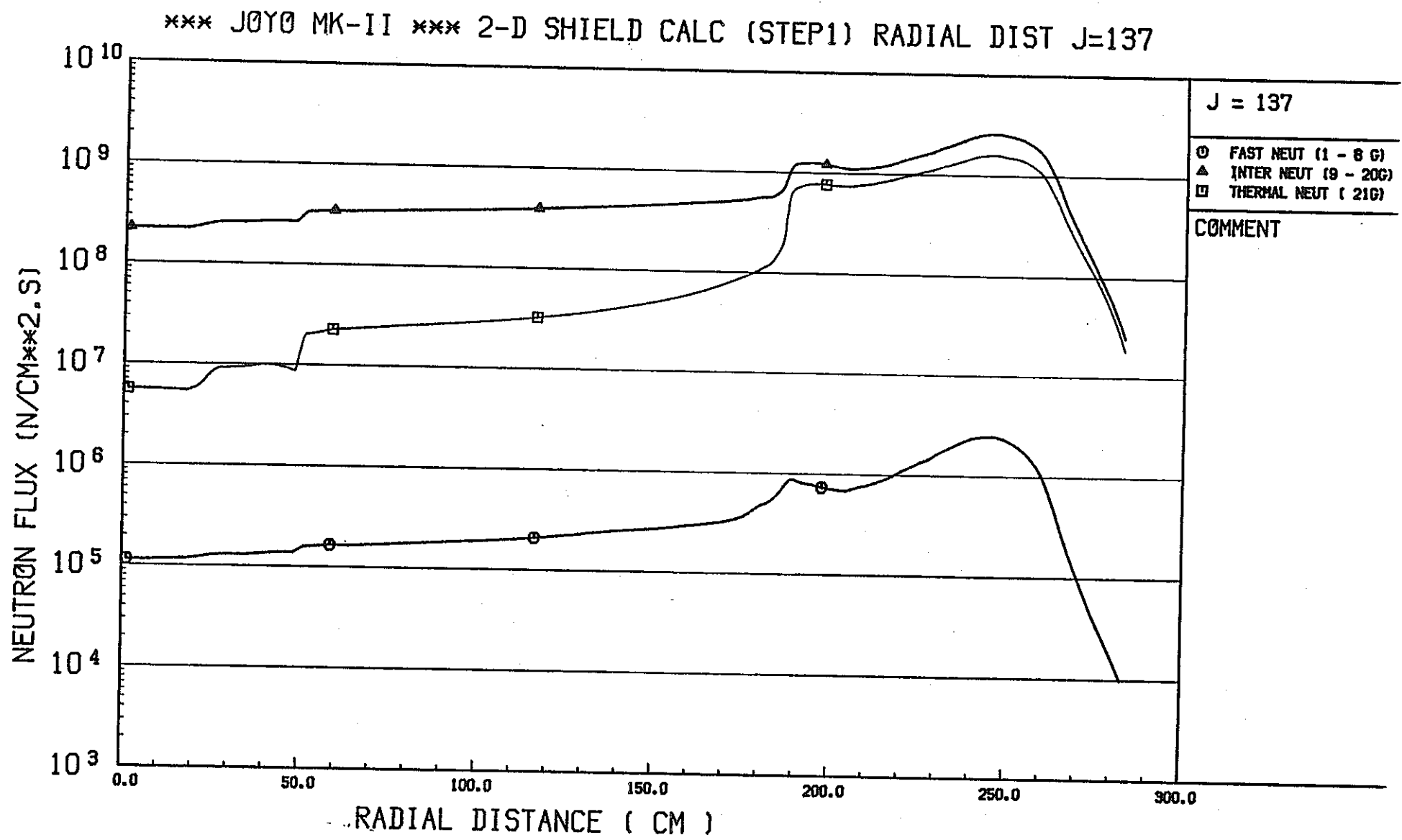


Fig. 2.4.13 Radial Flux Distribution for Step 1 Calculation at $Z=511.8$ cm (1/2)

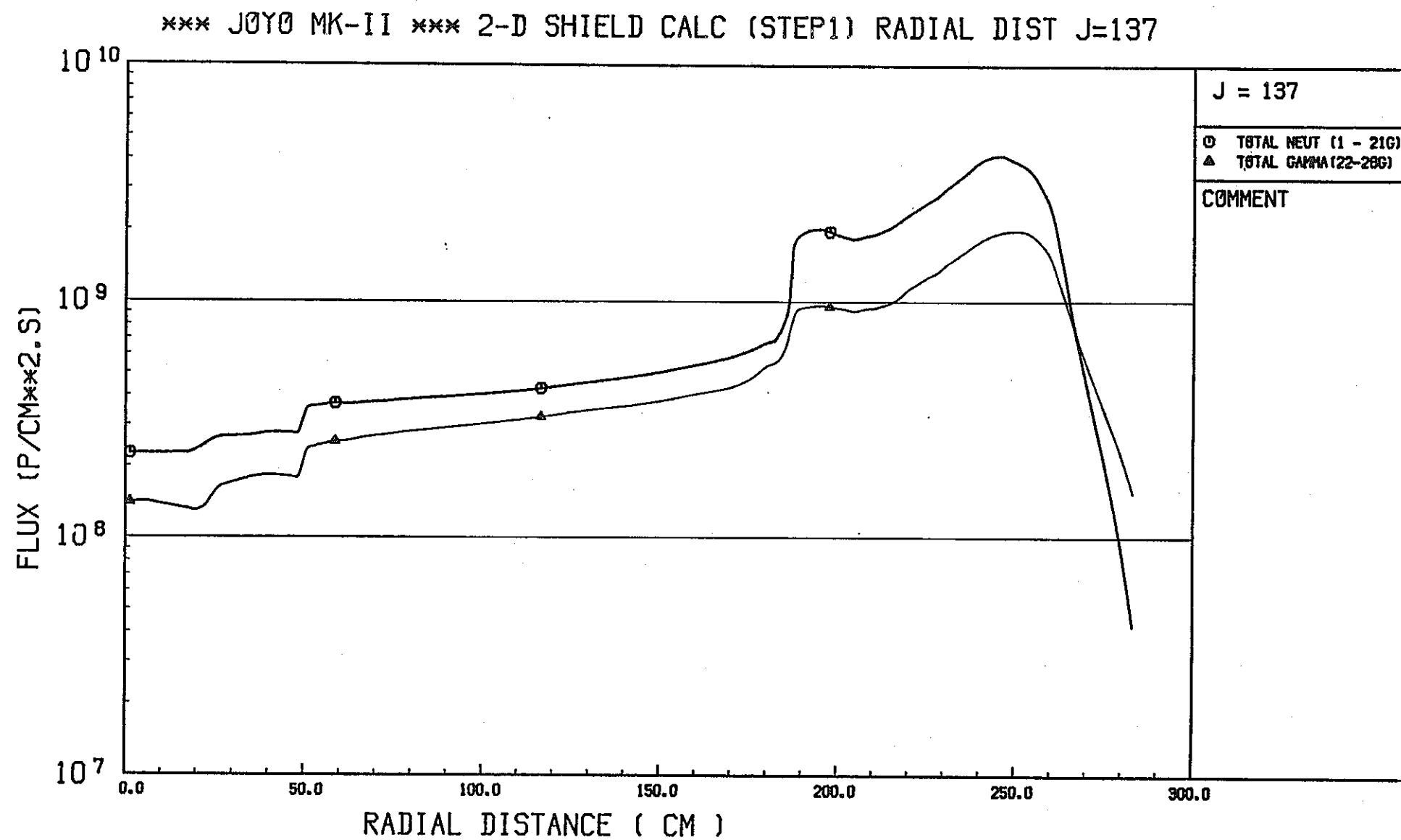


Fig. 2.4.13 (Continued) (2/2)

*** JOYO MK-II *** 2-D SHIELD CALC (STEP1) RADIAL DIST J=180

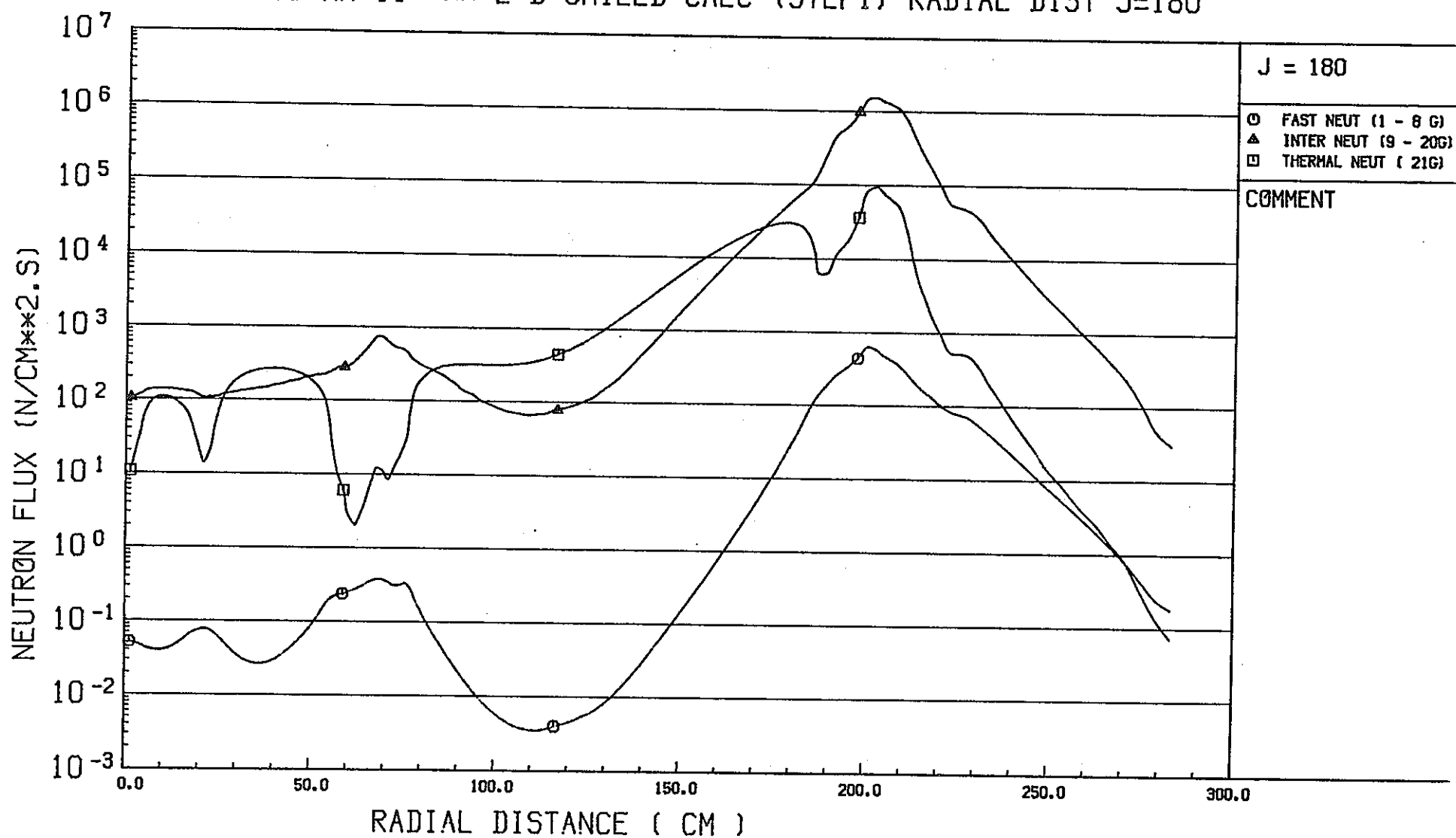


Fig. 2.4.14 Radial Flux Distribution for Step 1 Calculation at $Z=665.5$ cm (1/2)

2 - 80

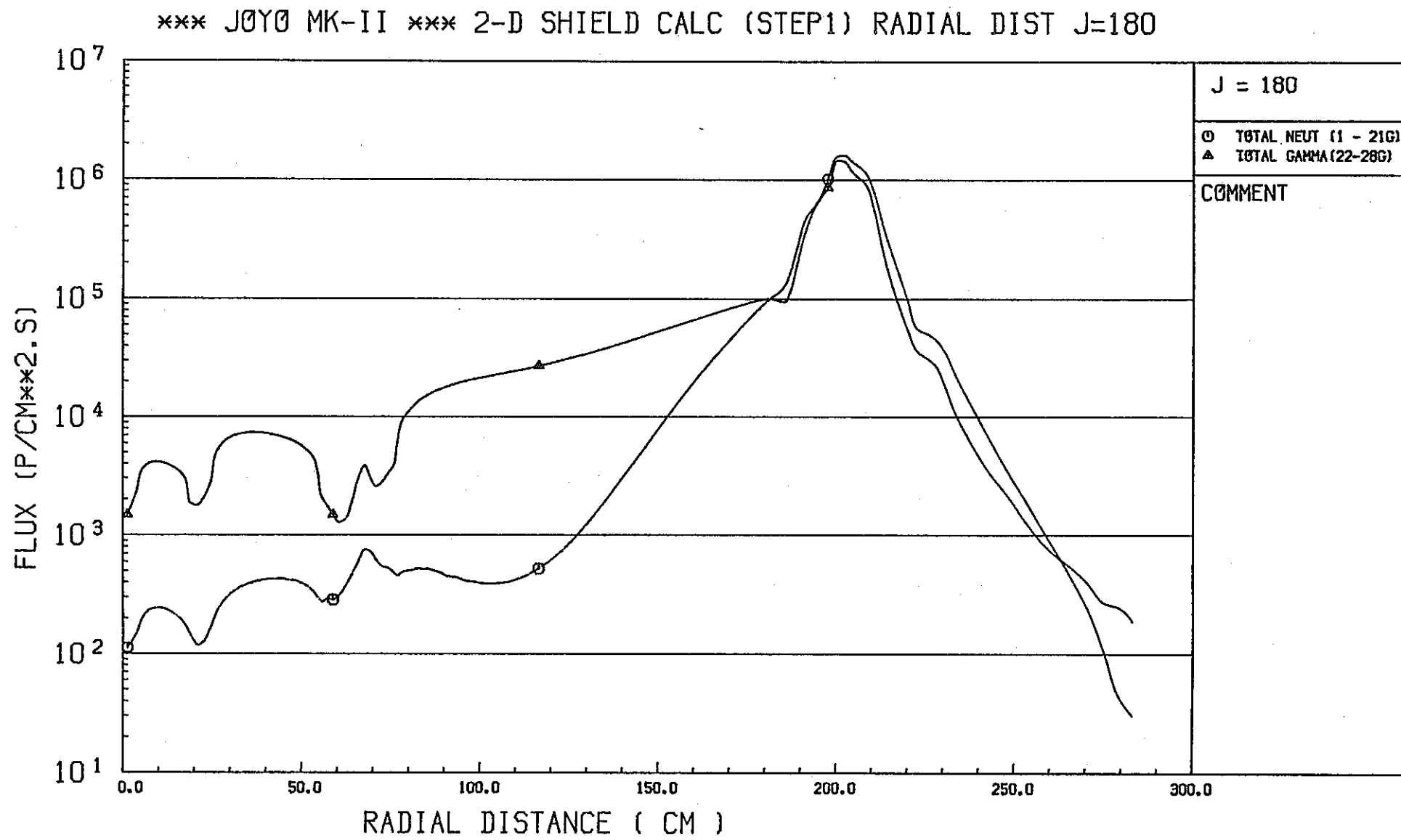


Fig. 2.4.14 (Continued) (2/2)

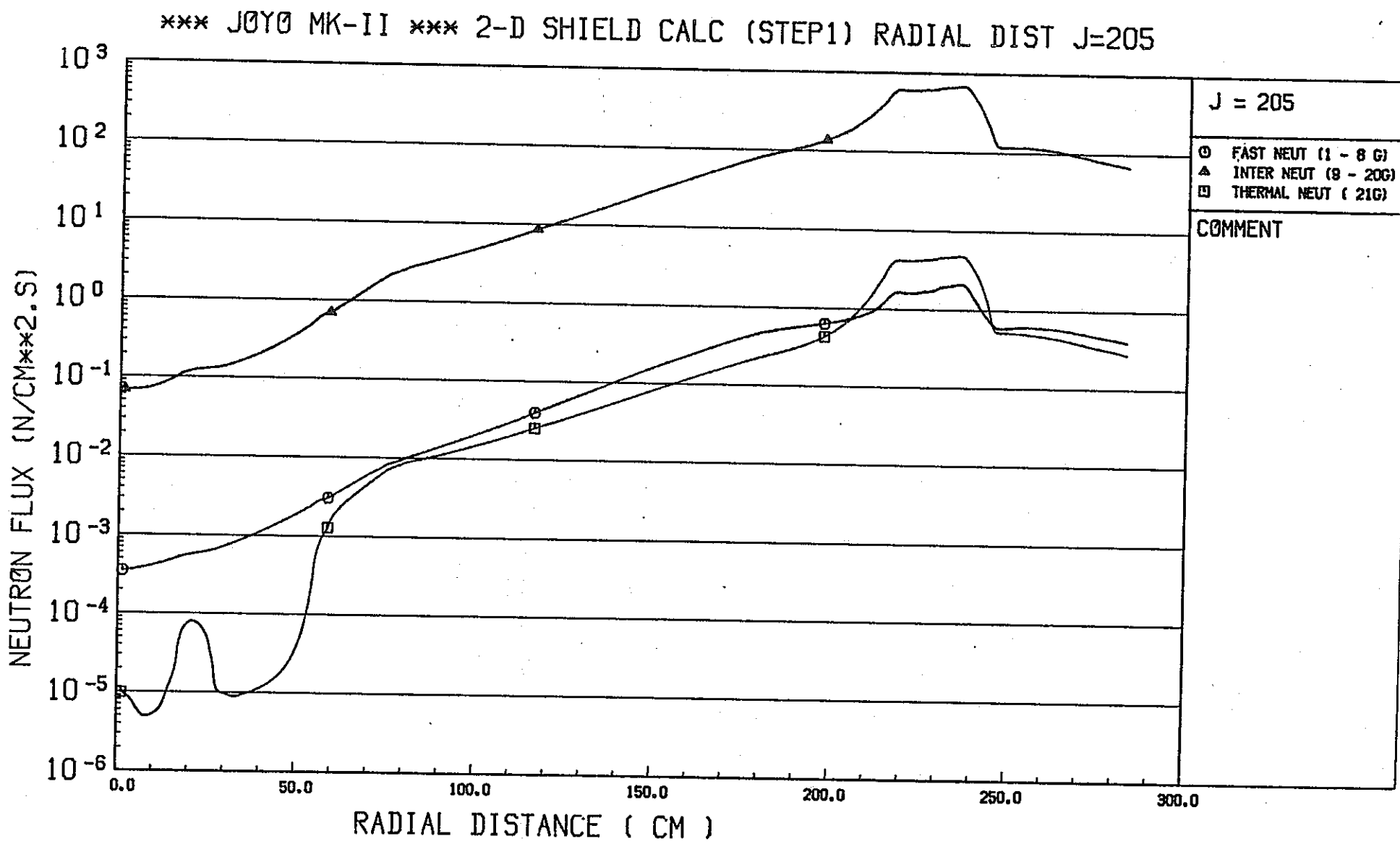


Fig. 2.4.15 Radial Flux Distribution for Step 1 Calculation at Z=745.8 cm (1/2)

*** JOY0 MK-II *** 2-D SHIELD CALC (STEP1) RADIAL DIST J=205

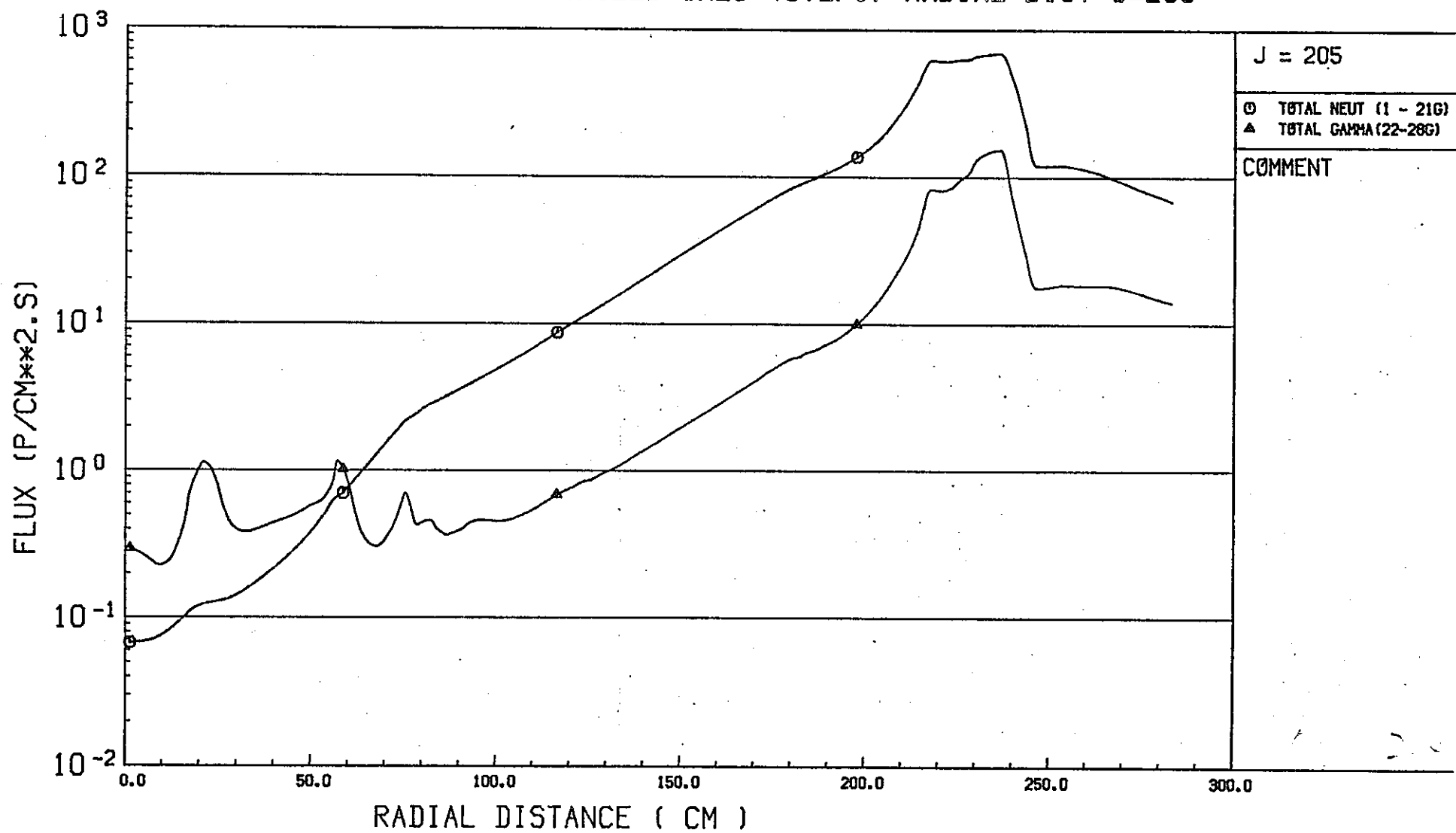


Fig. 2.4.15 (Continued) (2/2)

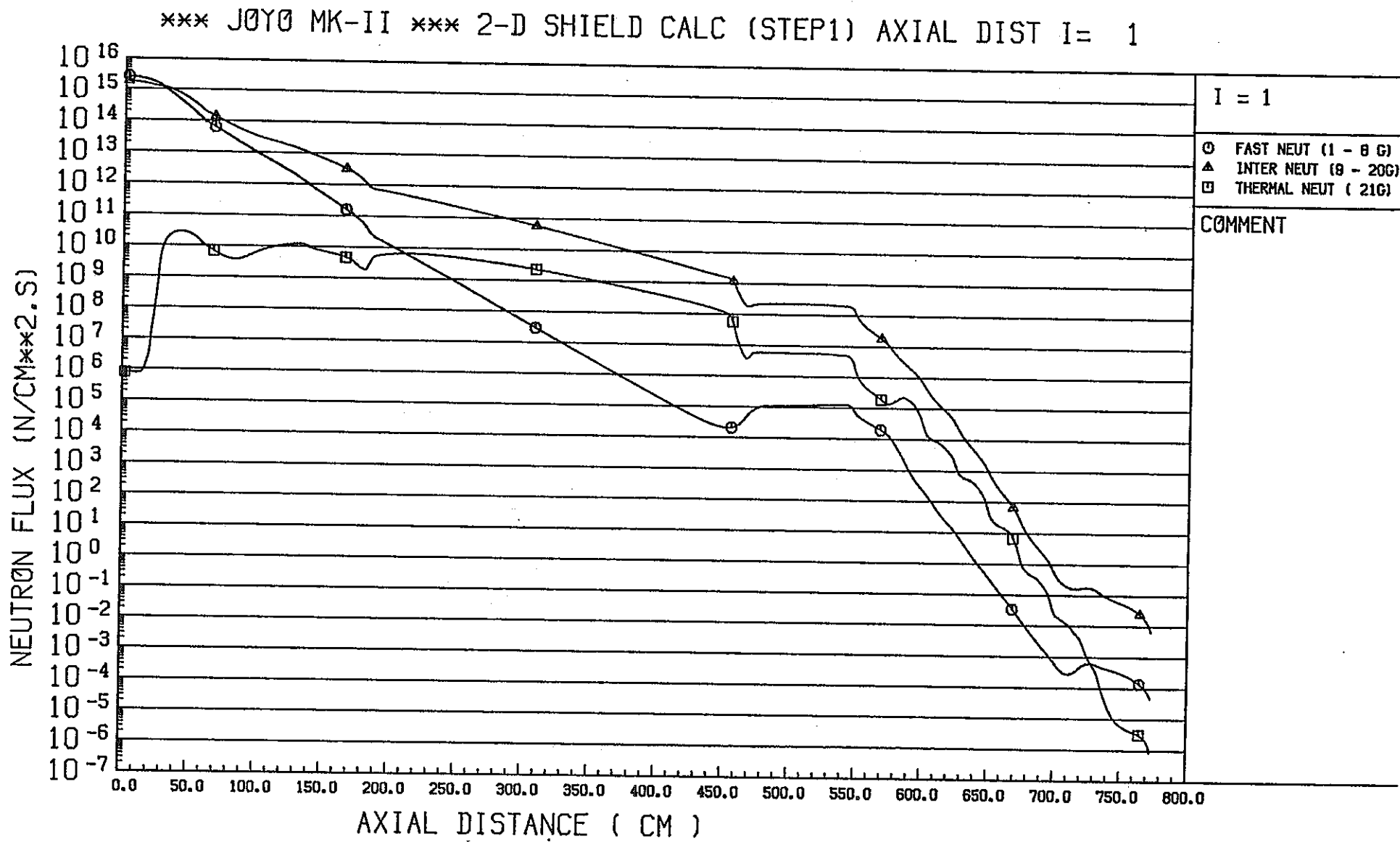


Fig. 2.4.16 Axial Flux Distribution for Step 1 Calculation at R=1.24 (1/2)

*** JOY0 MK-II *** 2-D SHIELD CALC (STEP1) AXIAL DIST I= 1

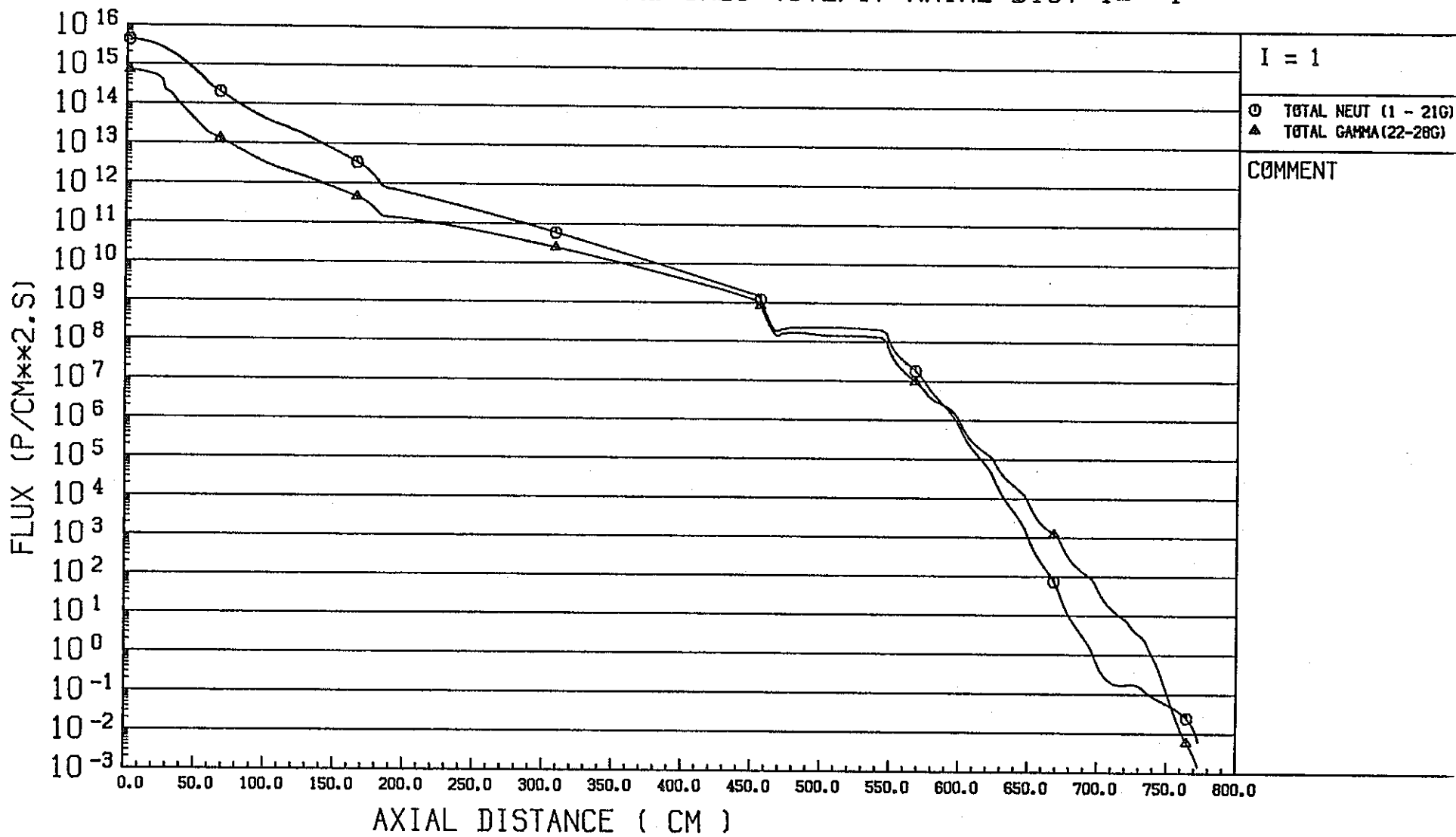


Fig. 2.4.16 (Continued) (2/2)

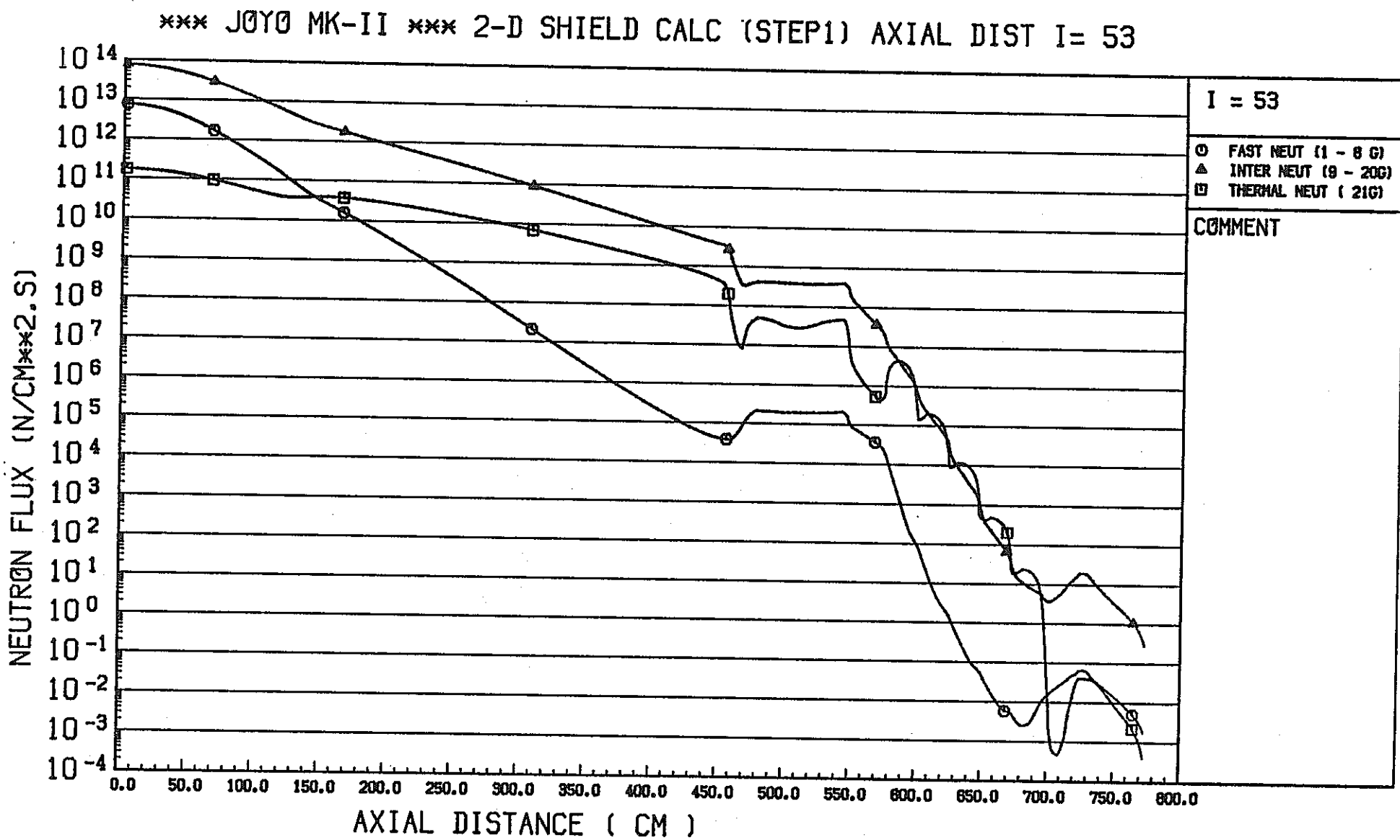


Fig. 2.4.17 Axial Flux Distribution for Step 1 Calculation at R=98.25cm (1/2)

*** JOYO MK-II *** 2-D SHIELD CALC (STEP1) AXIAL DIST I= 53

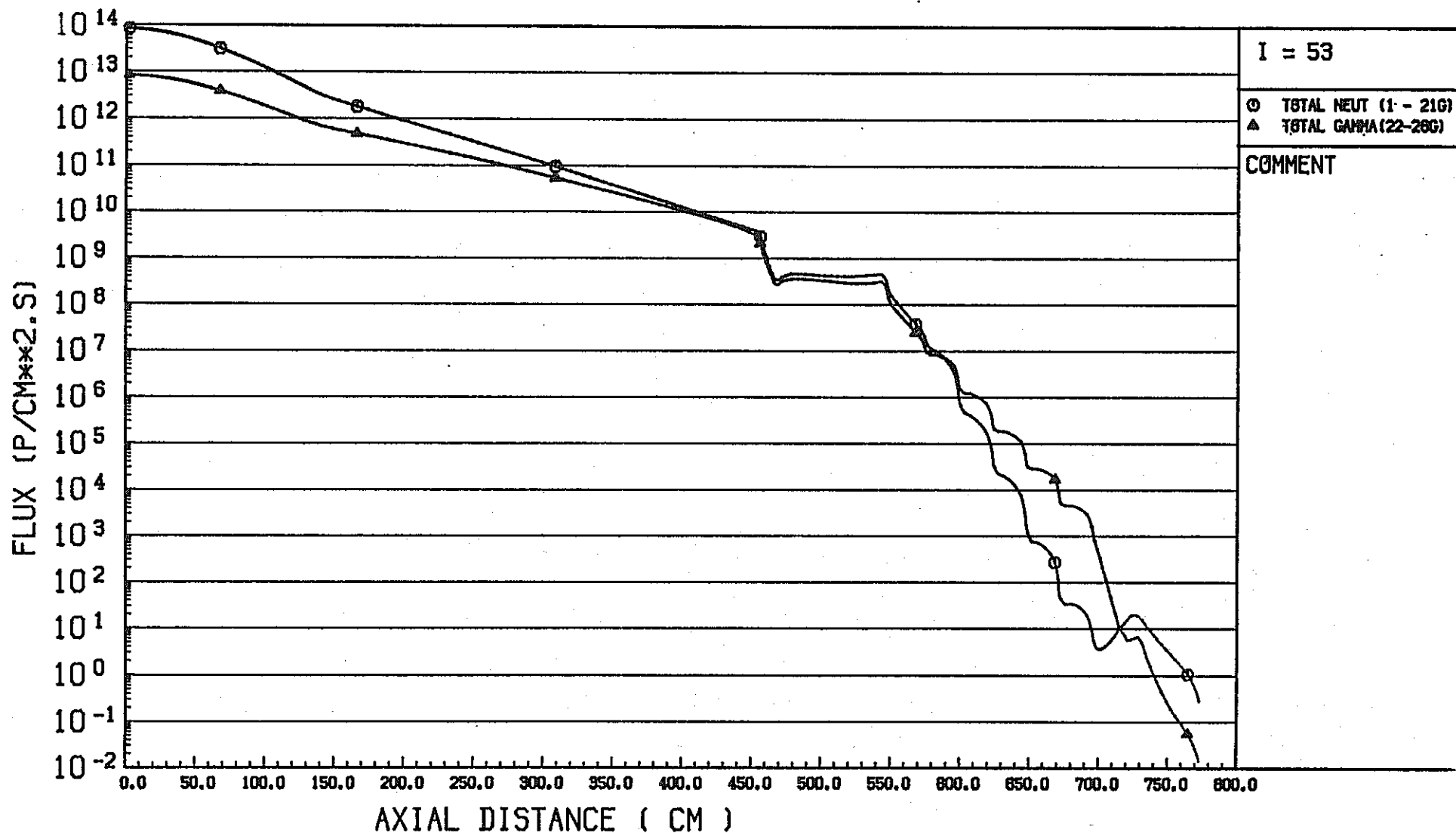


Fig. 2.4.17 (Continued) (2/2)

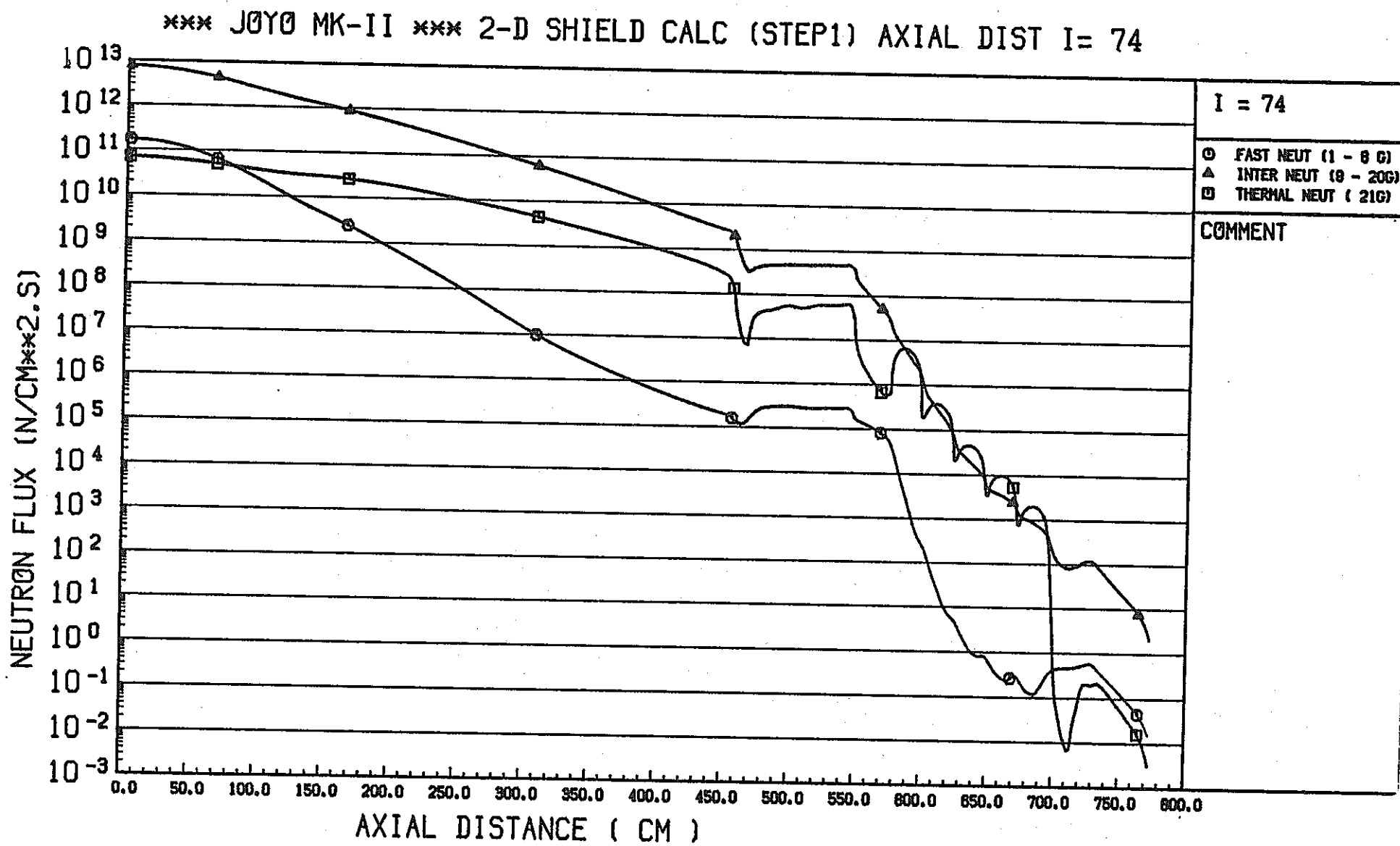


Fig. 2.4.18 Axial Flux Distribution for Step 1 Calculation at R=153.1cm (1/2)

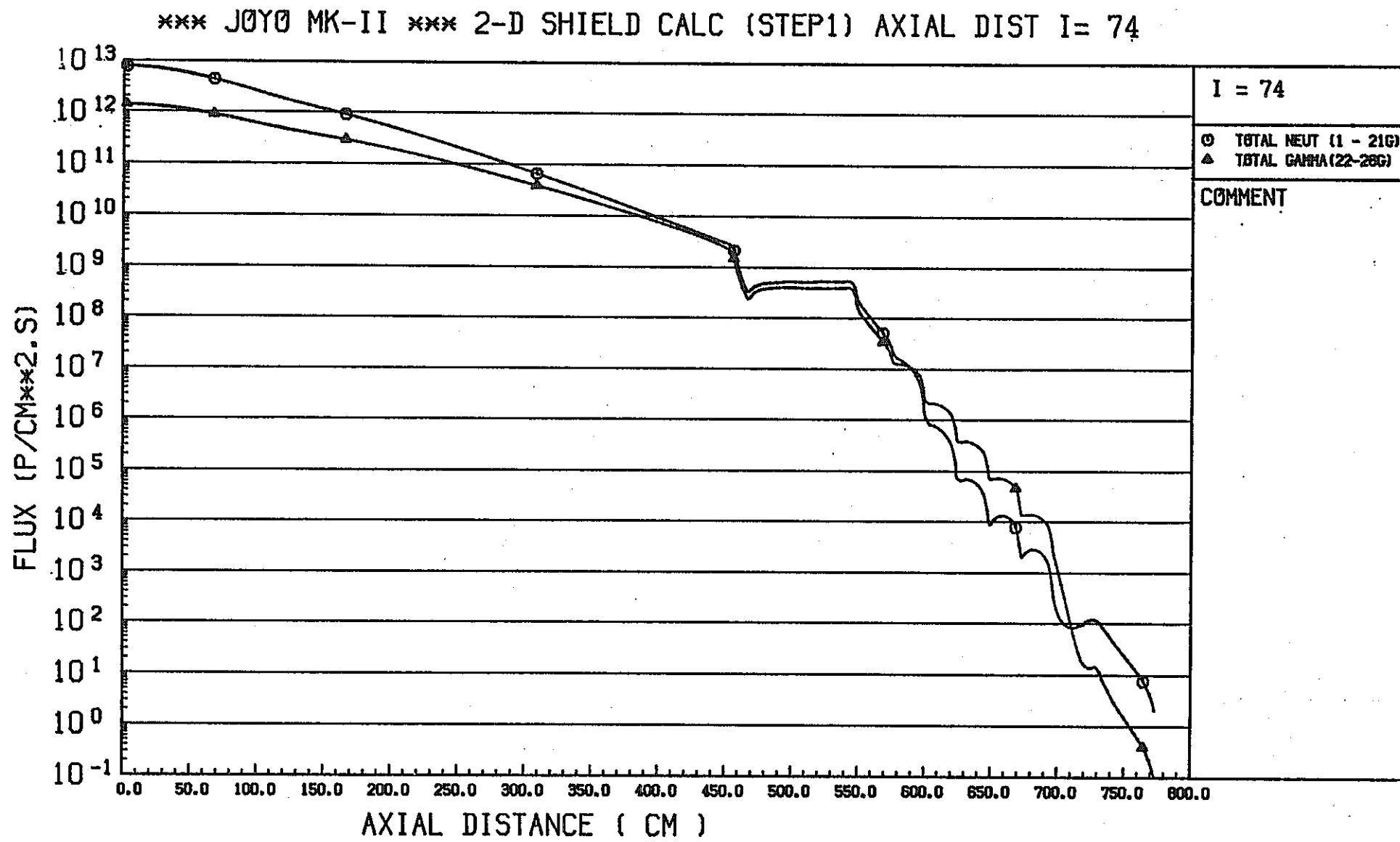


Fig. 2.4.18 (Continued) (2/2)

*** JOYO MK-II *** SHIELD CALC 2-D CALC (STEP1)

N0 1

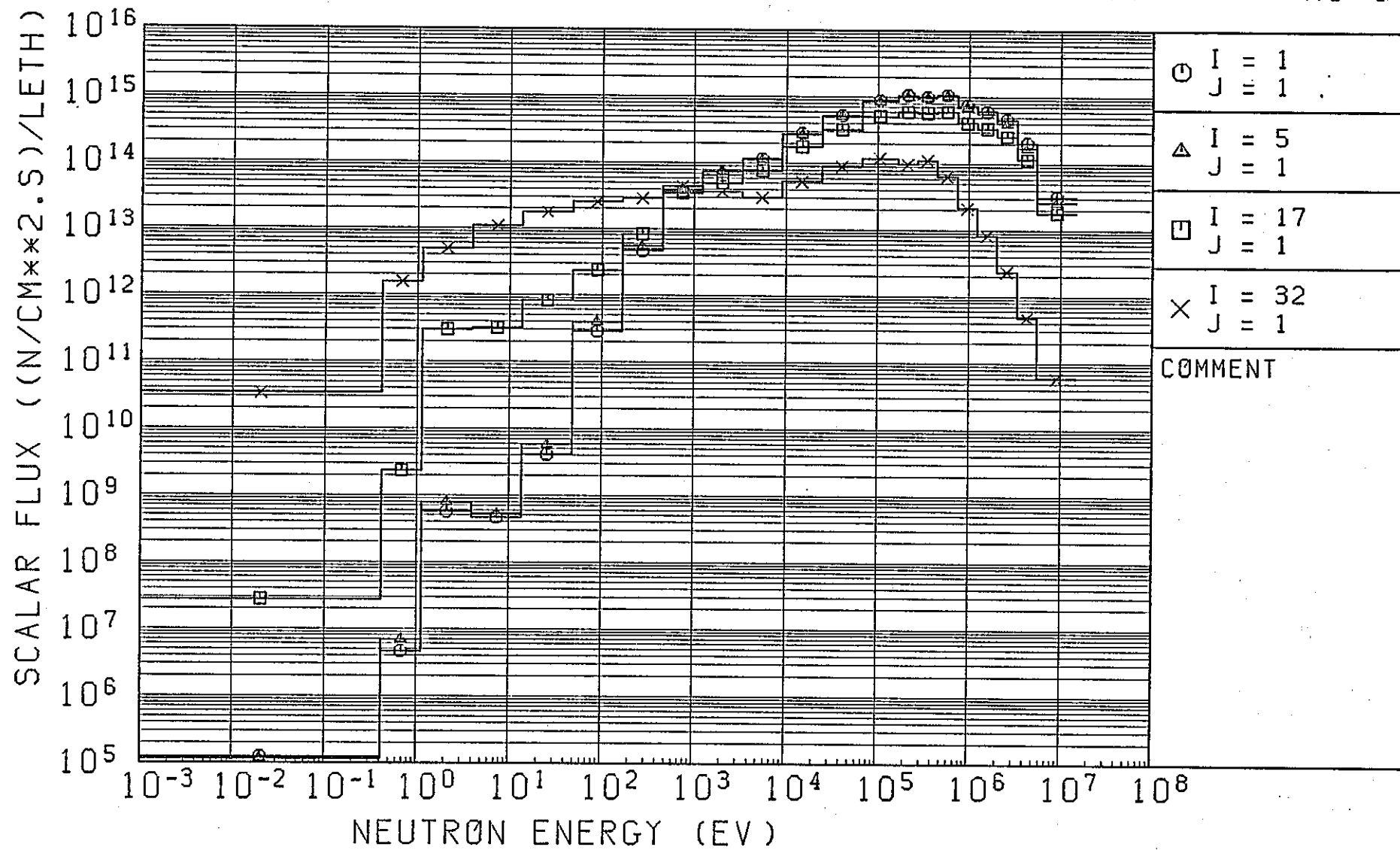


Fig. 2.4.19 Neutron Spectrum from Step 1 Calculation (1/3)

*** JOY0 MK-II *** SHIELD CALC 2-D CALC (STEP1)

NO 3

2 - 90

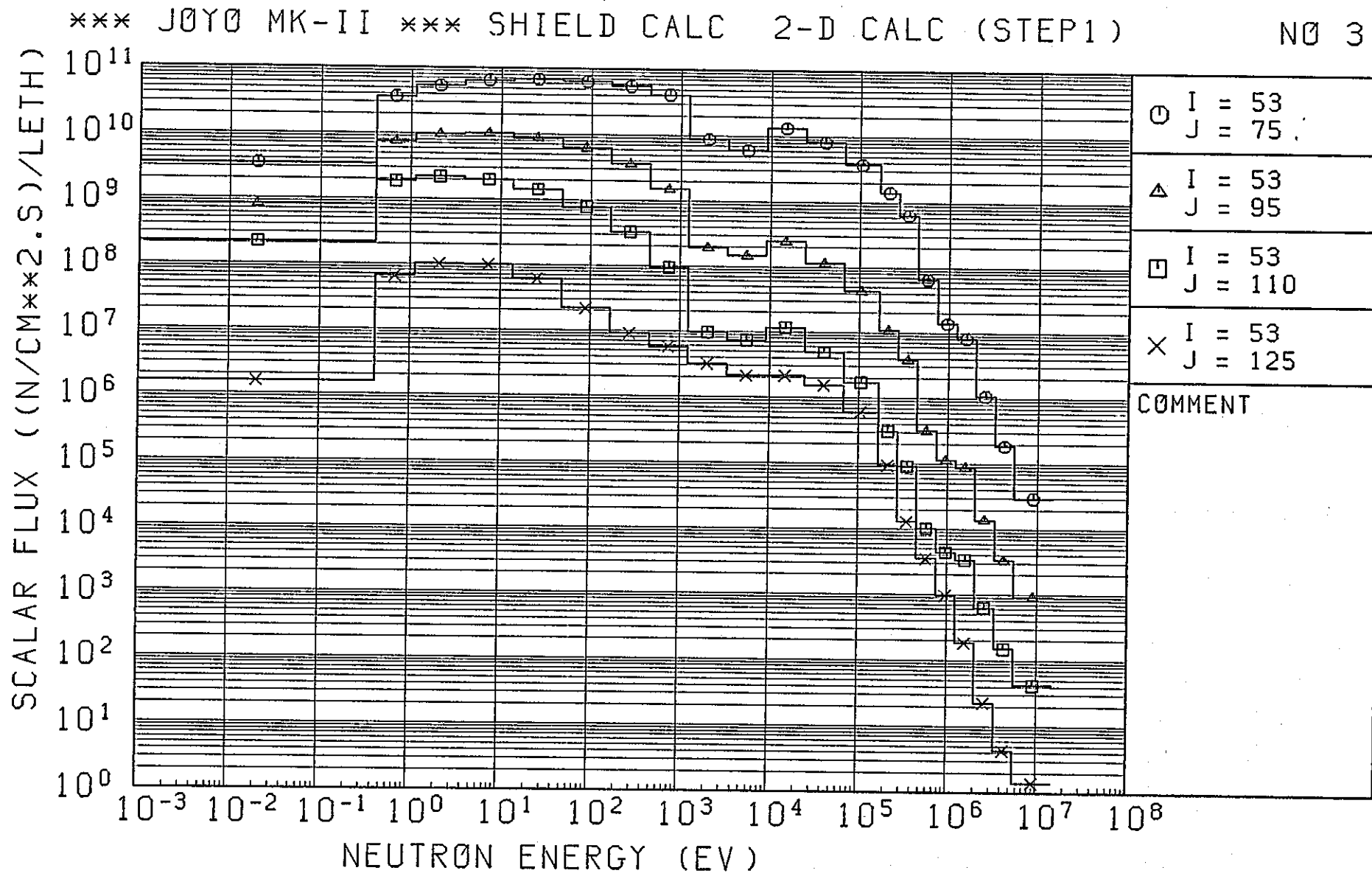


Fig. 2.4.19 (Continued) (2/3)

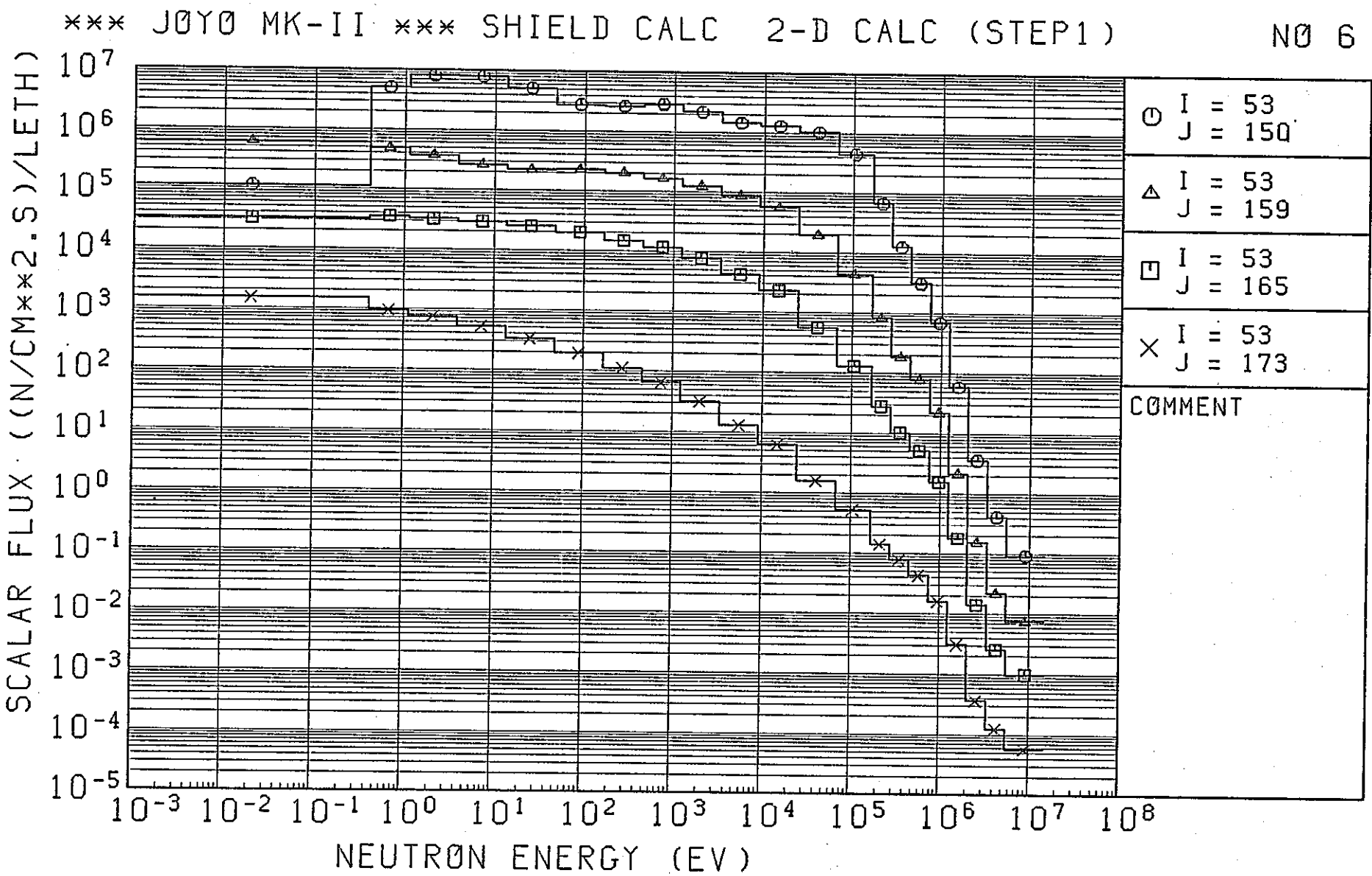


Fig. 2.4.19 (Continued) (3/3)

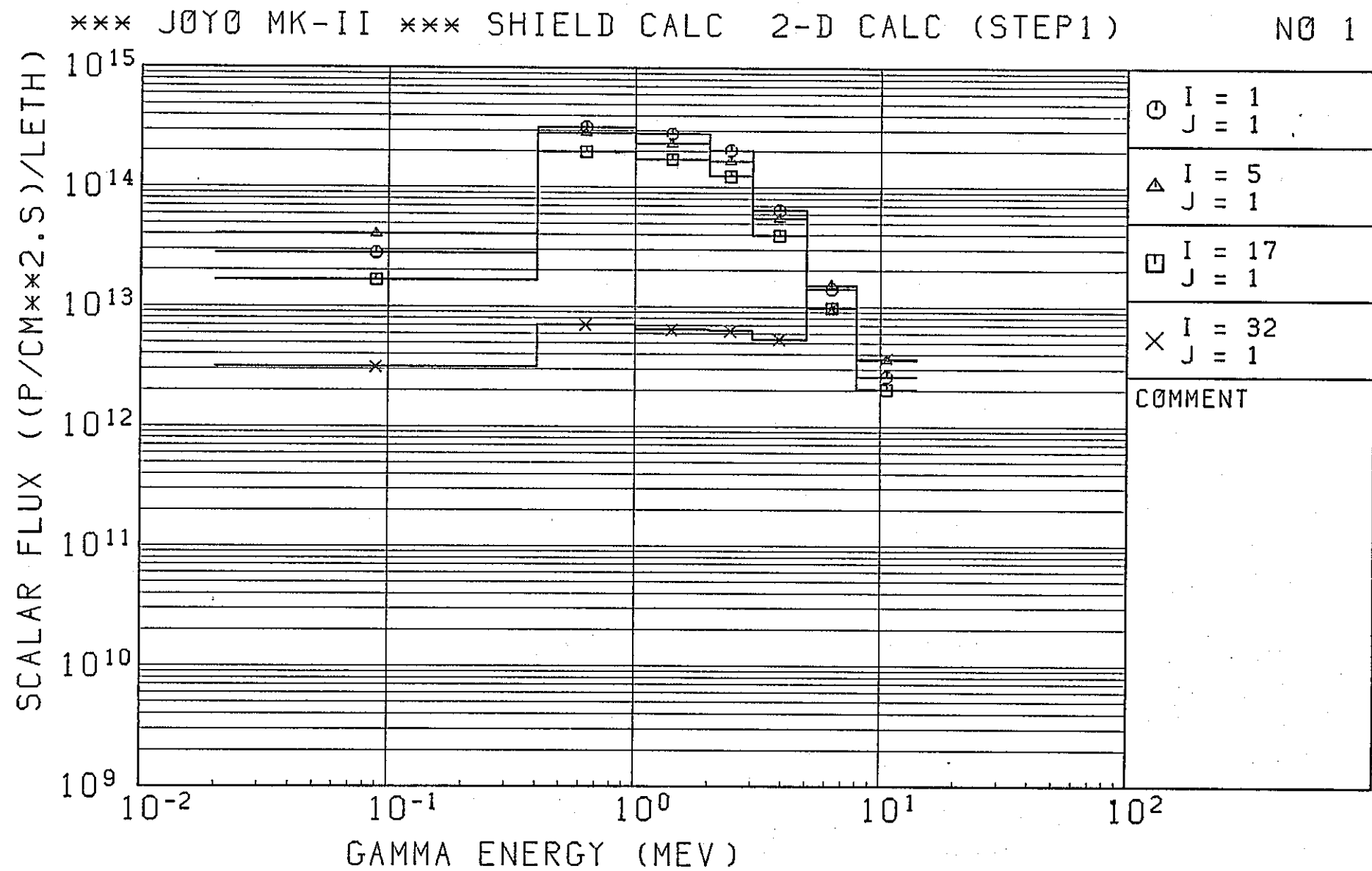


Fig. 2.4.20 Gamma-Ray Spectrum from Step 1 Calculation (1/3)

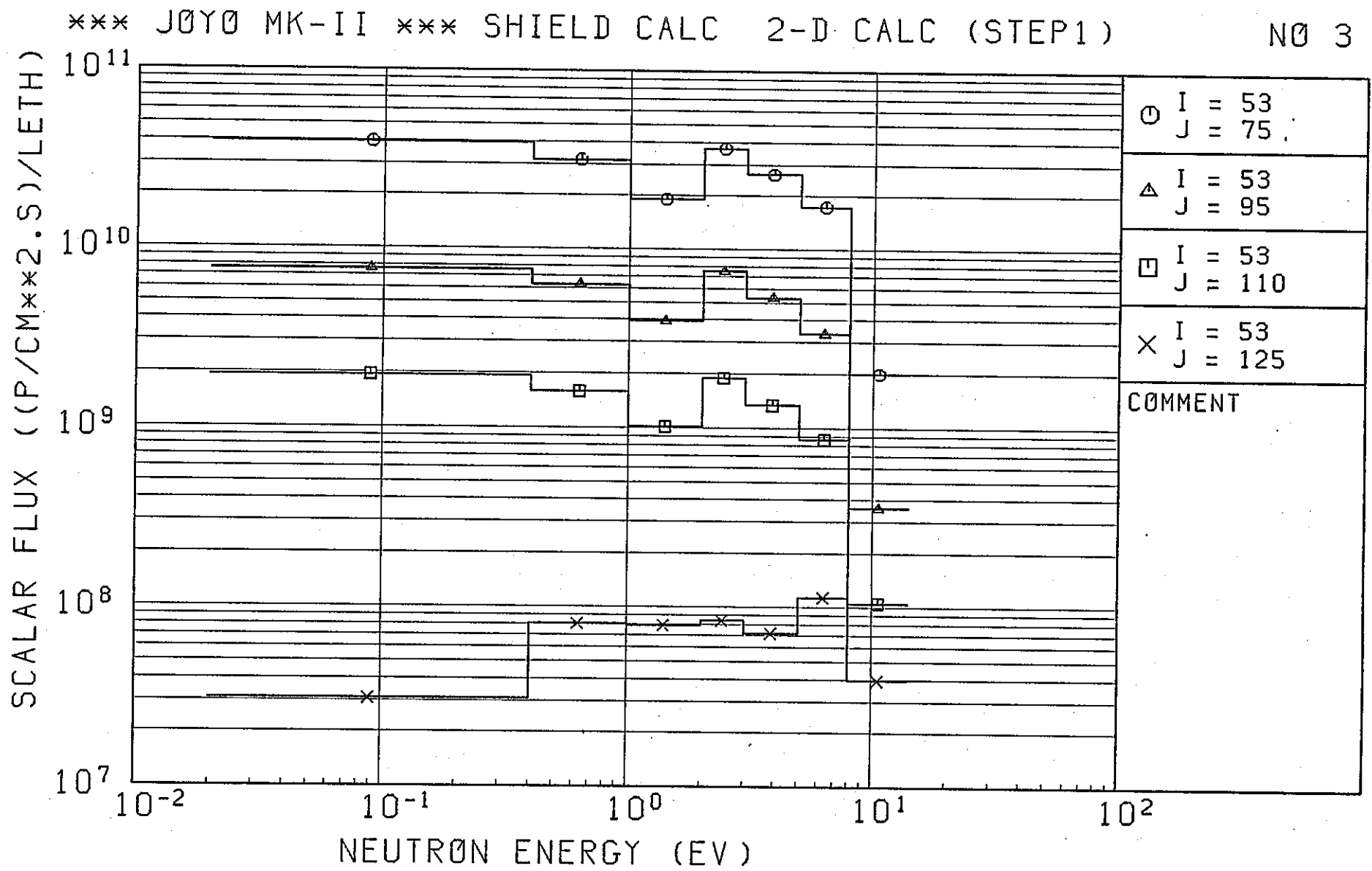


Fig. 2.4.20 (Continued) (2/3)

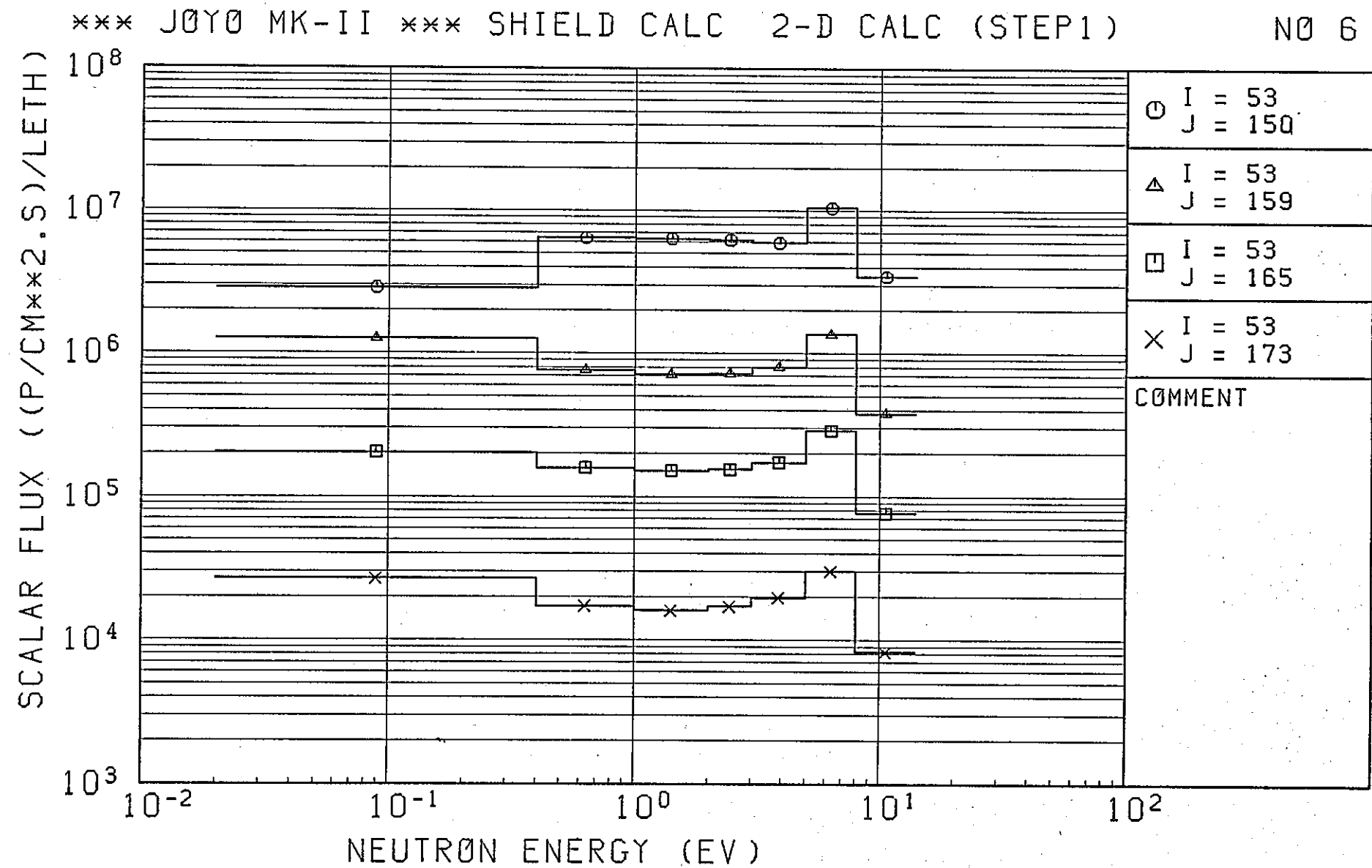


Fig. 2.4.20 (Continued) (3/3)

2.4.2 Step 2 Calculation

The zone map of the step 2 calculation geometry defined in section 2.2 is shown in Fig. 2.4.21 with the description of the zone material compositions shown in Table 2.4.7.

The angular quadrature set used was a biased 124 quadrature set in order to evaluate the annular streaming within good accuracy. This angular quadrature set is a combination of an S70 set for the upper direction and an S30 set for the lower direction. The largest η level was further devived into 11 levels using the 96 th order Gauss quadrature. The angular quadrature are given in Table 2.4.8.

The angular fluxes obtained in the Step 1 calculation were used as the boundary angular surce for the Step 2 calculation. The parameters used in the Step 2 calculation are summarized in Table 2.4.9.

Calculational results were editted in the same form as the Step 1 calculation and shown in Figs. 2.4.22 to 2.4.35.

Table 2.4.7 JOYO MK-II Partial R-Z Materials in Step 2 Calculation

<u>Zone</u>	<u>Material</u>	<u>Vol.Fraction</u>	<u>Zone</u>	<u>Material</u>	<u>Vol.Fraction</u>
1	Sodium	1.0	26	SS-304	1.0
2	Sodium	0.4	27	Heavy Concrete	1.0
	SS-304	0.6			
3	SS-304	1.0	28	Heavy Concrete	1.0
4	Nitrogen Gas	1.0			
5	SS-304	1.0			
6	SS-304	0.04			
7	Nitrogen Gas	1.0			
8	Graphite	1.0			
9	Graphite	1.0			
10	Graphite	1.0			
11	Nitrogen Gas	1.0			
12	Carbon Steel	1.0			
13	Nitrogen Gas	1.0			
14	Carbon Steel	1.0			
15	Carbon Steel	0.43			
16	Ordinary Concrete	1.0			
17	Ordinary Concrete	1.0			
18	Sodium	1.0			
19	Sodium	1.0			
20	Sodium	1.0			
21	Sodium	0.2			
	SS-304	0.8			
22	Sodium	1.0			
23	Sodium	1.0			
24	Nitrogen Gas	1.0			
25	Insulator	0.0833			

Table 2.4.8 Description of 124-Angle Quadrature (1/3)

ANGL	WEIGHT	ETA	MU
1	0.0	-0.9261766E+00	-0.3770773E+00
2	0.4403132E-01	-0.9261766E+00	-0.2666347E+00
3	0.4403132E-01	-0.9261766E+00	0.2666347E+00
4	0.0	-0.6815047E+00	-0.7318072E+00
5	0.3930132E-01	-0.6815047E+00	-0.6815047E+00
6	0.3930170E-01	-0.6815047E+00	-0.2666347E+00
7	0.3930170E-01	-0.6815047E+00	0.2666347E+00
8	0.3930132E-01	-0.6815047E+00	0.6815047E+00
9	0.0	-0.2666347E+00	-0.9637928E+00
10	0.4403132E-01	-0.2666347E+00	-0.9261766E+00
11	0.3930170E-01	-0.2666347E+00	-0.6815047E+00
12	0.4403141E-01	-0.2666347E+00	-0.2666347E+00
13	0.4403141E-01	-0.2666347E+00	0.2666347E+00
14	0.3930170E-01	-0.2666347E+00	0.6815047E+00
15	0.4403132E-01	-0.2666347E+00	0.9261766E+00
16	0.0	0.9996846E+00	-0.2491764E-01
17	0.6639869E-04	0.9996846E+00	-0.2406861E-01
18	0.6639869E-04	0.9996846E+00	-0.1761944E-01
19	0.6639869E-04	0.9996846E+00	-0.6449163E-02
20	0.6639869E-04	0.9996846E+00	0.6449163E-02
21	0.6639869E-04	0.9996846E+00	0.1761944E-01
22	0.6639869E-04	0.9996846E+00	0.2406861E-01
23	0.0	0.9983596E+00	-0.5717116E-01
24	0.1544963E-03	0.9983596E+00	-0.5522310E-01
25	0.1544963E-03	0.9983596E+00	-0.4042612E-01
26	0.1544963E-03	0.9983596E+00	-0.1479698E-01
27	0.1544963E-03	0.9983596E+00	0.1479698E-01
28	0.1544963E-03	0.9983596E+00	0.4042612E-01
29	0.1544963E-03	0.9983596E+00	0.5522310E-01
30	0.0	0.9959770E+00	-0.8955497E-01
31	0.2425599E-03	0.9959770E+00	-0.8650345E-01
32	0.2425599E-03	0.9959770E+00	-0.6332481E-01
33	0.2425599E-03	0.9959770E+00	-0.2317853E-01
34	0.2425599E-03	0.9959770E+00	0.2317853E-01
35	0.2425599E-03	0.9959770E+00	0.6332481E-01
36	0.2425599E-03	0.9959770E+00	0.8650345E-01
37	0.0	0.9925392E+00	-0.1218870E+00
38	0.3303774E-03	0.9925392E+00	-0.1177338E+00
39	0.3303774E-03	0.9925392E+00	-0.8618718E-01
40	0.3303774E-03	0.9925392E+00	-0.3154670E-01
41	0.3303774E-03	0.9925392E+00	0.3154670E-01
42	0.3303774E-03	0.9925392E+00	0.8618718E-01
43	0.3303774E-03	0.9925392E+00	0.1177338E+00
44	0.0	0.9880494E+00	-0.1541064E+00
45	0.4178479E-03	0.9880494E+00	-0.1488554E+00

Tabel 2.4.8 (Continued) (2/3)

ANGL	WEIGHT	ETA	MU
4 6	0.4178479E-0 3	0.9880494E+0 0	-0.1089697E+0 0
4 7	0.4178479E-0 3	0.9880494E+0 0	-0.3988570E-0 1
4 8	0.4178479E-0 3	0.9880494E+0 0	0.3988570E-0 1
4 9	0.4178479E-0 3	0.9880494E+0 0	0.1089697E+0 0
5 0	0.4178479E-0 3	0.9880494E+0 0	0.1488554E+0 0
5 1	0.0	0.9825125E+0 0	-0.1861706E+0 0
5 2	0.5048765E-0 3	0.9825125E+0 0	-0.1798270E+0 0
5 3	0.5048765E-0 3	0.9825125E+0 0	-0.1316425E+0 0
5 4	0.5048765E-0 3	0.9825125E+0 0	-0.4818450E-0 1
5 5	0.5048765E-0 3	0.9825125E+0 0	0.4818450E-0 1
5 6	0.5048765E-0 3	0.9825125E+0 0	0.1316425E+0 0
5 7	0.5048765E-0 3	0.9825125E+0 0	0.1798270E+0 0
5 8	0.0	0.9759346E+0 0	-0.2180419E+0 0
5 9	0.5913691E-0 3	0.9759346E+0 0	-0.2106123E+0 0
6 0	0.5913691E-0 3	0.9759346E+0 0	-0.1541789E+0 0
6 1	0.5913691E-0 3	0.9759346E+0 0	-0.5643340E-0 1
6 2	0.5913691E-0 3	0.9759346E+0 0	0.5643340E-0 1
6 3	0.5913691E-0 3	0.9759346E+0 0	0.1541789E+0 0
6 4	0.5913691E-0 3	0.9759346E+0 0	0.2106123E+0 0
6 5	0.0	0.9683222E+0 0	-0.2496849E+0 0
6 6	0.6772368E-0 3	0.9683222E+0 0	-0.2411771E+0 0
6 7	0.6772368E-0 3	0.9683222E+0 0	-0.1765539E+0 0
6 8	0.6772368E-0 3	0.9683222E+0 0	-0.6462312E-0 1
6 9	0.6772368E-0 3	0.9683222E+0 0	0.6462312E-0 1
7 0	0.6772368E-0 3	0.9683222E+0 0	0.1765539E+0 0
7 1	0.6772368E-0 3	0.9683222E+0 0	0.2411771E+0 0
7 2	0.0	0.9596838E+0 0	-0.2810649E+0 0
7 3	0.7623853E-0 3	0.9596838E+0 0	-0.2714880E+0 0
7 4	0.7623853E-0 3	0.9596838E+0 0	-0.1987430E+0 0
7 5	0.7623853E-0 3	0.9596838E+0 0	-0.7274497E-0 1
7 6	0.7623853E-0 3	0.9596838E+0 0	0.7274497E-0 1
7 7	0.7623853E-0 3	0.9596838E+0 0	0.1987430E+0 0
7 8	0.7623853E-0 3	0.9596838E+0 0	0.2714880E+0 0
7 9	0.0	0.9500282E+0 0	-0.3121488E+0 0
8 0	0.8467271E-0 3	0.9500282E+0 0	-0.3015126E+0 0
8 1	0.8467271E-0 3	0.9500282E+0 0	-0.2207226E+0 0
8 2	0.8467271E-0 3	0.9500282E+0 0	-0.8078998E-0 1
8 3	0.8467271E-0 3	0.9500282E+0 0	0.8078998E-0 1
8 4	0.8467271E-0 3	0.9500282E+0 0	0.2207226E+0 0
8 5	0.8467271E-0 3	0.9500282E+0 0	0.3015126E+0 0
8 6	0.0	0.9393659E+0 0	-0.3429025E+0 0
8 7	0.9616145E-0 3	0.9393659E+0 0	-0.3312184E+0 0
8 8	0.9616145E-0 3	0.9393659E+0 0	-0.2424688E+0 0
8 9	0.9616145E-0 3	0.9393659E+0 0	-0.8874965E-0 1
9 0	0.9616145E-0 3	0.9393659E+0 0	0.8874965E-0 1
9 1	0.9616145E-0 3	0.9393659E+0 0	0.2424688E+0 0

Table 2.4.8 (Continued) (3/3)

ANGL	WEIGHT	ETA	MU
9 2	0.9 6 1 6 1 4 5 E-0 3	0.9 3 9 3 6 5 9 E+0 0	0.3 3 1 2 1 8 4 E+0 0
9 3	0.0	0.8 6 5 0 5 8 9 E+0 0	-0.5 0 1 6 6 0 6 E+0 0
9 4	0.2 4 4 4 1 9 5 E-0 1	0.8 6 5 0 5 8 9 E+0 0	-0.4 3 3 3 9 2 9 E+0 0
9 5	0.1 2 9 2 0 8 8 E-0 1	0.8 6 5 0 5 8 9 E+0 0	-0.1 4 8 8 7 3 3 E+0 0
9 6	0.1 2 9 2 0 8 8 E-0 1	0.8 6 5 0 5 8 9 E+0 0	0.1 4 8 8 7 3 3 E+0 0
9 7	0.2 4 4 4 1 9 5 E-0 1	0.8 6 5 0 5 8 9 E+0 0	0.4 3 3 3 9 2 9 E+0 0
9 8	0.0	0.6 7 9 4 0 6 8 E+0 0	-0.7 3 3 7 5 5 4 E+0 0
9 9	0.2 7 0 1 0 8 4 E-0 1	0.6 7 9 4 0 6 8 E+0 0	-0.6 7 9 4 0 6 8 E+0 0
1 0 0	0.8 5 4 9 8 4 3 E-0 2	0.6 7 9 4 0 6 8 E+0 0	-0.4 3 3 3 9 2 9 E+0 0
1 0 1	0.1 9 2 1 0 4 2 E-0 1	0.6 7 9 4 0 6 8 E+0 0	-0.1 4 8 8 7 3 3 E+0 0
1 0 2	0.1 9 2 1 0 4 2 E-0 1	0.6 7 9 4 0 6 8 E+0 0	0.1 4 8 8 7 3 3 E+0 0
1 0 3	0.8 5 4 9 8 4 3 E-0 2	0.6 7 9 4 0 6 8 E+0 0	0.4 3 3 3 9 2 9 E+0 0
1 0 4	0.2 7 0 1 0 8 4 E-0 1	0.6 7 9 4 0 6 8 E+0 0	0.6 7 9 4 0 6 8 E+0 0
1 0 5	0.0	0.4 3 3 3 9 2 9 E+0 0	-0.9 0 1 1 9 9 8 E+0 0
1 0 6	0.2 4 4 4 1 9 5 E-0 1	0.4 3 3 3 9 2 9 E+0 0	-0.8 6 5 0 5 8 9 E+0 0
1 0 7	0.8 5 4 9 8 4 3 E-0 2	0.4 3 3 3 9 2 9 E+0 0	-0.6 7 9 4 0 6 8 E+0 0
1 0 8	0.2 7 4 6 8 2 4 E-0 1	0.4 3 3 3 9 2 9 E+0 0	-0.4 3 3 3 9 2 9 E+0 0
1 0 9	0.6 8 5 6 6 2 8 E-0 2	0.4 3 3 3 9 2 9 E+0 0	-0.1 4 8 8 7 3 3 E+0 0
1 1 0	0.6 8 5 6 6 2 8 E-0 2	0.4 3 3 3 9 2 9 E+0 0	0.1 4 8 8 7 3 3 E+0 0
1 1 1	0.2 7 4 6 8 2 4 E-0 1	0.4 3 3 3 9 2 9 E+0 0	0.4 3 3 3 9 2 9 E+0 0
1 1 2	0.8 5 4 9 8 4 3 E-0 2	0.4 3 3 3 9 2 9 E+0 0	0.6 7 9 4 0 6 8 E+0 0
1 1 3	0.2 4 4 4 1 9 5 E-0 1	0.4 3 3 3 9 2 9 E+0 0	0.8 6 5 0 5 8 9 E+0 0
1 1 4	0.0	0.1 4 8 8 7 3 3 E+0 0	-0.9 8 8 8 5 1 5 E+0 0
1 1 5	0.1 6 6 6 7 6 7 E-0 1	0.1 4 8 8 7 3 3 E+0 0	-0.9 7 3 9 0 2 5 E+0 0
1 1 6	0.1 2 9 2 0 8 8 E-0 1	0.1 4 8 8 7 3 3 E+0 0	-0.8 6 5 0 5 8 9 E+0 0
1 1 7	0.1 9 2 1 0 4 2 E-0 1	0.1 4 8 8 7 3 3 E+0 0	-0.6 7 9 4 0 6 8 E+0 0
1 1 8	0.6 8 5 6 6 2 8 E-0 2	0.1 4 8 8 7 3 3 E+0 0	-0.4 3 3 3 9 2 9 E+0 0
1 1 9	0.1 8 2 2 4 8 9 E-0 1	0.1 4 8 8 7 3 3 E+0 0	-0.1 4 8 8 7 3 3 E+0 0
1 2 0	0.1 8 2 2 4 8 9 E-0 1	0.1 4 8 8 7 3 3 E+0 0	0.1 4 8 8 7 3 3 E+0 0
1 2 1	0.6 8 5 6 6 2 8 E-0 2	0.1 4 8 8 7 3 3 E+0 0	0.4 3 3 3 9 2 9 E+0 0
1 2 2	0.1 9 2 1 0 4 2 E-0 1	0.1 4 8 8 7 3 3 E+0 0	0.6 7 9 4 0 6 8 E+0 0
1 2 3	0.1 2 9 2 0 8 8 E-0 1	0.1 4 8 8 7 3 3 E+0 0	0.8 6 5 0 5 8 9 E+0 0
1 2 4	0.1 6 6 6 7 6 7 E-0 1	0.1 4 8 8 7 3 3 E+0 0	0.9 7 3 9 0 2 5 E+0 0

Table 2.4.9 Description of Input Variables (Step 2)

Program DOT 3.5

Geometry type Two-dimensional cylinder

Problem type Fixed exterior boundary source

Number of energy groups IGM = 21 + 7

Number of radial intervals IM = 96

Number of axial intervals JM = 142

Number of angles A04 = 109 + 15

Order of scattering A03 = 3

Flux calculational model Weighted difference mode

Convergence Pointwise scaling, G06 = 0.01

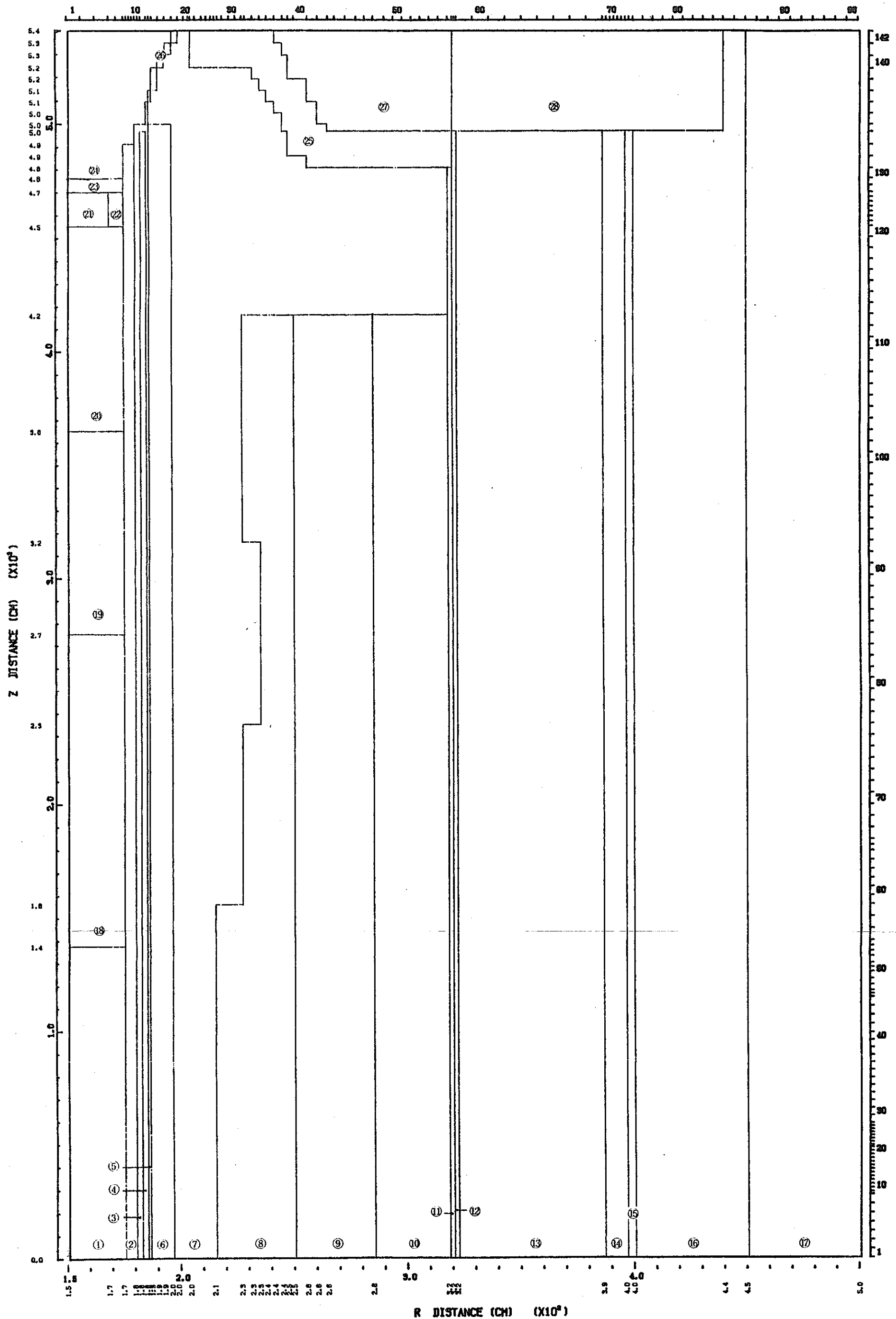
Boundary conditions

Left Fixed exterior boundary source

Right Vacuum

Bottom Reflection

Top Vacuum



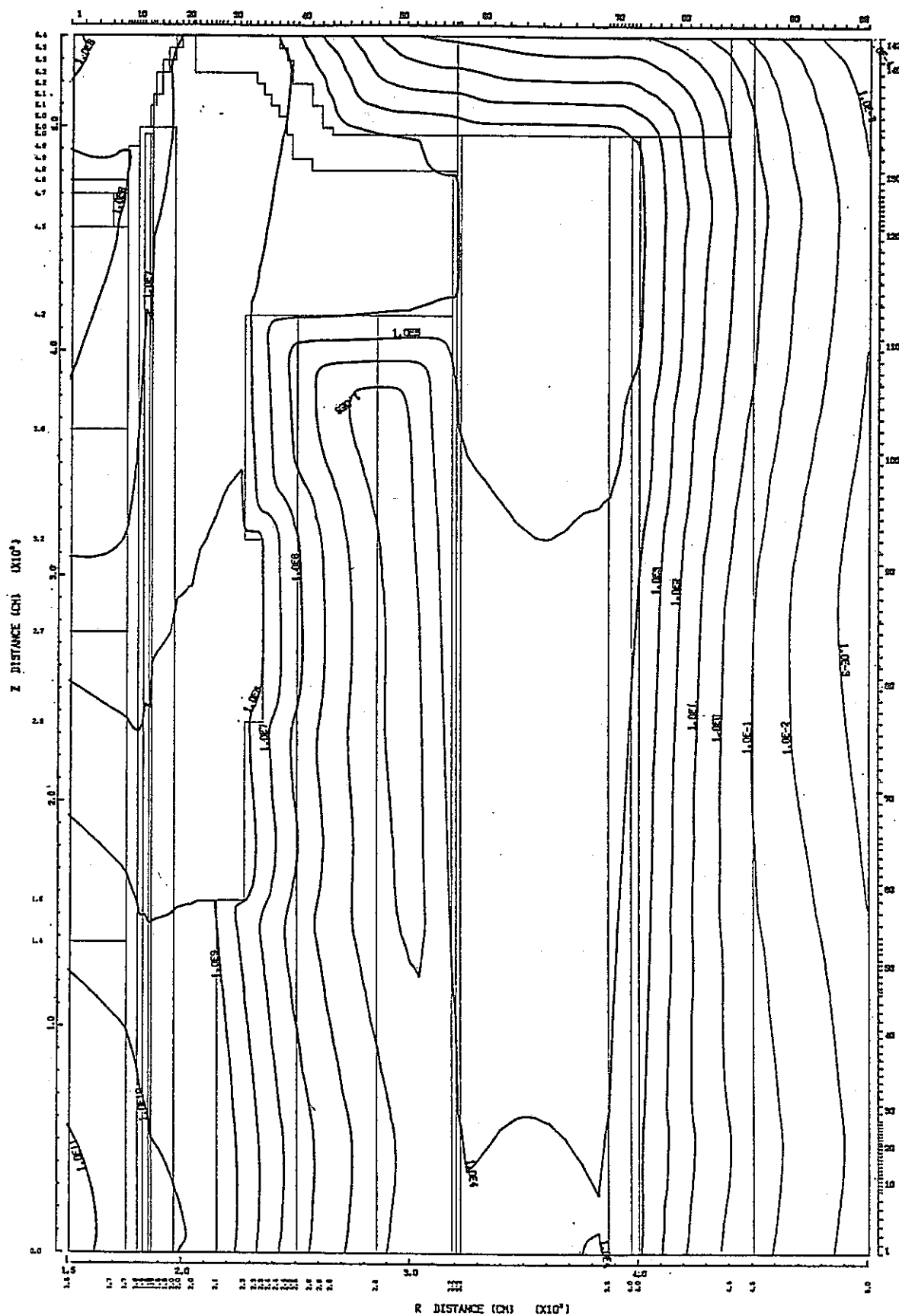


Fig. 2.4.22 Fast Neutron Isoflux Contours for Step 2 Calculation
 FAST NEUTRON FLUX (N/CM^{**2.S}) 1.4918E+07 - 1.6573E+05 (EV) (GROUP 1-8)

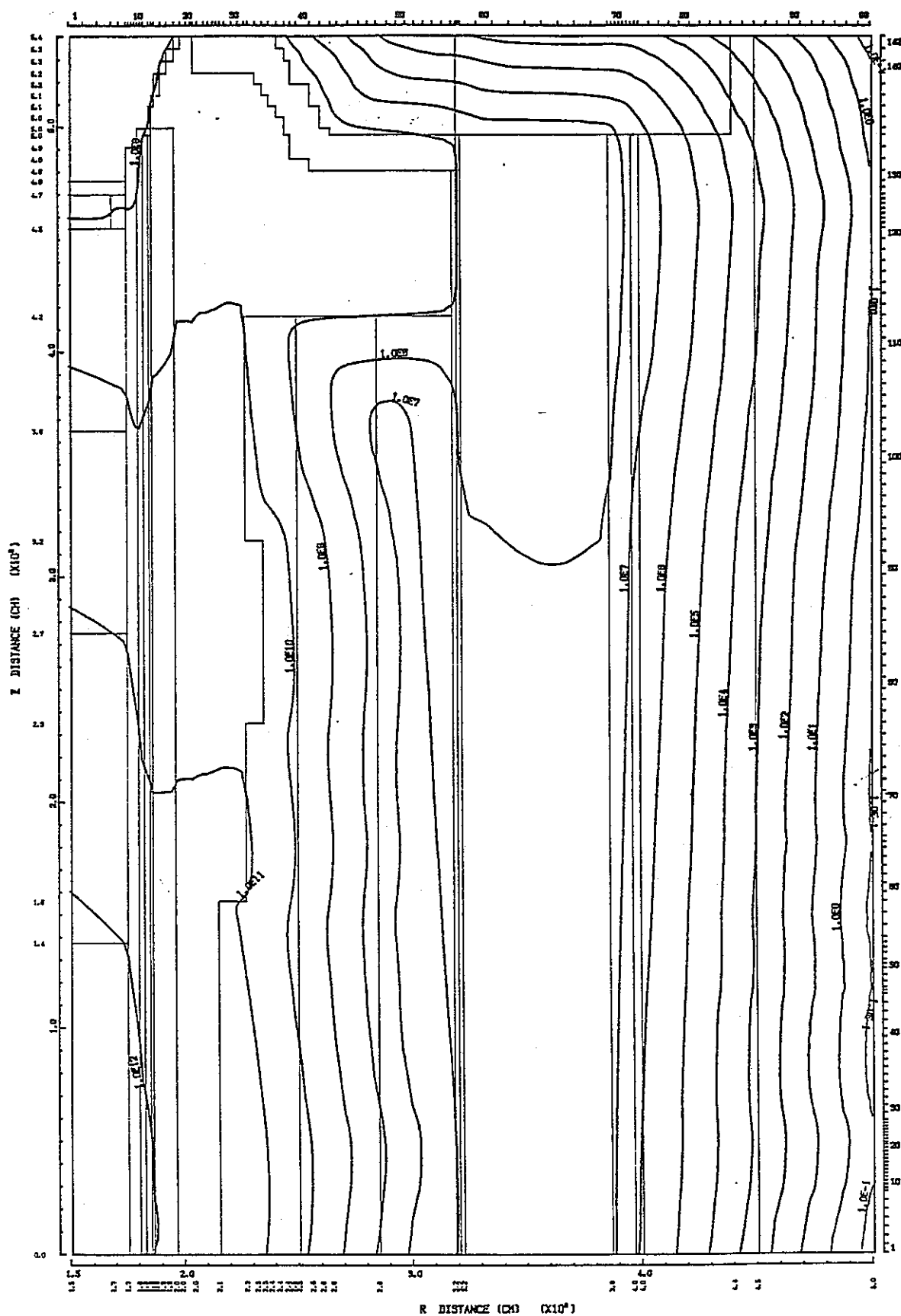


Fig. 2.4.23 Intermediate Neutron Isoflux Contours for Step 2 Calculation
 INTER NEUTRON FLUX (N/CM**2.S) 1.6573E+05 - 4.1399E-01 (EV) (GROUP 9-20)

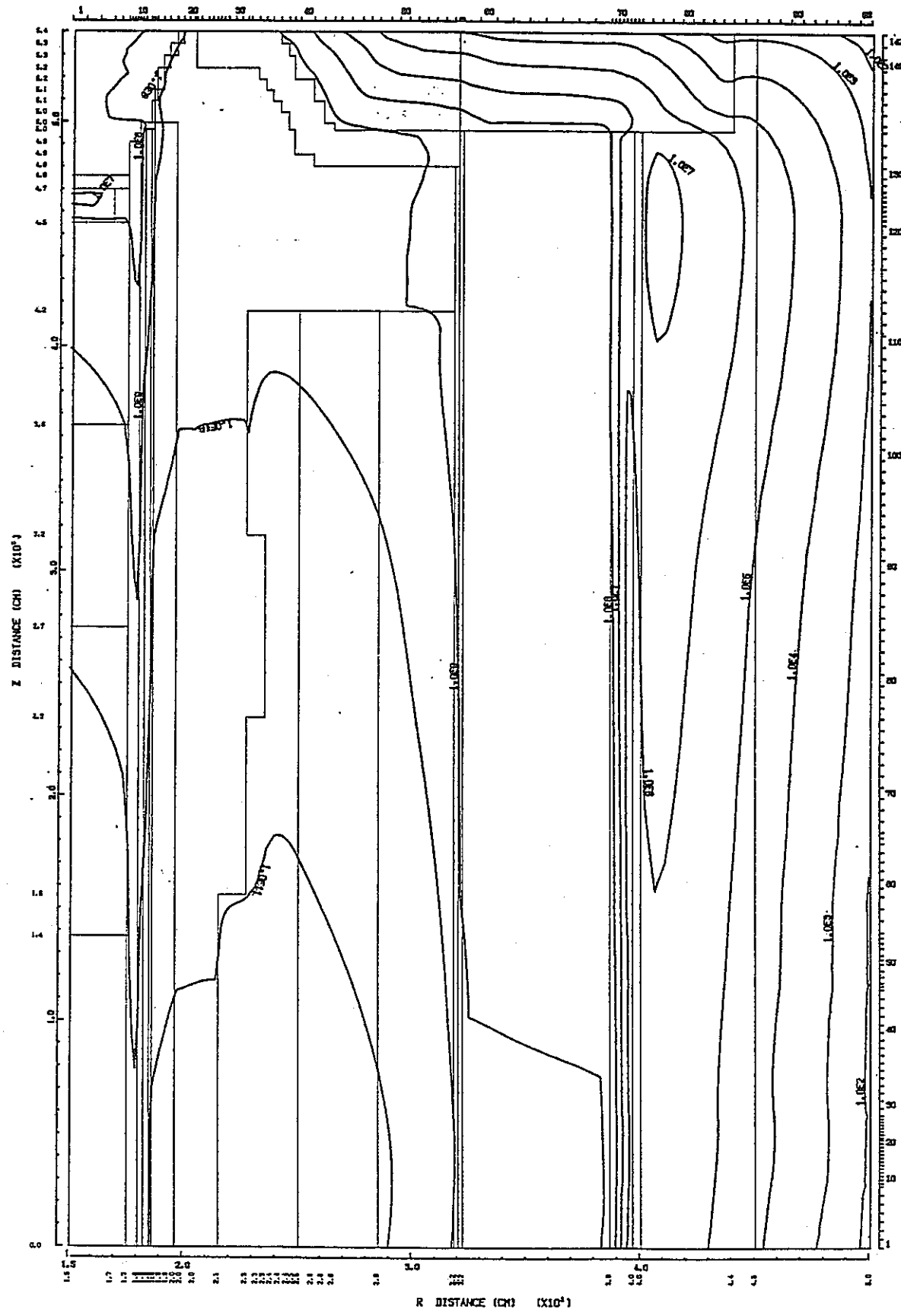


Fig. 2.4.24 Thermal Neutron Isoflux Contours for Step 2 Calculation
 NEUTRON FLUX (N/CM**2.S) 4.1399E-01 - 1.0000E-03 (EV) (GROUP 21)

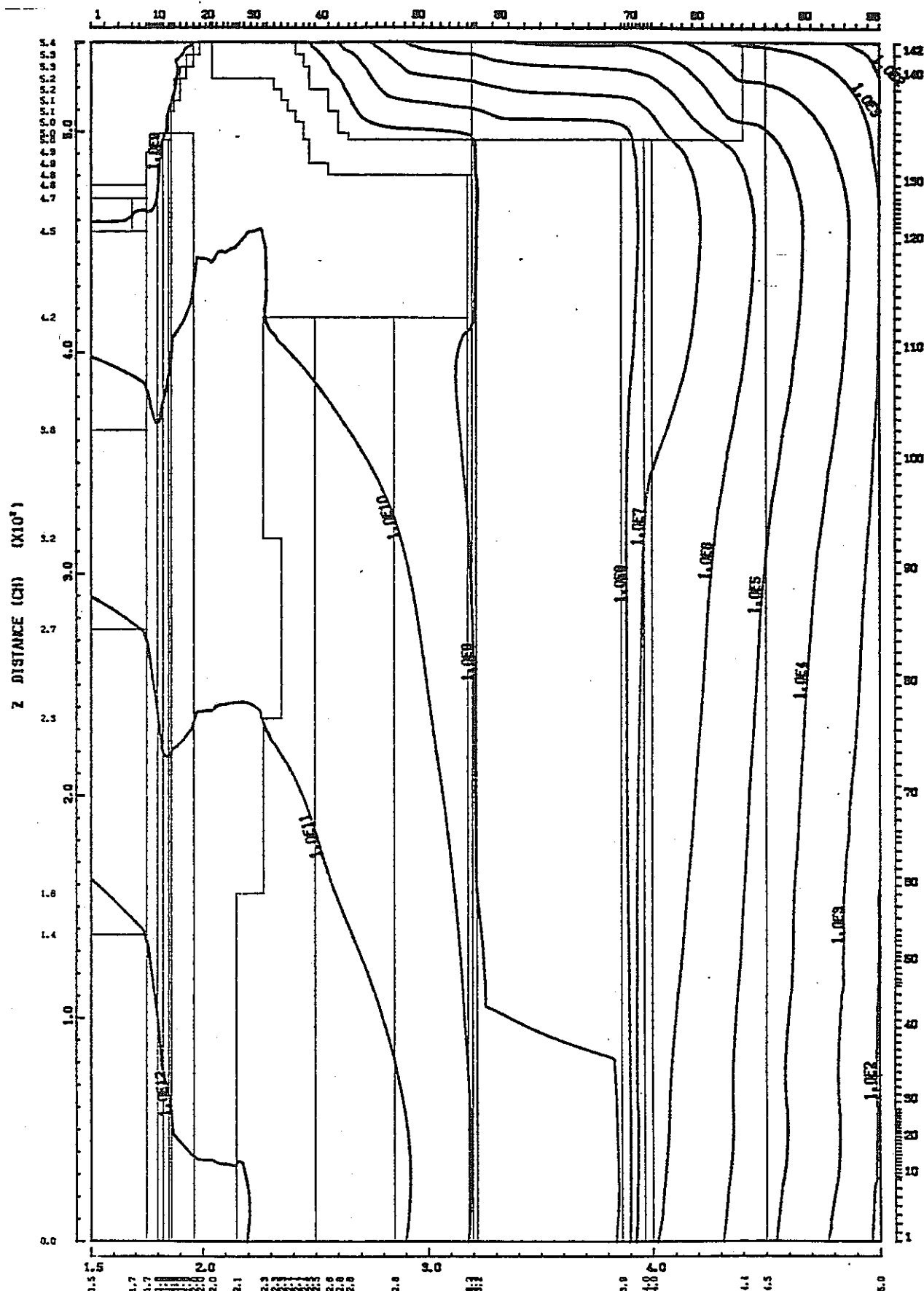


Fig. 2.4.25 Total Neutron Isoflux Contours for Step 2 Calculation
 TOTAL NEUTRON FLUX (N/CM**2.S) 1.4918E+07 - 1.0000E-03 (EV) (GROUP 1-19)



Fig. 2.4.26 Total Gamma-Ray Isoflux Contours for Step 2 Calculation
 TOTAL GAMMA FLUX (P/CM**2.S) 14.0 - 0.02 (MEV) (GROUP 22-28)

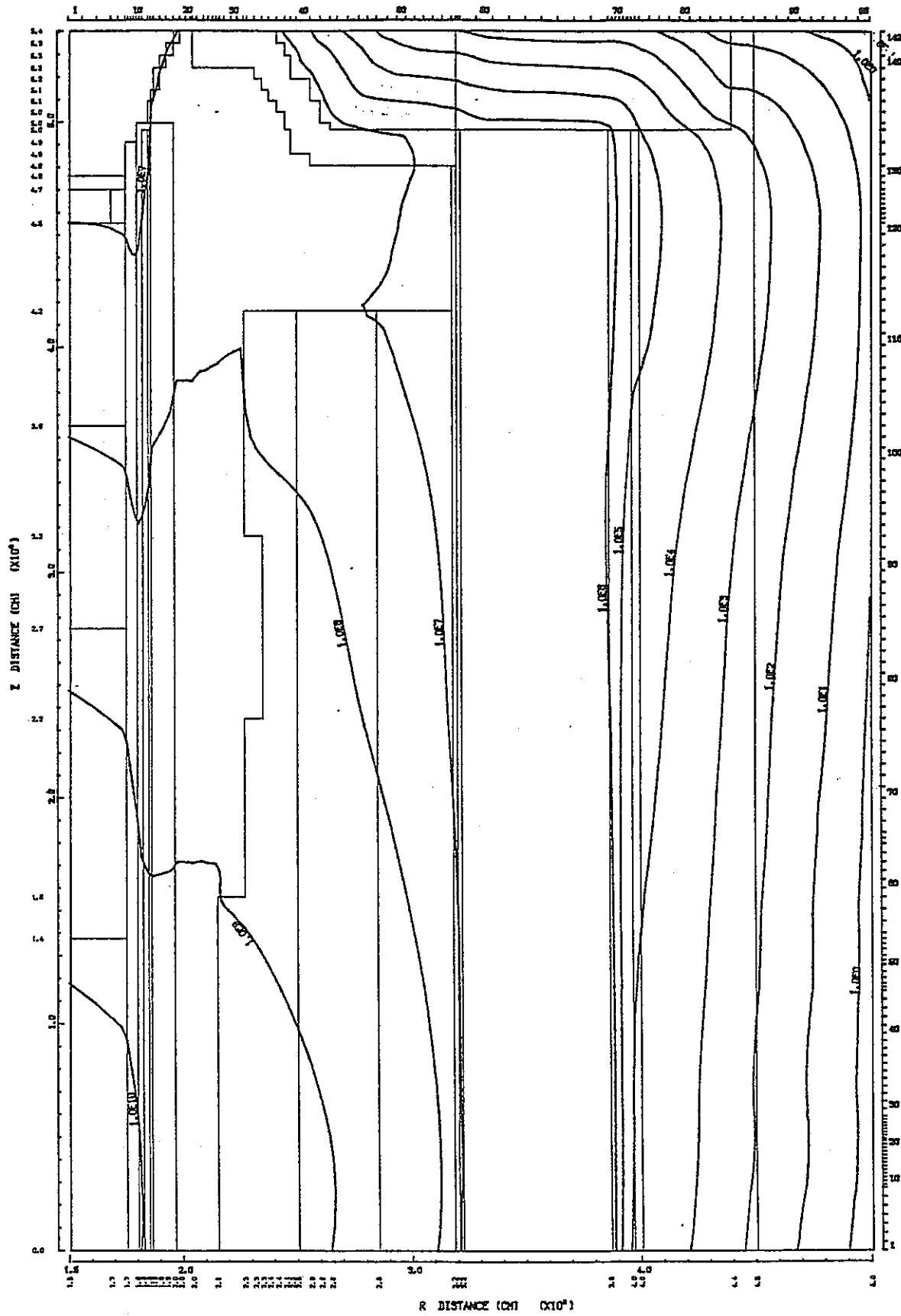


Fig. 2.4.27 Neutron Isodose Contours for Step 2 Calculation
 NEUTRON DOSE RATE (MREM/HOUR) $1.4918E+07 - 1.0000E-03$ (EV) (GROUP 1-21)



Fig. 2.4.28 Gamma-Ray Isodose Contours for Step 2 Calculation
 GAMMA DOSE RATE (MREM/HOUR) 14.0 - 0.02 (MEV) (GROUP 22-28)

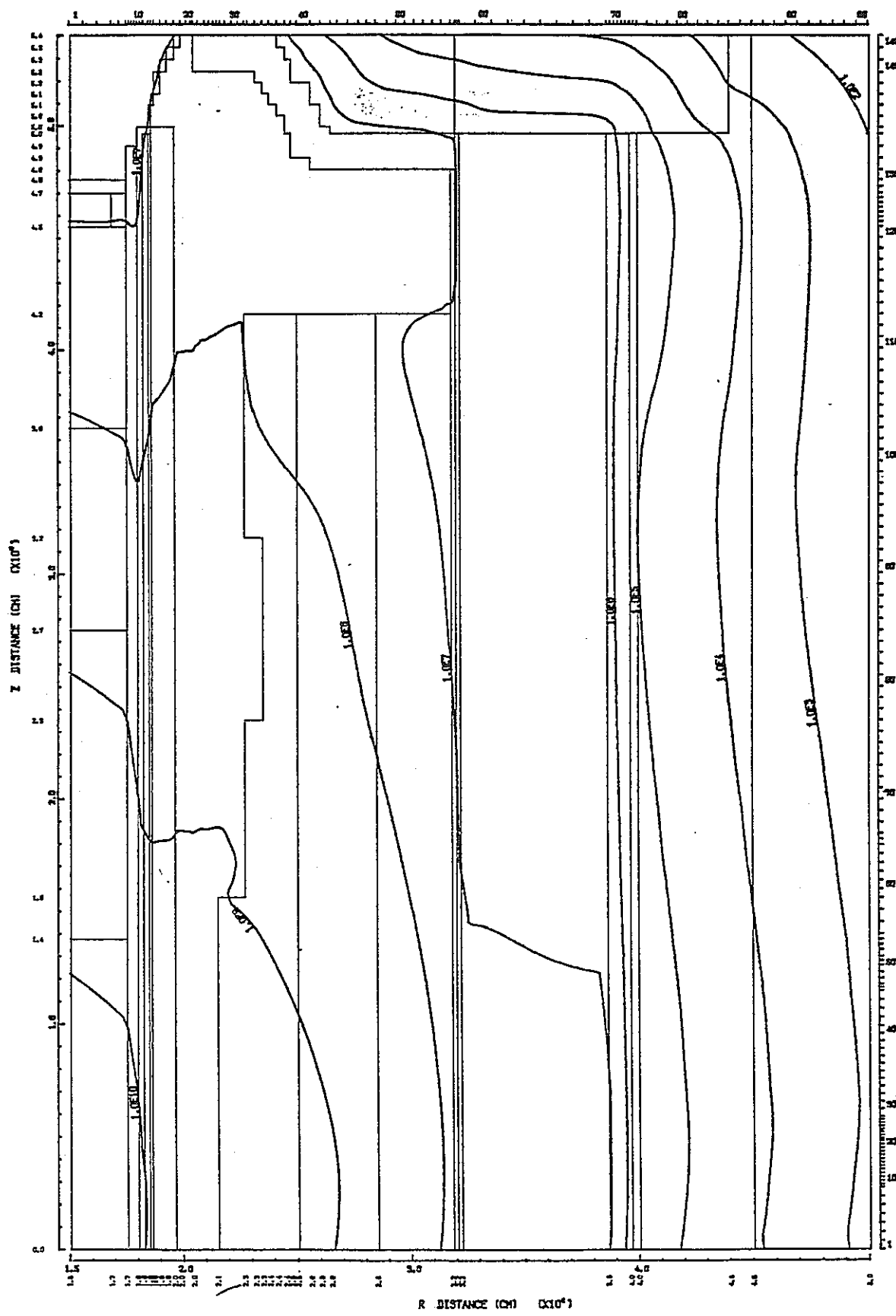


Fig. 2.4.29 Total Isodose Contours for Step 2 Calculation
 TOTAL DOSE RATE (MREM/HOUR) NEUTRON DOSE + GAMMA DOSE (GROUP 1-28)

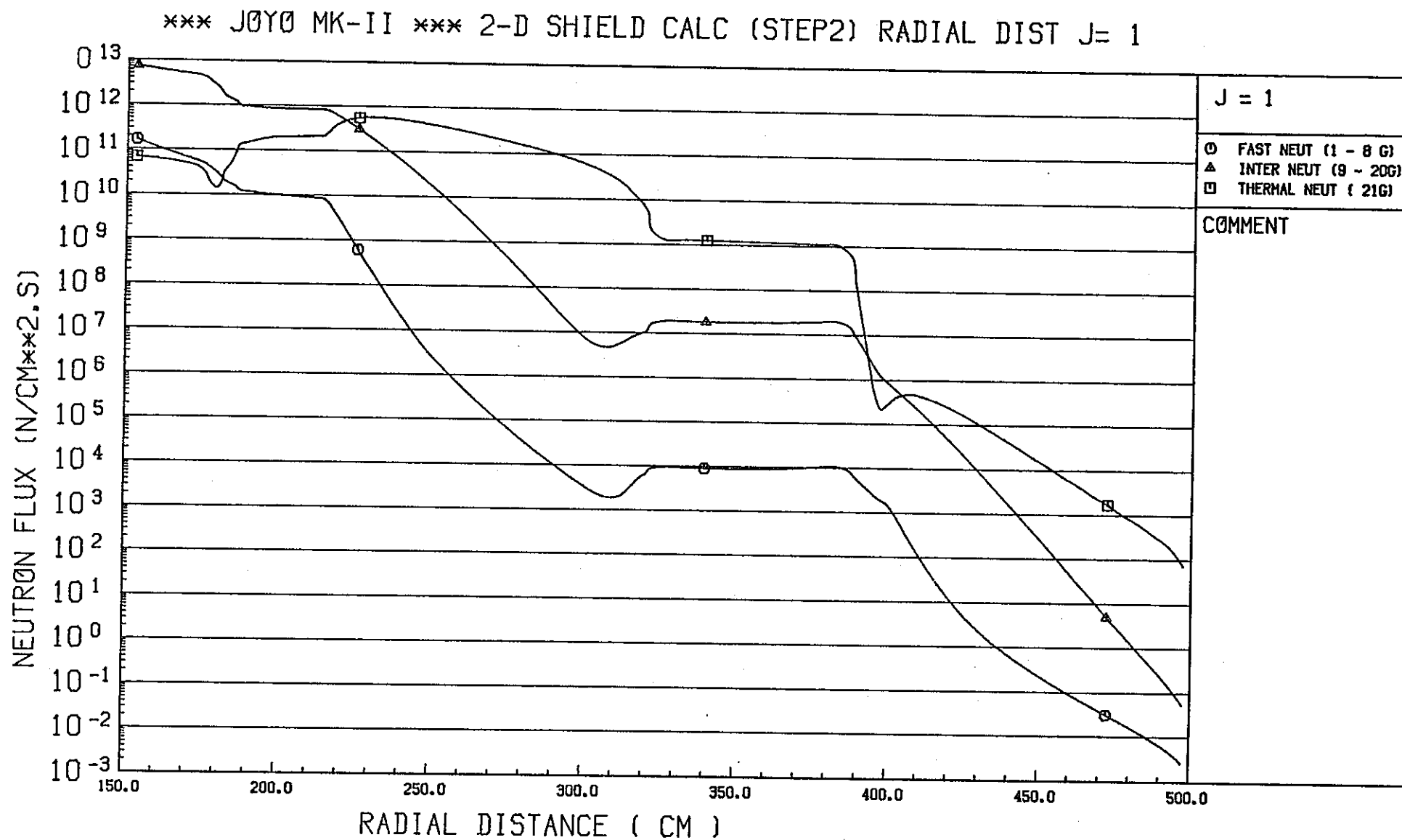


Fig. 2.4.30 Radial Flux Distribution for Step 2 Calculation at Z=1.97 cm (1/2)

*** JOYO MK-II *** 2-D SHIELD CALC (STEP2) RADIAL DIST J= 1

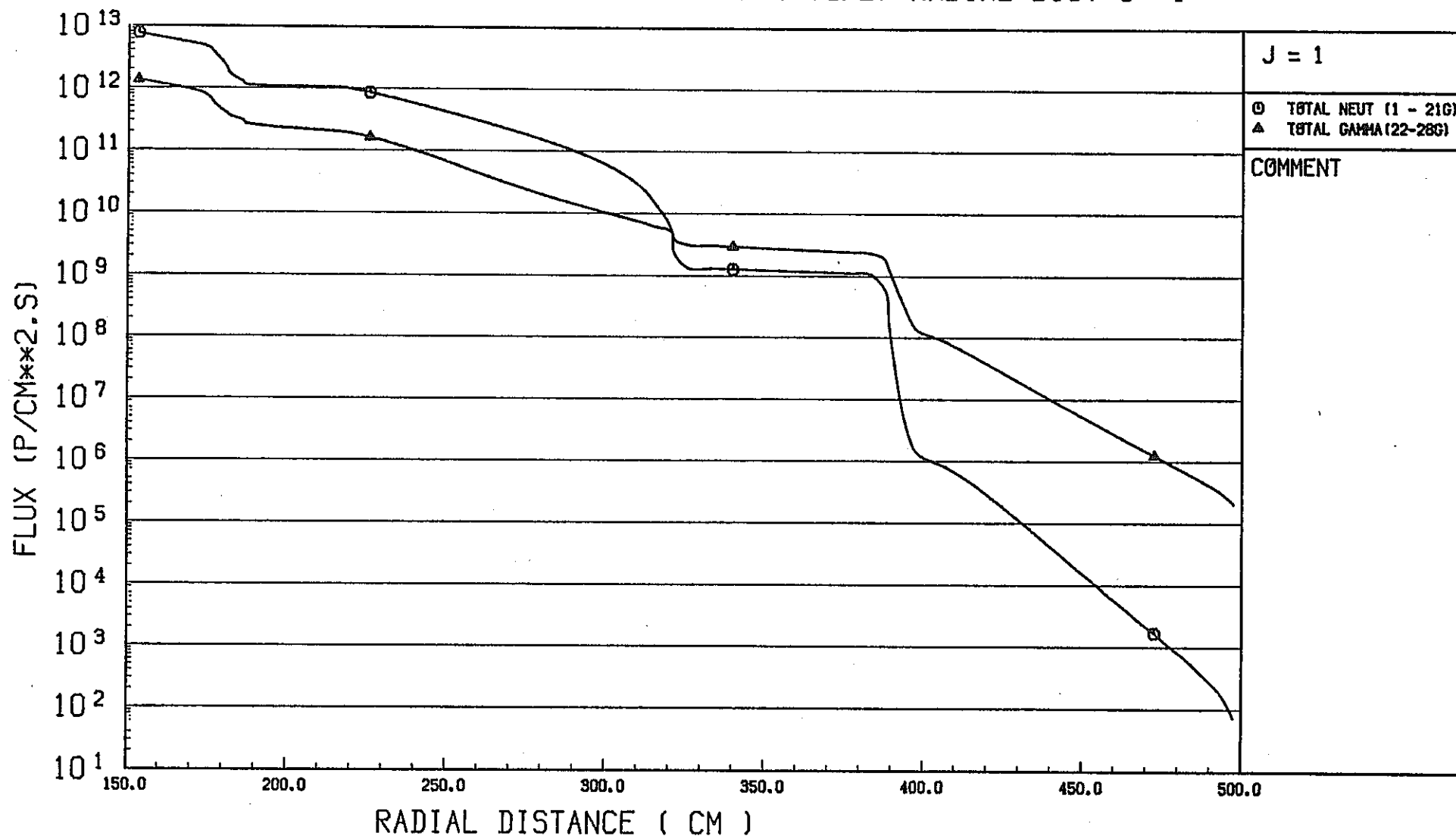


Fig. 2.4.30 (Continued) (2/2)

*** JOYO MK-II *** 2-D SHIELD CALC (STEP2) RADIAL DIST J=110

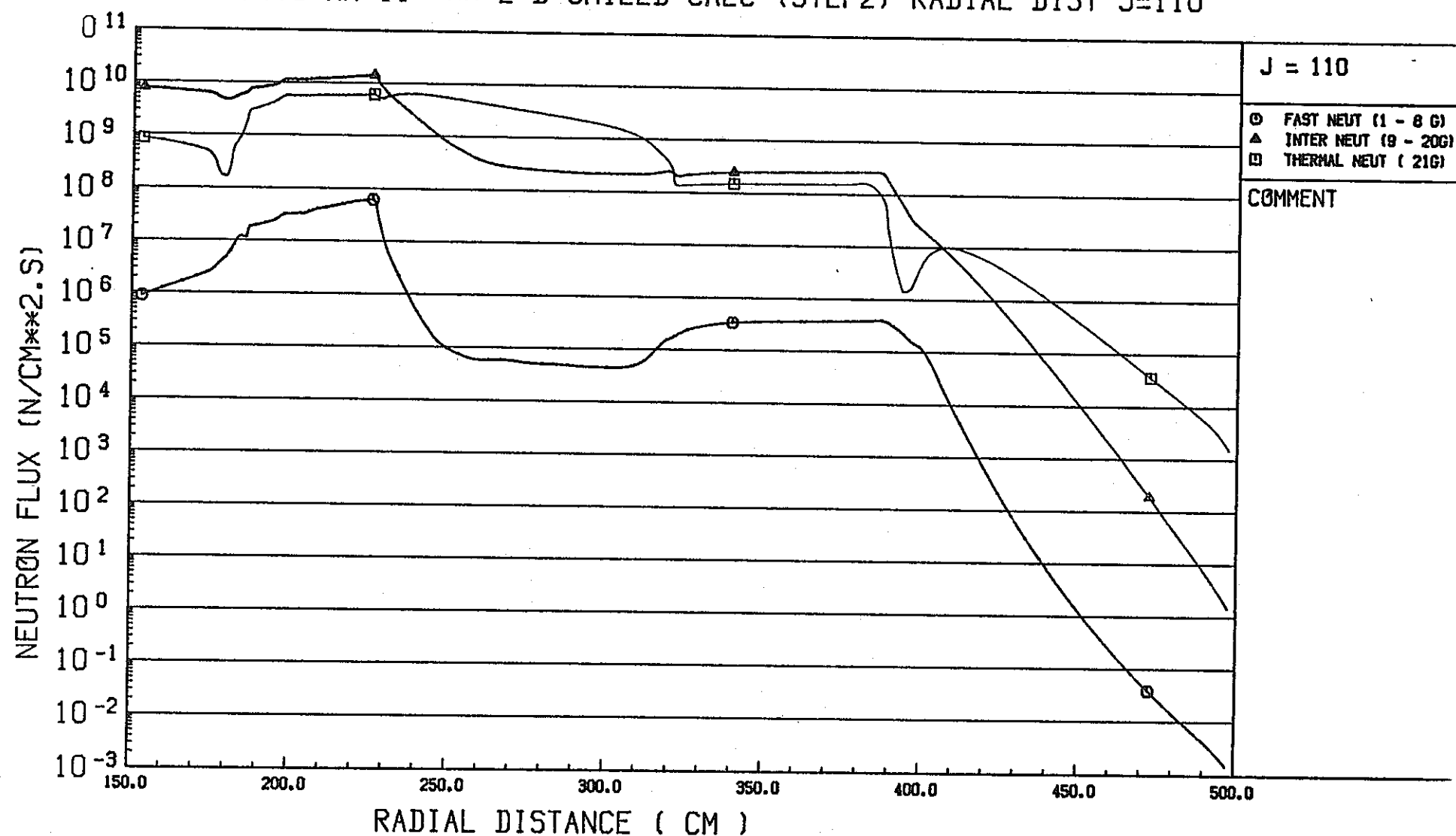


Fig. 2.4.31 Radial Flux Distribution for Step 2 Calculation at Z=403.3cm (1/2)

*** JOY0 MK-II *** 2-D SHIELD CALC (STEP2) RADIAL DIST J=110

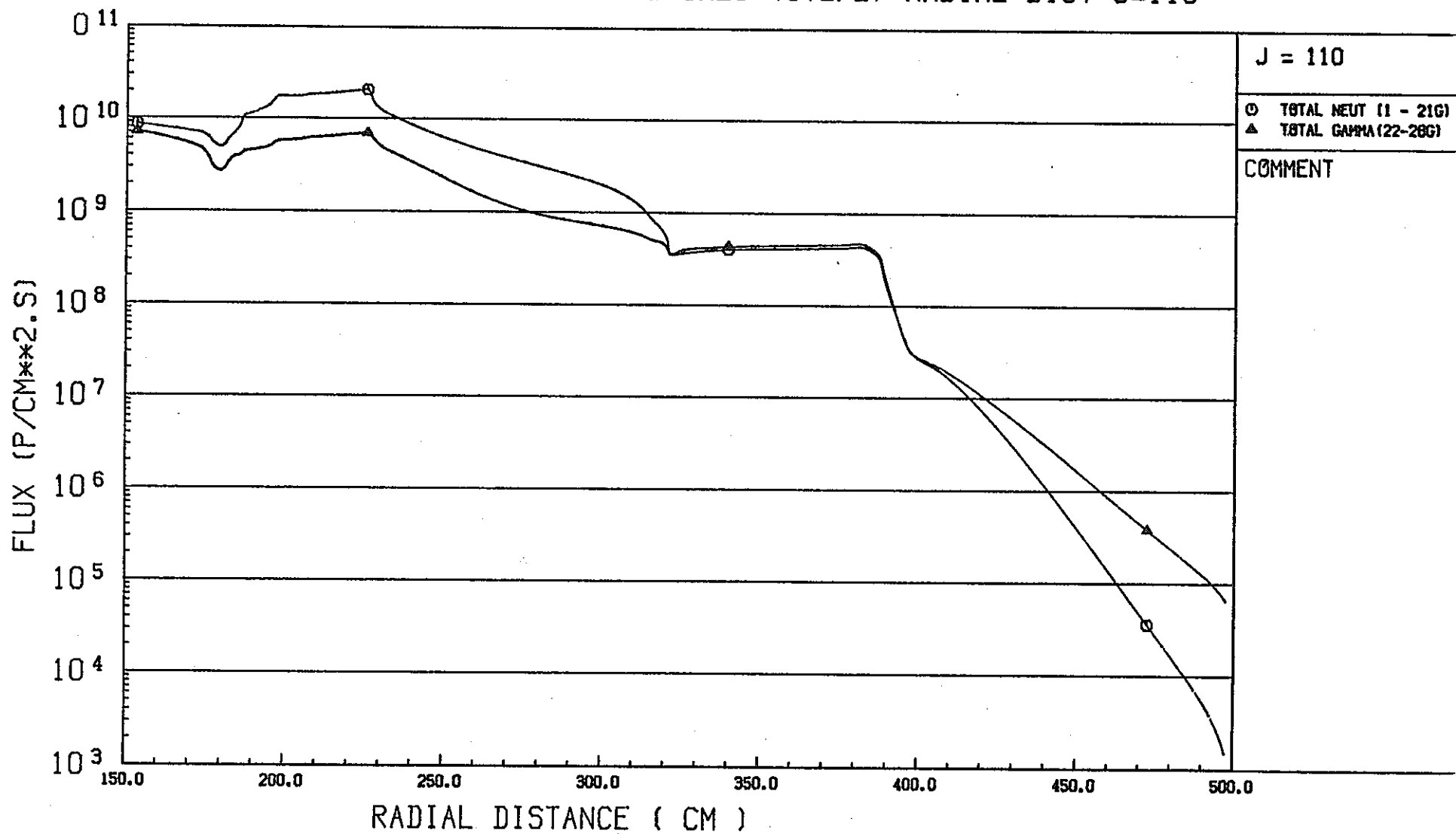


Fig. 2.4.31 (Continued) (2/2)

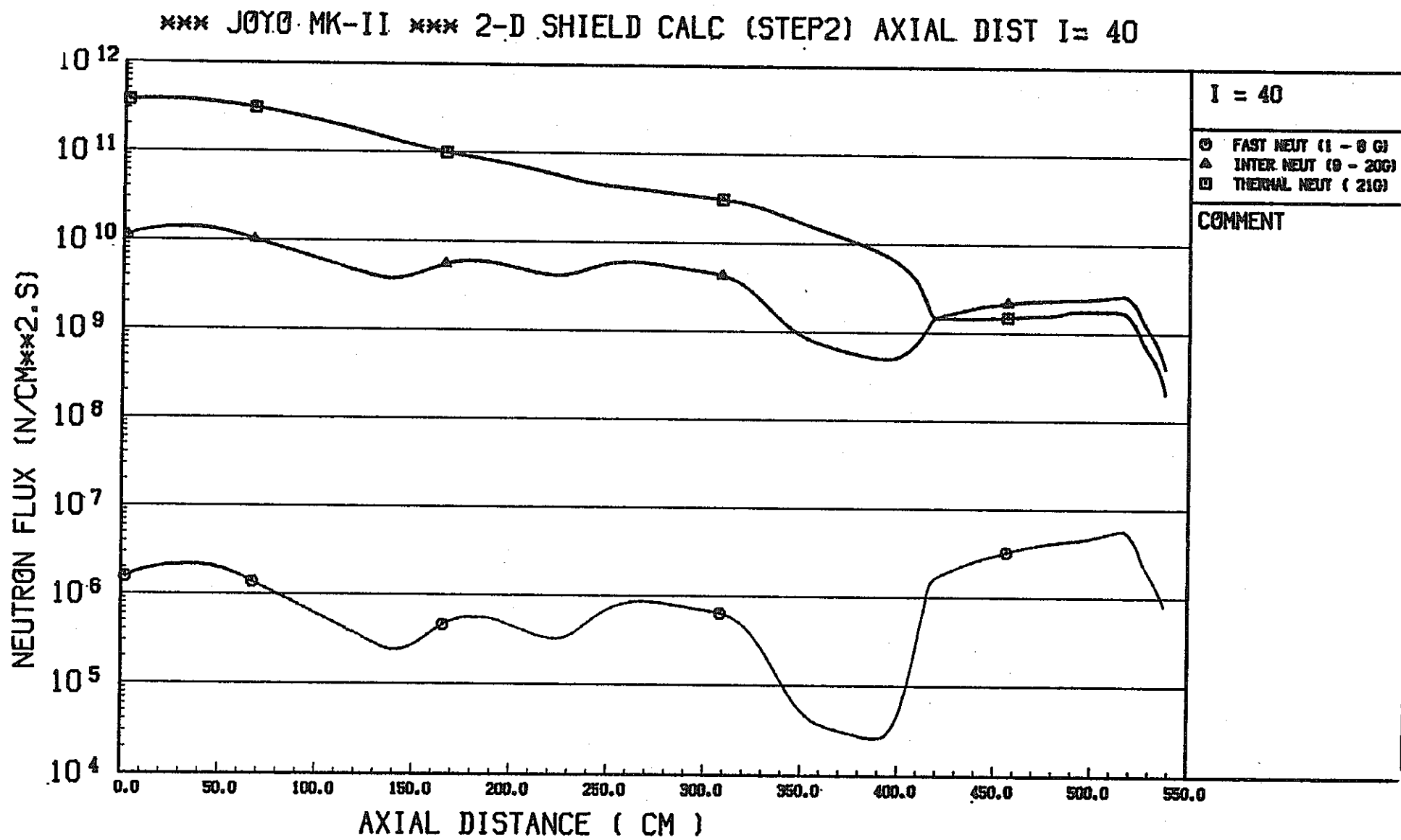


Fig. 2.4.32 Axial Flux Distribution for Step 2 Calculation at R=253.0cm (1/2)

*** JOYO MK-II *** 2-D SHIELD CALC (STEP2) AXIAL DIST I= 40

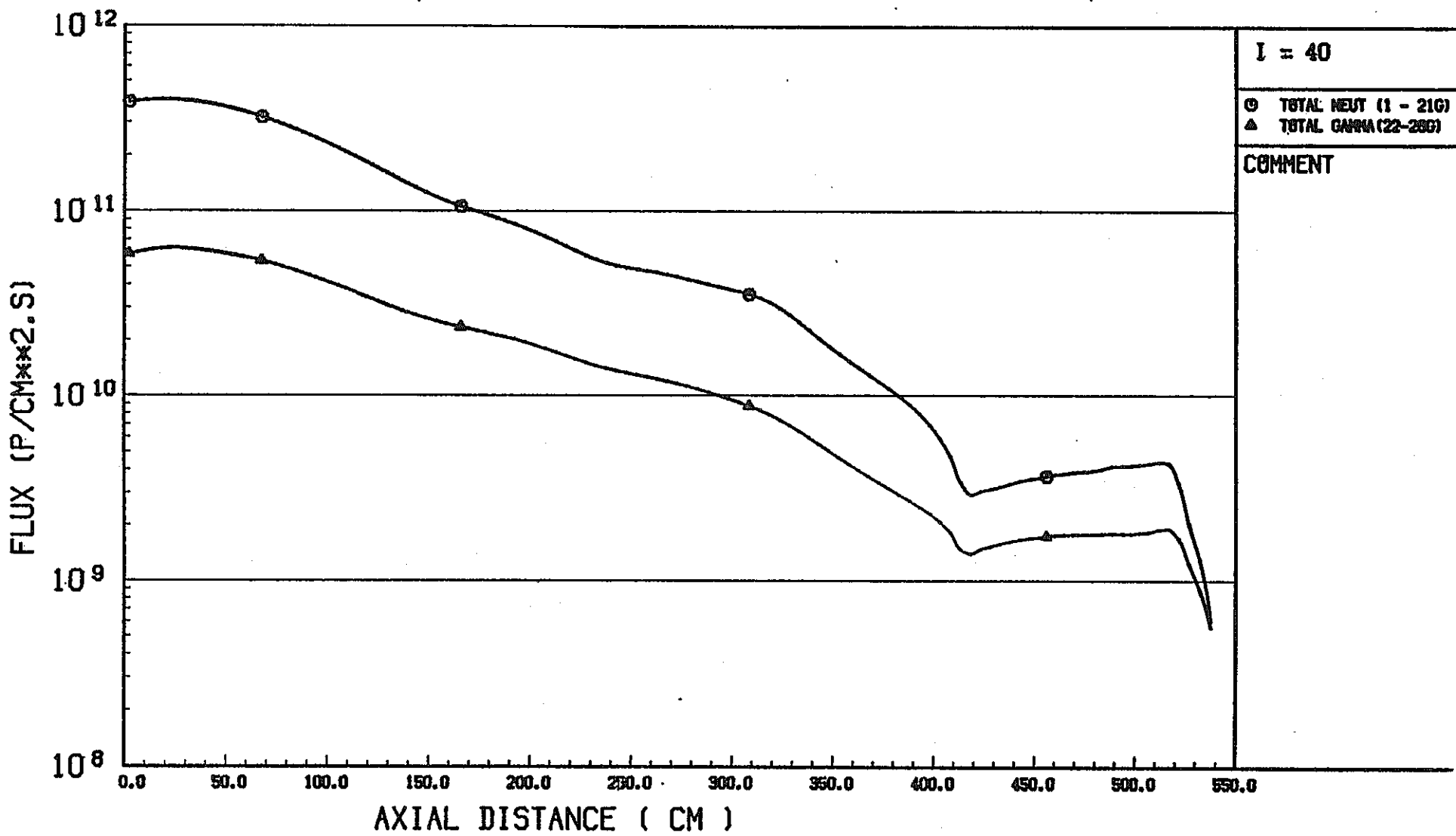


Fig. 2.4.32 (Continued) (2/2)

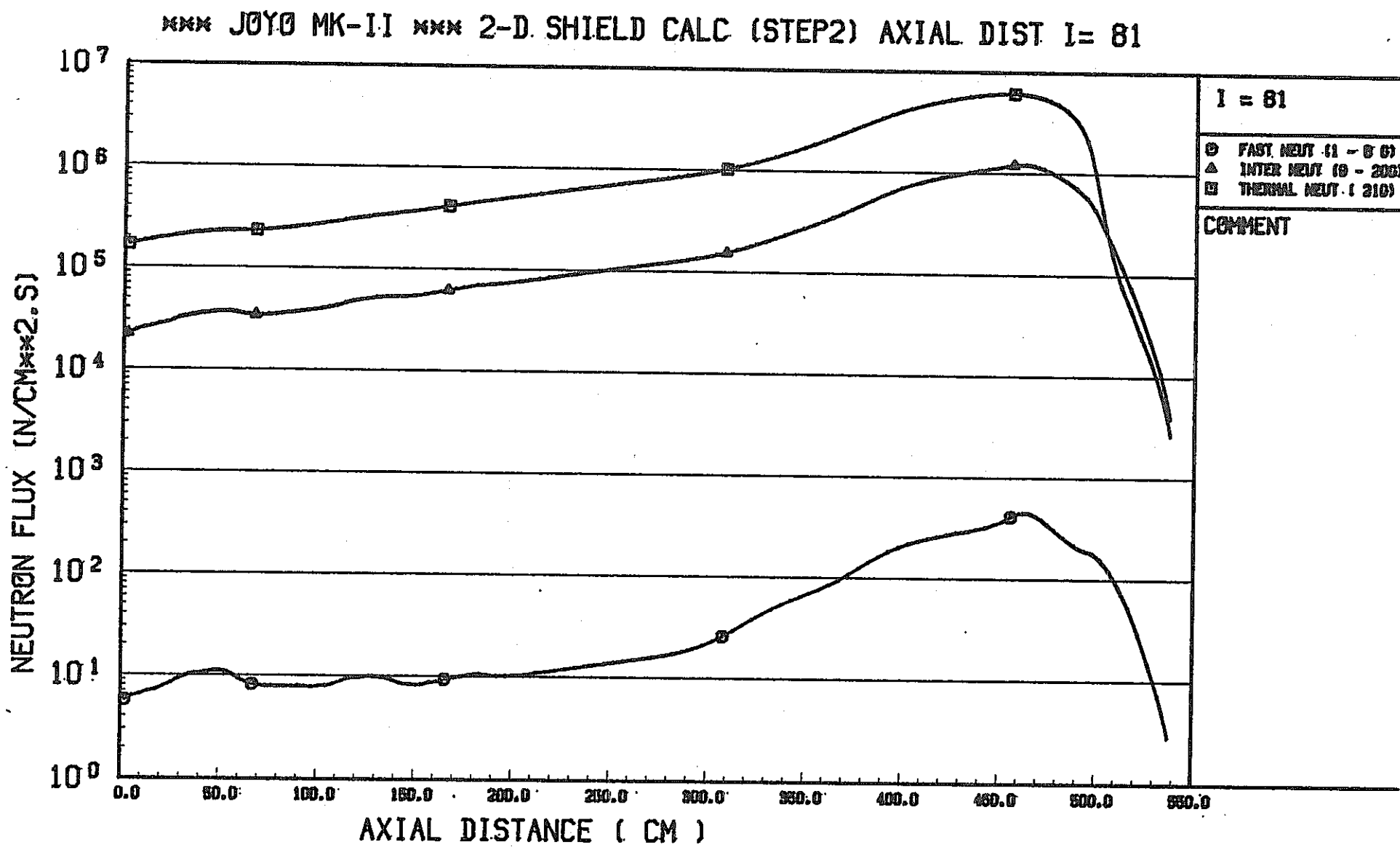


Fig. 2.4.33 Axial Flux Distribution for Step 2 Calculation at R=424.4cm (1/2)

*** JOYO MK-II *** 2-D SHIELD CALC (STEP2) AXIAL DIST I= 81

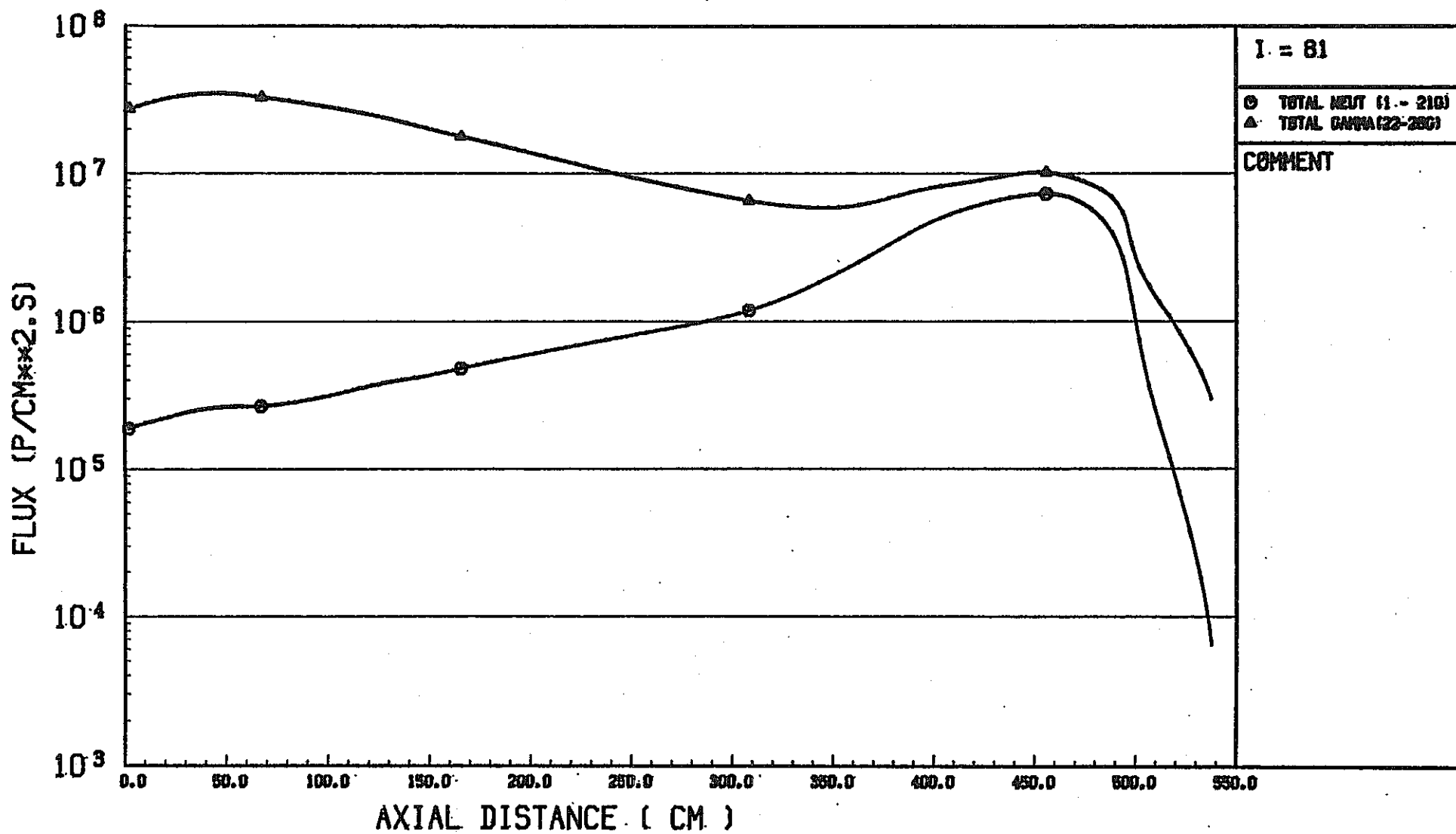


Fig. 2.4.33 (Continued) (2/2)

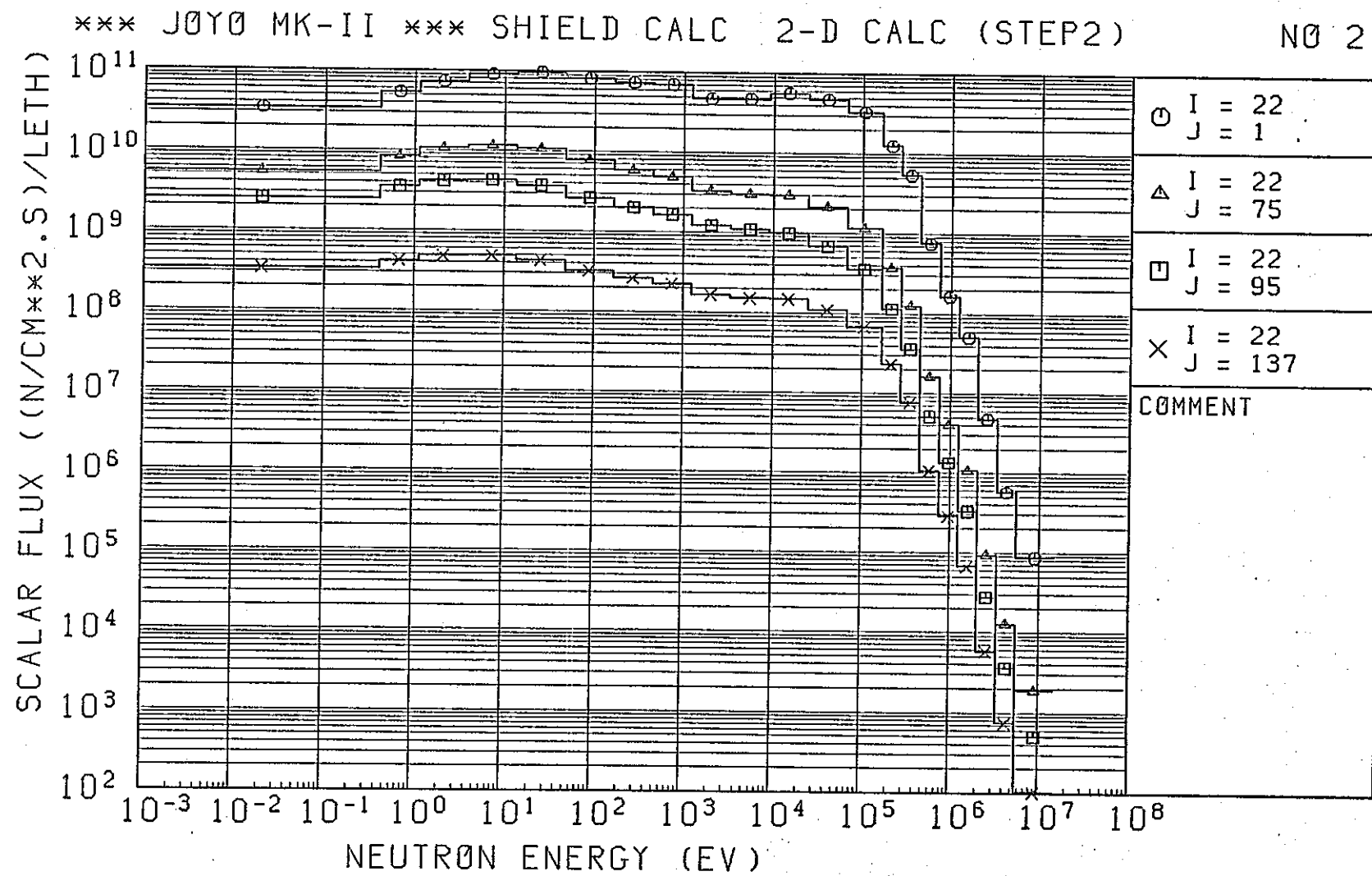


Fig. 2.4.34 Neutron Spectrum from Step 2 Calculation (1/2)

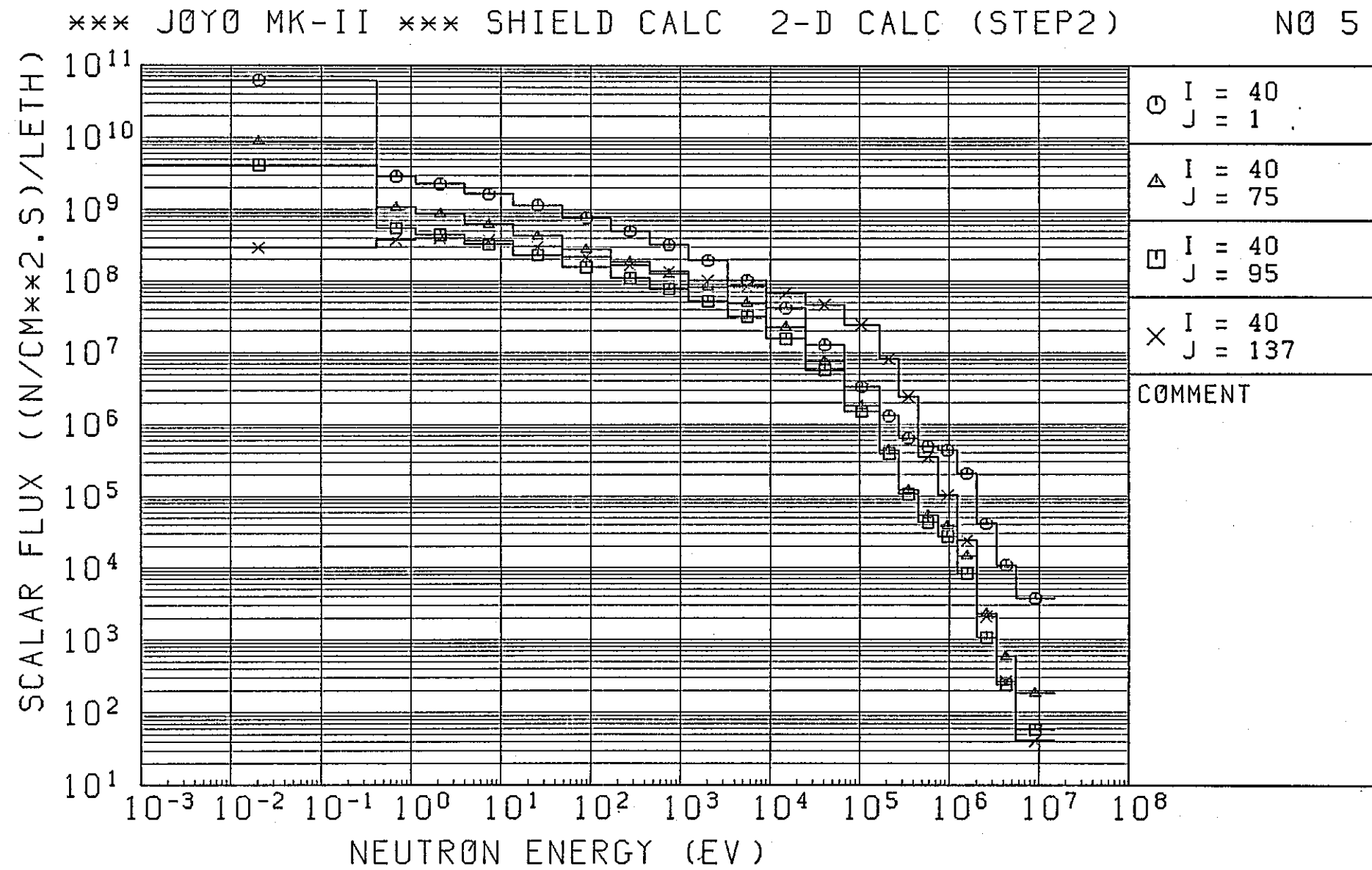


Fig. 2.4.43 : (Continued) (2/2)

*** JOYO MK-II *** SHIELD CALC 2-D CALC (STEP2)

NO 2

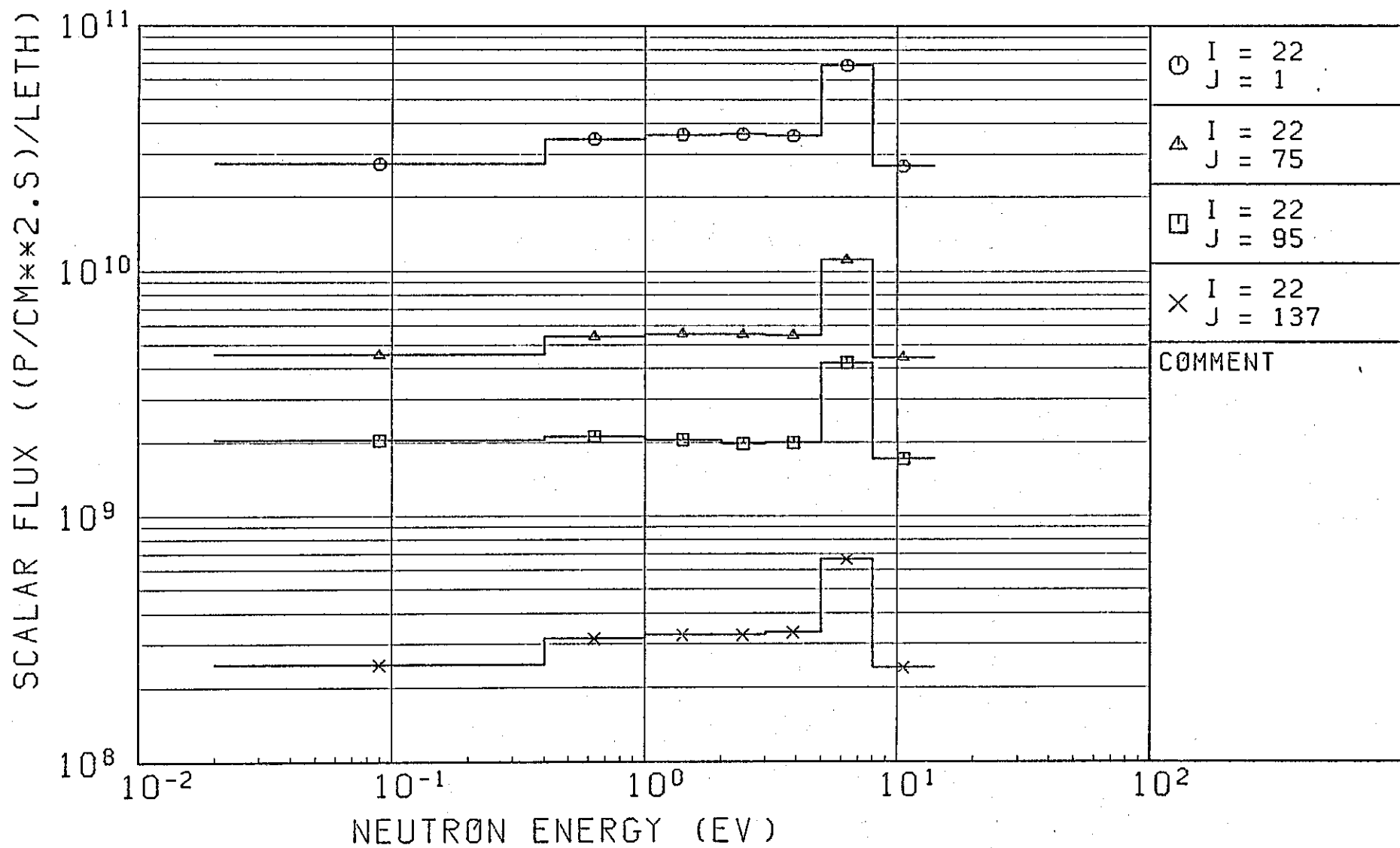


Fig. 2.4.35 Gamma-Ray Spectrum from Step 2 Calculation (1/2)

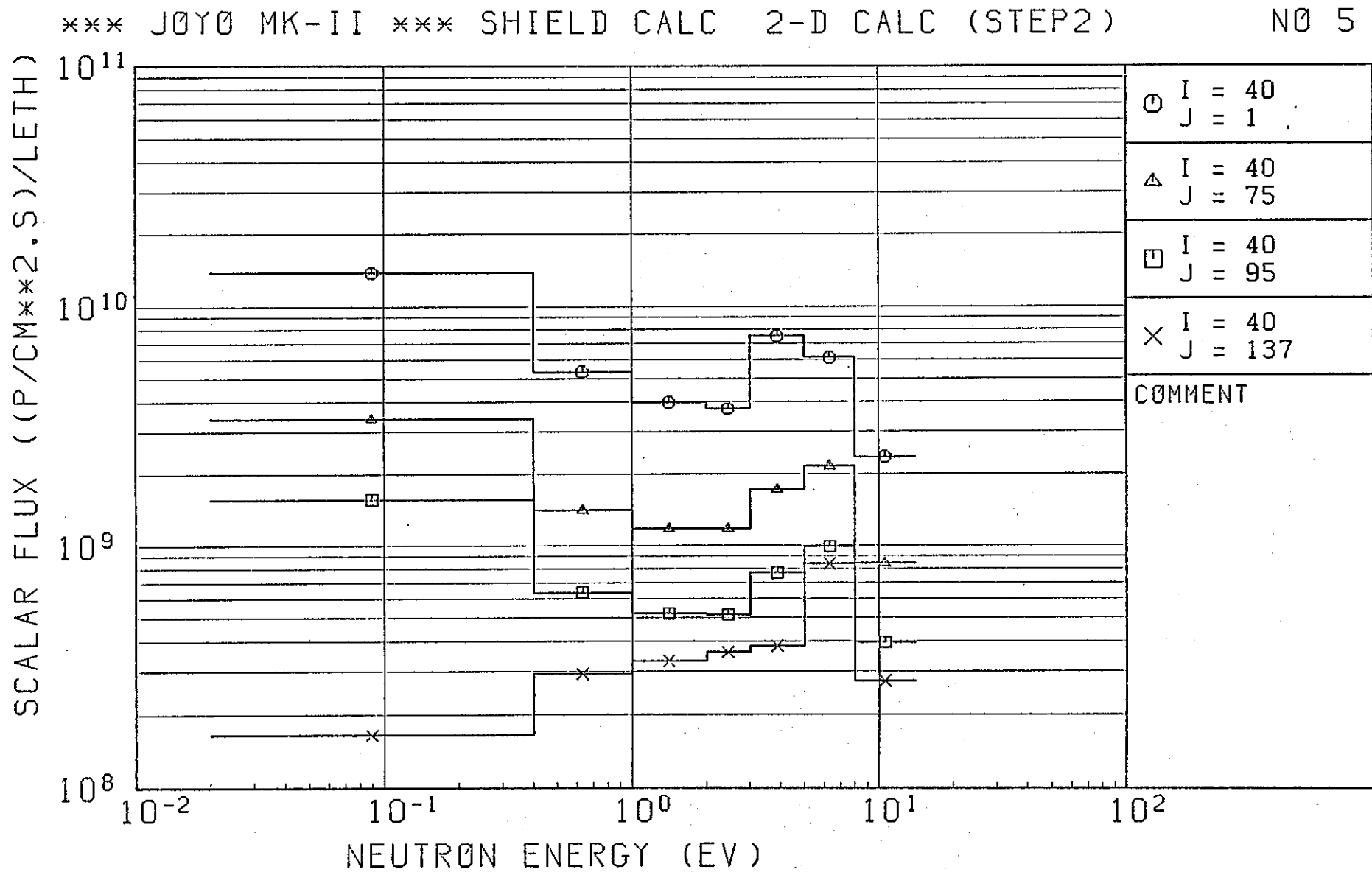


Fig. 2.4.35 (Continued) (2/2)

2.4.3 Comparison of the calculational results with MK-I results

The JOYO MK-II core assembly is different from the MK-I core assembly. The greatest difference is that the MK-II core has no blanket regions. Other differences between MK-II and MK-I analysis are the composition of the control rod guide tube, sodium temperature (200°C for MK-I and 500°C for MK-II) and the composition of the fuel storage rack (0.8 sodium and 0.2 SS for MK-I, and 1.0 sodium for MK-II). These difference result in the different core leakage neutrons. The structural compositions outside the near core, however, are the same for two analysis geometries. It is interesting to compare the difference of the neutron and gamma-ray attenuation characteristis between two geometries in order to examine the effect of the use of the difference cross-section data, taking into account the different core leakage.

The comparison was focussed on the representative positions shown in Fig. 2.4.36 and the comparison data are summalized in Table 2.4.7 for neutron and gamma-ray fluxes.

We can see from this table that the fast and intermediate neutron fluxes and the gamma-ray flux are almost the same for two geometries. The thermal neutron flux, however, is a factor of 6 higher in the MK-II analysis than in the MK-I analysis. Since the thermal power was normalized to 100MW for both analysis, the difference in the thermal flux at the core center attributes to the difference of cross-section data used. At positions from the fuel storage rack to the inner surface of the graphite shield (② to ⑤) along the core mid-plane, the MK-II fluxes are larger than the MK-I fluxes by a factor of about 2. At positions in and outside the graphite shield, the MK-II fluxes are smaller than the MK-I fluxes reflected the cross-section data differences. The MK-II fluxes are higher than the MK-I fluxes at the top of the fuel assembly (⑨) and at the top of the fuel storage rack (⑩), but are smaller only for fast energy at positions

in the sodium and argon cover gas region (13 to 16). In the control rod region the MK-II fluxes are much smaller than the MK-I fluxes because of the higher volume fraction of the absorber.

In general, the core leakage components for the MK-II core are a factor of about 2 higher than those for the MK-I core. The radiation levels at positions in graphite shield, in biological shield and in shield plug are smaller in fast energy components for the MK-II results than for the MK-I results.

Table 2.4.7 Comparison of the MK-I Calculational Results with the
MK-II Calculational Results (1/2)

No.	Positions	Fast Neutron Flux	Intermediate Neutron Flux	Thermal Neutron Flux	Total Neutron Flux	Total Gamma-Ray Flux
1	Core Center	* ¹ 2.77+15	1.69+15	1.30+5	4.46+15	7.13+14
		* ² 2.60+15	1.81+15	7.48+5	4.40+15	6.97+14
		* ³ 0.94	1.07	5.76	0.99	0.98
2	Fuel Storage Rack	4.36+12	4.64+13	5.18+10	5.08+13	4.33+12
		8.46+12	7.88+13	1.67+11	8.74+13	8.28+12
		1.94	1.70	3.23	1.72	1.91
3	Core Barrel	2.05+12	2.61+13	3.24+10	2.82+13	2.97+12
		3.97+12	5.36+13	8.48+10	5.76+13	5.71+12
		1.93	2.05	2.62	2.04	1.92
4	Reactor Vessel	1.81+10	8.54+11	9.79+9	8.78+11	1.53+11
		2.56+10	2.15+12	1.75+10	2.19+12	4.01+11
		1.42	2.53	1.79	2.50	2.62
5	Graphite Shield	4.74+9	2.96+11	1.14+11	4.14+11	7.32+10
		7.03+9	7.85+11	2.62+11	1.05+12	2.01+11
		1.48	2.66	2.30	2.55	2.75
6	Graphite Shield	8.76+4	3.61+7	4.49+10	4.49+10	5.77+9
		1.36+4	5.51+7	1.12+11	1.12+11	1.53+10
		0.16	1.53	2.50	2.50	2.66
7	Concrete	2.05+3	4.88+5	6.66+5	1.16+6	5.47+7
		1.94+3	1.21+6	2.15+5	1.42+6	1.38+8
		0.94	2.47	0.32	1.23	2.52
8	Concrete	3.78-2	1.08-1	1.02+2	1.02+2	6.55+4
		2.65-3	5.42-2	7.25+1	7.26+1	2.08+5
		0.07	0.50	0.71	0.71	3.17
9	Top of Fuel Assembly	5.19+11	3.42+12	6.78+8	3.94+12	3.96+11
		9.40+11	9.84+12	9.35+9	1.08+13	1.07+12
		1.81	2.88	13.8	2.74	2.69
10	Top of Fuel Storage Rack	5.44+10	1.57+12	1.19+10	1.64+12	2.89+11
		5.06+10	3.20+12	3.77+10	3.28+12	7.04+11
		0.93	2.03	3.17	2.01	2.44

*¹ Calculational Results with the MK-I

*² Calculational Results with the MK-II

*³ (Results with MK=III)/(Results with MK-I)

Table 2.4.7 (Continued) (2/2)

No.	Position	Fast Neutron Flux	Intermediate Neutron Flux	Thermal Neutron Flux	Total Neutron Flux	Total Gamma-Ray Flux
11	Graphite Shield	1.33+4	1.10+7	1.22+10	1.22+10	2.30+9
		2.08+3	2.31+7	4.39+10	4.39+10	7.52+9
		0.16	2.09	3.60	3.60	3.27
12	Graphite Shield	7.59+3	1.58+7	6.03+9	6.05+9	1.22+9
		1.15+3	3.00+7	1.72+10	1.73+10	3.54+9
		0.15	1.90	2.86	2.85	2.90
13	Sodium	1.68+6	7.28+9	4.36+8	8.26+9	4.63+9
		1.10+6	1.32+10	7.64+8	1.39+10	7.83+9
		0.66	1.69	1.75	1.69	1.69
14	Sodium	1.62+6	1.13+10	8.04+8	1.21+10	9.24+9
		1.10+6	2.36+10	2.49+9	2.60+10	1.92+10
		0.68	2.09	3.10	2.16	2.08
15	Argon Gas	1.26+5	9.85+7	4.51+6	1.03+8	8.33+7
		1.07+5	2.23+8	5.75+6	2.29+8	1.62+8
		0.84	2.26	1.27	2.22	1.94
16	Argon Gas	1.94+5	1.46+8	1.81+7	1.64+8	1.39+8
		1.94+5	4.01+8	4.21+7	4.43+8	3.45+8
		1.0	2.75	2.32	2.70	2.49
17	Insulator	1.33+6	6.42+8	6.53+8	1.30+9	5.15+8
		1.70+6	1.59+9	1.21+9	2.80+9	1.27+9
		1.27	2.48	1.85	2.16	2.47
18	Control Rod Driver	1.29+0	4.99+2	6.00+1	5.60+2	2.05+3
		5.11-2	1.02+2	1.07+1	1.12+2	1.48+3
		3.9-2	0.20	0.18	0.20	0.72
19	Shield Plug	6.83-2	9.74+1	3.82+2	4.80+2	1.01+4
		9.35-3	1.00+2	3.13+2	4.13+2	1.99+4
		0.14	1.03	0.82	0.86	1.97
20	Shield Plug	2.31-2	3.01+0	4.42-3	3.03+0	1.01-1
		4.52-3	9.55-1	1.99-3	9.62-1	5.02-2
		0.20	0.32	0.45	0.32	0.50

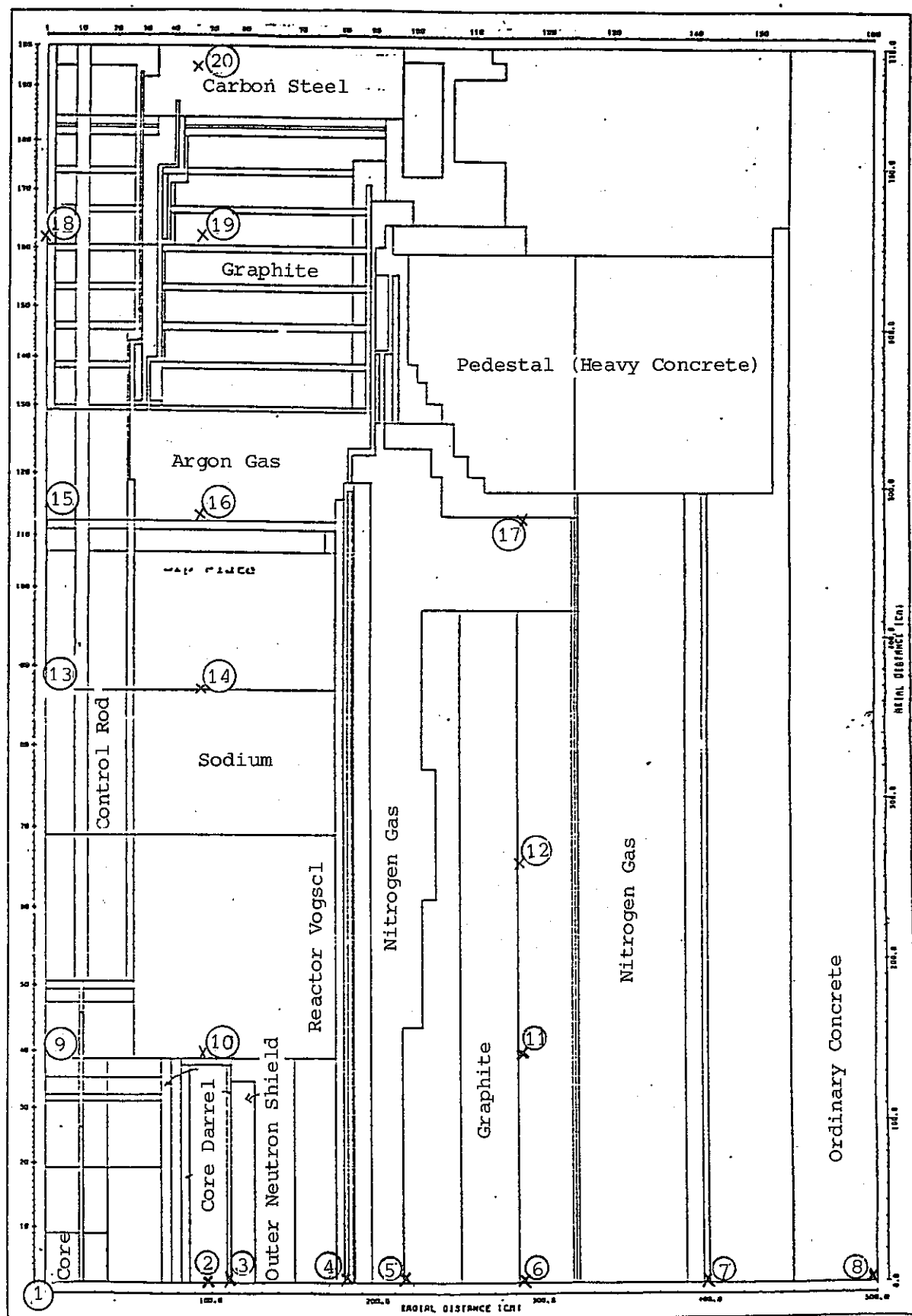


Fig. 2.4.36 Positions for Comparing of the MK-I Calculational Results with the MK-II Calculational Results

CHAPTER 3

COMPARISON OF THE CALCULATION RESULTS WITH MEASUREMENTS

3.1 Measurement

Many useful measurement have been taken during the JOYO MK-II core operation at the core center position, at positions in the reflector region, at positions in and on fuel storage racks, and at positions in the detector guide tube of channel A. These positions are shown in Fig. 3.1.1. Measurements in the fuel storage rack have been taken at three different racks, R-9, R-15 and R-25, as shown in Fig. 3.1.2. When the measurements were taken, there were six fuel storage racks with the fuels in them, R-8, R-9, R-10, R-15, R-19 and R-21. The measurements on the fuel storage rack was taken on the R-16 fuel rack. When the measurements along the detector guide tube were taken, there were seven fuel storage racks with the fuel assemblies in them as shown in Fig. 3.1.3.

The measured data are reaction rates of $^{235}_{\text{U}}(\text{n},\text{f})$, $^{238}_{\text{U}}(\text{n},\text{f})$, $^{238}_{\text{U}}(\text{n},\gamma)$, $^{197}_{\text{Au}}(\text{n},\gamma)$ and $^{58}_{\text{Ni}}(\text{n},\text{p})$ reactions.

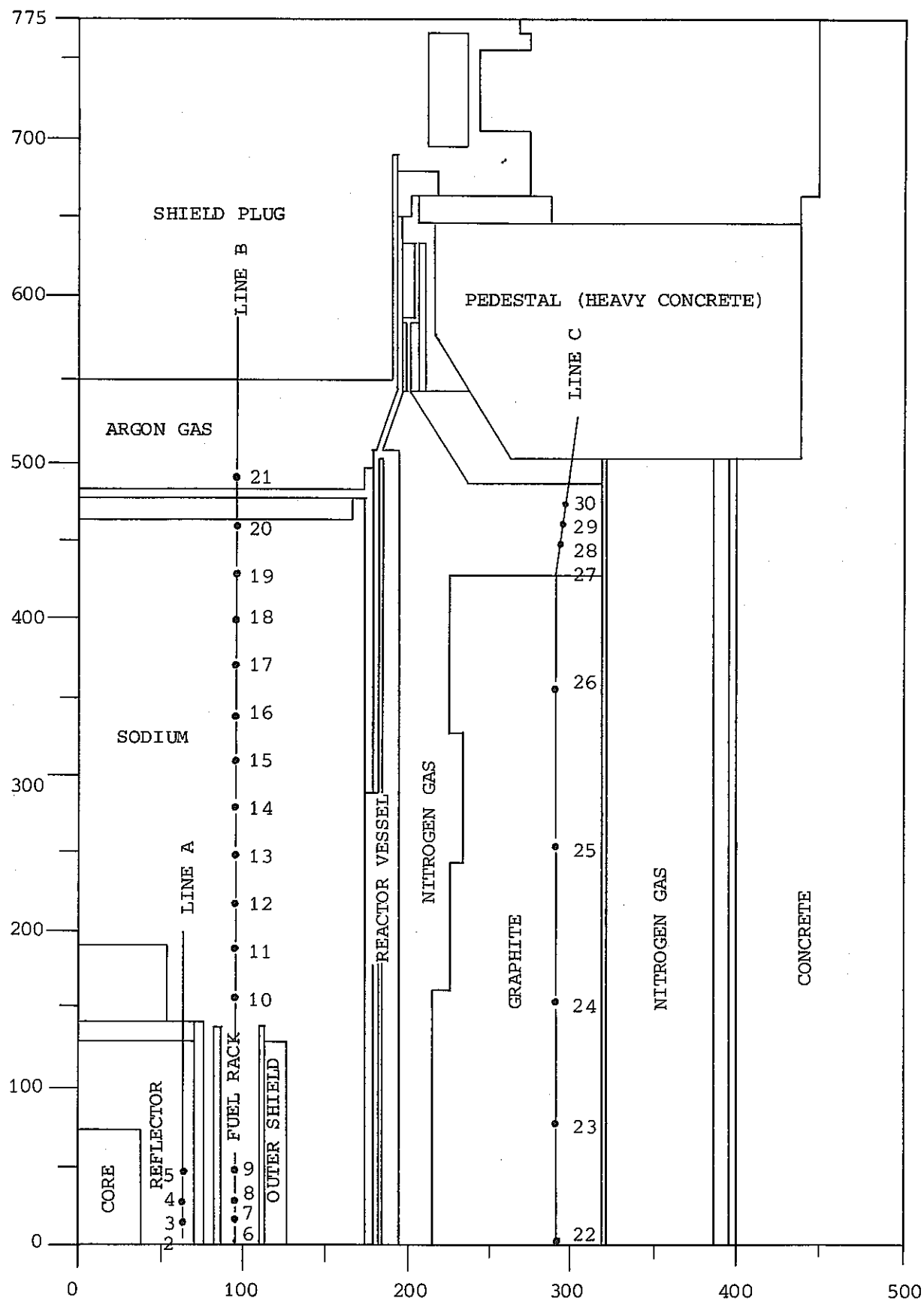


Fig. 3.1.1 Measurement Positions

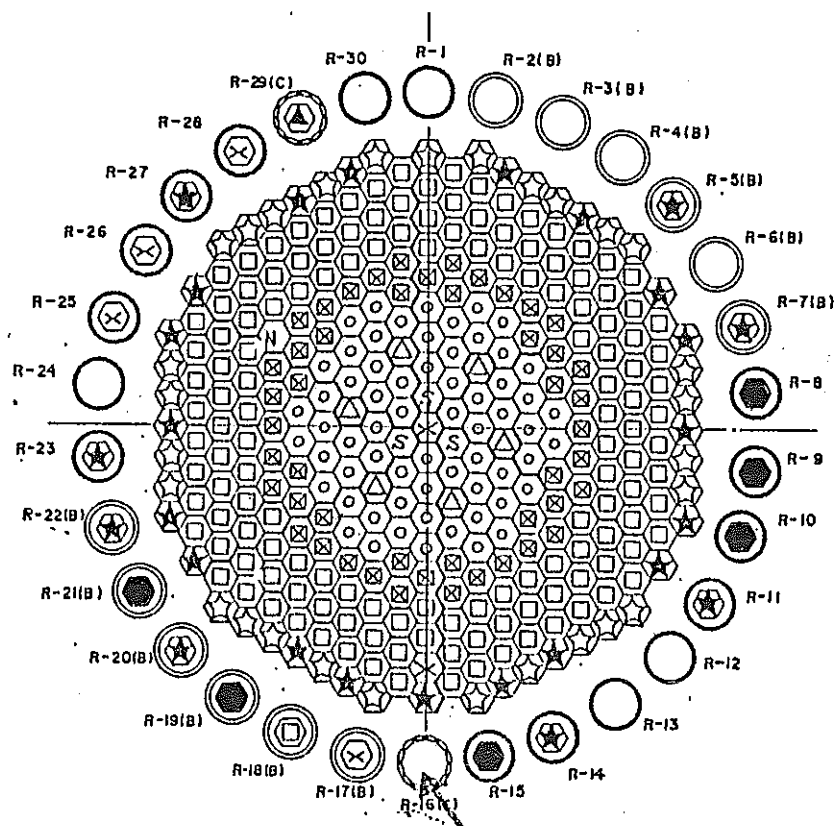


Fig. 3.1.2 In-Vessel Fuel Storage Configuration for Measurements in and on the Fuel Storage Rack

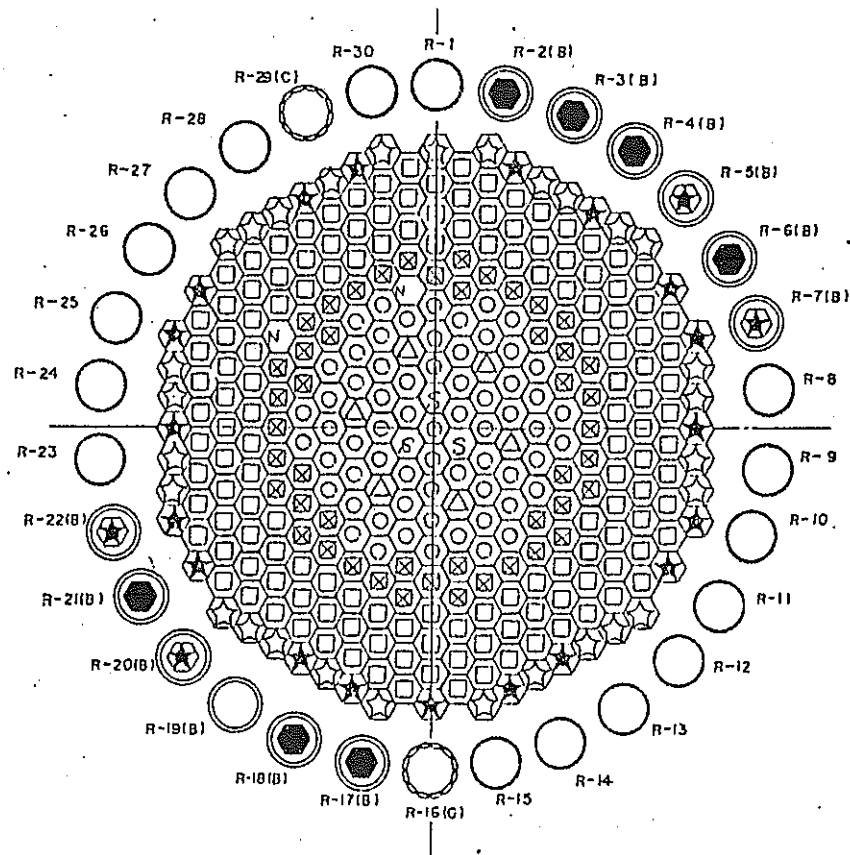


Fig. 3.1.3 In-Vessel Fuel Storage Configuration for Measurements in the Detector Guide Tube.

3.2 Comparison

3.2.1 At core center and in reflector

Measurements taken at the core center position are reaction rates of $^{235}\text{U}(\text{n},\text{f})$, $^{238}\text{U}(\text{n},\text{f})$, $^{238}\text{U}(\text{n},\gamma)$, $^{197}\text{Au}(\text{n},\gamma)$ and $^{58}\text{Ni}(\text{n},\text{p})$ reactions.

Measured reaction rates are shown in Table 3.2.1 in comparison with calculated reaction rates and the calculation to measurement ratio.

Calculated reaction rates supremely well agree with measured reaction rates. The maximum deviation occurs for the $^{58}\text{Ni}(\text{n},\text{p})$ fast neutron reaction at a value of 18%, but this deviation is still tolerable and small.

Measurements taken in the reflector region are $^{235}\text{U}(\text{n},\text{f})$, $^{238}\text{U}(\text{n},\text{f})$, $^{238}\text{U}(\text{n},\gamma)$ and $^{58}\text{Ni}(\text{n},\text{p})$ reaction rates and the results are shown in Table 3.2.2 for each reaction. The calculated $^{235}\text{U}(\text{n},\text{f})$ and $^{238}\text{U}(\text{n},\gamma)$ reaction rates fairly well agree with measurements. This means that the low energy neutron flux calculation is accurate. The calculated reaction rates of $^{238}\text{U}(\text{n},\text{f})$ and $^{58}\text{Ni}(\text{n},\text{p})$ which have the larger cross-section in the high neutron energy region are somehow smaller than the measured reaction rates. This result is attributed to the fact that the actual fuel storage rack contains fuel assemblies. The calculation was performed with the fuel assemblies in the fuel storage rack neglected. The actual high energy neutron source in the fuel storage rack increases the high energy neutrons in the reflector region. However, the effect of the fission source generated in the fuel storage rack on the neutron flux in the reflector region is small.

3.2.2 In and on fuel storage rack region

Measured reaction rates are shown in Table 3.2.3 in the order of $^{235}\text{U}(\text{n},\text{f})$, $^{238}\text{U}(\text{n},\text{f})$, $^{238}\text{U}(\text{n},\gamma)$, $^{197}\text{Au}(\text{n},\gamma)$ and $^{59}\text{Ni}(\text{n},\text{p})$ reactions. In the fuel storage racks R-9 and R-15 the fission neutrons are generated, while in the fuel storage rack R-25 there is no fuel assembly. This results

in that the actual $^{235}\text{U}(n,f)$ reaction rates in R-9 and R-15 are larger than in R-25. To compare properly with calculation and measurement it would be preferable to introduce the measurement in R-25. The calculation to measurement ratios are nearly equal to unity for almost all measurement positions. The calculation agrees well with the measurement.

The $^{238}\text{U}(n,f)$ reaction rate has a predominant response to high energy neutrons and the high energy neutrons are generated in the racks R-9 and R-15. There are much more high energy neutrons actually in the fuel rack region than the calculational fuel rack region. Therefore the calculational response of the reaction is smaller than the measurement as seen from the data in (2) of Table 3.2.3. It might be natural that the $^{238}\text{U}(n,\gamma)$ reaction rates are larger in measurement than in calculation.

The calculational results of the $^{197}\text{Au}(n,\gamma)$ agree well with the measurement but the calculation of the $^{58}\text{Ni}(n,p)$ reaction rates are far from the measurement because of the same reason as the $^{238}\text{U}(n,f)$ reaction.

3.2.3 In detector guide tube

The measured data in the detector guide tube are shown in Table 2.3.4 in comparison with the calculation results. This guide tube locates 290cm away from the core center and penetrates the graphite shield. In the previous analysis⁽¹¹⁾, it has been found that the measurement in this guide tube suffered the effect of the guide tube material.

The calculational reaction rates of $^{235}\text{U}(n,f)$ and $^{197}\text{Au}(n,\gamma)$ agree well with the measurements.

Table 3.2.1 Reaction Rate at Core Center

<u>Reaction</u>	<u>Measurement</u>	<u>Calculation</u>	<u>Cal./Mes.</u>
$^{235}_{\text{U}}(\text{n},\text{f})$	7.84 - 14	7.43 - 14	0.95
$^{238}_{\text{U}}(\text{h},\text{f})$	3.12 - 15	3.06 - 15	0.98
$^{238}_{\text{U}}(\text{n},\gamma)$	1.10 - 14	1.12 - 14	1.02
$^{197}_{\text{Au}}(\text{n},\gamma)$	2.19 - 14	2.07 - 14	0.95
$^{58}_{\text{Ni}}(\text{n},\text{p})$	1.09 - 15	8.92 - 16	0.82

Table 3.2.2 Reaction Rate in Reflector Region
(see line A in Fig. 3.1.1)

(1) $^{235}_{\text{U}}(\text{n},\text{f})$

<u>Height (cm)</u>	<u>Measurement</u>	<u>Calculation</u>	<u>Cal./Mes.</u>
0.0	4.01 - 14	3.76 - 14	0.94
12.5	3.61 - 14	3.51 - 14	0.97
25.0	3.12 - 14	2.97 - 14	0.95
45.0	1.86 - 14	1.75 - 14	0.94

(2) $^{238}_{\text{U}}(\text{n}, \text{f})$

<u>Height (cm)</u>	<u>Measurement</u>	<u>Calculation</u>	<u>Cal./Mes.</u>
0.0	1.56 - 17	9.17 - 18	0.59
12.5	1.31 - 17	8.01 - 18	0.61
25.0	9.36 - 18	5.62 - 18	0.60
45.0	2.50 - 18	1.61 - 18	0.64

(3) $^{238}_{\text{U}}(\text{n}, \gamma)$

<u>Height (cm)</u>	<u>Measurement</u>	<u>Calculation</u>	<u>Cal./Mes.</u>
0.0	2.83 - 14	3.43 - 14	1.21
12.5	2.56 - 14	3.22 - 14	1.26
25.0	2.20 - 14	2.74 - 14	1.24
45.0	1.31 - 14	1.67 - 14	1.27

(4) $^{58}_{\text{Ni}}(\text{n}, \text{p})$

<u>Height (cm)</u>	<u>Measurement</u>	<u>Calculation</u>	<u>Cal./Mes.</u>
0.0	3.27 - 18	1.23 - 18	0.38

Table 3.2.3 Reaction Rate in and on Fuel Storage Rack (1/3)
 (see line B in Fig. 3.1.1)

(1) $^{235}\text{U}(n,f)$

<u>Position</u>	<u>Height (cm)</u>	<u>Measurement</u>	<u>Calculation</u>	<u>Cal./Mes.</u>	<u>Remarks</u>
6	0.0	5.09 - 15	1.18 - 14	2.32	R-9
6	0.0	5.24 - 15	1.18 - 14	2.25	R-15
6	0.0	1.26 - 14	1.18 - 14	0.94	R-25
7	12.5	5.00 - 15	1.14 - 14	2.28	R-9
7	12.5	5.21 - 15	1.14 - 14	2.19	R-15
8	25.0	5.01 - 15	1.05 - 14	2.10	R-9
8	25.0	5.21 - 15	1.05 - 14	2.02	R-15
9	45.0	8.94 - 15	8.11 - 14	0.91	R-9
9	45.0	9.49 - 15	8.11 - 14	0.85	R-15
10	156.0	6.71 - 16	6.89 - 16	1.03	R-16
11	186.0	4.83 - 16	4.53 - 16	0.94	
12	216.0	3.09 - 16	2.87 - 16	0.93	
13	246.0	1.86 - 16	1.76 - 16	0.95	
14	276.0	1.07 - 16	1.00 - 16	0.93	
15	306.0	6.35 - 17	5.77 - 17	0.91	
16	336.0	3.76 - 17	3.31 - 17	0.88	
17	366.0	1.80 - 17	1.81 - 17	1.01	
18	396.0	9.56 - 18	9.77 - 18	1.02	
19	426.0	5.51 - 18	5.12 - 18	0.93	
20	456.0	2.23 - 18	1.78 - 18	0.80	
21	486.0	6.59 - 19	2.98 - 19	0.45	R-16

Table 3.2.3 (Continued) (2/3)

(2) $^{238}\text{U}(n, f)$

<u>Position</u>	<u>Height (cm)</u>	<u>Measurement</u>	<u>Calculation</u>	<u>Cal./Mes.</u>	<u>Remarks</u>
6	0.0	8.08 - 18	2.95 - 19	0.037	R-9
6	0.0	7.80 - 18	2.95 - 19	0.038	R-15
6	0.0	2.29 - 18	2.95 - 19	0.13	R-25
7	12.5	7.55 - 18	2.71 - 19	0.036	R-9
7	12.5	7.55 - 18	2.71 - 19	0.036	R-15
8	25.0	6.52 - 18	2.21 - 19	0.034	R-9
8	25.0	6.65 - 18	2.21 - 19	0.034	R-15
9	45.0	1.67 - 18	1.15 - 19	0.069	R-9
9	45.0	1.79 - 18	1.15 - 19	0.064	R-15

(3) $^{238}\text{U}(n, \gamma)$

<u>Position</u>	<u>Height (cm)</u>	<u>Measurement</u>	<u>Calculation</u>	<u>Cal./Mes.</u>	<u>Remarks</u>
6	0.0	4.18 - 15	1.13 - 14	2.70	R-9
6	0.0	4.51 - 15	1.13 - 14	2.51	R-15
6	0.0	1.77 - 14	1.13 - 14	0.64	R-25
7	12.5	4.38 - 15	1.09 - 14	2.49	R-9
7	12.5	4.74 - 15	1.09 - 14	2.30	R-15
8	25.0	4.76 - 15	1.01 - 14	2.12	R-9
8	25.0	4.81 - 15	1.01 - 14	2.10	R-15
9	45.0	7.92 - 15	7.92 - 15	0.58	R-9
9	45.0	1.30 - 14	7.92 - 15	0.61	R-15
10	156.0	1.11 - 15	3.82 - 16	0.34	R-16
11	186.0	8.05 - 16	2.32 - 16	0.29	
12	216.0	5.17 - 16	1.37 - 16	0.26	
13	246.0	2.70 - 16	7.78 - 17	0.29	
14	276.0	1.60 - 16	4.87 - 17	0.30	
15	306.0	7.76 - 17	2.59 - 17	0.33	
16	336.0	3.55 - 17	1.36 - 17	0.38	
17	366.0	1.72 - 17	9.73 - 18	0.57	
18	396.0	7.11 - 18	4.76 - 18	0.67	
19	426.0	3.28 - 18	2.35 - 18	0.72	
20	456.0	1.56 - 18	1.11 - 18	0.71	
21	486.0	3.48 - 19	1.68 - 19	0.48	R-16

Table 3.2.3 (Continued) (3/3)

(4) $^{197}\text{Au}(n,\gamma)$

<u>Position</u>	<u>Height (cm)</u>	<u>Measurement</u>	<u>Calculation</u>	<u>Cal./Mes.</u>	<u>Remarks</u>
6	0.0	1.38 - 14	4.13 - 14	2.99	R-25
7	12.5	1.36 - 14	4.00 - 14	2.94	R-25
8	25.0	1.27 - 14	3.72 - 14	2.93	R-25
9	45.0	1.04 - 14	2.95 - 14	2.84	R-25
10	156.0	8.15 - 16	6.23 - 16	0.76	R-16
11	186.0	6.02 - 16	3.96 - 16	0.66	
12	216.0	3.74 - 16	2.45 - 16	0.66	
13	246.0	2.32 - 16	1.47 - 16	0.63	
14	276.0	1.28 - 16	1.65 - 16	1.29	
15	306.0	7.75 - 17	9.21 - 17	1.19	
16	336.0	4.51 - 17	5.07 - 17	1.12	
17	366.0	1.98 - 17	6.05 - 17	3.06	
18	396.0	8.96 - 18	3.08 - 17	3.44	
19	426.0	4.86 - 18	1.57 - 17	3.23	
20	456.0	1.79 - 18	7.44 - 18	4.16	
21	486.0	4.75 - 19	1.51 - 18	2.42	R-16

(5) $^{59}\text{Ni}(n,p)$

<u>Position</u>	<u>Height (cm)</u>	<u>Measurement</u>	<u>Calculation</u>	<u>Cal./Mes.</u>	<u>Remarks</u>
6	0.0	2.37 - 17	2.72 - 20	1.1-3	R-9
6	0.0	2.35 - 17	2.72 - 20	1.2-3	R-15
7	12.5	2.35 - 17	2.47 - 20	1.1-3	R-9
7	12.5	2.22 - 17	2.47 - 20	1.1-3	R-15
8	25.0	1.94 - 17	1.96 - 20	1.0-3	R-9
8	25.0	1.89 - 17	1.96 - 20	1.0-3	R-15
9	45.0	5.13 - 19	9.22 - 21	0.018	R-9
9	45.0	2.94 - 19	9.22 - 21	0.031	R-15

Table 3.2.4 Reaction Rate in Detector Guide Tube (1/3)
(see line C in Fig. 3.1.1)

(1) $^{235}\text{U}(n,f)$: No correction for the effect of guide tube

<u>Position</u>	<u>Height (cm)</u>	<u>Measurement</u>	<u>Calculation</u>	<u>Cal./Mes.</u>
22	0.0	2.92 - 16	4.08 - 16	1.40
23	75.0	2.06 - 16	3.48 - 16	1.69
24	150.0	7.36 - 17	1.60 - 16	2.17
25	250.0	3.27 - 17	6.27 - 17	1.92
26	350.0	8.94 - 18	2.35 - 17	2.63
27	450.0	3.80 - 18	4.43 - 18	1.17
28	460.0	3.71 - 18	4.50 - 18	1.21
29	475.0	3.15 - 18	4.86 - 18	1.54
30	490.0	—	5.11 - 18	—

(2) $^{235}\text{U}(n,f)$: Correction for the effect of quide tube

<u>Position</u>	<u>Height (cm)</u>	<u>Measurement</u>	<u>Calculation</u>	<u>Cal./Mes.</u>
22	0.0	2.92 - 16	1.89 - 16	0.65
23	75.0	2.06 - 16	2.40 - 16	1.16
24	150.0	7.36 - 17	1.04 - 16	1.41
25	250.0	3.27 - 17	3.30 - 17	1.01
26	350.0	8.94 - 18	1.50 - 17	1.68
27	450.0	3.80 - 18	1.73 - 18	0.46
28	460.0	3.71 - 18	1.76 - 18	0.47
29	475.0	3.15 - 18	1.90 - 18	0.60
30	490.0	—	—	—

(3) $^{238}\text{U}(n,r)$: No correction for the effect of quide tube

<u>Position</u>	<u>Height (cm)</u>	<u>Measurement</u>	<u>Calculation</u>	<u>Cal./Mes.</u>
22	0.0	8.90 - 18	2.03 - 18	0.23
23	75.0	6.26 - 18	1.74 - 18	0.28
24	150.0	2.27 - 18	7.96 - 19	0.35
25	250.0	9.88 - 19	3.18 - 19	0.32
26	350.0	3.12 - 19	1.18 - 19	0.38
27	450.0	2.40 - 18	4.92 - 19	0.21
28	460.0	2.14 - 18	5.08 - 19	0.24
29	475.0	2.06 - 18	5.61 - 19	0.27
30	490.0	1.60 - 18	5.44 - 19	0.34

Table 3.2.4 (Continued) (2/3)

(4) $^{197}\text{Au}(n,\gamma)$

(No correction for the effect of detector guide tube)

<u>Position</u>	<u>Height (cm)</u>	<u>Measurement</u>	<u>Calculation</u>	<u>Cal./Mes.</u>
22	0.0	5.62 - 17	7.50 - 17	1.33
23	75.0	3.38 - 17	6.40 - 17	1.89
24	150.0	1.35 - 17	2.94 - 17	2.18
25	250.0	5.67 - 18	1.16 - 17	2.05
26	350.0	1.56 - 18	4.33 - 18	2.78
27	450.0	2.31 - 18	4.50 - 18	1.95
28	460.0	2.24 - 18	4.60 - 18	2.05
29	470.0	2.09 - 18	4.84 - 18	2.32
30	490.0	1.69 - 18	5.00 - 18	2.96

(5) $^{197}\text{Au}(n,\gamma)$

(Corrected for the effect of quide tube)

<u>Position</u>	<u>Height (cm)</u>	<u>Measurement</u>	<u>Calculation</u>	<u>Cal./Mes.</u>
22	0.0	5.62 - 17	3.53 - 17	0.63
23	75.0	3.38 - 17	4.50 - 17	1.33
24	150.0	1.35 - 17	1.97 - 17	1.46
25	250.0	5.67 - 18	6.36 - 18	1.17
26	350.0	1.56 - 18	2.99 - 18	1.91
27	450.0	2.31 - 18	2.77 - 18	1.20
28	460.0	2.24 - 18	2.83 - 18	1.26
29	470.0	2.09 - 18	2.98 - 18	1.42
30	490.0	1.69 - 18	3.08 - 18	1.82

Table 3.2.4 (Continued (3/3)

(6) Thermal Flux by Au Foil

(No correction for the effect of detector quide tube)

<u>Position</u>	<u>Height (cm)</u>	<u>Measurement</u>	<u>Calculation</u>	<u>Cal./Mes.</u>
22	0.0	6.52 + 5	1.12 + 6	1.72
23	75.0	3.91 + 5	9.56 + 5	2.45
24	150.0	1.57 + 5	4.39 + 5	2.80
25	250.0	6.60 + 4	1.72 + 5	2.61
26	350.0	1.75 + 4	6.45 + 4	3.69
27	450.0	5.76 + 3	1.09 + 4	1.89
28	460.0	—	—	—
29	470.0	7.55 + 3	1.14 + 4	1.51
30	490.0	—	—	—

(7) Thermal Flux by Au Foil

(Corrected for the effect of quide tube)

<u>Position</u>	<u>Height (cm)</u>	<u>Measurement</u>	<u>Calculation</u>	<u>Cal./Mes.</u>
22	0.0	6.52 + 5	4.20 + 5	0.64
23	75.0	3.91 + 5	5.33 + 5	1.36
24	150.0	1.57 + 5	2.33 + 5	1.48
25	250.0	6.60 + 4	7.63 + 4	1.16
26	350.0	1.75 + 4	3.53 + 4	2.02
27	450.0	5.76 + 3	2.44 + 3	0.42
28	460.0	—	—	—
29	470.0	7.55 + 3	2.52 + 3	0.33
30	490.0	—	—	—

CHAPTER 4

CONCLUSIONS

Shielding analysis around the reactor vessel of JOYO has been performed for the condition of the mark II core constitution. The interesting feature lay in that the JENDL-2 base cross-sections were used in place of the ENDF/B-IV base cross-sections that had been used for the analysis of JOYO with mark I core constitution. The comparison of the results between the one-dimensional analysis using the JENDL-2 base cross-sections and the ENDF/B-IV cross-sections has revealed that neutron fluxes by the JENDL-2 are small than those by the ENDF/B-IV, especially the fast neutron fluxes in the graphite shield and the fast and intermediate neutron fluxes in the concrete are much smaller.

The difference of the mark II core constitution from the mark I core constitution relating to the shielding analysis was that the JOYO MK-II has no blanket region outside the fuel assemblies. The analysis has shown that the leakage neutrons from the mark II core are a factor of 2-3 larger than that from the mark I core.

There was a difference in the region composition between the analysis and the real reactor. The JOYO MK-I core has been operated with some fuels in the fuel storage racks outside the core barrel, while the fuels in the storage racks were neglected and replaced by sodium in the analysis. Comparison of the calculational results with the measurements has shown that the calculational results agree with the measurements within a factor of 3 for the low energy neutron fluxes. This result has obtained through the measurements of $^{235}\text{U}(n,f)$, $^{238}\text{U}(n,\gamma)$, and $^{197}\text{Au}(n,\gamma)$ reaction rates, and has shown that the fuel assemblies in the fuel storage rack have a little effect on the low energy neutron fluxes.

Comparison of $^{238}\text{U}(n,f)$ and $^{58}\text{Ni}(n,p)$ reaction rates obtained by the calculation and the measurements has shown that the calculational results are much smaller than the measurements. It has been found that the fuel assemblies in the fuel storage racks have a great effect on the fast neutron fluxes.

The measurements were obtained also in the graphite shield region along the detector guide tube of channel A, and compared with the calculation. The comparison has shown that the calculation agrees with the measurement within a factor of 5.

ACKNOWLEDGEMENT

It is a pleasure to thank Dr. N. Ohtani for many helpful discussions and suggestions. Thanks are also to Mr. T. Ikegami and Mr. T. Kawakita for presenting many shielding data of JOYO.

REFERENCES

- (1) PNC, "Radiation Shielding Analyses of JOYO." SN 241 81-29, November, 1981.
- (2) RSIC Computer Code Collection, "DOT 3.5, Two-Dimensional Discrete Ordinates Radiation Transport Code," CCC-276 (1978)
- (3) S.Miyasaka, et al : "Code System for the Radiation-Heating Analysis of a Nuclear Reactor, RADHEAT," JAERI - M 5794 (1974).
- (4) K.Koyama, et al : "RADHEAT - V3, A Code System for Generating Coupled Neutron and Gamma-Ray Groups Constants and Analyzing Radiation Transport," JAERI - M 7155 (1977).
- (5) PNC, "Development of Nuclear Group Constants for Shielding" SN 298 82-02 (in Japanese).
- (6) MAPI, "Development of Nuclear Group Constants for Radiation Shielding Calculation," PNC J 206 83 - 02 (1983).
- (7) K.Koyama, et. al., "Multi-group Cross Section sets for shield Materials," JAERI-M 6928 (1977), (in Japanese).
- (8) W.E.Ford III, : "The POPOP4 Library of Neutron Induced Secondary Gamma-Ray Yield and Cross Section Data, " CTC-42(1970)
- (9) RSIC Computer Code Collection, "ANISN-W, Multigroup One-Dimensional Discrete Ordinates Transport Code with Anisotropic Scattering," CCC-82 (1968)
- (10) MAPI, "Fission Neutron Source Distribution in Core Region," 721013-RP-36A, 1973 (in Japanese).
- (11) Hitachi, "Supplement to Radiation Shielding analyses of JOYO - (C)," SJ.202 82-03, 1982.